CHARACTERIZING AND MODELING ARCTIC SHRUB EXPANSION ON THE NORTH SLOPE OF ALASKA, USA

A Dissertation

by

ADAM T. NAITO

Submitted to the Office of Graduate and Professional Studies of
Texas A&M University
in partial fulfillment of the requirements for the degree of

DOCTOR OF PHILOSOPHY

Chair of Committee,	David M. Cairns
Committee Members,	Charles W. Lafon
	Oliver W. Frauenfeld
	William E. Grant
Head of Department,	Vatche P. Tchakerian

August 2014

Major Subject: Geography

ABSTRACT

Shrub expansion is one of the most recognized components of terrestrial Arctic change and has been documented in studies involving fine-scale experimental manipulations or broad-scale satellite remote sensing. The characteristics and drivers of this phenomenon at the landscape scale, however, are understudied. The motivation of this dissertation was to develop an improved understanding of the historic spatial characteristics of shrub expansion on the North Slope of Alaska and its environmental drivers at this landscape scale. This work has three objectives, which include: 1) mapping and quantifying historic shrub expansion patterns; 2) examining a relationship between shrub expansion and its hydrological controls; and 3) designing and implementing a spatially-explicit simulation model to develop hypotheses regarding the landscape-scale drivers of shrub expansion (i.e., modes of reproduction, hydrological constraints, and their interactions). Shrubs maps were generated from semi-automated classification of historic vertical aerial photographs and contemporary high-resolution satellite imagery within a GIS. The spatial patterns of historic shrub expansion were quantified using FRAGSTATS and the multi-scale information fractal dimension. Relationships between shrub expansion and local hydrology was determined statistically through associations between areas that gained shrub cover and topographic wetness index values derived from a digital elevation model. The contribution of shrub reproductive characteristics was determined by developing a C#-based spatially-explicit simulation model that simulates clonal and sexual reproduction of shrubs. The

reproductive mode(s) producing spatial patterns most similar to the observed patterns was determined through principal components analyses. Results from this work suggest that: 1) the shrub-tundra ecotone within river valleys on the North Slope is has either initiated or completed a phase transition from tundra to shrubland; 2) shrub development is promoted in areas where the potential for water accumulation or throughflow is higher; and 3) vegetative reproduction appears to have been dominant mode of reproduction . Considering our current understanding of the fine-scale relationships between shrub expansion and hydrology, surface energy balances, and C and nutrient cycling, continued expansion may have considerable implications for circumpolar tundra ecosystems. These findings will facilitate the development of improved projections of the structure and function of these ecosystems and their feedbacks to climate change.

ACKNOWLEDGEMENTS

I have a number of people to thank and acknowledge for their contributions to, and their support of, this work.

First and foremost, I would like to thank my committee chair, Dr. Cairns, for his valuable support and his mentorship. Because of him, I have been able to pursue opportunities in the PhD program at Texas A&M University that I would not have been able to pursue elsewhere (yes, that includes running to catch the airplane on the airstrip in Anaktuvuk Pass, Alaska to get my backpack back). I would also like to thank Dr. Charles Lafon, Dr. Oliver Frauenfeld, and Dr. William Grant, for their guidance and support.

The National Science Foundation for provided financial support for this work (grants ARC-0806506 and BCS-1203444). Ms. Elizabeth Doerr at the GeoEye Foundation, and Ms. Patricia Dahnka at SPOT Astrium furnished the free satellite imagery for the North Slope of Alaska. Mr. Jeremy Hale (i-Cubed) and Ms. Katie Nelson (Apollo Mapping) helped furnish additional QuickBird imagery. I would like to acknowledge Ms. Krista Roznovsky, Ms. Denise Mackan, and Mr. Clayton Hollee at Office of Sponsored Research at Texas A&M University for their assistance with grant management.

Thank you to Dr. Richard M. Feldman in the Department of Industrial & Systems Engineering at Texas A&M University for developing the shrub simulation model. I am also indebted to Ellen R. Gass, Jeremy S. Johnson, Tiffany Roe, Collin Kohlmeyer,

Virginia Cain, and Patrick Hourahan for their assistance in processing the aerial imagery. Special thanks go to Morgan Buob for traveling with me to Fairbanks, Alaska to scan the images at the Fish and Wildlife Service Office.

Ms. Faustine Bernadac, Ms. Emily Roseberry, Mr. Joshua Bacon, and Mr. Douglas Whiteman of CH2MHill provided valuable logistical support and accommodations for the education and outreach trips to the North Slope of Alaska. Mr. Walt Audi and Ms. Merilyn Audi provided additional accommodations in Kaktovik, Alaska. The scientists at the Barrow Arctic Science Consortium (BASC) also provided important logistical support, and I apologize that I do not remember all your names. Thank you also to the people of Anaktuvuk Pass, Atqasuk, Barrow, and Kaktovik, Alaska.

Thank you to Ms. Janet Jorgenson at the Fish and Wildlife Service in Fairbanks, Alaska for providing logistical and intellectual support for the work on the coastal plain of the Arctic National Wildlife Refuge. Dr. David Swanson at the National Park Service in Fairbanks Alaska provided additional imagery.

I would like to thank Dr. Ken D. Tape for his support of this work and his valuable manuscript comments. I also appreciate his hospitality while Ms. Buob and I were in Fairbanks. Dr. Xinyuan “Ben” Wu and Dr. Bradford Wilcox of the Department of Ecosystem Science and Management at Texas A&M University provided additional thoughtful comments on manuscripts stemming from this work.

NOMENCLATURE

ALT	Soil Active Layer Thickness
BRNS	The Brooks Range and North Slope Uplands of Alaska
C	Carbon
GPP	Gross Primary Productivity
GIS	Geographic Information Systems
ka BP	Thousand Years Before Present
ISODATA	Iterative Self-Organized Data Analysis Technique
LGM	Last Glacial Maximum
N	Nitrogen
NDVI	Normalized Difference Vegetation Index
TWI	Topographic Wetness Index

TABLE OF CONTENTS

Page

LIST OF FIGURES

Page

Page

Page

Page

Page

Page

Page

LIST OF TABLES

Page

Page

Page

Page

1. INTRODUCTION

1.1 Context and Problem Statement

The expansion of shrubs in the Alaskan tundra is a phenomenon that has occurred over much of the 20th century. Along with permafrost thaw and sea-ice melt, shrub expansion is one of the most widely recognized components of Arctic change. Evidence of this change has been documented in studies involving both fine-scale experimental manipulations (Bret-Harte et al. 2002; Walker et al. 2003a; Chapin et al. 2005; McGuire et al. 2006; Blok et al. 2010; Elmendorf et al. 2012; Walker et al. 2012; Myers-Smith & Hik 2013) and broad-scale satellite remote sensing (Goetz et al. 2005; Jia et al. 2006; Pouliot et al. 2008; Verbyla 2008; Forbes et al. 2010; Beck & Goetz 2011). In particular, the expansion of tall shrubs (> 0.5 m in height) and their associated feedbacks will have considerable ecosystem consequences for surface energy balances, permafrost degradation, and soil nutrient availability (Myers-Smith et al. 2011a). The precise characteristics of this expansion are less understood. A study using repeat oblique aerial photography of the northern Brooks Range and North Slope uplands (BRNS) from the 1940s and early 2000s revealed expansion ranging from 3 to 80% (Tape et al. 2006). In addition, the greatest increases in shrub cover occurred in floodplains and valley slopes. Based upon results of this study, Tape et al. (2006) proposed that:

1) shrub expansion manifests itself as an increases in the number and size of patches and a decrease in the distance between patches;

2) most of the increases in shrub cover occur on the floodplains and the valley slopes; and,
3) a simple logistic growth model has the capacity to explain past and predict future expansion.

As foundational as this study has been to current terrestrial Arctic change studies, however, Tape et. al's (2006) study did not explain the *process* behind expansion at this scale.

1.2 Research Questions and Associated Objectives

In this dissertation, I focused on quantifying the historic spatial characteristics of shrub expansion in the BRNS and developing an improved understanding of how landscape-scale environmental characteristics influence its development. My specific research questions of this work are as follows:

1) What is the manner of expansion with regard to shrub patch density, shrub patch size, and distance between patches? In addition, what is the potential for an ecological phase transition from tundra to shrubland as shrubs continue to expand?
2) If shrub expansion is preferentially occurring in floodplains and valley slopes, is the manner of (potential) water flow or accumulation in these geomorphic units promoting or constraining their patterns of development? Specifically, does shrub expansion occur in areas where the potential availability of water is greater? In addition, is there a relationship between floodplain shrub developmen

development and river channel characteristics?

3) What is the contribution of clonal and/or sexual reproductive characteristics to observed patterns of expansion?

To answer these questions, my objectives were as follows:

1) Quantify the historic dynamics of shrub expansion in river corridors at ten sites in the BRNS using historic vertical imagery, current satellite imagery, and pattern metric analysis.
2) Determine an association between shrub expansion patterns and topographically-derived hydrologic characteristics and fluvial characteristics at five of the sites in the BRNS from Objective 1.
3) Determine the contribution of shrub reproductive characteristics to observed patterns of shrub expansion using a spatially-explicit computer simulation model.

Although the scientific community is beginning to understand some of the processes involved in the observed changes in the Arctic shrub-tundra, the patterns of shrub change are not yet well understood, especially at the landscape scale. Landscape pattern can inform us about the trajectory of shifts between vegetation types (in this case, from tundra to shrubland) and the processes that drive this shift. The emphasis of this research is to quantify the spatial patterns of shrub expansion in an effort to improve scientific understanding of its processes in the BRNS. Given that this phenomenon is circumpolar in extent, developments from this work, including the simulation model, could potentially be applied to other regions in the Arctic since the processes driving

expansion are thought to be similar. Through the integration of additional field-derived measurements, improved remote sensing products, new remote sensing techniques, this work will contribute to advancing understanding of Arctic ecological interactions and possible shifts in shrub reproductive characteristics, as well as predicting the future state of the Arctic. Refinement of this understanding will also help improve coupling to global-scale climate and atmospheric models to improve predictions of Arctic environmental changes.

1.3 Dissertation Organization

Section 1 provides a general overview of the work herein. Section 2 provides an overview and synthesis of the literature on shrub expansion as a global phenomenon. In addition, there are other subsections that discuss literature pertinent to specific objectives of the work presented herein. Section 3 briefly describes the study area. Section 4 introduces the methods used in this work and discusses the process of acquiring the imagery and conducting the GIS-based analyses. Section 5 details the considerations and components of the SimSHRUB spatially explicit simulation model used in this work. It has been separated from Section 4 to improve clarity. Section 6 provides an overview of the results of the pattern analysis, the influence of hydrologic characteristics, and the simulation model runs. Section 7 provides a discussion on the results, their potential contribution to current knowledge, the limitations of the work, and future research avenues. Section 8 provides concluding remarks about the findings of the work.

2. LITERATURE REVIEW AND SYNTHESIS [*]

2.1 Introduction

The range of woody shrubs is expanding globally, and this phenomenon involves a transition from herbaceous to woody cover (Ghersa et al. 2002; Gibbens et al. 2005; Lunt et al. 2010). Such expansion will likely become an important constituent of future land management schemes as issues of biodiversity and sustainability come to the fore. Furthermore, shrub expansion also has dramatic implications for net primary production, nutrient cycling, and the global C balance (Archer et al. 1995; Sturm et al. 2001a; Jackson et al. 2002; Bai et al. 2009). As such, an understanding of the magnitude and pattern of shrub expansion is necessary to predict future changes in the ranges of shrub species and thus contribute meaningfully to the debates regarding this global phenomenon.

The most recent reviews of global and regional shrub expansion focused on subtropical savannas and temperate rangelands (Archer et al. 1995) and North American semiarid and arid grasslands (Van Auken 2000, 2009). The most recent review (Naito & Cairns 2011a) summarizes additional studies from these regions and incorporates a discussion on the patterns and processes of Arctic shrub expansion, which has been missing from previous reviews. In addition, this review also summarizes technological and analytical developments involving remote sensing, GIS, and computer simulation

[*] Reprinted with permission from "Patterns and processes of global shrub expansion" by Naito, A.T. & Cairns, D.M. 2011. *Progress in Physical Geography*, 35(4): 423-442, Copyright [2011] by Adam T. Naito and David M. Cairns. The online abstract is available at http://ppg.sagepub.com/content/35/4/423.abstract.

models. A summary of this work is included in the following subsections.

2.2 Patterns and Processes of Global Shrub Expansion

The extent and degree of the occurrence of shrub expansion is variable, and it is contingent on spatial and temporal scale as well as environmental characteristics. Patterns of shrub expansion are scale-dependent; therefore, studies that implement multi-scalar approaches provide a more comprehensive understanding of observed patterns and their causes and will facilitate land management efforts (Johnson & Miller 2006). There are few current estimates of the total land area undergoing expansion. Knapp et al. (2008) suggested that perhaps 220 – 330 million ha of non-forest land in the United States are undergoing a transition to woody shrubs. Estimates are often difficult to make because individuals of the same species can be common to different geographic areas (Van Auken 2009). This results in varying classifications of the landscape. While numerous studies have quantified local changes, total estimates appear to be largely absent from the literature.

The following discussion of shrub expansion patterns is categorized by rangeland type, which include desert grasslands, mesic grasslands, and savannas. While the type distinctions are not clear-cut, and the literature uses these terms interchangeably, these divisions are only to facilitate clarity and follow the classifications indicated by the literature cited within each section. Fig. 1 also provides an overview map of the location of and primary mechanism of plot-based studies summarized in this subsection.

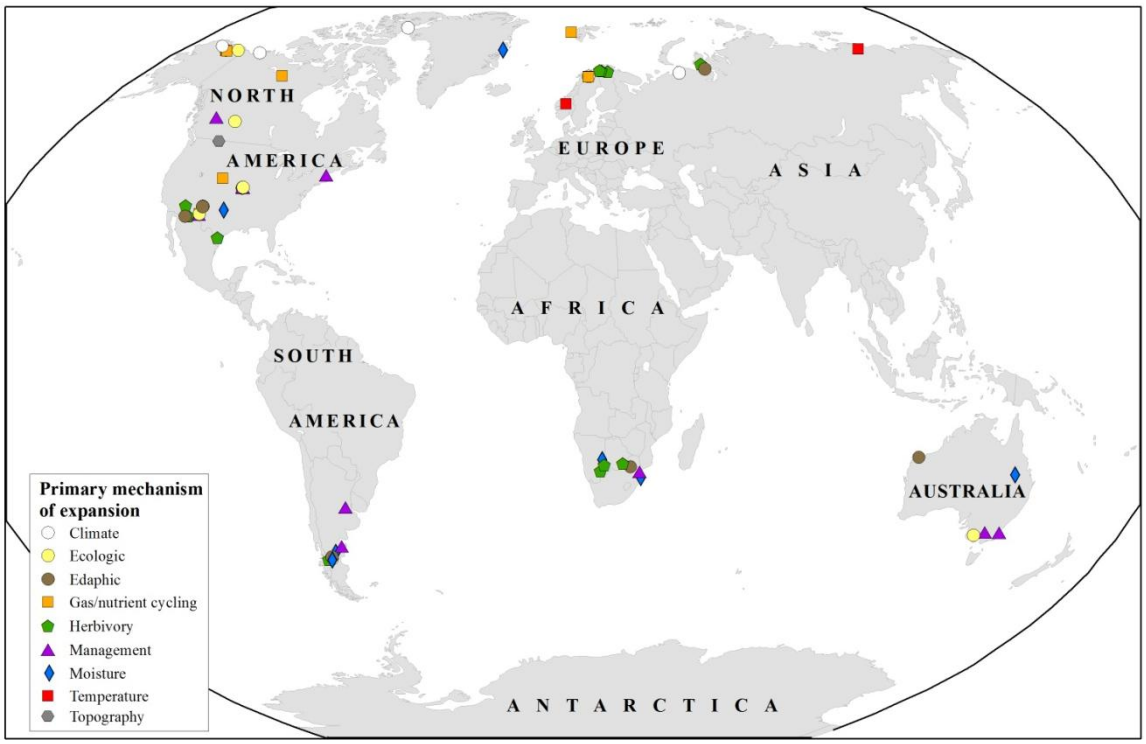

Figure 1: Location and primary mechanism of plot-based studies summarized in Subsection 2.1. Broad-scale modeling and paleorecord studies are not included in this map.

2.2.1 Patterns and Processes in Desert Grasslands

2.2.1.1 Desert Grassland Patterns

Deciduous species of the genus *Prosopis* (mesquite) have been a primary focus of studies regarding shrub expansion in desert grasslands. Their native range is in the south-central and southwestern United States (Archer 1990), but they have been introduced to Western Australia (van Klinken et al. 2006; Robinson et al. 2008)

The Jornada Basin of New Mexico, United States has been the focus of numerous studies of *Prosopis* expansion. Buffington and Herbel (1965) provided what is perhaps the first comprehensive review of vegetation changes in this region. Using the

Jornada Experimental Range (JER) in New Mexico as their focus, Buffington and Herbel (1965) noted that, between the 1850s and 1960s, areas dominated by *Prosopis* grew from 6,000 ac to more than 60,000 ac. Expanding upon Buffington and Herbel's (1965) work, Gibbens et al. (2005) used additional vegetation surveys and recent aerial photography to provide updated trends in shrub expansion at the JER and the Chihuahan Desert Rangeland Research Center (CDRRC), both within the Jornada Basin. Between 1915 and 1998, the land area occupied by *P. glandulosa* as the dominant or subdominant species in JER increased from 26 to 84%. At the CDRRC between 1938 and 1998, the land area occupied by *P. glandulosa* increased from 44 to 51% (Gibbens et al. 2005). These shrub increases were concomitant with a significant decline in the area occupied by grasses. Goslee et al. (2003) utilized historic aerial photographs to identify three trends in spatial patterns of *Prosopis* expansion over time in the Chihuahan Desert. These included: an increase in the amount of shrub cover and patch size, trending to stabilization; an increase, then decrease, of patch-size complexity as a consequence of increasing shrub size, shrub merging, and subsequent infilling; and considerable shrub clustering at fine scales and random distribution at large scales in 1936, trending towards regular distribution by 1983 (Goslee et al. 2003).

Members of the *Prosopis* genera were deliberately introduced to Western Australia in the 1930s to provide both shade for livestock and an alternate source of fodder in times of drought (Robinson et al., 2008). Patterns of *Prosopis* establishment in this region are not identical to those in the southwestern United States, however. First, total and adult *Prosopis* density and size of the sapling bank are larger in Australia.

Dense stands are also capable of totally excluding an underlying herbaceous layer (van Klinken et al. 2006). Van Klinken et al. (2006) also attribute the presence of hybrid (*P. glandulosa* x *P. velutina* x *P. pallida*) species to differences in these patterns. Robinson *et al.* (2008) note, however, that the time-span (~70 yr) and rate (~0.4 – 1.2%/yr^{-1}) of expansion in Western Australia is comparable to that observed in the southwestern United States.

Edaphic characteristics are also an important influence in *Prosopis* expansion. Soils dominated by *Prosopis* are often of a coarse texture, with low levels of nutrients and moisture (Paulsen 1953). Robinson et al. (2008) determined that patterns of *Prosopis* expansion in northwestern Australia were different based upon land type. The greatest change in *Prosopis* cover occurred in riparian and upland-red loamy land types in terms of initial colonization rates, canopy cover increases, and patch sizes. Browning et al. Browning et al. (2008)argued that sandy soils are important for *Prosopis* shrub seedling establishment in Australia, while clayey soils with their higher nutrient and moisture content are more important for post-establishment shrub persistence.

Shrub species of the genus *Larrea* (creosotebush) are evergreen and are found in the southwestern United States and the Patagonian Monte of South America. *Larrea* species invading Chihuahan Desert grasslands are found on sandy loam soils (Peters et al. 2006). Peters et al. (2006) discovered that invasibility by *Larrea* was contingent on seed dispersal, propagule pressure, local environmental conditions such as soil structure, and the abundance of grass species such as *Boutelouda gracilis*. A greater abundance of *B. gracilis* could therefore limit the expansion of *Larrea*, but the size, density, and

configuration of patches of *B. gracilis* in order to accomplish this are unknown (Peters *et al.*, 2006). Gibbens et al. (2005) noted that the land area occupied by *L. tridentata* as the dominant species in JER increased from 4.5% to 24.6% between 1915 and 1998. Between 1938 and 1998, the land area occupied *L. tridentata* as the dominant or subdominant species in CDRRC increased from 43 to 59%. The Patagonian equivalent, *L. divaricata*, functions as both an initiator of new patches in bare soils and as a colonizer that serves to increase the size of current shrub patches, particularly when competition from grasses is reduced (Bisigato & Bertiller 2004). Similar to species in North America, typical soils in this region include sandy or sandy loam soils (Bertiller 1996). Given adequate competition from herbaceous cover, it appears that *Larrea* shrub populations can be limited or reduced.

2.2.1.2 Desert Grassland Processes

Desert grassland shrubs possess unique structural characteristics that allow them to withstand harsh conditions and persist on the landscape. These strategies provide shrubs with advantages in terms of uptake of soil moisture and nutrients. Although one might assume deciduous and evergreen shrubs have different survival strategies, work in the Jornada Basin by Reynolds et al. (1999) found that the deciduous *P. glandulosa* and evergreen *L. tridentata* are very similar in that regard. These strategies include an ability to utilize different levels of soil for moisture as well as temporally shifting its growth and physiological activity periods to access moisture resources. Experimental work by Connin et al. (1997) discovered that *Prosopis* can produce woody biomass at a soil level

beneath most perennial grasses. As a consequence, they note that total and deep root biomass has increased since shrub expansion began. In addition, long-term C sequestration has been enhanced since this below-ground woody biomass acts as a C sink (Connin et al., 1997). While desert shrubs may positively respond to elevated levels of CO_2, this relationship is complicated by other interacting edaphic and surface characteristics for which empirical evidence is lacking (Van Auken 2009). Schlesinger et al. (1999; 2000) noted that experiments involving rainfall-induced runoff in the Chihuahuan Desert contributed to an increased loss in N from shrub-dominated systems compared to grass-dominated systems. McAuliffe (1994) noted a high prevalence of *L. tridentata* at the base of slopes despite cold air drainage and a preference for deep-rooting in coarse-grained soil covering deeper, more developed horizons. Likewise, deciduous Patagonian shrubs such as *Mulinum spinosum* and *Adesmia campestris* concentrate their roots in the lower soil layers where moisture levels are greater, resulting in their ability to persist on the landscape (Aguiar et al. 1992; Paruelo & Sala 1995). More recently, precipitation experiments in the Patagonian steppe revealed that extreme precipitation events resulted in a leaching of limiting-N and nitrate from upper soil layers. Nutrients are likely to remain in deeper soil layers, thereby favoring deep-rooted shrubs (Yahdjian & Sala 2010).

Herbivory effects also play a crucial role in influencing the development of shrub patterns in desert grasslands, with higher levels of herbivory contributing to greater shrub presence. The presence of livestock can increase the landscape's susceptibility to shrub expansion by lowering available grass fuels that can otherwise carry fires at

temperatures sufficient to kill shrubs, producing manure that serves as a vector for scarified shrub seed, compacting soil that reduces moisture availability and otherwise restricts shrub development, and eliminating perennial grasses that would otherwise provide competition to shrubs (Bahre & Shelton 1993). Heavy livestock grazing leads to a removal of grass cover and subsequent overland flow of water (Schlesinger et al. 1990; Aguiar & Sala 1994; Schlesinger et al. 1996). This leads to increased heterogeneity of soil characteristics that favor shrubs like *L. tridentata* and the development of "islands of fertility" (Schlesinger et al. 1990; Schlesinger et al. 1996). In Patagonia, sheep grazing leads to soil and wind erosion. This reduces moisture- and nutrient-retention capacity and improves environmental conditions for xeric shrubs (Bertiller et al. 1995). Sheep and macropods are the primary dispersal agents of the hybrid *Prosopis* species in Western Australia (Robinson et al. 2008).

2.2.2 Patterns and Processes in Mesic Grasslands

2.2.2.1 Patterns in Mesic Grasslands

Mesic grasslands of central North America and Australia are undergoing a transition from C_4 herbaceous cover to C_3 woody shrub cover (Lett & Knapp 2003; Lett & Knapp 2005). Examples of shrubs include *Acacia sophorae* (coastal wattle), *Betula glandulosa* (American dwarf birch), *Cornus drummondii* (rough-leaved dogwood), and *Leptospermum scoparium* (tea tree). *B. gladulosa* often appears in grazed valley bottoms in Alberta in acidic, well-drained, nutrient-poor soils (de Groot et al. 1997; de Groot & Wein 2004). Analysis of historical aerial photographs have revealed patterns of

expansion in these areas since 1958 (Burkinshaw & Bork 2009). The deciduous *C. drummondii* can be found in prairies of the central United States in silty loam or alluvial soils (Lett & Knapp 2003; Briggs et al. 2005; Craine et al. 2010). In addition, in the absence of graminoid competition, they can form dense patches via rhizomatous stems (Lett & Knapp 2003). The deciduous *A. sophorae* and the evergreen *L. scoparium* are predominately found in southeastern Australia and New Zealand (Costello et al. 2000; Stephens et al. 2005; Price & Morgan 2008). *A. sophorae* has been replacing vegetation on woodlands and heathlands near coastal areas, particularly critical native tussock grasses (Costello et al. 2000). *L. scoparium* is readily adapted to extreme environments and infertile or wet soils not conducive for the development of climax forest (Stephens et al. 2005). Patches of *L. scoparium* have also been associated with decreased species richness and ground-level biomass (Price & Morgan 2008). Because mesic grassland shrubs have a high tolerance for poor soils and are able to exclude more desirable species, they have important biogeographic implications.

2.2.2.2 Processes in Mesic Grasslands

A combination of survival strategies, fire exclusion, and high-intensity grazing has created environmental conditions conducive for shrub expansion in mesic grasslands (Bragg & Hulbert 1976; Bai et al. 2004; Briggs et al. 2007; Burkinshaw & Bork 2009). Heisler et al. (2004) determined that significant re-sprouting of *C. drummondii* occurred after fire. As a consequence, areas co-dominated by the shrub can persist even with frequent fire, thereby preventing the reversion to mesic grassland without significant

manipulation (Briggs et al. 2005). Similarly, *B. gladulosa* in Alberta is well-adapted to a range of fire regimes and possesses a competitive advantage due to its ability to re-sprout after a fire (de Groot & Wein 2004). Grazing activities in American grasslands provide an effective vector for shrub propagules (Briggs et al. 2002). In contrast, fences established for grazing areas in Australia have limited the spread of *A. sophorae* because it is palatable to cattle. In addition, expansion of *A. sophorae* was greatest after cattle exclusion in the late 1970s (Costello *et al.*, 2000).

Shrub influences on soil nutrient cycling in mesic grasslands appear less important than in other rangeland types. Instead, C storage and vegetation productivity are more affected. For example, *C. drummondii* does not significantly influence soil C and N resources. Instead, *C. drummondii* cover limited incoming light, contributing to a reduction of graminoid cover and subsequent above-ground net primary productivity (Lett & Knapp 2003). A later study indicated that *C. drummondii* increased aboveground C storage and reduced soil CO_2 flux (Lett et al. 2004). Similar processes occur in southeastern Australia, where *L. scoparium* reduced biomass and species richness as a result of decreased light reaching the soil (Price & Morgan 2008).

2.2.3 Patterns and Processes in Savannas

2.2.3.1 Patterns in Savannas

Savannas are another rangeland type of concern with regards to shrub expansion. Experimental manipulations, image analysis, and simulation modeling have all provided insights into the developing patterns of expansion in savannas.

In savannas of the Americas, *Prosopis* is again a primary research focus and will only receive light treatment here. *Prosopis* typically occupies alluvial clay loam sites in these ecosystems (e.g., Ansley et al. 2001). Aerial photograph analysis between 1941 and 1983 led Archer (1990) to hypothesize that while drought may eliminate small patches of *Prosopis*, normal or wet years offset losses. This resulted in an overall increasing trend in area converted to shrubland or woodland and a coalescence of patches (Archer et al. 1988; Archer 1990; Ansley et al. 2001). Spatial patterns of shrub expansion in savanna drylands are also hierarchically structured (Wu & Archer 2005). Spatial analysis incorporating the use of aerial photographs and digital elevation models revealed subsoil texture variability controls patch-scale upland expansion of *P. glandulosa*, and surface hydrologic characteristics control catena-scale patterns (Wu & Archer 2005).

Acacia and *Grewia* species are implicated in the conversion of southern African savannas to shrubland and woodland (e.g., van Vegten 1984). Jeltsch et al. (1997) noted that shrub expansion is detrimental to the carrying capacity of Kalahari savannas for livestock. In non-overgrazed areas with nutrient-poor soils, *A. mellifera* (black thorn) developed patterns of high aggregation and plant size due to the removal of competition from herbaceous cover (Skarpe 1991). O'Connor (1995) suggested that much of the observable *A. karroo* (sweet thorn) establishes within herbaceous swards. Upon removal of competition from surrounding herbaceous cover due to herbivory, *A. karroo* manifests itself as groups of even-aged stands (O'Connor 1995). Similarly, the deciduous *G. flava*

(brandybush) forms dense thickets and depend upon *A. erioloba* (camelthorn) trees to maintain suitable recruitment sites (Tews et al. 2006).

2.2.3.2 Processes in Savannas

Interactions between atmospheric CO_2, moisture availability, fire, and livestock grazing at variable frequencies and spatial scales all have contributed to savanna shrub expansion (Skarpe 1991; Brown & Archer 1999; Roques et al. 2001). Assigning primacy to any one of these mechanisms is difficult (e.g., Archer et al. 1995), but recent evidence from experimental manipulation of CO_2 levels in open-top chambers suggests that rising atmospheric CO_2 levels are indeed contributing to the expansion of shrubs in part (Morgan et al. 2007). While increased CO_2 levels are thought to have facilitated the shift from grassland to shrubs at broader spatial scales, livestock grazing and avoidance of unpalatable species have facilitated expansion at the fine scale (Morgan et al. 2007). Higher levels of moisture are indicative of greater woody plant cover (e.g., Knoop & Walker 1985). Aerial photograph and statistical analysis indicated that increased rates of change of shrub development in Queensland, Australia is primarily due to increased rainfall (Fensham et al. 2005). Observed patterns of *A. karroo* are due to intraspecific competition for moisture resources. As these resources are fully utilized, size increases result in density decreases (Skarpe 1991). Similarly, seedling emergence was contingent on higher moisture availability (O'Connor 1995). Livestock reduction (which serves as a vector for shrub seed dispersal) and the introduction of a fire regime making use of fine fuels have been recommended as measures to mitigate expansion (e.g., Archer 1990).

Computer simulation models have incorporated livestock interactions, as well as environmental and ecological processes to develop an improved understanding of expansion in savannas. Jeltsch et al. (1997) argued that simulation modeling is ideal for understanding savanna ecological function because changes are slow-paced and end-results are highly variable. In their study, Jeltsch et al. (1997) utilized a preliminary grid-based simulation model that incorporated parameters for stocking rates, soil moisture, precipitation, and probability of grass fire. They determined that high stocking rates (between 22 and 33 ha per livestock unit) combined with high precipitation levels resulted in dramatic expansion of shrubs. In addition, a non-linear relationship existed between stocking density and shrub cover where shrub cover increased dramatically above a particular density given low precipitation, and given normal stocking rates, shrub cover is likely to increase dramatically over the next century (Jeltsch et al. 1997). Spatially-explicit modeling also suggests that livestock can disperse *Grewia* shrub seed beyond natural limits imposed by fire, precipitation, and seeding intensity alone (Tews et al. 2004).

2.3 Patterns and Processes of Arctic Shrub Expansion

Despite the fact that the Arctic is undergoing rapid environmental change, reviews on the patterns and processes on Arctic shrub expansion are largely absent in the literature. In the following subsection, the current state of knowledge regarding the historic patterns and processes of shrub expansion inferred from the paleorecord is reviewed. From there, current observed patterns and their processes are discussed.

2.3.1 Historic Patterns and Processes of Arctic Shrub Expansion

2.3.1.1 Historic Patterns of Arctic Shrub Expansion

Extensive work has focused on generating an improved understanding Arctic vegetation dynamics using the paleorecord. Analysis of ice cores and sediment cores (containing samples of pollen, diatoms, and plant macrofossils) have allowed scientists to construct timelines and spatially-explicit representations of these changes. Fig. 2 presents six maps of historic Arctic vegetation change based upon a synthesis of the literature described below.

Historic vegetation patterns of Beringia are of great interest. Its now partially submerged state, however, limits our ability to extract meaningful records. Some of the earliest paleoecological work in this region (e.g., Livingstone 1955, 1957) elucidated patterns of vegetation development. For example, Livingtone (1955) analyzed *Betula*, *Alnus*, and *Salix* pollen present in lake sediment core samples from the present-day North Slope of Alaska. Based upon his results, Livingstone (1955) contended that this region served as a refugium for these species during the last glacial period. Later work led to hypotheses that mesic shrub and herb tundra dominated Beringia during the Wisconsin glacial period (Guthrie 2001; Yurtsev 2001). Most recently, during the Wisconsin glaciation (up until approximately 15 ka BP), much of Beringia was comprised of graminoid tundra (Fig. 2B) (Ager & Phillips 2008). By the Holocene, much of the vegetation tranisitioned to shrub-dominated tundra, such as *Betula* (Ager & Phillips 2008) (Fig. 2C and 2D).

Anderson and Brubaker (1994) summarized pollen records acquired from north-central (generally, extending south from the Brooks Range to the Yukon lowland, and east from Kotzebue Sound to the Porcupine River) Alaska. They note that much of the tundra was dominated by herbs between 18 ka and 14 ka BP (Figure 2A). *Betula* species expanded rapidly over the tundra 14 ka BP, particularly in eastern Alaska and became the dominant shrub by 12 ka BP (Figure 2B)**.** By 9 ka BP, *Betula* was giving way to *Alnus* species, particularly in the western Brooks Range (Figure 2D). By 4 ka BP, *Alnus* declined, and resulted in the present distribution of tundra and forest vegetation (Anderson & Brubaker 1994) (Figure 2F). Pollen records from Tukuto and Etivlik lakes reveal similar trends (Oswald et al. 1999). At the end of the late glacial period (~10 ka BP), the tundra was dominated by *Betula*, *Eriophorum*, and *Salix* (Figure 2C)**.** From 6 ka BP to the present, *Alnus* became the dominant shrub tundra species (Oswald et al. 1999) (Figure 2E and 2F)**.** Anderson (1985) noted that the greatest and most rapid expansion of *Betula* and *Alnus* in northern Alaska in the paleorecord occurred in river valleys and lowlands. *Salix*, *Betula*, and *Alnus* were most firmly established in lowland, well-drained areas during their respective periods of dominance (Anderson & Brubaker 1994).

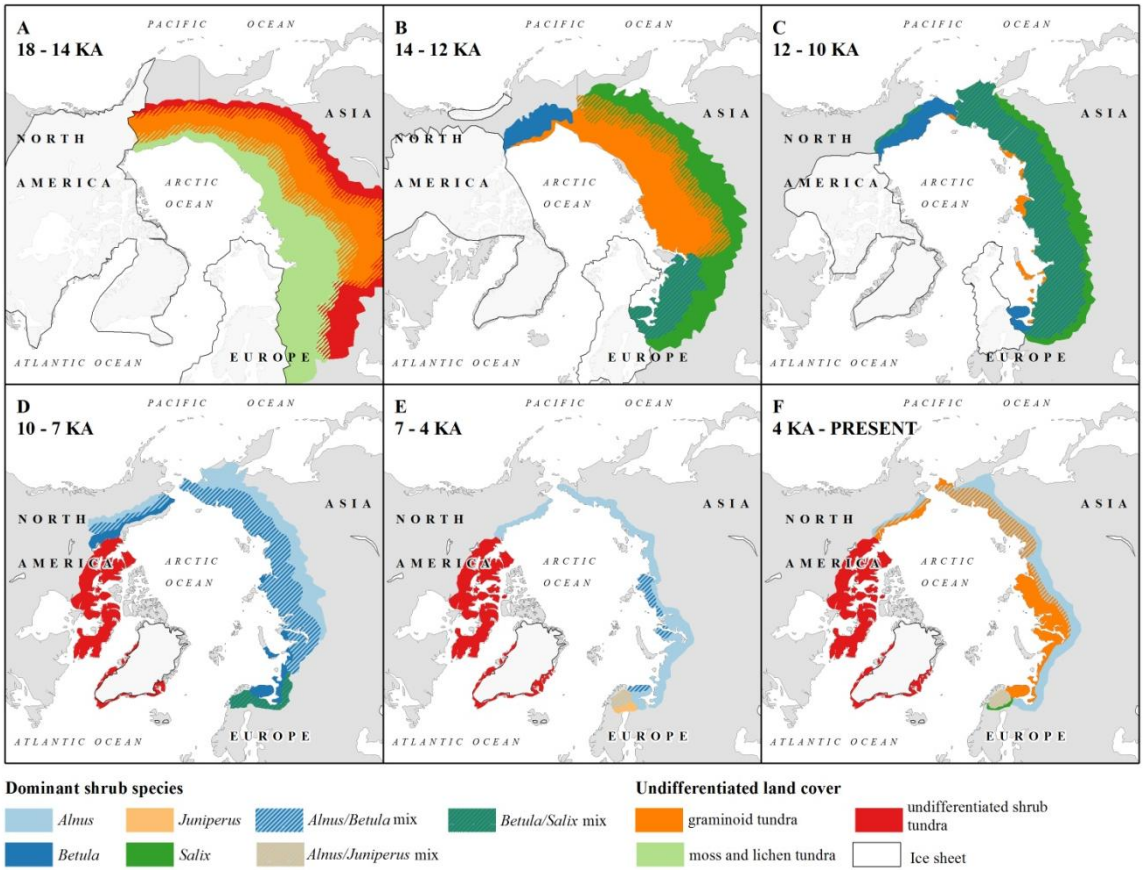

Figure 2: Generalized changes in patterns of dominant shrub (*Alnus, Betula, Juniperus*, and *Salix*) occurrence in the Arctic since the LGM. (A) Determined from synthesis of Anderson and Brubaker (1994), Bigelow et al. (2003), and Kaplan et al. (2003). (B) Determined from synthesis of Ager and Phillips (2008), Anderson (2002), Anderson and Brubaker (1994), Kremenetski et al. (2004), and Werner et al. (2010). (C) Determined from synthesis of Ager and Phillips (2008), Anderson et al. (2002), Andreev et al. (2003), Kremenetski et al. (1998), Lohzkin et al. (2007), and Oswald et al. (1999). (D) Determined from synthesis of Ager and Phillips (2008), Anderson and Brubaker (1994), Barnekow (1999), Bigelow et al. (2003), Bjune et al. (2004), Kaplan et al. (2003), and Seppa¨ et al. (2002). (E) Determined from synthesis of Bigelow et al. (2003), Bjune et al. (2004), Kaplan et al. (2003), Kremenetski et al. (2004), and Oswald et al. (1999). (F) Determined from synthesis of Anderson and Brubaker (1994), Bjune et al. (2004), Kremenetski et al. (2004), and Oswald et al. (1999). Glacial extents determined from synthesis of Forsstrom and Greve (2004), Siegert and Marsiat (2001), and Strong and Hills (2005).

Development of historic migration and development of shrubs has also been inferred from paleoecologic records in the European Russian Arctic (e.g., Oksanen et al. 2001; Valiranta et al. 2006) and Siberia (e.g., Lozhkin et al. 2007). During the Younger Dryas of approximately 12 ka BP, herbaceous species dominated much of northeastern Siberia, while species such as *Betula* and *Alnus* were rare (Werner et al. 2010) (Figure 2B). Although populations were possibly low, *Salix* appeared to be the most common shrub up to 12 ka BP in eastern Siberia (e.g., Anderson et al. 2002) (Figure 2B). *Betula* and *Salix* rapidly replaced herb tundra in response to postglacial warming occurring 10.8 ka BP (Figure 2C). While the landscape reverted to herb tundra approximately 10 ka BP, *Betula* and *Salix* reestablished shortly after and progressed to *Betula*-*Alnus*-dominated tundra by approximately 9 ka BP (Anderson et al. 2002) (Figure 2D). Similar trends were observed from radiocarbon dating of wood and shrub macrofossils (Kremenetski et al. 1998) and analysis of pollen from the Taymyr Peninsula of northern Russia (Andreev et al. 2003) and northeastern Siberia (Lozhkin et al. 2007). The Kola Peninsula was dominated by shrubs (e.g., *Betula* and *Salix*) during the lateglacial period (Figure 2B) (Kremenetski et al. 2004). *Salix* diminished during the Younger Dryas, and *Betula* peaked at the Late Glacial-Holocene transition (Figure 2C). As the Holocene progressed, the Kola Peninsula experienced an influx of birch, then subsequently pine (figure 2D). By 7.8 ka BP, *Alnus* reached a peak, followed by a decrease in *Betula* influx about 5 ka BP (Figure 2E). Finally, the present-day tundra established approximately 3.1 ka BP (Kremenetski et al. 2004) (Figure 2F).

Some palynological work revealing Holocene shrub dynamics has also been conducted in northern Fennoscandia. In Norway, *Betula* and *Salix* dominated much of the early Holocene until approximately 7.7 ka BP (Figure 2D) (Bjune et al. 2004). From 7.7 – 5.5 ka, *Alnus* and *Juniperus* shrubs increased (Figure 2E), leading to a trend of increasing ericaceous shrubs by 2.8 ka, followed by an increase of *Salix* until the present (Bjune et al. 2004) (Figure 2F). Lake cores from other locations in Fennoscandia have revealed similar patterns for *Betula* (Barnekow 1999; Seppä et al. 2002).

Modeling has facilitated broad scale predictions of Arctic vegetation change in the paleorecord. For example, Bigelow et al. (2003) used the BIOME4 model to reconstruct pan-Arctic vegetation (e.g., forests, dwarf shrub tundra low- and high-shrub tundra) patterns since the LGM. Their model results suggest that, at the LGM, herbaceous tundra was a major constituent of the vegetation in much of the unglaciated Beringia land bridge and eastern Siberia (Figure 2A). By the mid-Holocene, low- and high-shrub tundra had replaced the herbaceous vegetation, and was approximately 500 km north of its present location, with dwarf-shrub tundra occupying extreme northern Siberia and Canada, as well as coastal Greenland (Bigelow et al. 2003) (Figure 2D and E).

Review of the studies of vegetation dynamics in the paleorecord suggest several pan-Arctic trends. First, *Salix* was the dominant shrub species in a primarily graminoid Arctic tundra up until the end of the LGM. The early Holocene was marked by a substantitive increase in *Betula* and *Alnus* species, and a general decrease of *Salix.* The dominance of *Betula* and *Alnus* fluctuated through much of the Holocene, with shrub-

and treeline extending far north of its present extent. These lines receded southward in the late Holocene to their present locations today.

2.3.1.2 Historic Processes of Arctic Shrub Expansion

While early work generated hypotheses of glacial and post-glacial vegetation changes, identifying dominant mechanisms for these changes was more challenging. More extensive sampling and improvements in analysis techniques over the decades, however, have allowed scientists to generate more accurate inferences of these environmental mechanisms.

Climatic influences appear to play a significant role in driving vegetation changes in the Arctic. Work by Colinvaux (1964) suggested that warmer climates were responsible for increases in dwarf birch (*Betula nana*) and development of tussock tundra in Beringia. Anderson and Brubaker (1994) noted that transitions from herb tundra to shrub tundra, particularly in north-central Alaska were indicative of climate amelioration. Kaplan et al.'s (2003) climate simulation modeling using BIOME4 revealed several Arctic climatic trends in the paleorecord. First, dry, cold climates dominated Beringia at the LGM and possibly explains the presence of graminoid tundra in that region. This corroborates well with earlier palynological work (e.g., Colinvaux 1964; Anderson 1985; Anderson & Brubaker 1994). Second, increased summer insolation occurred in the early- to mid-Holocene. This led to increased Arctic temperatures and partially explains the poleward shift north in the treeline (Kaplan et al. 2003). A later synthesis of terrestrial and marine climate dynamics since the early

Cenozoic reflects many of these patterns (Miller et al. 2010). Overpeck et al. (1997) summarized climatic trends in the Arctic over the past 400 years from tree ring and pollen records across the Arctic. While acknowledging widespread natural variability in climatic responses across the Arctic, Overpeck et al. (1997) noted a transition from an abnormally cold 19th century to peak warm conditions in the 20th century.

In a related theme, moisture availability was also an important historic mediator of Arctic vegetation change (Mann et al. 2002). For example, Mann et al. (2002) stated that increased precipitation in northern Alaska was associated with rising sea levels in response to glacial retreat. This led to increased alluviation and paludification. The expansion of shrubs roughly coincided with this increased moisture, and they are still associated with acidic, nutrient-poor soils formed from paludification (e.g., Mandre et al., 2010). Rühland et al. (2009) suggested that the rise of *Alnus* during the mid-Holocene (7.5 ka BP) was due to a cooler growing season and the greater effective moisture as a result. Using the CCM1 simulation model, Bartlein et al. (1998) noted a strong east-to-west moisture gradient over Beringia between 14 ka and 6 ka BP. This corresponds well with the transition from graminoid to shrub tundra (e.g., Anderson & Brubaker 1994).

2.3.2 Current Patterns and Processes of Arctic Shrub Expansion

2.3.2.1 Current Patterns of Arctic Shrub Expansion

Generally, circumpolar and regional or plot-level scales have been the focal scales for studies of Arctic shrub expansion and its environmental drivers. Circumpolar

or regional scale studies have utilized the normalized difference vegetation index derived from low-resolution satellite data and *in situ* measurements to infer changes in productivity. These increases in productivity, or 'greenness,' were found to be correlated with increases in temperature (Myneni et al. 1997; Jia et al. 2003; Goetz et al. 2005; Bunn & Goetz 2006; Jia et al. 2006; Pouliot et al. 2008; Verbyla 2008; Beck & Goetz 2011). Intermediate-scale studies have largely employed the use of analysis of coarse and high resolution satellite imagery and/or aerial photographs to quantify changes in shrub patches (e.g., Tape et al. 2006; Forbes et al. 2010; Beck & Goetz 2011; Beck et al. 2011; Frost et al. 2013). In fact, the Arctic is the focus of what is perhaps the most extensive and comprehensive mapping work to quantify and understand ongoing vegetation dynamics in a region. The first large and comprehensive circumpolar mapping effort was initially discussed in a series of workshops (Walker et al. 1995) and culminated in the generation of the Circumpolar Arctic Vegetation Map (CAVM) (Walker et al. 2005). In concert with the CAVM project, Gould et al. (2003) developed a vegetation map of northern Canada for use in GIS databases and calculation of biomass and productivity. While coarse-scale maps provide useful information, the recognition of fine-scale heterogeneity (e.g., the transition from tall shrub tundra to dwarf shrub tundra) and its dynamics are also an important consideration (Lantz et al. 2010).

Research by Sturm et al. (2001a; 2001b) brought the issue of current Arctic shrub expansion to the fore. They determined that between 1948 and 2000, shrub development occurred as patch in-filling and increases in height and diameter. Subsequent analysis of 202 pairs of repeat photographs across the BRNS of Alaska indicated increases in shrub

cover ranging from 3% to 80%, with the greatest increases occurring in floodplains and along valley slopes and only minimal changes on interfluves (Tape et al. 2006). In addition, shrub expansion patterns manifest themselves as an increase in the size and number of patches, as well as in-filling of patches (Tape et al. 2006). These patterns have been confirmed elsewhere in the Arctic (Hallinger et al. 2010; Myers-Smith et al. 2011). The transition from tall shrub tundra to dwarf shrub tundra is contingent upon latitude (Lantz et al. 2010). As dominance and patch size of tall shrub tundra diminished, the dominance and patch size of dwarf shrub tundra increased (Lantz et al. 2010). Rigorous quantification and pattern metric analysis of fine-scale shrub cover change, however, still appears to be lacking.

Observed patterns of shrub expansion are now recognized to be heterogeneous in nature (Lantz et al. 2010; Tape et al. 2012; Walker et al. 2012; Raynolds et al. 2013).; Tape *et al*. (Tape et al. 2012) note both expanding and stable patches are present in Northern Alaska. Expanding patches are associated with higher resource environments (e.g., floodplains, stream corridors), while stable patches are associated with low-resource environments (e.g., poorly drained tundra). Shrub expansion also tends to be promoted in areas where the potential for water throughflow and accumulation is greater (Naito & Cairns 2011). These findings collectively suggest that landscape features are important considerations when predicting the future state of the Arctic vegetation cover. Interactions between climate and landscape features may also promote nonlinear ecological responses (Burkett et al. 2005).

2.3.2.2 Current Processes of Arctic Shrub Expansion

Climatic warming is greatest in the Arctic, and it is believed to be the dominant broad-scale driver of Arctic vegetation development (Overpeck et al. 1997; Press et al. 1998; Walker 2000; Walker et al. 2006), and transitions between Arctic vegetation zones (e.g., High and Low Arctic) (Epstein et al. 2004). The recent climatic warming trend in the Arctic, which is unique over the past 400 years, is accelerating shrub expansion and altering the terrestrial component of the Arctic ecosystem (Chapin et al. 1995; Serreze et al. 2000; Chapin et al. 2005; Goetz et al. 2005; Zhang et al. 2005; Jia et al. 2006; McGuire et al. 2006; Pouliot et al. 2008; Verbyla 2008; Blok et al. 2010; Beck & Goetz 2011). Since the 1950s, average annual Arctic temperatures have risen 2 to 3°C, and this increasing trend is expected to continue (Hinzman et al. 2005). In particular, warming is believed to contribute to the expansion of deciduous shrubs such as *B. nana* and the decline of evergreen shrubs such as *Ledum decumbens* (dwarf Labrador tea) (e.g, (Wahren et al. 2005). In contrast, however, a later observational study indicated that an increase in vegetation productivity was associated with evergreen shrub and bryophyte increases, while deciduous shrub cover did not change (Hudson & Henry 2009).

Experimental and modeling work have revealed that shrub development and establishment is influenced by edaphic characteristics and their interactions with climatic warming. It is critical to note, however, that experimental manipulation of temperature and nutrients often involve inputs many times greater than that which would be available or produced under changing conditions (Bret-Harte et al. 2002). Increased temperatures accelerate cycling of C, N, and decomposition in the soil (Chapin & Shaver 1996;

Hobbie 1996; Bret-Harte et al. 2001; Bret-Harte et al. 2002; Wahren et al. 2005) and this stimulates microbial activity and further shrub development (Jonasson et al. 1999; Gordon et al. 2001; Sturm et al. 2001b; Sturm et al. 2005). Hobbie et al. (2002) argued that, while temperature is important, other factors such as N and phosphorus may play a role in nutrient cycling. They highlighted that the long-term impacts of these inputs are understudied (Hobbie et al. 2002). Likewise, Walker et al. (2003a) argued that soil pH and temperature have greater control on vegetation productivity versus solely air temperature. Chapin et al. (1995) suggested that the Arctic is sensitive to small alterations in these characteristics. Sturm (2005) indicated that taller and denser vegetation facilitated the retention of snowpack. The snow provides an insulative effect on the underlying soil, thereby enhancing decomposition and nutrient cycling during the winter (Liston et al. 2002). As a consequence of summer melting, soil moisture and runoff increased considerably. These mechanisms acting together contribute to accelerated shrub growth via a positive feedback (Sturm et al. 2001a; Sturm et al. 2005). Illeris et al. (2003) found the addition of precipitation improved soil respiration and moisture and enhanced microbial activity. Litter inputs in birch stands were found to accelerate soil N availability (Buckeridge et al. 2010). Sturm et al. (2005) used a computer simulation model for simulating microbial activity along a north-south gradient in the Kuparak Basin of Alaska. Microbial activity was extended by up to two months in areas experiencing accelerated shrub growth (Sturm et al. 2005). Using the Plant-Soil Model to elucidate past, present, and future trends in ecosystem C balance, Stieglitz et al. (2006) determined that while a loss of soil C would occur, there would be

no net loss of ecosystem C. This broadly corroborates findings from similar previous modeling exercises (e.g., McKane et al. 1997; Mack et al. 2004; Rastetter et al. 2005). Epstein et al. (2000) devised the predictive model ArcVeg as a means of simulating nutrient cycling and ecological characteristics over long time intervals. Yu et al. (2009) used the model ArcVeg in the context of the Yamal Arctic Transect to determine that soil nutrient availability was the limiting factor in vegetation development and its response to climate change. Recently, a circumpolar synthesis of plot-level studies have revealed that warming has promoted increases in mean canopy height and shrub height (Elmendorf et al. 2012).

Some recent work has sought to use dendrochronological methods to investigate climatic influences on shrub dynamics. Bär et al. (2007) developed the first ring-chronology for the dwarf shrub *Empetrum nigrum* subsp. *hermaphroditum* in the central Norwegian Scandes Mountains. This study suggested that temperature, and perhaps partly microtopography, control growth rates. Hallinger et al.(2010) investigated dynamics of *Juniperus nana* in Abisko, Sweden. Similar to expansion patterns observed by Tape et al. (2006) in northern Alaska, Hallinger et al. (2010) observed an increase in shrub radial and vertical growth at all elevation levels, recent colonization at higher elevations, and a high correlation between shrub ring widths and summer temperatures that led to accelerated growth in more recent years. *Salix lanata* ring widths spanning 1942 – 2005 from the Nenets Autonomous Okrug in Russia were highly correlated with summer temperatures and NDVI values (Forbes et al. 2010).

In contrast to the grassland types mentioned, recent work has revealed that herbivory reduces shrub development in the Arctic. Activities by large herbivores such as reindeer (feeding, trampling, and feces deposition) enhance nutrient cycling and productivity and reduce shrub cover (van der Wal 2006). As a result, shifts to graminoid vegetation forms can occur (Olofsson et al. 2001; Olofsson et al. 2004; Olofsson et al. 2009). Forbes et al. (2010) also note that shrubs that exceed the browsing height of reindeer (~1.8 m) typically remain unaffected. Building on previous work by rner (2003) and Dullinger et al. (2004), Cairns and colleagues argued that hypotheses regarding climatic influences on treeline dynamics in Fennoscandia failed to consider the influence of herbivory (Cairns & Moen 2004; Cairns et al. 2007; Moen et al. 2008). Pajunen (2009) collected measurements of *Salix glauca* and *Salix lanata* on the Yamal Peninsula and counts of reindeer feces as a proxy for grazing intensity, and discovered that *Salix* growth was positively associated with mean summer temperatures, and negatively associated with reindeer grazing. This suggests that reindeer grazing can partially counteract the effect of increasing temperatures on Arctic shrubs.

2.4 Synthesis of Pattern-Process Relationships in Global Shrub Expansion

Based upon the review of the literature provided in the previous subsection, some important comparisons and contrasts between the Arctic and the desert or mesic grasslands and savannas of the temperate regions of the world may be drawn.

2.4.1 Comparisons and Contrasts of Global Shrub Expansion Patterns

Patterns of shrub expansion manifest themselves in specific positions on topographic, hydrologic, and edaphic gradients, facilitated by their structural characteristics. Generally, as patch size increases, total cover increases, and the complexity of patch characteristics and overall species diversity decreases. Lowland and riparian areas have undergone the greatest transition to shrubs (Tape et al. 2006; Robinson et al. 2008; Burkinshaw & Bork 2009; Lunt et al. 2010). Species implicated in expansion are often found in coarse or wet clayey soils (e.g., Gibbens et al. 2005; Craine et al. 2010; Craine & Nippert 2010). In either case, these soils are nutrient-poor. Coarse, sandy soils facilitate the drainage of moisture into deeper soil horizons. Structural advantages of both deciduous and evergreen shrubs such as deep-rooting allow shrubs to take advantage of these moisture stores that are otherwise inaccessible to shallow-rooted herbaceous or graminoid cover. As a result, both types of shrubs are expanding in grasslands and savannas. By contrast, there is debate regarding the nature of expansion of Arctic deciduous shrubs versus evergreen shrubs (e.g., Wahren et al. 2005; Hudson & Henry 2009).

2.4.2 Comparisons and Contrasts of Global Shrub Expansion Processes

The intensification of livestock grazing has promoted the expansion of woody shrubs in grasslands. This degradation often includes soil compaction, reduction of fine fuels and water infiltration due to the removal of perennial and graminoid species by grazing (e.g., Bahre & Shelton 1993). Livestock also serve as an effective vector for the

dissemination of shrub seeds to new areas (e.g., Archer 1990). Given economic needs such as livestock, reversion back to grassland is unlikely (Brown & Archer 1999).

By contrast, Arctic expansion is driven by an interaction of environmental variables such as temperature, decomposition, and nutrient cycling. While nutrient cycling is the dominant fine-scale driver, broad-scale temperature increases are amplifying its effects due to a positive feedback loop (Sturm et al. 2001b; Sturm et al. 2005). Review of the previously-mentioned studies suggests then that nutrient cycling controls shrub expansion at fine scales. Climatic warming, while having a more indirect effect, drives this feedback (e.g., Sturm et al. (2005). Studies of herbivory suggest that such activities counteract the effect of climatic warming on shrub growth (e.g., Pajunen 2009).

Grasslands, savannas, and the Arctic tundra are foci of scientific inquiry and concern because they form a significant terrestrial component of the biosphere. Because shrub expansion may hold critical future environmental and economic implications, appropriate land management policies must be informed by increasingly extensive and rigorous data sets (e.g., spatially-explicit records of land use, aerial photography) and tools (e.g., GIS and spatially-explicit models).

Space-for-time substitution, experimental manipulations, and observational work are three important methods of analysis in studies of ecological changes such as shrub expansion. The studies in this section employed, or were informed by, at least one of these methods. While their utility will not be debated in detail here, each method is plagued by issues of scale. Space-for-time substitution methods are limited beyond site-

specific studies due to the varying environmental interactions (e.g., climatic changes, alterations in land use) on shrub expansion patterns at broader-scales. Experimental manipulations have provided insights on the interrelationships between shrub, edaphic, and atmospheric characteristics. They suffer from the same problems as space-for-time substitutions, however, in that results are not easily extrapolated to broader scales. The now widespread availability of aerial photography and high-resolution satellite imagery provide scientists with a rich source of historic and present observational data. Unfortunately, significant financial resources and labor are required to acquire, process, and analyze these data over broad scales. In addition, the availability of historic imagery at sufficient spatial and temporal scales can be limited. As a consequence, establishing trends or pulses in shrub expansion or decline with high confidence is difficult. Land use records may supplement this information. The utility of these records can be hampered, however, by limited spatial and temporal coverage, or by problems in accuracy and completeness.

Considering these limitations, spatially-explicit modeling, informed by continued observational and experimental work, is critical for understanding future trends in shrub expansion. Grid-based (e.g., Jeltsch et al. 1997; Rupp et al. 2000) and spatially-explicit (e.g., Alftine & Malanson 2004; Tews et al. 2004) simulation models provide the greatest utility for accurately representing patterns of vegetation and their mechanisms over scales critical for land management interests. Observational data from historical and current sources provide a means for establishing the initial pattern parameters. The simulation of processes driving alterations in patterns can draw from environmental

relationships established by experimental work and associated aspatial models. Manipulation of these parameters results in the generation of future plausible patterns of shrub expansion. These model outputs can then be used to inform land management strategies, or they can provide a basis for further hypothesis generation. This modeling strategy may be particularly applicable to the Arctic, since the patterns and processes of shrub expansion are presumed to be regional in extent.

2.5 Reciprocal Interactions Between Fluvial and Riparian Vegetation Dynamics

Riparian systems in floodplains are highly diverse and complex ecosystems (Tockner & Stanford 2002; DeWine & Cooper 2007). They provide critical habitat corridors for plant and animals (Junk 1999). This complexity and diversity is enhanced by the high level of disturbance due to flooding (Glenz et al. 2006). Fluvial landforms and other similar land surface processes were previously a focus of only geomorphologists. However, reciprocal interactions between fluvial processes and their associated biological communities (predominately woody vegetation, i.e., trees and shrubs) have become increasingly recognized (Naiman et al. 1999; Seyfried & Wilcox 2006; Corenblit et al. 2007). As a result, these areas are now the focus of intensive interdisciplinary research that spans biogeography, geomorphology, geology, pedology, ecology, and limnology.

Riparian vegetation development is heavily influenced by water flow dynamics (Malanson 1993). Characteristics of these dynamics include flooding (Bendix & Hupp 2000; Glenz et al. 2006; Bejarano et al. 2011), channel type (DeWine & Cooper 2007),

channelization (Hupp 1992; Poff et al. 1997), and physical gradients (Friedman et al. 2006) can introduce disturbances that modify the vegetation communities. These disturbances allow for the development of vegetation communities that are "a compromise between the stress caused by the environment, the disturbance level, and the competition among plants: stress and disturbance control the intensity of competition" (Corenblit et al. 2007). Long-term measurements of these characteristics and their dynamics provide a basis for understanding future trends in vegetation and fluvial landform development.

The aim of this subsection is to provide a brief review of recent studies examining: a) geomorphic influences on woody vegetation development in fluvial corridors and surrounding areas, and b) impacts of climate change on rivers and floodplain dynamics. While there is an emphasis on temperate and semi-arid/regions, extended comments on recent studies in the Arctic will also be included because the number of studies or reviews of studies from this region are more rare.

2.5.1 Geomorphic Influences on Woody Vegetation Development

Geomorphic processes in riverine corridors are highly influenced by disturbance. These geomorphic processes in turn, can shape vegetative characteristics. Water flow effects are often attributed as the greatest source of disturbance to local geomorphology. This, in turn, has an effect on the vegetation. Poff (1997) identified five fluvial characteristics that regulate the development of these communities: 1) magnitude, 2) frequency, 3) duration, 4) timing, and 5) rate of change of water events. Poff et al.

(1997) defines magnitude as the amount of water flowing past a fixed location in a given unit of time. Duration refers to the period of time associated with a specific flow condition. The timing of flow is in reference to the regularity of the occurrence of a flow event. Finally, the rate of change refers to how quickly flow changes from one condition to another (Poff et al. 1997). Once it is firmly established in the system, however, vegetation can then act as a reciprocal influence on the geomorphology and its resistance to disturbance (Corenblit et al. 2007).

Lowland and riparian areas have undergone the greatest transition to woody vegetation (Tape et al. 2006; Robinson et al. 2008; Burkinshaw & Bork 2009; Lunt et al. 2010; Naito & Cairns 2011a). In his study of vegetation succession along the Platte River in Nebraska, Johnson (1998) proposed a graphical model to facilitate understanding of the reciprocal interactions between vegetation and the local geomorphology. This graphical model is divided into time periods: 1) pre-regulation, and 2) post-regulation adjustment. The first period is marked by significant geomorphologic shifts. Braided rivers begin to channel-narrow and meandrous rivers cease to meander. Shifts in vegetation composition also occur and are largely influenced by extreme weather events and climatic changes. In addition, pioneer species such as *Salix* and *Populus* expand. The second period marks the end of major geomorphologic shifts, while pioneer woodland species decline and are replaced by later successional species (Johnson 1998).

Flooding events can facilitate the development of sediment deposits. These deposits provide a substrate for primary succession of woody vegetation (Douglas 1989).

However, their survival is not guaranteed because they are susceptible to erosion or channel migration (Konrad et al. 2011). Riparian vegetation can provide stability to the geomorphologic structure of fluvial systems. For example, these plants can reduce pore-water pressure and providing reinforcement via their roots (Abernethy & Rutherfurd 2001). This root reinforcement is usually provided through buttressing and arching. The presence of plants can also enhance evapotranspiration and the reduction of soil moisture (Darby 1999).

Arctic streams play a critical role in Arctic ecosystem due to the otherwise relatively low levels of biodiversity in the region. The transport of freshwater to the ocean also plays a critical role in high-latitude oceanographic properties (e.g., decreasing salinity). Despite this, Arctic hydrology is understudied. Arctic stream dynamics and associated tundra vegetation are unique due to associations with permafrost and extreme seasonality effects. In addition, Arctic streams carry proportionally less sediment than their temperate counterparts due to factors such as few freeze-thaw cycles, frozen ground, snow as the primary form of precipitation, low-severity storms, and low amounts of flood erosion (Mann et al. 2010). Paleoecologic work by Mann et al. (2010) suggested that two mass-wasting events occurred during the Pleistocene-Holocene transition in northern Alaska. Rivers in this region have become increasingly decoupled from valley slope sediment inputs. While deposition and erosion of sediment still occur, the rivers have transported much of the sediment input from those events (Mann et al. 2010). This suggests that overall sediment input has decreased over time, thereby reducing overall sediment loads in the channels. The presence of vegetation can stabilize

otherwise ephemeral features like sediment bars, reducing their susceptibility to erosion (Konrad et al. 2011). This has the effect of restricting channel migration.

Topography is the primary control on hydrologic characteristics in non-floodplain areas in the Arctic (Sorensen et al. 2006). However, this relationship has been poorly studied until recently due to difficulty in accessing study sites and a relative lack of historic and current spatial data. Tape et al. (Tape et al. 2006) noted that most of the increases in woody vegetation cover in the Arctic occurred in the floodplains, but potential causes of this were not discussed in great detail.

2.5.2 Effects of Fluvial Dynamics on Seed Dispersal and Recruitment

Examination of the fluvial effects of seed dispersal has also received recent attention. Many of these studies took place in temperate regions, while the literature of seed dispersal dynamics in arid regions is much sparser. In their examination of seed dispersal and spatial variability in recruitment of *P. nigra* on the Garonne River, Guilloy-Froget et al. (2002) concluded that while overall seed survivorship was low, there was significant variability between trees and over time. Consistently wet conditions favored germination and seedling survival, while transitions to submerged or dry conditions reduced the likelihood of recruitment and survival (Guilloy-Froget et al. 2002). Barsoum (2001) investigated the abundance of sexual and asexual recruits of *P. nigra and S. alba* along the Drome River in southeastern France. Barsoum (2001) noted that periodic flooding provided a means for vegetation regeneration. While recruitment from sexual reproduction was initially dominant, flooding restricted widespread survival

of these recruits. As a consequence, asexually reproduced individuals had a greater overall survivorship. Johnson (2000) studied recruitment of *Populus* and *Salix* seeds over a 14 year period in a riparian corridor in Nebraska. He noted that seed and seedling mortality was exceedingly high due to summer stream flow pulses that eroded or buried germinants, and moving ice in winter restructured the river bed to preclude seedling recruitment (Johnson 2000).

2.5.3 Climate Change Effects on Reciprocal Interactions

Rangelands that are inhabited by large numbers of herbivorous animals (e.g., megafauna such as elephants, or domestic cattle) are likely to become increasingly arid as climate change progress. This effect is exacerbated by overgrazing, and riparian vegetation is highly susceptible to this (Poff et al. 2011). Hoffman and Rohde (2011) noted that a combination of increased grazing and aridity is leading to a sharp reduction in riparian vegetation in South Africa. Neary and Medina (1996) note that grazing also contributes to trampling of riparian vegetation and soil, reducing the overall bank stability and increasing its susceptibility to erosion.

Climatic changes can often be reflected in stream dynamics and productivity. Stromberg et al. (2010a) noted that increased flow intermittency of the San Pedro River in Arizona would lead to a shift from hydric riparian species (e.g., *Populus*, *Salix*) to more mesic species (*Tamarix*) (Stromberg et al. 2010a; Stromberg et al. 2010b). Increased flooding, on the other hand, would increase the prevalence of xeric shrub species and replace perennial individuals with annuals that have reduced ability to

stabilize sediment cover (Stromberg et al. 2010a). Climate changes can also cause direct and even competing effects on stream ecosystems. Mulholland et al. (2009) found that an unusual spring freeze in the southeastern United States led to defoliation and increased levels of light reaching the stream. This led to increases in gross primary productivity (GPP) largely from algae, as well as lower levels of nitrate and higher populations of herbivorous snails. This introduces a competing effect however, since climate change will both: a) extend the time period available for foliar development (and therefore a reduction in stream GPP), and b) increase the likelihood of extreme weather events such as the freeze (leading to increased light reaching the stream, and increasing GPP) (Mulholland et al. 2009). Poff et al. (2011) observed that drought-induced stress reduces the ability of moisture- demanding species (e.g., *Populus*) to photosynthesize and uptake moisture. Exotic species are also overtaking native species in these increasingly arid riparian corridors (e.g. *Tamarix* spp., *Elaeagnus angustifolia*). These species are likely to be better adapted to the drier conditions in comparison to their native counterparts and therefore can outcompete them (Poff et al. 2011).

The effects of climatic warming are most pronounced in the Arctic, with many of the terrestrial changes (e.g., woody shrub expansion, permafrost thawing) attributable to this phenomenon (Overpeck et al. 1997, Walker 2000, Walker et al. 2006). However, the processes driving shrub expansion in floodplains or other similar riparian areas are poorly understood due to a lack of research in Arctic hydrology and riparian ecosystems (Woo et al. 2008, Mann et al. 2010). Hinzman et al. (2005) provides a useful overview of the effect of climate change on Arctic Rivers. The lack of data and gauge monitoring

of Arctic rivers is a primary limitation of scientific ability to extract trends in river and discharge characteristics. Discharge levels of rivers with glacial sources are increasing due to accelerated glacial melt. The continued melting of permafrost beneath these rivers will likely lead to increased infiltration and decreased surface runoff (Hinzman et al. 2005). Strom et al. (2011) anticipates that increased Arctic warming will lead to a narrowing of riparian corridors in northern Sweden . Specifically, upstream riparian communities will be replaced by terrestrial communities due to reduced flooding events. Downstream riparian communities will be replaced by more aquatic communities due to higher fall and winter flooding (Strom et al. 2011). It would be expected that a warming climate would likely cause a uniform expansion of shrubs. However, Tape et al.'s (2006) study demonstrates that this is not the case. In a later study, Tape et al. (Tape et al. 2012) suggested that expanding shrub patches occurred in areas of tundra that were well-drained and resource-rich, while static shrub patches tended to be associated with resource-poor and stagnant areas.

A number of competing interactions contribute to fluvial response by herbivory in Arctic riparian zones. Modeling by Butler et al. (2007) suggested that herbivory typicallly reduced early successional vegetation (e.g. *Salix* spp.) and increased levels of later successional vegetation (e.g., *Alnus* spp.). Erosion and accretion exhibited the opposite effect. When considering the interaction of these efffects, Butler et al. (2007) noted that high erosion and low herbivory led to increased levels of Salix, while high erosion and high herbivory led to increased levels of *Alnus* spp. This latter effect was

also apparent under conditions of intermediate erosion/accretion and low herbivory levels (Butler et al. 2007).

2.6 Shrub Expansion Effects on Permafrost

Permafrost is defined as soil at a temperature at or below 0°C for 2 or more years. It commonly occurs throughout the Arctic tundra and the boreal regions to the south. It is estimated that 18-22% of exposed ground in these regions are underlain by permafrost (Zhang et al. 1997). Two recognized zones of permafrost occur in Alaska. These include the zones of continuous permafrost and discontinuous permafrost. The BRNS generally falls in the zone of continuous permafrost.

Over the last century, temperatures in the Arctic have increased 2-4° C (Lachenbruch & Marshall 1986; Anisimov & Nelson 1996; Anisimov et al. 1997; Osterkamp & Romanovsky 1999; Serreze et al. 2000). The consequences of this warming include the deepening of the ALT, the reduction in the thickness and extent of permafrost (Anisimov et al. 1997; Hinzman et al. 2005; Lawrence & Slater 2005), the facilitation of water percolation and subsequent drying of the tundra (Lloyd et al. 2002), and the release of massive quantities of C and methane to the atmosphere (Walker et al. 2003b; Dutta et al. 2006; Schuur et al. 2008).

Large amounts of C are stored in the soil organic matter of the Arctic (Mack et al. 2004; Zimov et al. 2006). Gorham (1991) estimated that 455 Pg C are stored in the top 1 m of the soil profile in the Arctic. Because of the low temperatures and waterlogged conditions, decomposition rates are slow. As a result, organic matter can

readily accumulate (Dutta et al. 2006). A major scientific concern is that, as conditions continue to warm, C flux to the atmosphere will increase. This will act as a positive feedback effects to climate warming (Chapin et al. 2005).

Studies conducted over the last two decades have offered contrasting views of the effects of permafrost degradation on vegetation development. Earlier studies suggested that the degradation of permafrost generally promotes vegetation development on the tundra (e.g. Lloyd et al. 2003). Warmer ALT can promote increased N mineralization from decomposition (e.g., Waelbroeck, 1997; Jorgenson et al. 2001). Permafrost degradation can also promote improved water filtration (Woo et al. 1992) Recently, however, fine-scale studies involving either transects or plots suggest that summer shading from tall shrubs could offset permafrost losses. Blok et al. (2010) found that ALT under shrub canopy was shallower than under open tundra. Tall shrub canopy also facilitates snow trapping in winter (e.g., Sturm et al. 2001b), and snow reduces the transfer of heat energy from near-surface air to areas below ground (Stieglitz et al. 2003). In addition, tall shrubs facilitate shading of the soil in summer, effectively reducing heat flux and the potential thaw depth (Walker et al. 2003a). However, studies incorporating broad-scale climate models suggest that land-atmosphere feedbacks resulting from shrub expansion will amplify climate warming through the reduction in permafrost (Lawrence & Swenson 2011).

2.7 Ecological Phase Transition Theory

Loehle et al. (1996) proposed ecological phase transition theory to explain ecotone dynamics in response to environmental change. A vegetation phase refers to the state of a dominant life-form (e.g., trees, shrubs, grasslands) that is different from other states in the ecosystem (Li 2002). Uzunov (1993) defines a phase transition as "a qualitative change in the state of a system under a continuous infinitesimal change in external parameters." Therefore, shifts between vegetation phases are roughly analogous to the changes that occur between different phases of matter (Milne et al. 1996; Li 2002). In a biological system, a phase is susceptible to transition if biological or environmental variability exceeds its range of self-regulation (Gillson & Ekblom 2009). Combinations of extreme events and/or biotic and abiotic factors may cause a reorganization of ecosystem structure and function, initiating a phase transition. In such a transition, interactions are reorganized, and a new phase can emerge (Gillson & Ekblom 2009). In the context of tundra ecosystems, climatic warming is a primary external forcing that could override finer-scale processes (Chapin et al. 2005; McGuire et al. 2006; Lawrence & Swenson 2011), thereby resulting in a phase transition.

Ecological phase transition theory is based on percolation processes in thermodynamic models and employs fractal analysis to characterize ecosystem heterogeneity and ecotonal dynamics (Milne et al. 1996; Li 2002; Alados et al. 2005), making it well-suited to studying plant invasion. Critical values derived from percolation theory can be used to evaluate the potential for ecotone migration (Loehle et al. 1996). These critical points are universal and are insensitive to fine-scale spatial configurations

of the focal vegetation. As a result, they can be applied to a variety of ecotones. Phase transitions have been observed in a number of ecosystems, including the North American savannas, Mediterranean scrubland, boreal forests, and alpine treeline (e.g., (Rocchini et al. 2006; Zeng & Malanson 2006; Danby & Hik 2007; Alados et al. 2009; Gillson & Ekblom 2009; Scheffer et al. 2012). Phase transition theory has not yet been applied to Arctic ecosystems.

An ecotone is a transitional area between individual phases (Loehle & Li 1996; Milne et al. 1996). Ecotones are typically situated on environmental gradients that can affect key ecological processes or organism distribution or on more gradual gradients where thresholds or nonlinear responses to these gradients can lead to significant changes in ecosystem dynamics and dominant species distribution. If environmental conditions change such that it is beneficial for one of the phases, the patch size of the focal phase will increase in the ecotone system (Risser 1995). This will lead to the invasion of previously unsuitable habitats. Since ecotones already occur at the physiological limits of species in the adjacent communities, an external forcing like climate change could promote the invasion of one species by another (Risser 1995).

Loehle et al. (1996) used the multi-scale information fractal dimension (d_I) to characterize spatial patterns of forest spread into prairie in eastern Kansas. The d_I is a measure of deviation from spatial homogeneity used to detect phase transitions at multiple spatial scales. The median d_I describes the state of the entire landscape, and the d_I profiles provide an interpretation of landscape heterogeneity as scale changes. The d_I values range between 0 and 2, where $d_I < 1$ indicates a fragmented landscape, $1 < d_I < 2$

indicates a heterogeneous landscape, and $d_I = 2$ indicates a homogenous landscape (Loehle & Li 1996). Loehle et al. (1996) propose that an ecotone is present on a landscape for critical values $1.56 \leq d_I \leq 1.8958$; at $1.7951 \leq d_I \leq 1.8285$, the invading phase can spread to the entire landscape and initiate a phase transition. These critical values used in interpreting landscapes are based on percolation theory and can be related to percent cover using linear regression to derive critical forest percent cover values needed to initiate a phase transition (Loehle et al. 1996). In the Kansas case, forest cover could spread to the entire landscape after reaching a critical value of 18.5%. Since their data indicated that forest cover was approaching 20%, Loehle et al. (1996) argued that their landscape was undergoing a phase transition.

2.8 Clonal and Sexual Reproductive Characteristics

Abiotic stressors such as low average annual temperatures, low levels of insolation, and limitations on soil moisture and nutrient availability can limit the development of Arctic shrubs. Most shrub species therefore grow slowly and must make use of a short growing season. Because energy and nutrient demands required of sexual reproduction are prohibitive given these constraints, it is believed that most shrub species exhibit clonal, or vegetative, reproduction. Clonal species tend to be long-lived (de Witte & Stocklin 2010; Myers-Smith et al. 2011a) and can develop ramets of the same genotype. This is advantageous because each ramet is capable of independent growth and reproduction (Chen et al. 2006). Physical, underground connections between individual ramets provides for resource sharing, particularly in heterogeneous, nutrient-

limited environments such as the Arctic tundra. This also allows deteriorating ramets to be replaced by new ones, giving the impression that clonal patches are "immortal" (de Witte & Stocklin 2010). Once established, these clonal shrub patches could theoretically continue to expand. Greater below-ground biomass also likely improves survival during variable weather conditions (Shevtsova et al. 1995). There is also evidence that clonal patches may facilitate new recruits by behaving as "nurse plants" (Carlsson & Callaghan 1991).

Sexual recruitment is possible in the Arctic, although it is thought to be rare (Bell & Bliss 1980) and stochastic (Alsos et al. 2007). Focal species for these studies, however, have largely been prostrate- or mat-forming shrubs such as *Cassiope Empetrum*, *Dryas*, *Salix*¸ and *Saxifraga* spp. Biotic interactions and the absence of bare ground created by disturbance can restrict seedling recruitment (Cooper et al. 2004; Gough 2006). Herbivory can also reduce seed bank density (Pajunen 2009; Gonzalez et al. 2010). However, due to rapid warming in the Arctic, the growing season will increase in duration. As a consequence, shrubs may shift their reproductive strategies from vegetative means to sexual means (Douhovnikoff et al. 2010). Other studies have suggested that sexual reproduction is already common in several High Arctic species. For example, *Salix arctica* (Steltzer et al. 2008) and *Saxifraga cernua* (Kjolner et al. 2006) exhibited high genetic diversity thought to be made possible through frequent sexual reproduction. Sexual reproduction potential (Klady et al. 2011) and germination potential (Graae et al. 2008; Walck et al. 2011) was also found to be enhanced with climate change. Because sexual reproduction produces offspring with higher genetic

variability, it is believed that their chances for survival in changing environmental conditions will improve considerably (Klady et al. 2011). If sexual reproduction became dominant throughout the terrestrial Arctic, the landscape would look very different from its present state. Increased sexual reproduction and germination potential, combined with findings that river corridors are in or have completed a phase transition from tundra to shrubland (see Section 7.1.2) would have significant consequences for surface energy balances, permafrost degradation, and nutrient availability.

In the case of the Low Arctic in northern Alaska, it is currently unknown in what combination these reproductive strategies have been present at landscape scales. The slow growth of shrub species and the requirements for long-term field monitoring, seed censuses, and genetic analyses limit the feasibility of such investigations of multiple sites at landscape scales.

2.9 Concluding Remarks

In the preceding subsections, I highlighted the important processes driving Arctic shrub expansion. However, most of these studies have been conducted at either fine- or circumpolar/regional spatial scales. As I discussed above, differences in potential consequences to ecosystem functioning as a result of continued shrub expansion are partly the result of the spatial scale of study. It is less understood how these patterns and processes of shrub expansion link at landscape scales. In this work, I sought to improve the scientific understanding of this pattern-process linkage at the landscape scale.

3. STUDY AREA*

The BRNS occupies approximately 220,000 km^2 in northern Alaska. The basin is bound by the Arctic coastal plain in the north, the Brooks Range in the south, the Noatak and Kokolik Rivers in the west, and the Jago River in the east. River valleys separated by higher elevation interfluves are key characteristics of this landscape. The BRNS lies largely within the Low Arctic, a vegetation zone dominated by tall and dwarf shrubs (Walker et al. 2005). This zone is commonly referred to as Arctic Bioclimate Subzone E (Walker *et al.*, 2005). Dominant species include *Alnus* spp., *Betula glandulosa, B. nana,* and *Salix* spp. (Viereck *et al*. 1995; Walker et al. 2000; Walker *et al*., 2005; Tape *et al*., 2006; USDA 2011). This region generally overlays an area of continuous permafrost cover. The ALT is usually deeper beneath rivers.

I named sites in river valleys in this study in accordance with their associated river. To meet Objective 1, I examined shrub pattern dynamics at nine sites, which included Ayiyak, Canning, Chandler, Colville, Killik, Kurupa, Nanushuk 1, Nanushuk 2, and Nimiuktuk. To meet Objective 2, I examined the shrub pattern dynamics and their association with hydrologic characteristics at Colville, Killik, Nanushuk 1, Nanushuk 2, and Nimiuktuk. To meet Objective 3, I applied the simulation model to subsets of the landscapes at Ayiyak and Colville (Fig 3).

---

* Part of this section is reprinted with permission from "Relationships between Arctic shrub dynamics and topographically-derived hydrologic characteristics" by Naito, A.T. & Cairns, D.M. 2011. *Environmental Research Letters*, 6(4) : 045506, Copyright [2011] by Institute of Physics. The online abstract is available at: http://iopscience.iop.org/1748-9326/6/4/045506/fulltext/. The Institute of Physics Copyright Policy is available at: http://www.iop.org/copyright/.

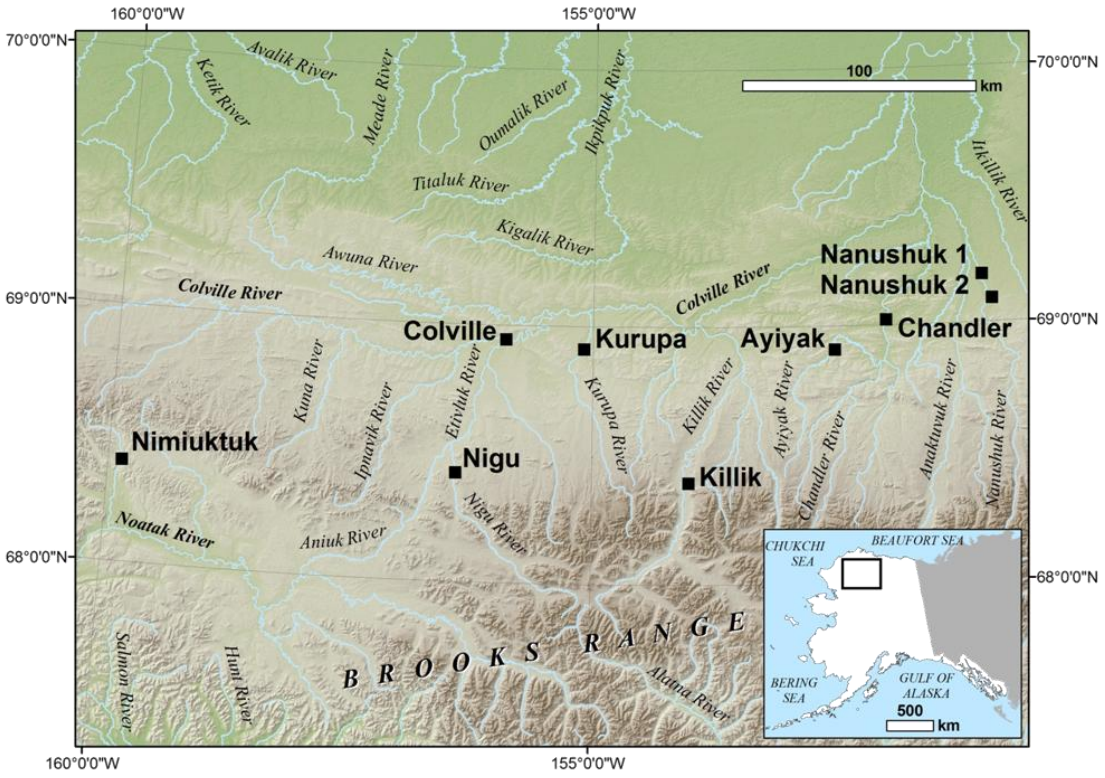

Figure 3: Location of the nine study sites within river corridors examined in this work. Site names are associated with the river in the corridor.

4. METHODS*

4.1 Aerial Photograph Acquisition and Processing

I acquired digital scans (14 micron scanning resolution) of 9" x 9" historic vertical aerial photographs (true color, color infrared, and panchromatic) for the nine sites from the United States Geological Survey Earth Resources Observation and Science (USGS EROS). These images were photographed in the mid-1950s, 1970s, and 1980s (Table 1, Fig. 4). These are the best data publicly available over the period of known changes in shrub cover that are relatively cloud-free and provide sufficient resolution to delineate tall shrubs. QuickBird/Worldview (QB-02) (0.5 m resolution), GeoEye-1, and IKONOS 2 (0.5-0.8 m resolution) (GE-1 and IK-2) imagery for each site was also acquired from archives at DigitalGlobe, Inc and the GeoEye Foundation. The QB-02 imagery is a pan-sharpened multispectral product. In the case of the GE-1 and IK-2 products, the panchromatic and multispectral bands were acquired separately. I pan-sharpened the multispectral bands for GE-1 and IK-2 in ENVI 4.7 (Exelis Information Solutions 2009) using the Gram-Schmidt transformation. These high resolution images are preferred because they facilitate visual interpretation of landscape characteristics and can serve as a source for spatially referencing other imagery (Lantz et al. 2010). Ancillary information from ground control point networks and high-resolution

* Part of this section is reprinted with permission from "Relationships between Arctic shrub dynamics and topographically-derived hydrologic characteristics" by Naito, A.T. & Cairns, D.M. 2011. *Environmental Research Letters*, 6(4) : 045506, Copyright [2011] by Institute of Physics. The online abstract is available at: http://iopscience.iop.org/1748-9326/6/4/045506/fulltext/. The Institute of Physics Copyright Policy is available at: http://www.iop.org/copyright/.

elevation data sets are not available in northern Alaska.

I processed and co-registered the USGS EROS photographs from the 1950s, 1970s, and 1980s to the QB-02/GE-1/IK-2 imagery using 80-100 ground control points and the Delaunay triangulation transformation (Fig. 5. Fig. 6A). I then resampled all imagery to a common pixel resolution of 1 m.

4.2 Imagery Classification

I identified and delineated tall shrub patches on both sets of imagery using a semi-automated classification approach. First, I applied the ISODATA unsupervised classification algorithm using a maximum setting of 20 classes and 20 iterations in ENVI 4.7 to each image (Fig. 6B). I then isolated spectral classes most closely resembling shrubs and converted them to polygons while maintaining the original raster boundaries at a resolution of 1 m (Fig. 6C). I did not distinguish between different shrub genera because of similarities in their spectral characteristics (e.g., Robinson et al. 2008). The process of converting the shrub spectral classes to polygons was used only to aid in the correction process, and polygons were not simplified in order to preserve the original raster boundaries. I corrected errors in classification manually using visual interpretation by overlaying the polygons on the images within a Geographic Information System developed using ArcGIS 10.1 (ESRI 2012) and checked for correspondence. This was particularly important because the ISODATA procedure usually identified dark shrubs and water bodies as the same spectral class. Individual polygons representing shadows and water could then be removed. Finally, I classified shrub polygons in each map as

present (1, green) or absent (0, transparent) (Fig. 6D). I repeated this procedure for the next available image at each site (Fig. 7). This process resulted in the creation of 26 maps representing changes in shrub (Figs. 8-10).

In situ field observations to validate the classification of the satellite imagery were not possible. However, I used the repeat oblique aerial photographs from Tape et al.'s (2006) study as a substitute for ground validation for the earliest and most recent imagery. In this situation, oblique aerial photographs provided the best source for ground information as shrub patches depicted in these photographs are clearly distinguishable from the underlying tundra matrix.

Table 1: Description and source of the images used for the Ayiyak, Chandler, Colville, Killik, Kurupa, Nanushuk 1, Nanushuk 2, and Nimiuktuk study sites. [a]USGS Earth Explorer archive image, [b]GeoEye-1 image, [c]WorldView 01 image, [d]QuickBird 02 image, [e]IKONOS-2 image. [1]Colour infrared image, [2]Panchromatic image, [3]Panchromatic multispectral image.

Site specifications				Image specification		
Site	**Location**	**Dim. (m)**	**Area (ha)**	**Source**	**Type**	**Acq. date**
Ayiyak	68º 54' N 152º 27' W	1534 x 2048	314	USGS[a] USGS GE[b]	CIR[1] CIR Pan[2]	13 Jul, 1979 2 Aug, 1985 2 Jul, 2010
Chandler	69º 0' N 151º 56' W	2500 x 2560	640	USGS USGS WV[c]	CIR CIR Pan	28 Jun, 1978 19 Aug, 1985 7 Jul, 2010
Colville	68º 57' N 155º 57' W	2048 x 4068	944	USGS USGS QB[d]	Pan CIR Pan MS	19 Jul, 1977 19 Aug, 1985 17 Aug, 2008
Killik	68º 22' N 154º 0' W	7168 x 2048	1468	USGS USGS IK2[e]	CIR CIR Pan MS	1 Jun, 1978 1 Aug, 1982 20 May, 2009
Kurupa	68º 55' N 155º 4' W	3000 x 5100	1530	USGS USGS USGS	CIR CIR CIR	26 Jul, 1977 2 Aug, 1985 6 Jul, 2007
Nanushuk 1	69º 9' N 150º 52' W	1024 x 1536	157	USGS USGS GE	Pan CIR Pan MS	1 Jun, 1955 28 Jun, 1978 14 Aug, 2010
Nanushuk 2	69º 7' N 150º 51' W	1997 x 1536	306	USGS USGS GE	Pan CIR Pan MS	1 Jun, 1955 28 Jun, 1978 14 Aug, 2010
Nigu	68º 25' N 156º 25' W	3072 x 2048	629	USGS USGS QB	CIR CIR Pan	19 Jul, 1977 19 Aug, 1985 5 Sep, 2008
Nimiuktuk	68º 23' N 159º 51' W	2560 x 2560	655	USGS GE	Pan Pan	19 Jul, 1977 27 Jun, 2010

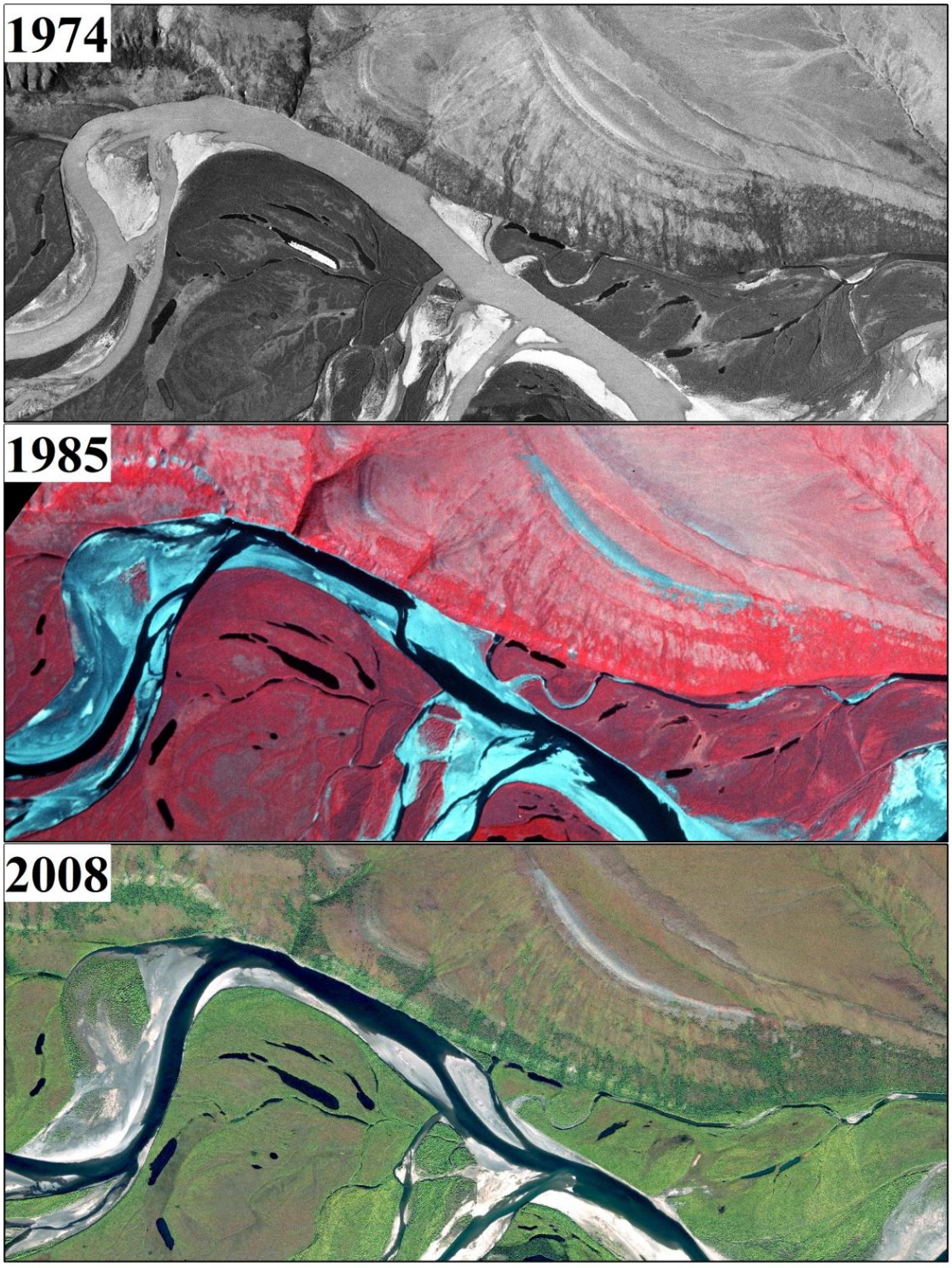

Figure 4: 1974 panchromatic vertical aerial photograph, 1985 color-infrared vertical aerial photograph, and 2008 QuickBird satellite image of the Colville River site.

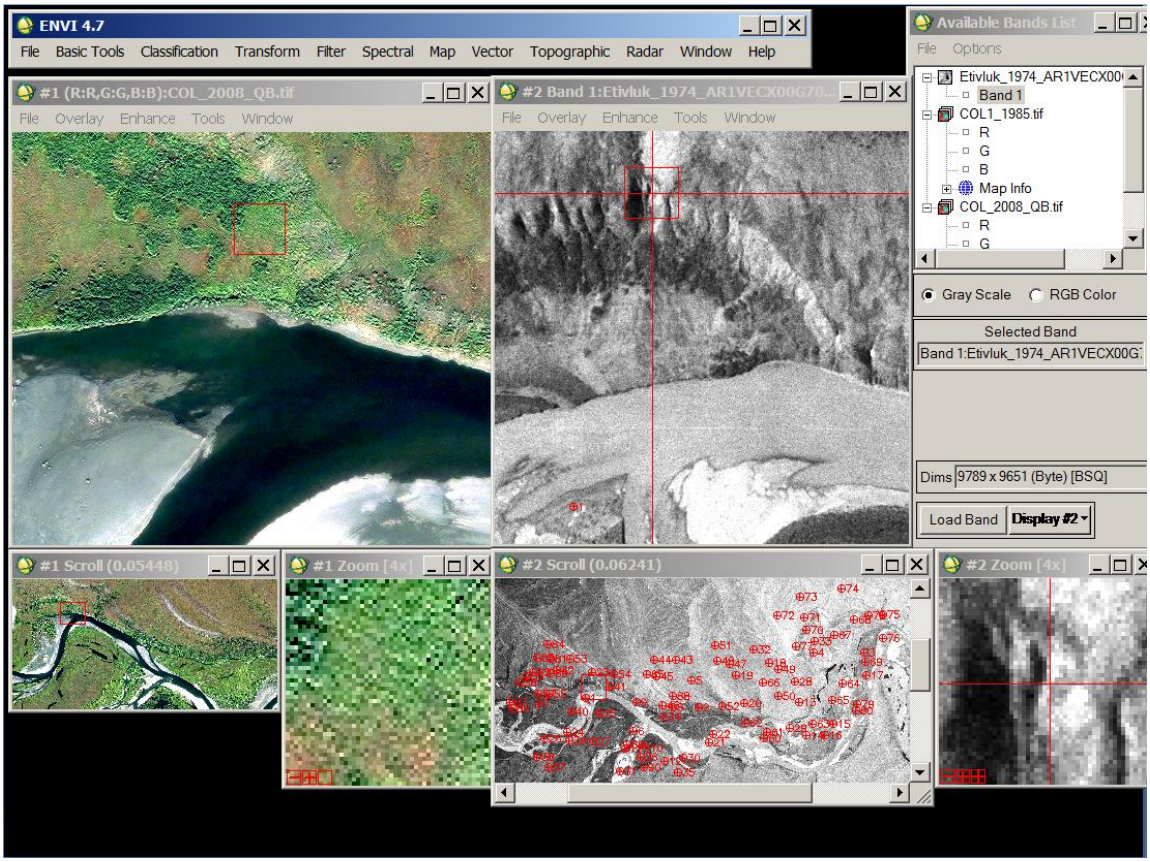

Figure 5: Co-registering the 1974 panchromatic aerial photograph of the Colville site (right) to the 2008 satellite image of the site using ENVI 4.7.

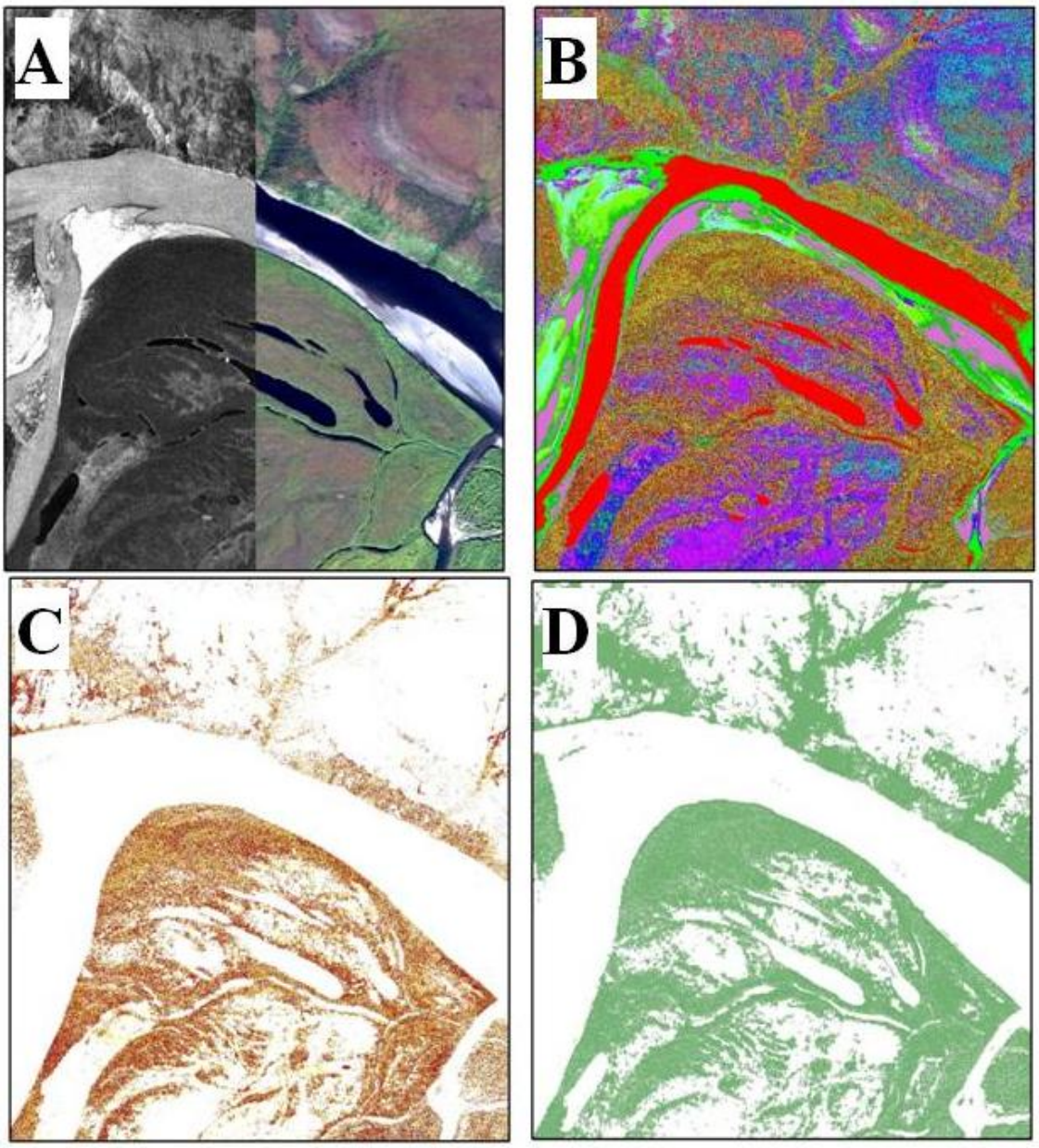

Figure 6: Procedure for processing and classifying digital images. (A) Panchromatic aerial photograph of Colville River from 1974 georectified to pan-sharpened color QuickBird image from 2008. (B) Spectral classes on 2008 image identified by ISODATA classification algorithm. (C) Isolated spectral classes from (b) most closely representing shrubs. (D) Corrected polygons from (C) converted to presence (green) and absence (white).

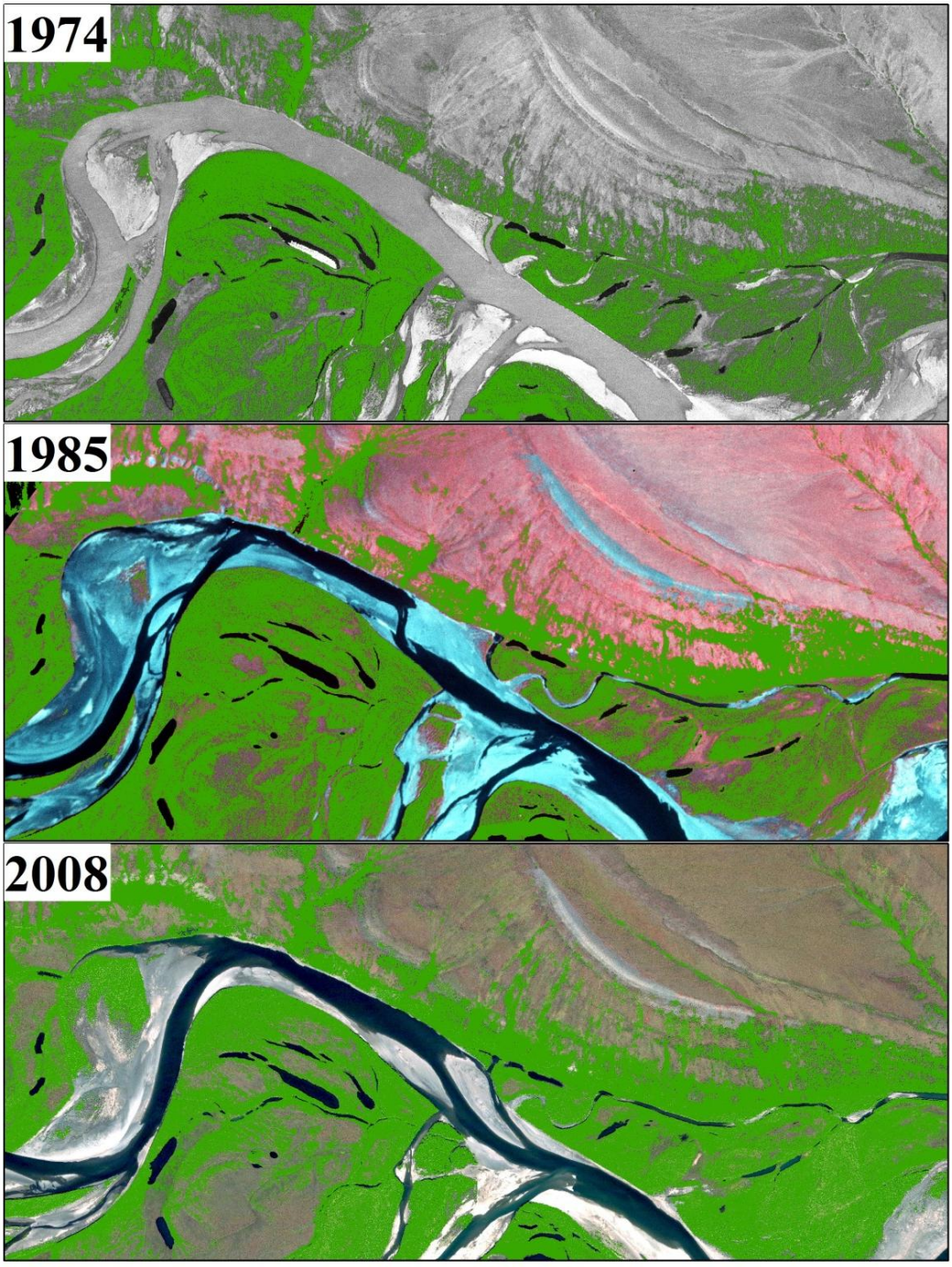

Figure 7: Maps of changes in shrub cover (in green) at the Colville site from 1974 to 2008. While the patterns of development are much more dynamic in the floodplains due to flooding and minor changes in the river course, there are net increases in the floodplains and on the valley slope (near the top of each image).

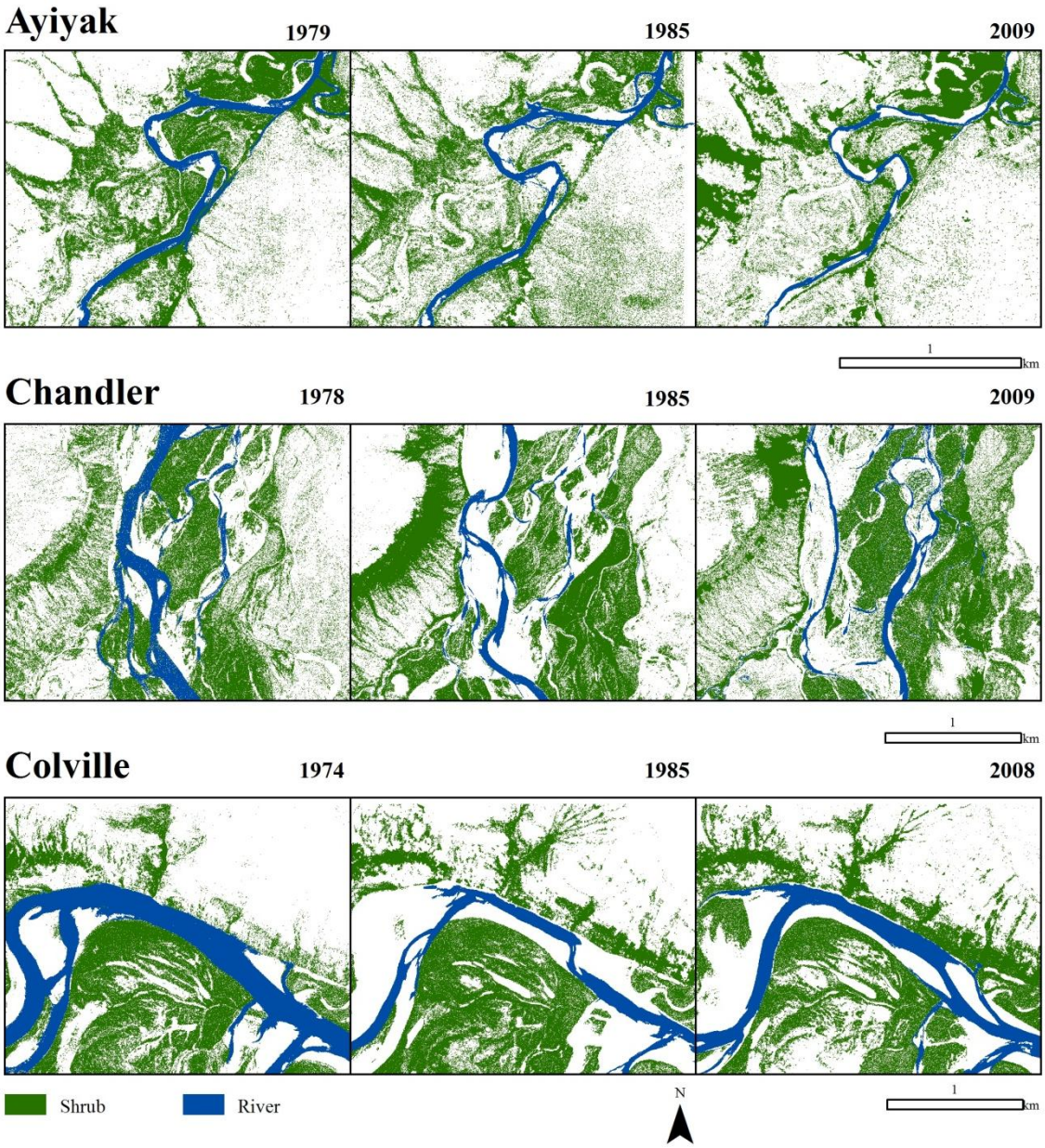

Figure 8: Maps of shrub cover changes at the Ayiyak, Chandler, and Colville sites. For clarity, only a portion of each site is depicted in each frame.

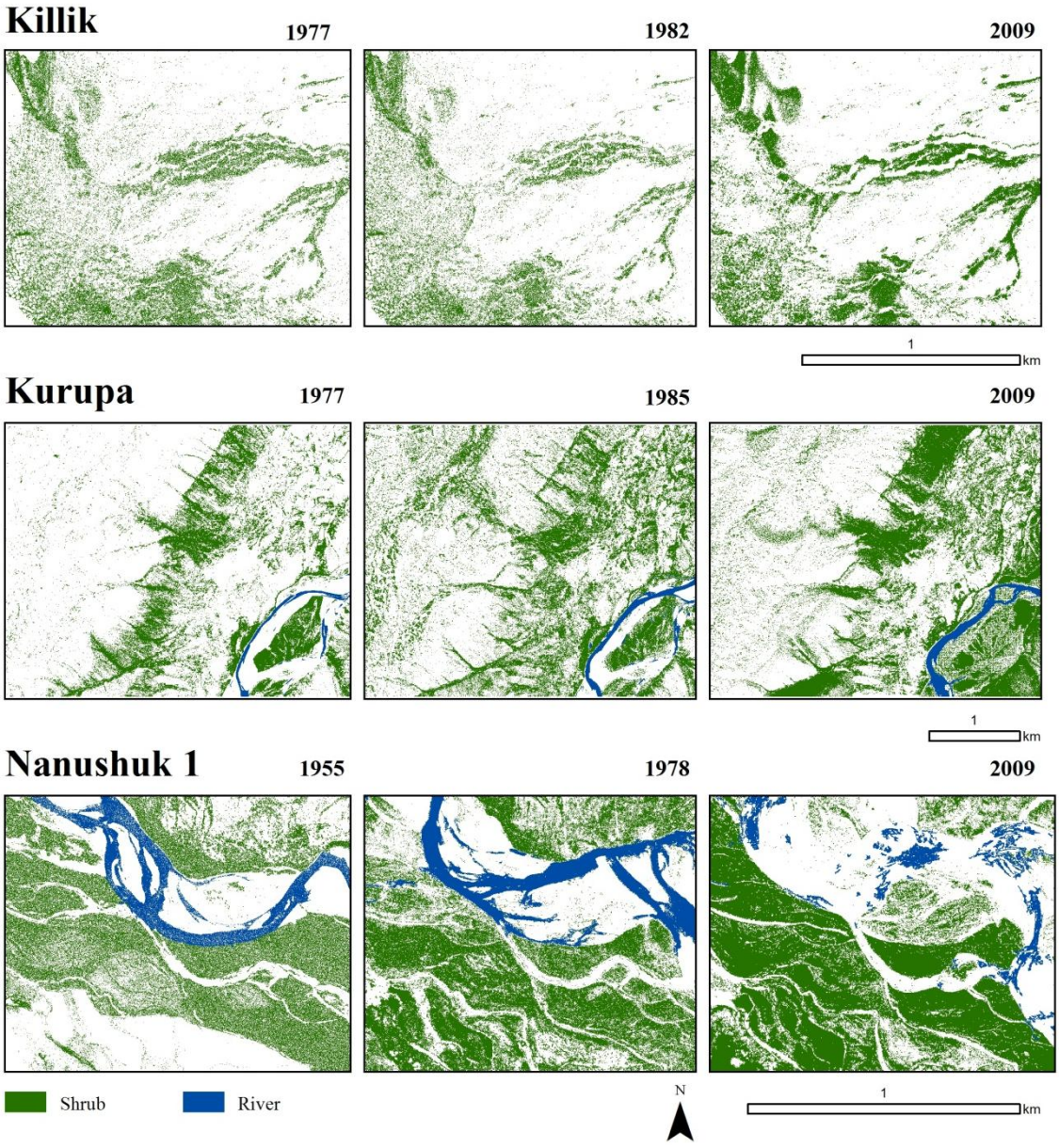

Figure 9: Maps of shrub cover changes at the Killik, Kurupa, and Nanushuk 1 sites. For clarity, only a portion of each site is depicted in each frame.

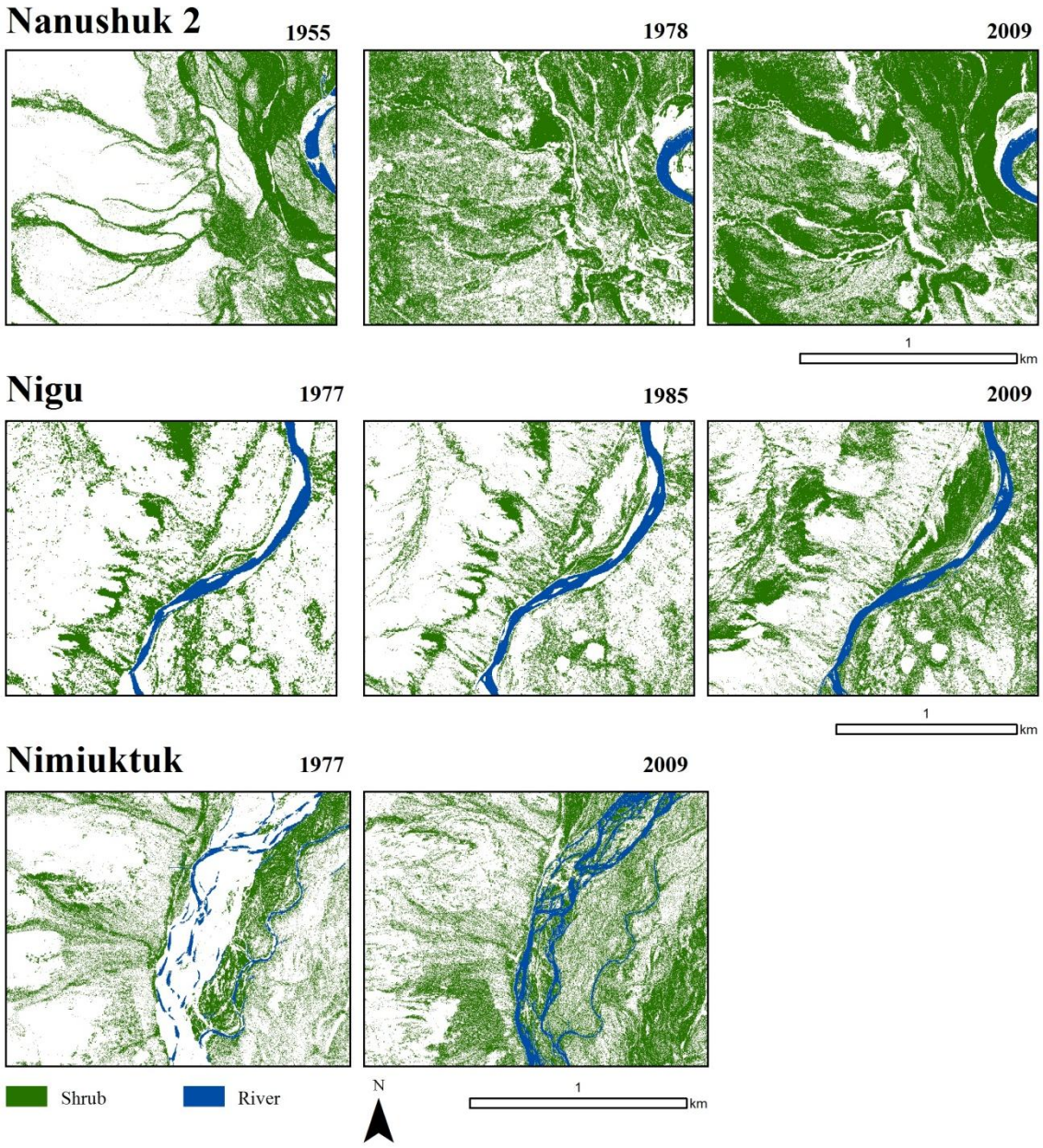

Figure 10: Maps of shrub cover changes at the Nanushuk 2, Nigu, and Nimiuktuk sites. For clarity, only a portion of each site is depicted in each frame.

4.3 Data Preparation for Pattern Metric Analysis and Determination of the Existence of a Phase Transition

4.3.1 Conceptual Landscape Models and Pertinent Pattern Metrics

I conceptualized two possible cases of landscape configurations undergoing phase transition in a 512 m x 512 m quadrat (Fig. 11). These conceptual landscapes help illustrate changes in d_I and pattern metrics over time and provides a basis for comparison with the observed landscapes.

Four pattern metrics provide a means for assessing the presence and trends of the types of shrub expansion at landscape scales. These include PCTCOV (percent area covered by shrubs), PADENS (shrub patch density per ha), CVSIZE (coefficient of variation of patch size expressed as a percent), and MEDIST (mean Euclidean nearest neighbor distance between patches). CVSIZE is an indicator of variability about the mean patch size and facilitates greater comparability of patch size between landscapes of different sizes over mean patch size alone (McGarigal & Marks, 1995). FRAGSTATS (McGarigal et al., 2012) is a software package that enables rapid quantification of spatial patterns and can easily calculate those four metrics.

Based upon the conceptual landscapes and previously published descriptions of shrub expansion patterns (Tape et al., 2006; Myers-Smith et al., 2011), I expected that an increase in PCTCOV, a variety of PADENS responses, a continual decrease in MEDIST, and an inflection of the trend in CVSIZE sometime during or after a local-scale phase transition would be observed. I assumed that variability would be detected at different scales, owing to environmental heterogeneity with respect to topography, soil conditions,

and hydrologic factors.

4.3.2 Calculation of the d_I

I calculated the median d_I and d_I profiles for Ayiyak, Canning, Chandler, Colville, Killik, Kurupa, Nanushuk 1, Nanushuk 2, and Nimiuktuk by generating grids containing equal-sized square cells using Geospatial Modelling Environment 0.7.2.1 (Beyer, 2012) and overlaying them on each landscape. Each grid consists of successively larger cell sizes, and sizes are based on a geometric sequence (e.g., 1, 2, 4, 8, …) (Fig. 12). Each pixel in the landscape is assigned a 0 or 1 for absence or presence of the invading shrub phase. These values are divided by the total number of shrub pixels in the entire landscape, resulting in a probability value of occupation. These probabilities are then summed for each overlying cell in an individual grid. Cells with a higher number of shrub pixels and/or have larger dimensions will therefore have a higher probability of occupation. This calculation is repeated for each grid. The d_I is then calculated by using Equation 1:

$$d_I(\varepsilon) = \frac{\sum_{i=1}^{K(\varepsilon)} P_i(\varepsilon) \log P_i(\varepsilon) - \sum_{i=1}^{K(\gamma)} P_j(\gamma) \log P_j(\gamma)}{\log\left(\frac{1}{\varepsilon}\right) - \log\left(\frac{1}{\gamma}\right)} \quad (1)$$

where P represents the probability of occupation, (ε) i s the number of cells of width ε, and $K(\Upsilon)$ is the number of cells of the next larger cell size to ε in the geometric sequence.

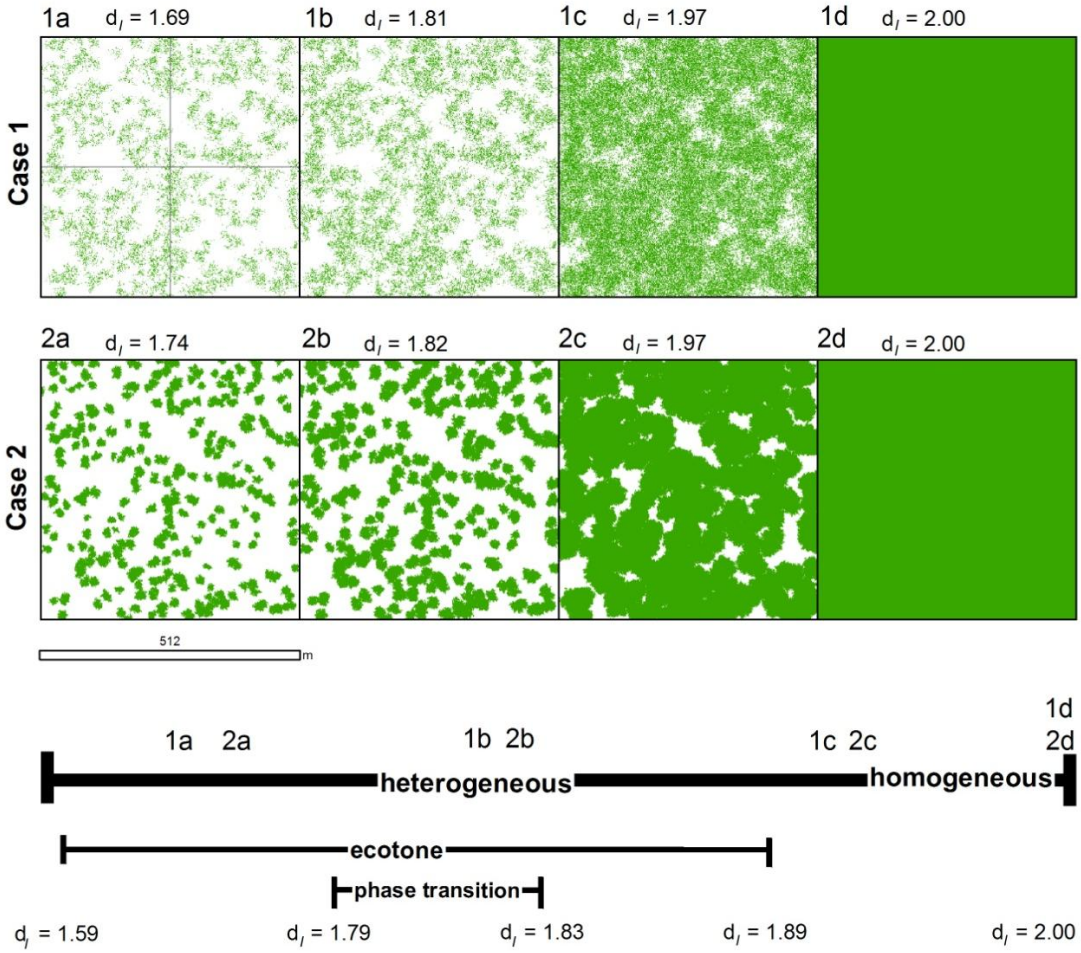

Figure 11: Conceptual maps of shrub patch dynamics at two landscapes (Case 1 and Case 2) categorized as ecotones with different configurations of the invading phase (green pixels). As time increases from Step a to Step d, the median information fractal dimension (d_I) increases to a value of 2.00. 1a and 2a are representative of landscapes in an ecotone. 1b and 2b are representative of the landscapes in an ecological phase transition. 1c and 2c represent landscapes approaching spatial homogeneity for the invading phase. 1d and 2d represent landscapes completely homogenous for the invading phase**.**

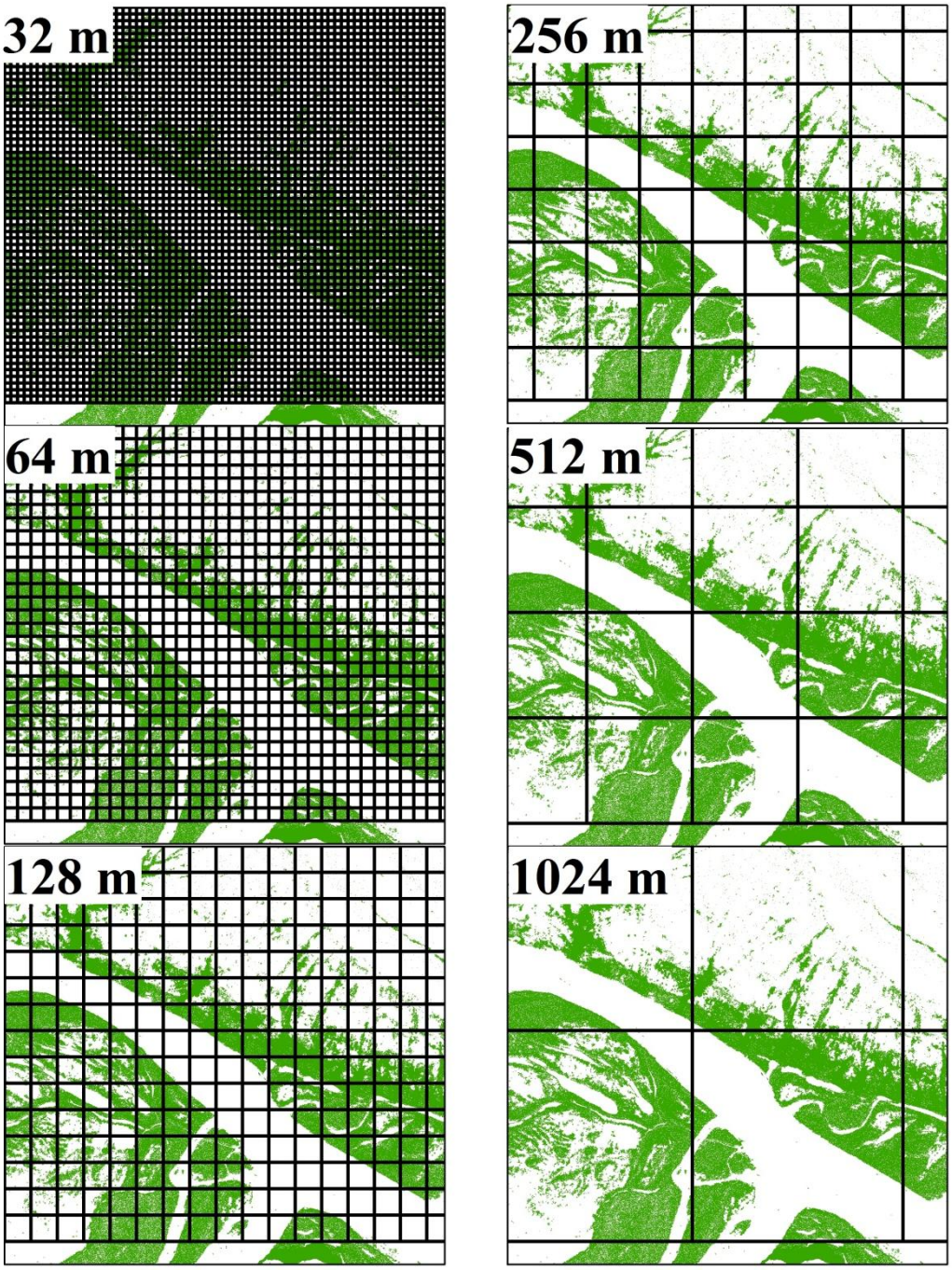

Figure 12: Example grids in a geometric sequence (32, 64, 128, 256, 512, and 1024 m on a side) overlaid on the Colville site for calculating the multiscale information fractal dimension (d_I).

A linear regression model between the median d_I value for all grids in a landscape and its corresponding PCTCOV determined from the pattern metric analysis. I used the Shapiro-Wilk test to verify normality for both the d_I and PCTCOV datasets ($p > 0.05$). This regression model was used to predict percent shrub cover required to initiate phase transition using the critical d_I values of Loehle *et al*. (1996).

4.4 Data Preparation for Examining Relationships Between Shrub Expansion and Hydrologic Characteristics

4.4.1 Change Detection

Change detection between the raster maps for the first (1970s) and last dates (2000s) at the Colville, Killik, Nannushuk 1, Nanushuk 2, and Nimiuktuk sites were facilitated by using map algebra to "subtract" the 2000s map from the 1970s map (Fig. 13). The resulting maps classified pixels into one of three categories (1, 0, and -1), representing gain, no change, and loss, respectively (Figure 14).

4.4.2 Calculation of the TWI

I investigated the association between the presence of shrubs and hydrological characteristics as a function of topography using the TWI proposed by Beven and Kirkby (Beven & Kirkby 1979). This index is defined as the natural log of the ratio between the upslope contributing area (a) and slope percent (tan b) (Eq. 2):

$$TWI = \ln\left(\frac{a}{\tan b}\right) \quad (2)$$

Pixels possessing larger TWI values are located in areas with a greater upslope catchment area (large value of *a*), and have more potential to be wetter than surrounding areas (Wu & Archer 2005). Specifically, areas of high values can either be well-drained (high value of *a* and tan *b*) or relatively stagnant due to a minimal slope gradation (small value of tan *b*) (Zinko et al. 2005). In the context of the BRNS, valley slope drainages and floodplains are likely to possess high TWI values. If local hydrology is influencing patterns of expansion such that shrub expansion is preferentially occurring where the potential for water accumulation or throughflow is greater, then most of the increases in shrub cover should be occurring in areas of higher TWI values.

I acquired mosaics of 1 arc-second, 30.88 m resolution ASTER GDEMs of the entire North Slope from the Alaska Mapped Statewide Digital Mapping Initiative. These were mosaicked together. I calculated the TWI using the TauDEM 5.0 (Terrain Analysis Using Digital Elevation Models) software suite (Tarboton 2010). The TWI values were then binned into integer categories ranging from 0 – 21 (Fig. 15).

I used the Geospatial Modeling Environment (GME) (Beyer 2012) software to generate 2000 randomly selected points within the Colville, Killik, Nanushuk 1, Nanushuk 2, and Nimiuktuk sites. Each point was then spatially associated to its corresponding pixel values for the difference map (1, 0, -1) and TWI map. This generated frequency distributions of TWI values within each of the three change categories. Points from each site were then merged into one dataset (Fig. 16)

I carried out statistical tests using S-Plus 8.1 (TIBCO, 2008). Because the TWI frequency distributions were not normally distributed, I used non-parametric Kruskal-Wallis and Wilcoxon rank-sum tests to determine the significance of shifts in the frequency distribution of TWI values within each change category.

4.4.3 Regression Analysis of the Relationship Between Floodplain Shrub Development and River Channel Characteristics

I isolated spectral classes created by the ISODATA process most closely matching the river channels and converted them to polygons. I then collapsed these polygon features into single centerlines that extended the longitudinal length of the main channel of the river. GME facilitated the generation of points at 5 m intervals along the centerlines. These served as the origins for lines perpendicular to the center that extended to the banks of the river. The lengths of these lines were then calculated within the GIS to determine channel width at each point along the centerline. I then determined the distance from the river bank by generating raster layers representing straight-line Euclidean distance from the river polygon boundaries using the ArcGIS Spatial Analyst (ESRI 2009).

From here, I subset the sample points from the TWI analysis to those present only in the floodplains. Points associated with no change in shrub cover were removed from this subset. The remaining points were then spatially associated with the distance raster layers. Floodplain sample points were matched with their closest river centerline point to determine the distance to a river and the width of the river at that point. Each

floodplain sample point therefore contained attributes representing binomial change in shrub cover, TWI value, distance from the river bank in the 1970s and 2000s, and river channel width. Additional attributes were created for bank distance and channel width differences between the two decades. These attributes were used to create a binomial generalized linear model using logistic regression in S-PLUS 8.1 (TIBCO, 2008) (Fig. 17).

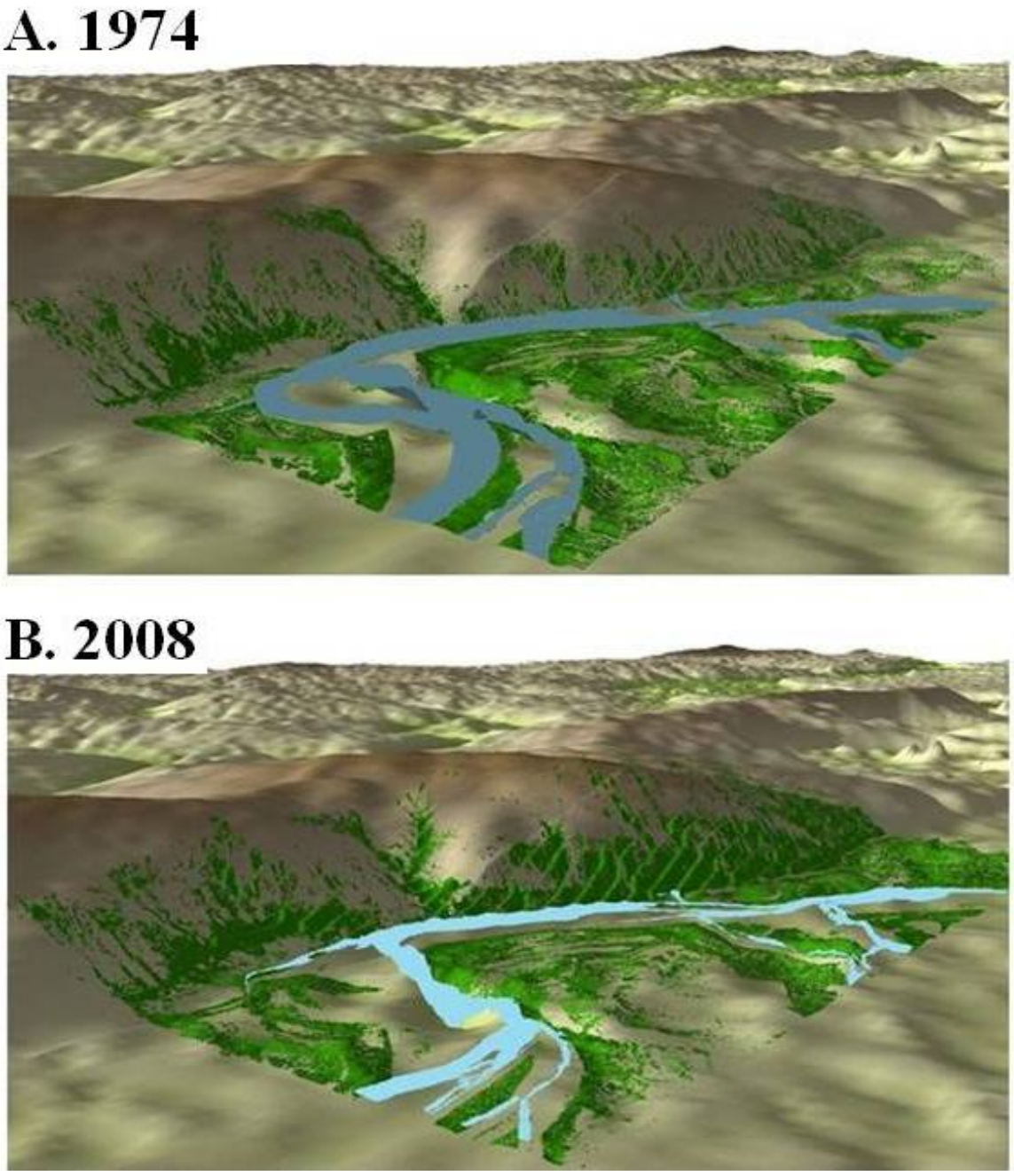

Figure 13: Shrub cover maps for 1974 and 2008 at the Colville site. The shrub maps (in green) are overlaid on three-dimensional exaggerated representations of the landscape using the digital elevation model (DEM) data.

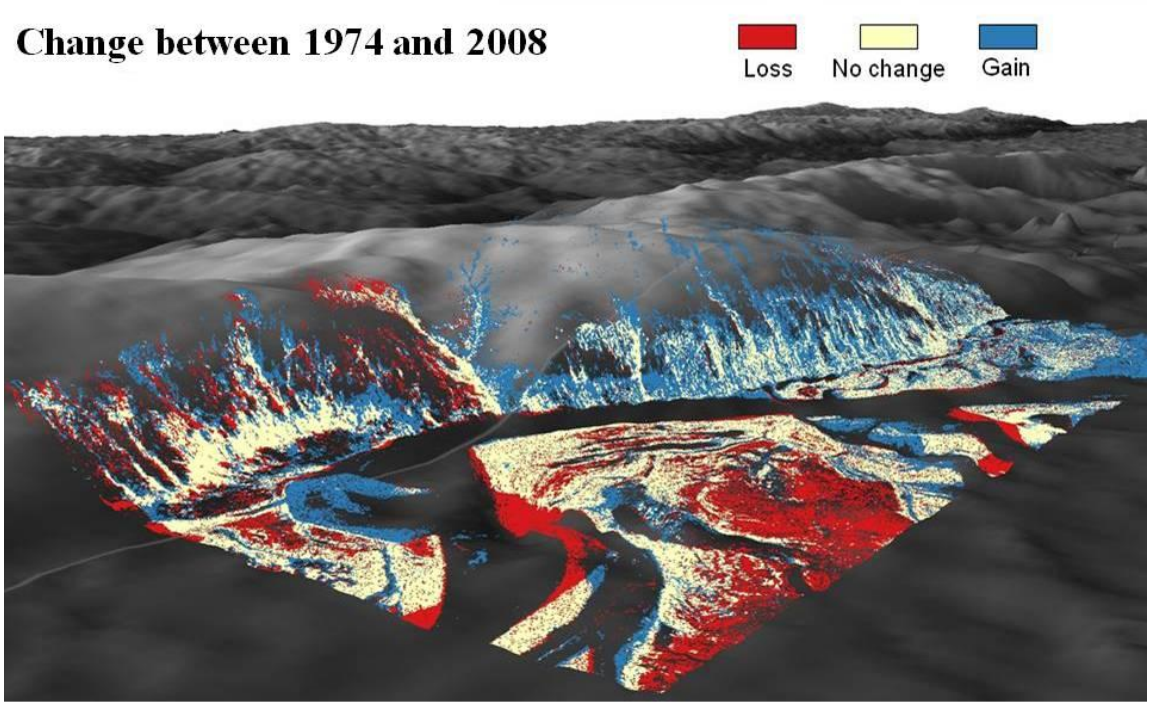

Figure 14: Change detection between the 2008 and 1974 shrub cover maps to determine which areas lost shrub cover, gained cover, or remained unchanged. Note the considerable gains on the valley slopes. The floodplains are highly dynamic due to flooding and channel migration. As a result, trends in local shrub cover change at very fine scales is variable, although there is a net gain.

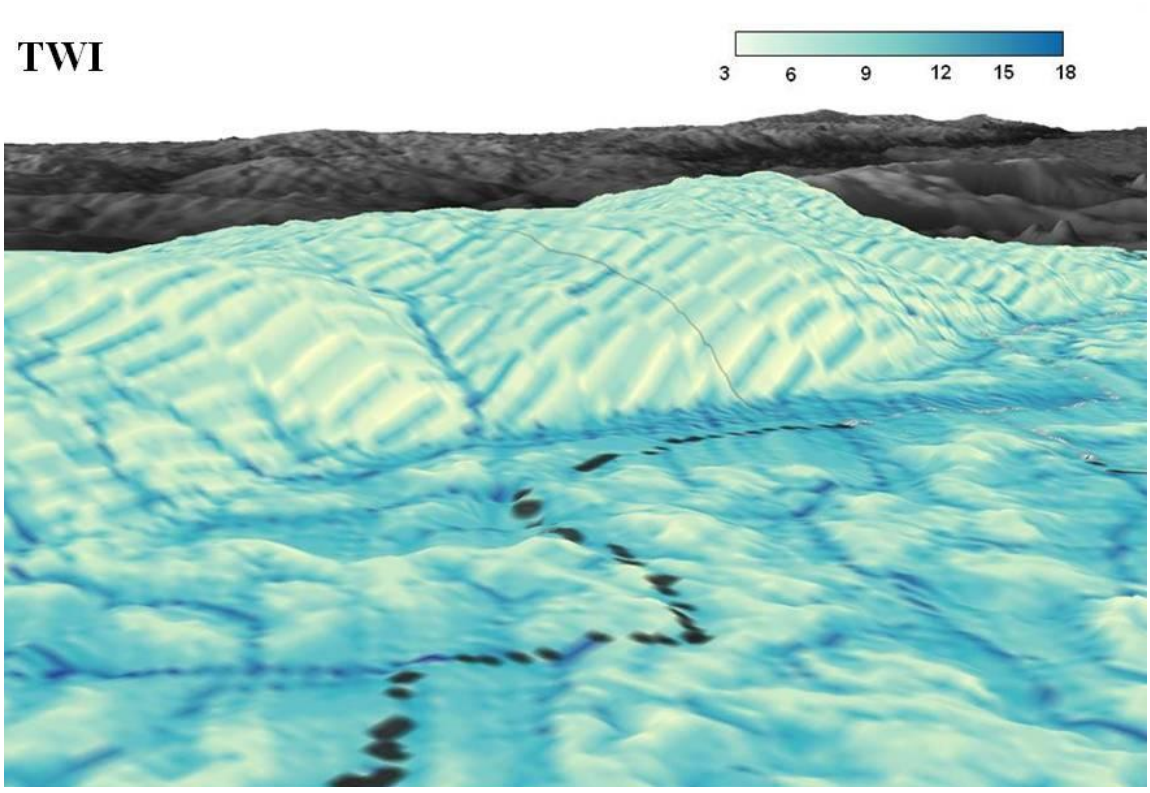

Figure 15: Map of the TWI for the Colville site. Notice that areas with higher TWI values (therefore, greater potential for water throughflow or accumulation) occur in the floodplains and the drainage channels on valley slopes.

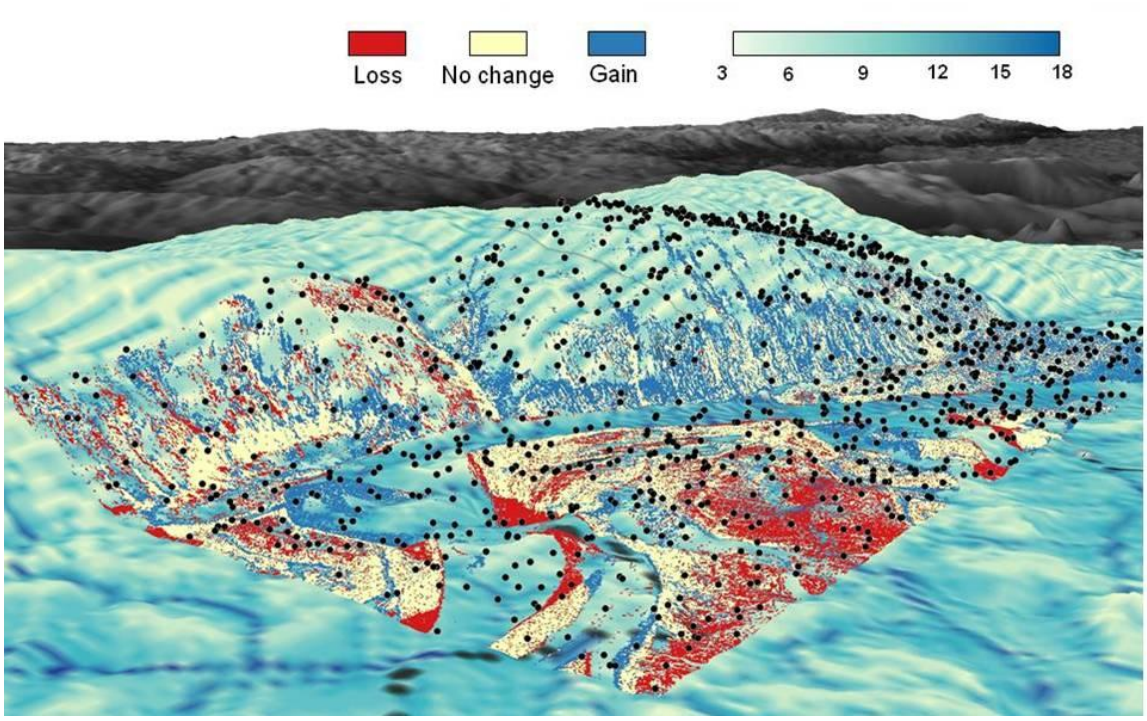

Figure 16: Overlay of the change detection map and the TWI map, and the location of sample points. The landscape was heavily sampled (n = 2000). By spatially associating each point with a category for shrub cover change and TWI value, frequency distributions of TWI values for each change category were generated.

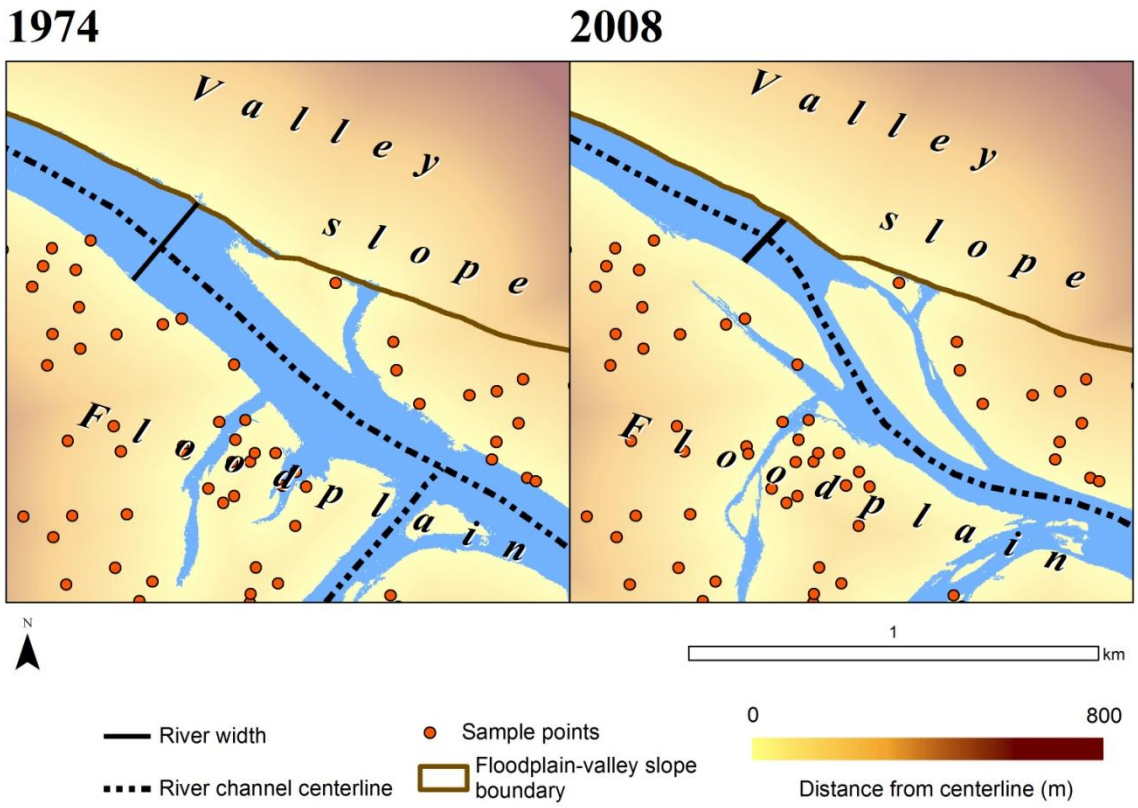

Figure 17: The location of the random sample points, the centerlines of the main river channels, sampled river width, distance from the centerline, and geomorphic boundaries between floodplains and valley slopes at the Colville site.

5. THE SimSHRUB MODEL

5.1 The Conceptual Model

5.1.1 Model Objectives and Bounds of Modeled System

Arctic shrub expansion is hypothesized to be controlled by a number of environmental factors, including increasing temperatures, topographically-controlled hydrologic variability (de Molenaar 1987; Naito & Cairns 2011b), clonal or sexual reproductive processes (Malanson & Cairns 1997; Douhovnikoff et al. 2010), snow-induced positive feedbacks (Sturm et al. 2005) and their interactions (Myers-Smith et al. 2011b). The degree to which each of these processes and their interactions drive observed patterns of shrub expansion, however, is still unknown. Spatially-explicit computer simulation modeling provides a means for rapidly generating plausible spatial patterns of shrub expansion through the manipulation of these processes in an effort to generate hypothesis regarding the true nature of its drivers. This approach can facilitate linkages between plot-level and landscape-level processes because long-term experimental studies at the landscape scale are often prohibitive.

The model developed for this work is a spatially-explicit, stochastic cellular model that can simulate patterns of expansion on an input landscape via different modes of reproduction. Because the contribution of shrub reproductive modes to observed patterns of expansion are poorly understood, this model includes quantitative and qualitative components. This approach should allow the model to accommodate environmental heterogeneity while limiting computational intensity. The strictly

quantitative components include: 1) a cell-based (raster) map of shrub cover from the earliest date at a site of interest, 2) an optional raster map of associated TWI values from that site of interest, and 3) the expected annual growth rate as determined by Tape et al. (2006). Based upon the results in Section 6.4, I expected that there would be a range of TWI values that facilitate shrub expansion. Above this range, the ground will be too wet to support shrub growth, and below this range, the ground will be too dry to support shrub growth. Therefore, shrub growth should be constrained to cells in which their TWI values falls within this range (hereafter, realized TWI niche). This range should vary by landscape. In the absence of detailed plot-level data, the model uses some qualitative components such as the use of random assignment of new shrubs on the landscape that meet certain criteria for the chosen mode of reproduction.

This modeling approach generally follows the one outlined by Alftine and Malanson (2004). The objective of that study was to investigate the processes driving recruitment of *Pinus albicaulis* at treeline at Lee Ridge in Glacier National Park, Montana. Alftine and Malanson (2004) collected field-based data regarding the spatial pattern of newly recruited *P. albicaulis* individuals as well as site characteristics. They also developed a spatially-explicit cellular simulation model that incorporated parameters relating to mortality, site characteristics, random establishment, neighbor effects, and associated directional feedbacks.

Operating under the assumption that rates of shrub growth are site-specific, Tape et al. (2006) fit a series of logistic curves to their measured rates of expansion. They

predicted that the intrinsic rate of increase was approximately 0.029 per year. This rate was incorporated into the simulation model as a means of testing its usefulness.

5.1.2 Model Components

This model has been constructed to include the following components (see also Fig. 18):

1) a means for a user to input a raster-based map (either square or rectangle) with some percentage of shrub cover at a 1 m resolution.
2) a means for a user to input a raster-based map with TWI values associated with the input shrub cover map as an optional input. The dimensions of this map must be the same as in 1), and the model should be able to check this agreement and warn the user if there is not agreement. The user can also specify the realized TWI niche that permits shrub growth.
3) a means for a user to choose a specific mode of reproduction to simulate. These modes include ubiquitous dispersal, sexual dispersal via seed, and two clonal (vegetative) types of reproduction (clonal reproduction with a "mass effect," and clonal reproduction without a "mass effect").
4) a means for a user to specify the length of the simulation period. The time step of the model t is one year.
5) a means to consider the number of "shrub" cells at the current time step S, the corresponding number of "empty" cells in the input landscape N, the maximum number of cells that can be invaded (i.e., the entire landscape) K, the intrinsic

rate of growth r, the mean expected growth in the next time step ΔS, and the actual probability p of an "empty" cell i becoming a "shrub" cell at $t+1$. The calculation of N and p varies by the chosen reproductive mode. N is also modified by the realized TWI niche.

6) a means of randomly assigning cells as "shrub" in the next time step that have a $p > 0$.
7) a means of outputting the simulation results that can be viewed as a map in GIS software. The user should be able to specify the time step increment for output.

5.1.3 Considerations in Each of the Reproductive Modes

5.1.3.1 Ubiquitous Dispersal Mode

In the ubiquitous dispersal mode, all empty cells in the landscape should have equal probability of becoming shrub cells. The input configuration drives the operation of the model, but remains unaffected because mortality is not a model parameter. Values for the shrub population S at any time step, the maximum size of the landscape K, and the number of empty cells N are collected from the input configuration. N is simply be the difference between S and K at each time step. Based upon values for S, K, and N, as well as the user-specified constant for the intrinsic growth rate r, the mean (expected) increase in shrub cover ΔS is calculated. Because the model is stochastic with regard to actual assignment, the sum of p should approximate ΔS. The model then proceeds to randomly assign cells as shrub cells such that the equation of the sum of p is approximately equal to ΔS is satisfied. This assignment results in new growth. This

mode should help identify whether local or more regional-scale processes might be driving expansion (Fig. 19).

5.1.3.2 Clonal Reproduction Without "Mass Effect" Mode

In the clonal reproduction without "mass effect" mode, all empty cells that are contiguous to a shrub cell have equal probability of becoming a shrub cell in the next time step. The values for *S*, *K*, and *N*, and the calculation of ΔS proceed in a manner similar to the process presented in the ubiquitous mode. However, *N* is constrained to only those cells that are contiguous to a shrub cell. *N* could be modified by the realized TWI niche values which remain constant throughout the simulation run. The model checks to ensure that the TWI value of each of the neighboring cells falls within the range of values. If so, that cell can be considered as part of *N*; otherwise, it is excluded. The calculation of *p* and the final random assignment is then constrained to N (Fig. 20).

5.1.3.3 Clonal Reproduction with "Mass Effect" Mode

In the clonal mode with a mass effect, the model operates in a manner similar to the clonal reproduction without "mass effect" mode. All empty cells with a neighboring shrub cell have some probability of becoming a shrub cell in the next time step. In this case, however, empty cells with more than one shrub cell neighbor will have higher probability of becoming a shrub cell than those that have one neighbor. Ecologically, this is meant to convey the idea that a patch of bare ground surrounded by shrubs will very likely become covered in shrub itself. On the other hand, the potential for bare

ground surrounding a single shrub changing to shrub will be much smaller. The values for *S*, *K*, and *N*, and the calculation of ΔS proceed in a manner similar to the process presented in the clonal reproduction without "mass effect" mode. Again, *N* should be modified by the realized TWI niche (Fig. 21).

5.1.3.4 Sexual Reproduction Mode

In the sexual dispersal mode, the user will be able to specify the maximum distance at which shrubs can recruit from a current "shrub" cell. Within this distance, probability of recruitment varies. Specifically, probability of recruitment is highest near to a current "shrub" cell. The probability reduces dramatically as distance increases. This consideration is intended to simulate the dispersal kernel. To reduce computational demands, the model does not trace a relationship between a specific parent plant and its seed that produces another shrub in a cell within a set distance away. *N* is therefore restricted to all empty cells within the specified distance of a shrub cell, and *p* increases as distance decreases. Again, *N* should be modified by the realized TWI niche (Fig. 22).

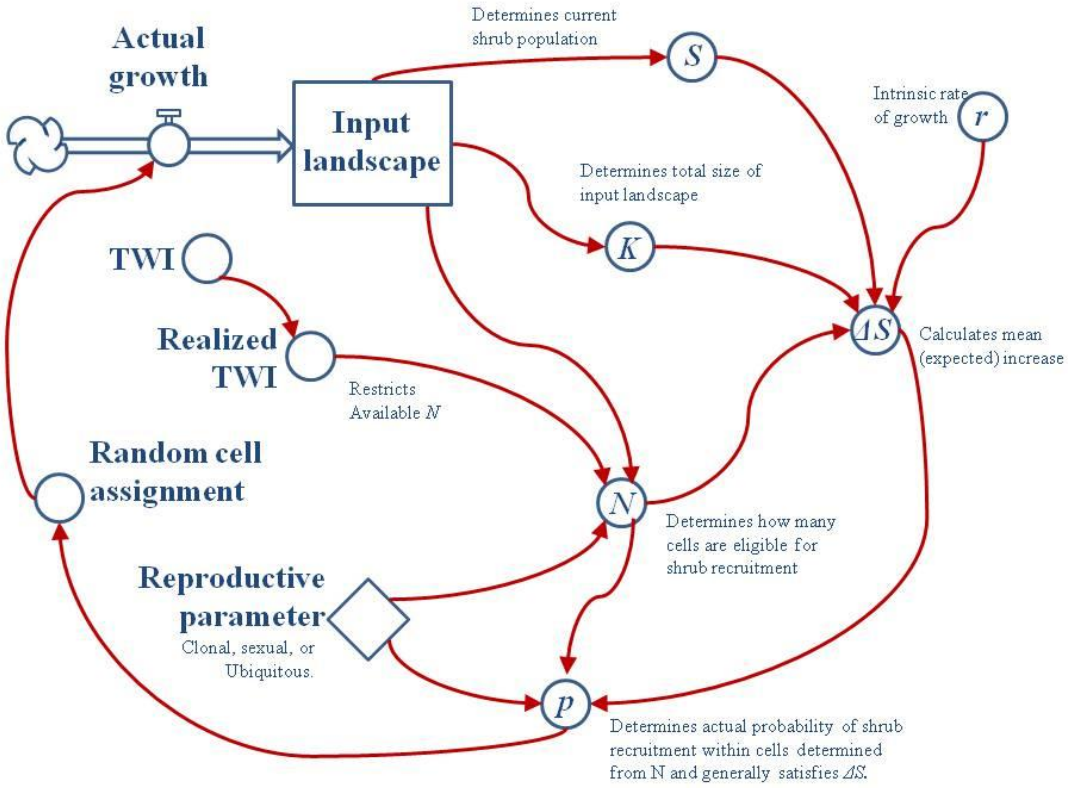

Figure 18: A conceptual model outlining the basic model considerations upon model initialization. This figure uses the same systems dynamics iconography as in Forrester diagrams and STELLA Modeling and Simulation Software. The ubiquitous dispersal mode operates similarly to this, since all *N* has equal probability of becoming a shrub cell in the next time step.

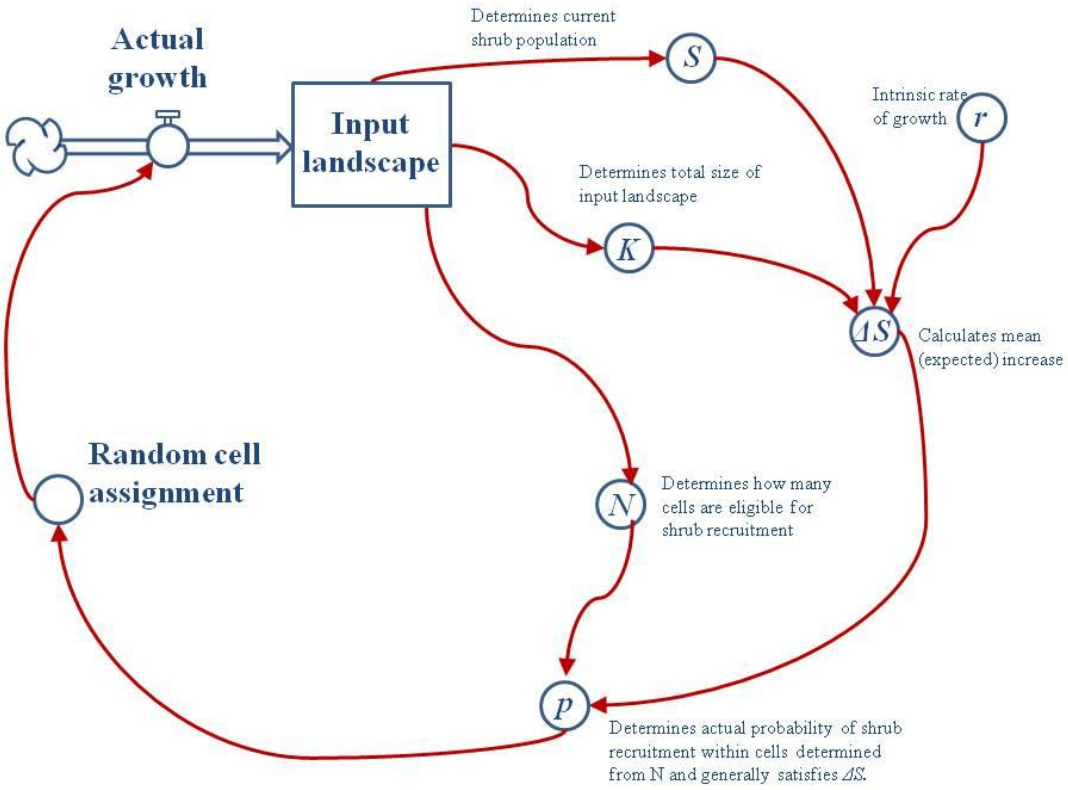

Figure 19: A conceptual model outlining the basic model considerations upon model initialization using the ubiquitous dispersal mode. The realized TWI niche is not considered in this run.

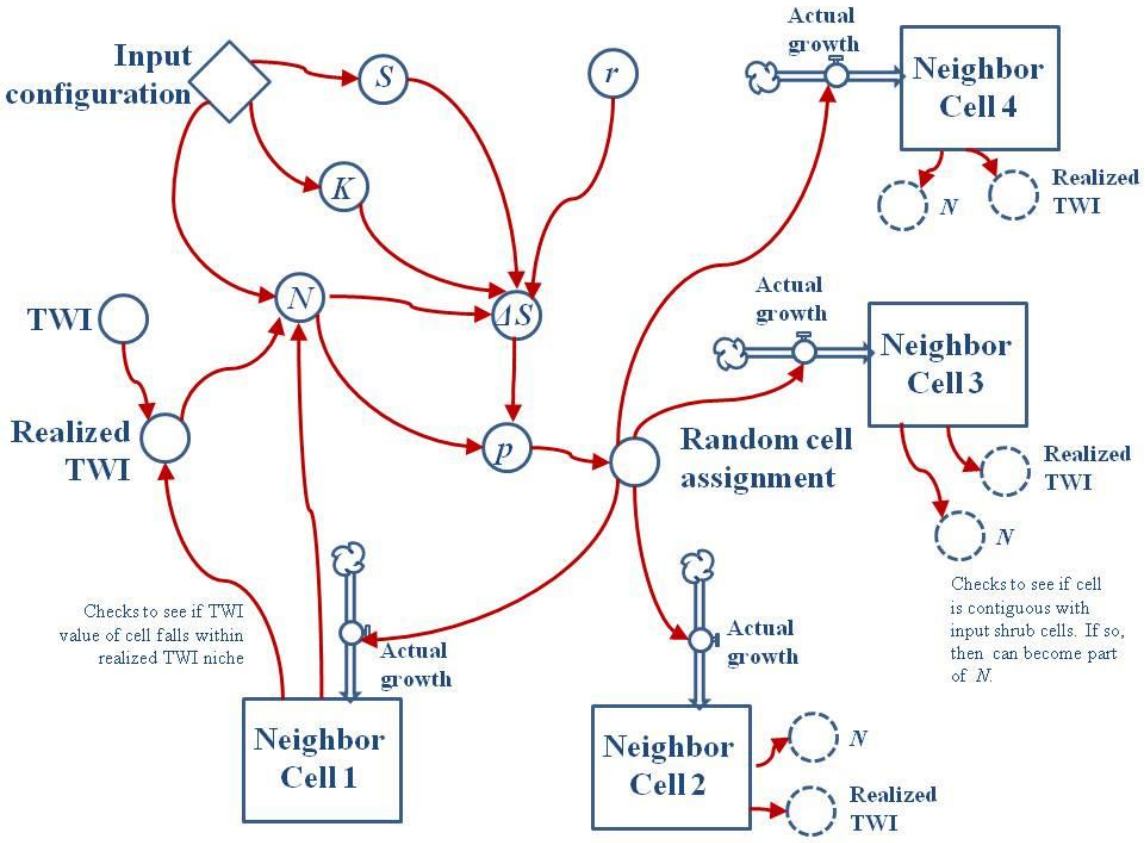

Figure 20: A conceptual model outlining the basic model considerations upon model initialization using the clonal reproduction without "mass effect" mode. Here, neighbor cells are assumed to be contiguous with the input configuration. The decision process regarding the realized TWI niche only proceeds if the user specifies it as input.

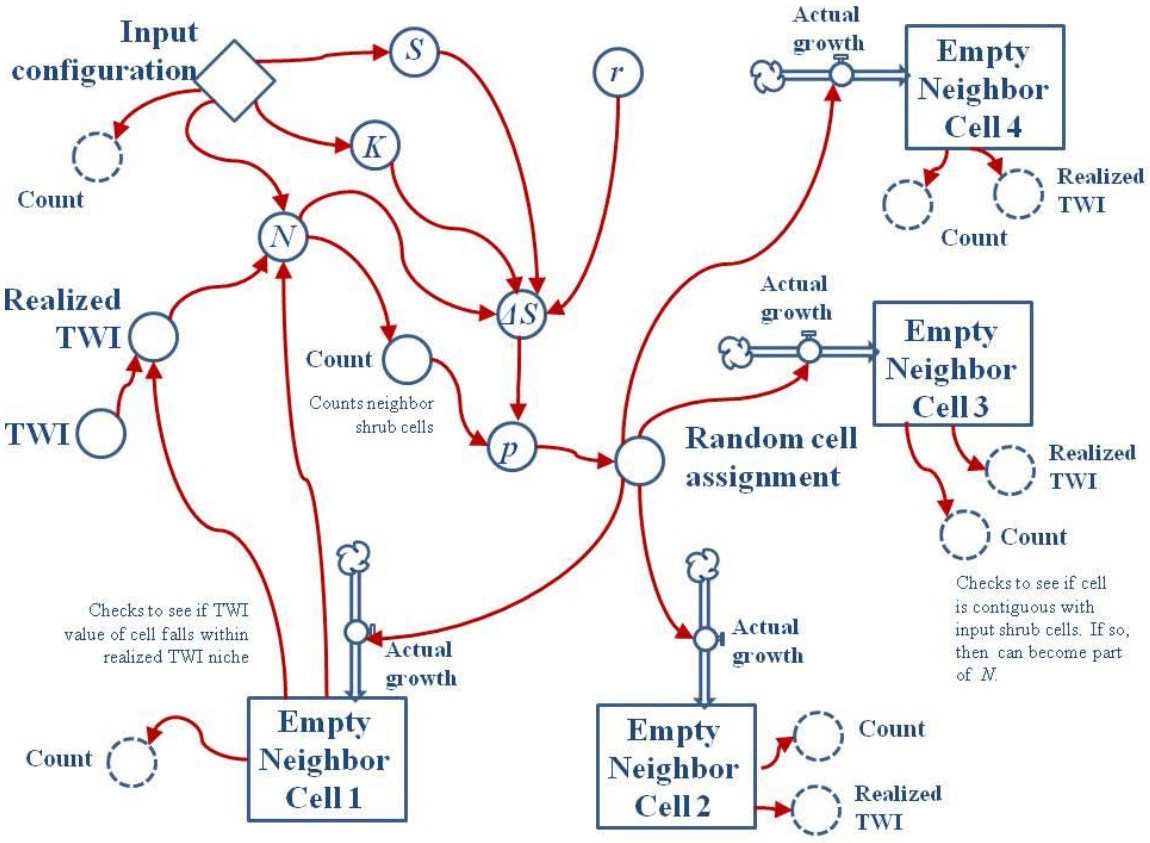

Figure 21: A conceptual model outlining the basic model considerations upon model initialization using the clonal reproduction with "mass effect" mode. Here, neighbor cells are assumed to be contiguous with the input configuration. The decision process regarding the realized TWI niche only proceeds if the user specifies it as input. The value of *p* increases with a greater number of neighbors. Conceptually, this means the introduction of a "Count" auxiliary variable that modifies *N* so that *p* is greater with a greater number of neighboring shrub cells. "Count" considers both the input configuration and neighbor cells that "indicate" their state of being empty.

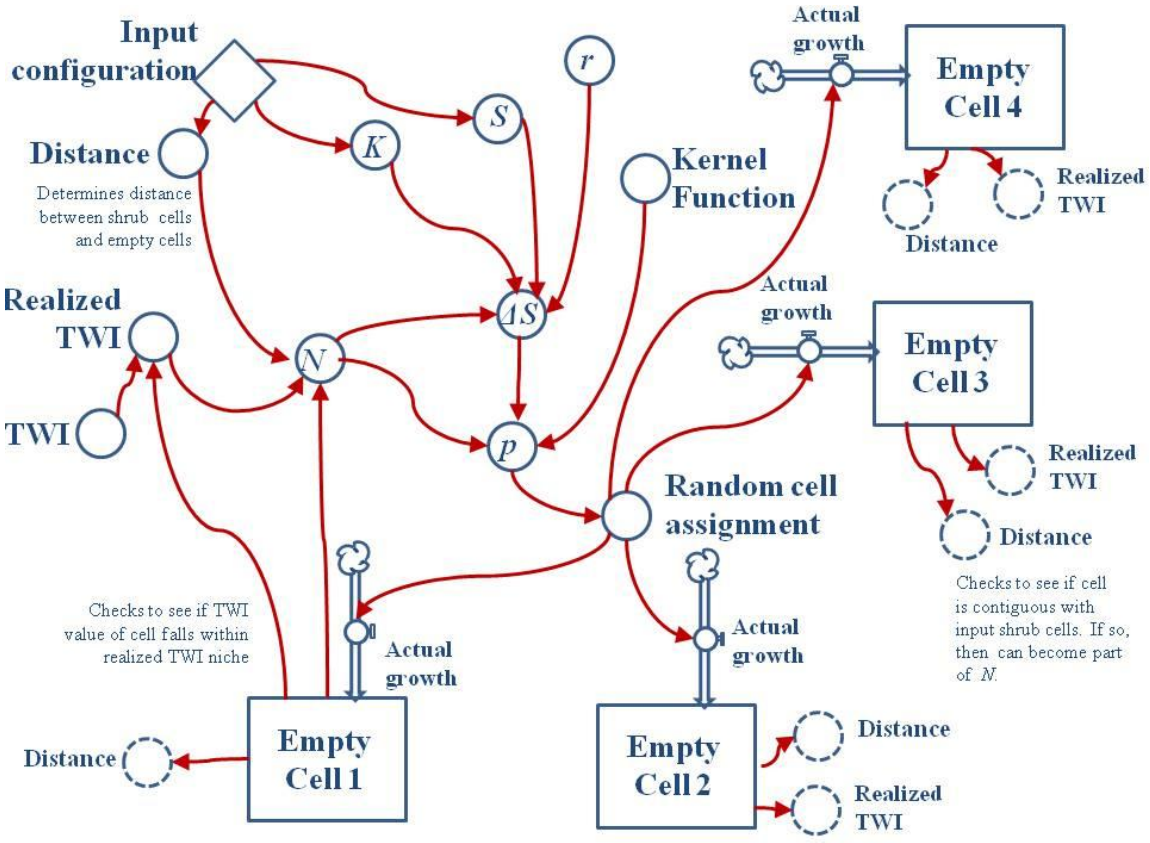

Figure 22: A conceptual model outlining the basic model considerations upon model initialization using the sexual reproduction mode. Here, an auxiliary variable "distance" calculates the distance between shrub cells and empty cells in order to determine *N*. Again, the decision process regarding the realized TWI niche only proceeds if the user specifies it as input. The value of *p* is modified further by the introduction of the dispersal kernel function, where higher probabilities of recruitment occur at short distances and lower probabilities of recruitment occur at long distances.

5.1.4 Expected Model Behavior

1) Patterns of shrub expansion produced through sexual dispersal and ubiquitous dispersal should appear very different from those produced through clonal expansion. Clonal expansion should generate shrub cells that are spatially contiguous. Sexual dispersal involving longer dispersal distances should generate shrub cells that are less spatially contiguous.
2) Given the coarse resolution of the DEMs and subsequent TWI maps, it is unlikely there will be a significant variation between the patterns produced with simulation runs using the TWI compared to those not using the TWI.

5.2 The Quantitative Model

5.2.1 Model Description

This simulation model was built using Visual C# (Microsoft Visual Studio 10). Visual C# is an object-oriented language that allows the user develop executable programs with a graphical user interface (GUI). An image of the GUI is provided in Fig. 23. The user must provide a map of shrub cover as a text file. Shrub cells must have a value of 1, and empty cells must have a value of 0. If the user chooses, s/he can provide a map of associated TWI values as a text file and the range of values that allow shrubs to grow (Fig. 23).

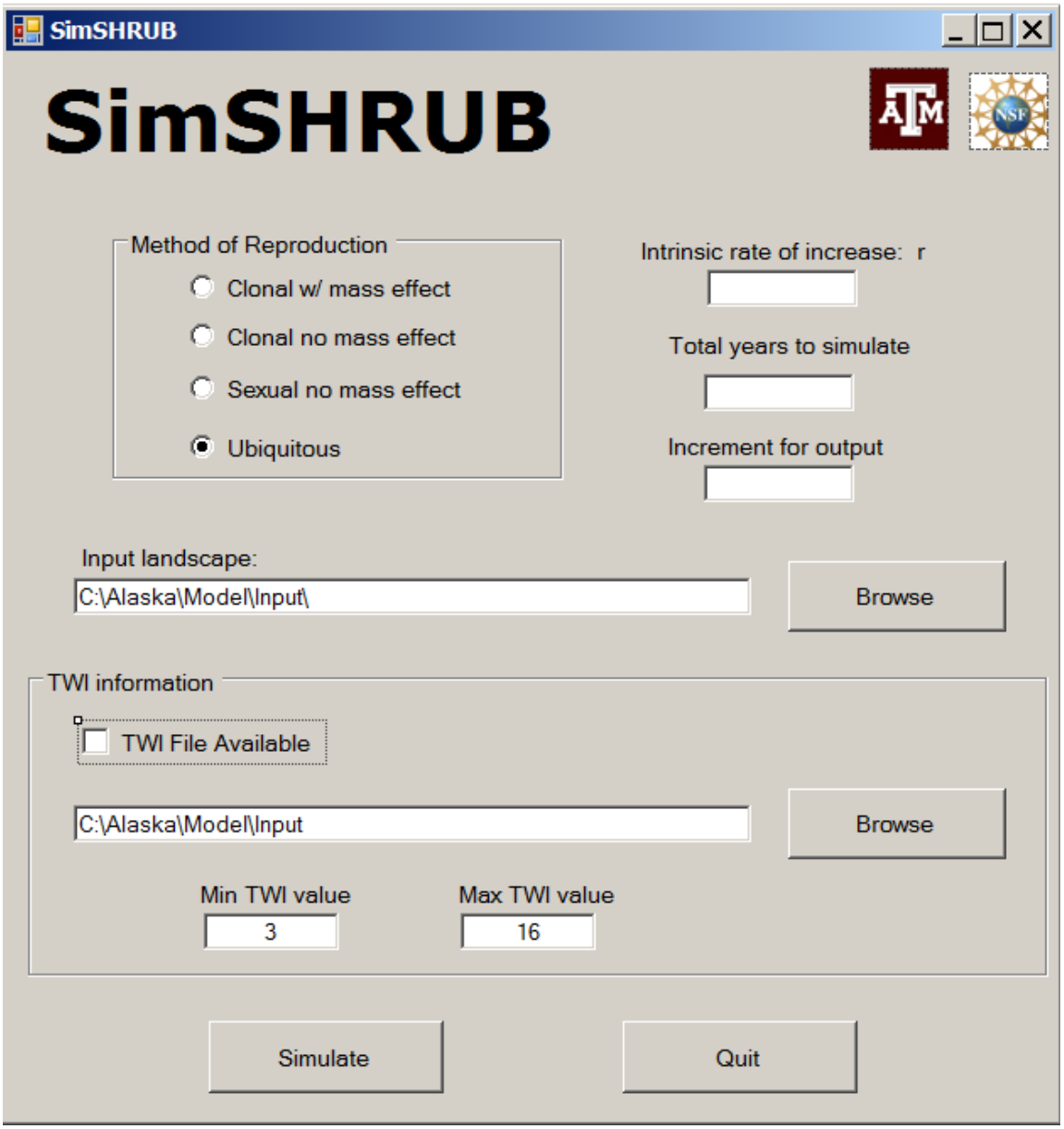

Figure 23: The graphical user interface (GUI) for SimSHRUB.

5.2.2 Quantitative Considerations Within Each Reproductive Mode

The mean expected increase in shrub cover *ΔS* is derived from Tape et al.'s (2006) logistic equation. The model calculates *S*, *N*, and *K* from the input landscape in order to determine *ΔS*. This relationship is given in Eq. 3:

$$\Delta S = r * S * (1 + \frac{S}{K}) \quad (3)$$

However, it would be expected that the actual growth at each time step would vary due to the stochastic nature of the model. Therefore, the *average* amount of growth at a time step from multiple simulation runs should approximate *ΔS*. The model assigns *p* to each cell *i* in *N* that meets the criteria for the chosen mode of reproduction. The calculation of *p* and *N* both vary with the mode of reproduction at each time step, but the sum of *p* should approximate *ΔS*. This relationship is given in Eq. 4:

$$\Delta S = \sum_{i}^{N} p_i \quad (4)$$

From there, the model uses Eq. 4 to identify empty cells with a probability of becoming a shrub cell, and randomly assigns empty cells as new shrub cells until the equation is satisfied.

In the ubiquitous mode, all *N* at each time step have equal *p*. *N* is calculated using Eq. 5, and *p* is calculated using Eq. 6. Since this acts as a "control" run and will help facilitate the determination of whether local or more regional processes are driving expansion, simulation runs did not include a realized TWI niche (Fig. 24).

$$N = K - S \quad (5)$$

$$p = \frac{\Delta S}{N} \quad (6)$$

In both clonal modes, *N* is restricted to empty cells that have at least one neighbor as a shrub cell. A neighbor is defined as a shrub cell with a common border or vertex with an empty cell. This allows each empty cell to have a maximum of eight neighbors. In the clonal mode without "mass effect," all empty cells with at least one neighbor shrub cell have equal probability of recruitment. Upon determining *N*, the model attempts to satisfy Eq. 6 (Fig. 25). Similarly, the clonal mode with "mass effect" considers all empty cells with at least one neighbor shrub cell to have some probability of recruitment. In this case, however, the probability increases with a greater number of neighbors. In this case, the model examines empty cells with a neighbor shrub cell and determines the probability of remaining empty q_1 in the next time step. For a empty cell with a single neighbor shrub cell along its border, this relationship is represented by Eq. 7:

$$p = 1 - q_1 \quad (7)$$

If this empty cell instead had a neighbor shrub cell with a common vertex, the probability of remaining empty q_2 would instead be represented by Eq. 8:

$$1 - q_2 = \frac{1 - q_1}{\sqrt{2}} \quad (8)$$

These relationships can then be applied to any empty cell with k_1 neighbors sharing a border and k_2 neighbors sharing a vertex, in which its probability of remaining empty q is determined using the equation:

$$q = q_1^{k_1} * q_2^{k_2} \quad (7)$$

The model then randomly assigns those cells to become new shrub cover. This continues until there is agreement with Eq. 4 (Fig. 26).

In the sexual mode, the model accepts the user-specified maximum distance *x* at which recruitment can occur in the next time step. This also incorporates an equation of probabilities as function of distance, with the user-specified distance value acting as the maximum value for distance (Fig. 27). Both a basic inverse distance function (Eq. 8) and leptokurtic dispersal kernels for derived from observational data in this work were tested (see Section 5.2.4). Leptokurtic dispersal kernels were calculated for the Ayiyak floodplain (Eq. 9), the Ayiyak valley slope (Eq. 10), the Colville floodplain (Eq. 11), and the Colville valley slope (Eq. 12).

$$p = \frac{1}{x^2} \quad (8)$$

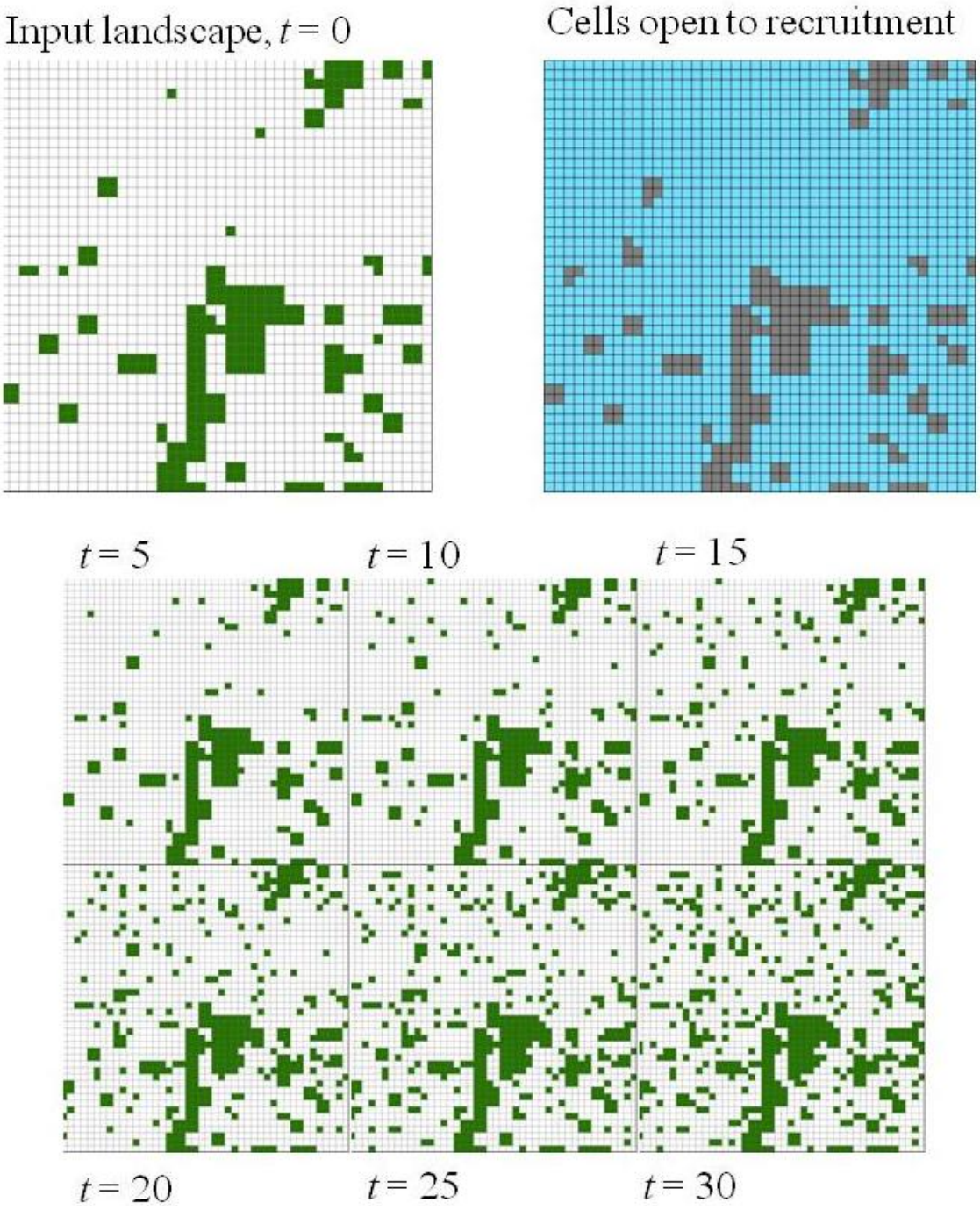

Figure 24: Example simulated maps of shrub growth using the ubiquitous dispersal mode. Clockwise from upper left: the input landscape at time t=0; the cells eligible for recruitment in the next time step highlighted in blue; and the shrub cover increases at time t=5 years, 10 years, 15 years, 20 years, 25 years, and 30 years.

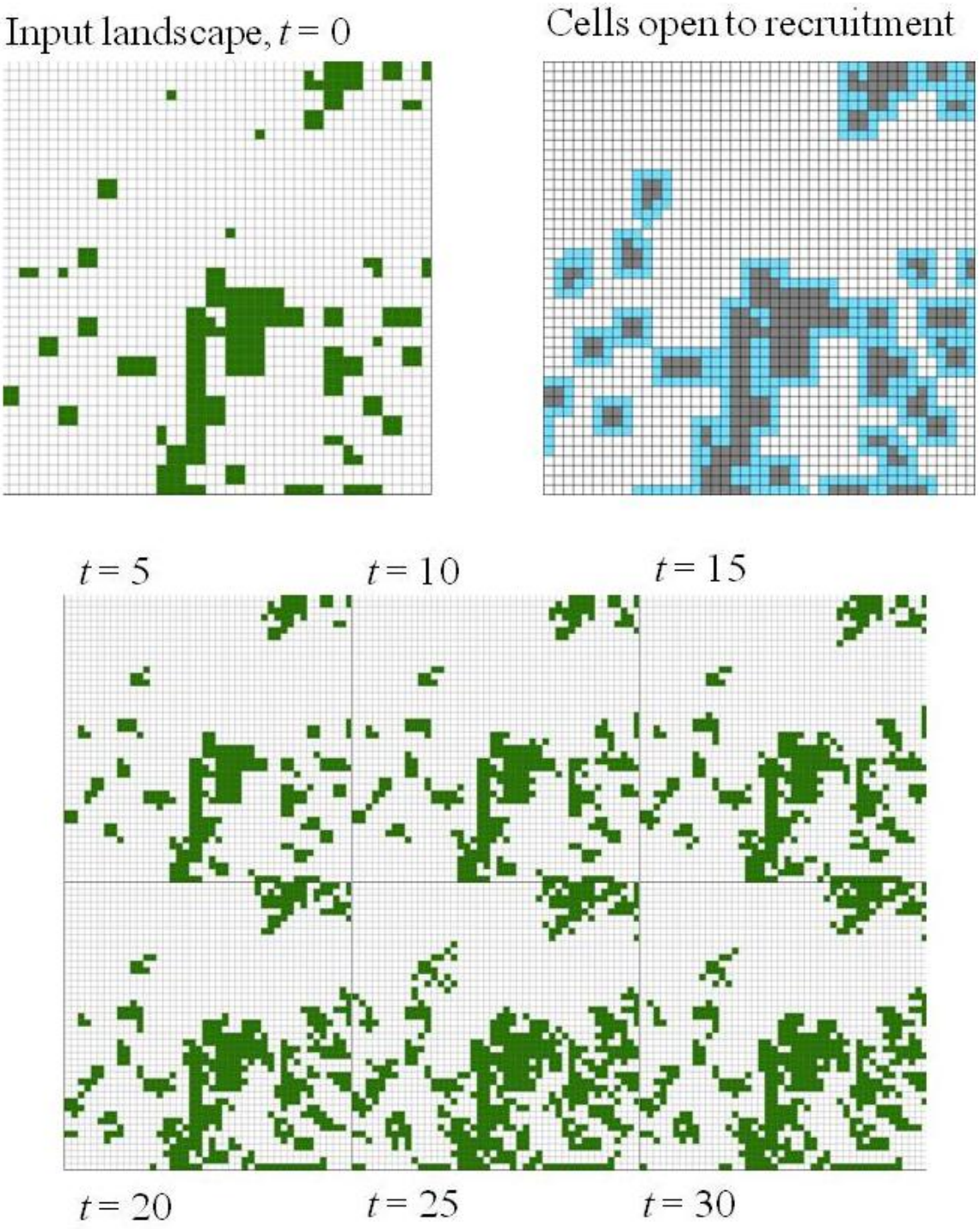

Figure 25: Example simulated maps of shrub growth using the clonal reproduction without "mass effect" mode. Clockwise from upper left: the input landscape at time t=0; the cells eligible for recruitment in the next time step highlighted in blue; and the shrub cover increases at time t=5, 10, 15, 20, 25, and 30 years.

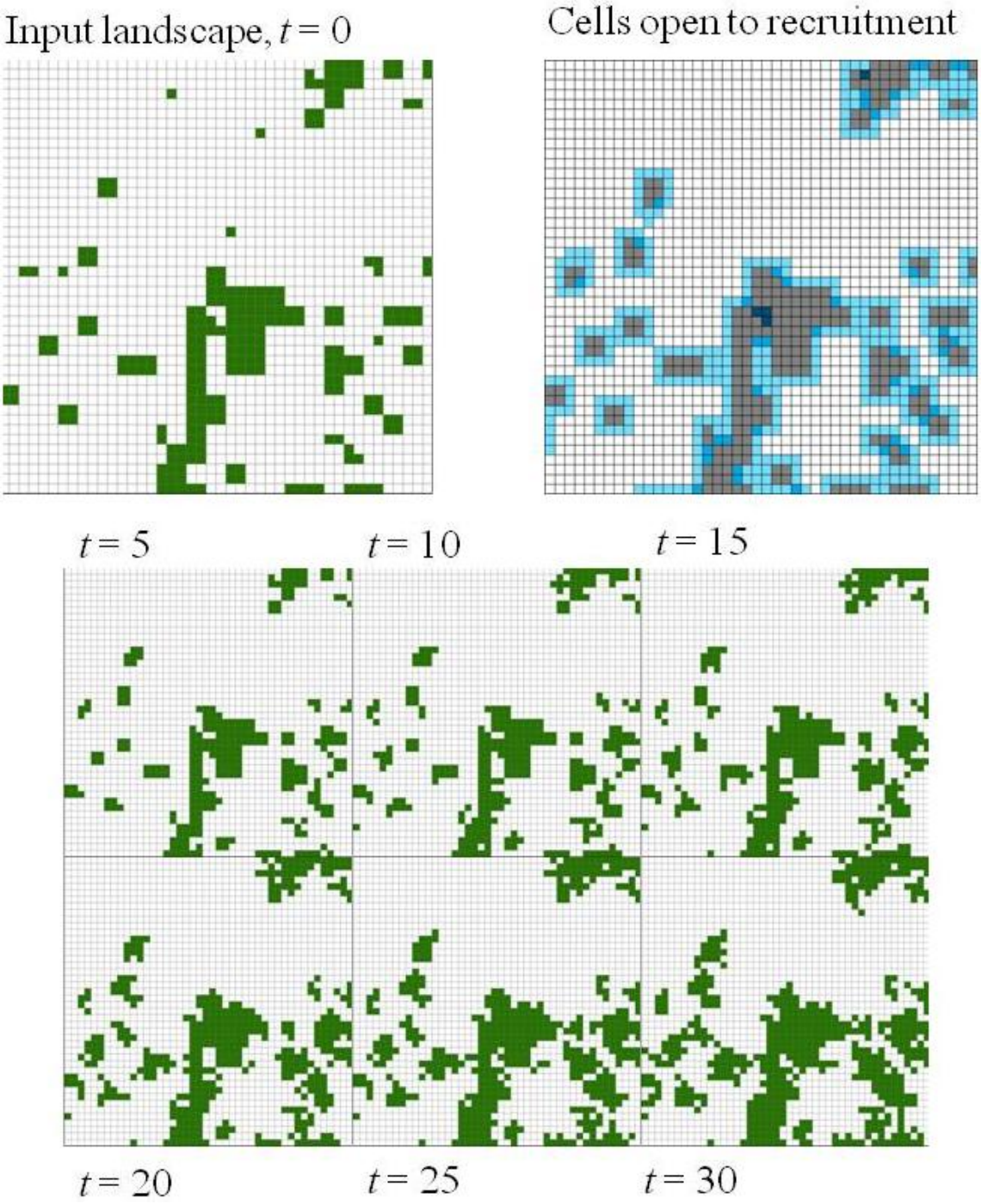

Figure 26: Example simulated maps of shrub growth using the clonal reproduction with "mass effect" mode. Note that cells with a higher probability of recruitment have more neighbors and are darker blue.

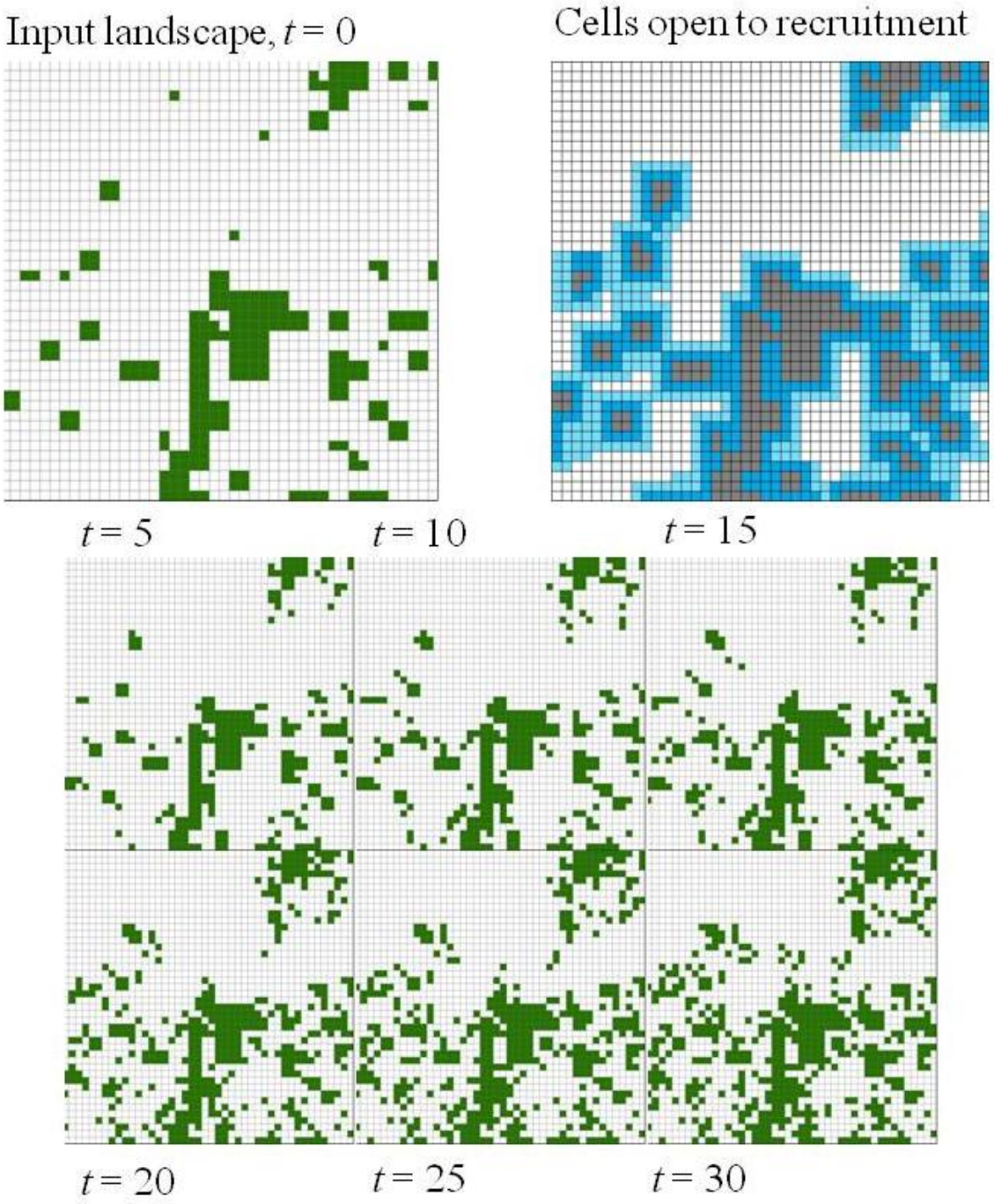

Figure 27: Example simulated maps of shrub growth using the sexual dispersal mode with a maximum distance of 2 m. Note that cells with a higher probability of recruitment are closer to parent patches.

5.2.3 The Dispersal Kernel

The dispersal distance of seeds from a parent plant can be mathematically represented using a dispersal kernel. This kernel is a probability density function that represents seed arrival at a distance *x* from the parent plant (Clark et al. 1998). Dispersal kernels may take on several functional forms, including Gaussian (Fujiwara et al. 2006), inverse distance, negative exponential (e.g., Willson 1993), and leptokurtic (e.g., Clark et al. 1998; Robledo-Arnuncio & Garcia 2007). In the leptokurtic form, the highest probabilities of seed arrival will occur closest to the parent patch (Clark et al. 1998; Clark et al. 1999) and probability declines as distance increases. These kernels are also known to possess a "fat tail" where the probability of long-distance dispersal is also relatively high.

In the absence of seed dispersal data from the sites in this work, I calculated potential dispersal kernels using spatial pattern for both Ayiyak and Colville sites. This involved the creation of rasterized difference maps between the 1970s and 2000s to identify areas that gained shrub cover (e.g., Naito & Cairns 2011b). These maps were converted to points. From there, I calculated the nearest neighbor distance between the points that represented a gain in cover in the 2000s and the points representing cover in the 1970s. These points were then segregated by floodplain and valley slope due to the assumption that the kernel would vary across the landscape due to of differences in shrub species composition, geomorphologic characteristics, and resource availability. Probability density distributions were generated using these distances *x* (Figs. 28-31). Weibull functions were then fit to each probability distribution for the Ayiyak

floodplains (Eq. 9), the Ayiyak hillslopes (Eq. 10), the Colville floodplains (Eq. 11), and the Colville valley slopes (Eq. 12). The Weibull functions served as the leptokurtic dispersal kernel for the sexual reproduction modes and were hard-coded into the model.

$$y = \frac{0.561}{10.142} \times \left(\frac{x}{10.142}^{0.561 - 1} \right) \times e^{-\left(\frac{x}{10.142}^{0.561} \right)} \quad (9)$$

$$y = \frac{1.178}{3.113} \times \left(\frac{x}{3.113}^{1.178 - 1} \right) \times e^{-\left(\frac{x}{3.113}^{1.178} \right)} \quad (10)$$

$$y = \frac{0.646}{10.783} \times \left(\frac{x}{10.783}^{0.646 - 1} \right) \times e^{-\left(\frac{x}{10.783}^{0.646} \right)} \quad (11)$$

$$y = \frac{0.773}{5.888} \times \left(\frac{x}{0.773}^{0.773 - 1} \right) \times e^{-\left(\frac{x}{5.888}^{0.772} \right)} \quad (12)$$

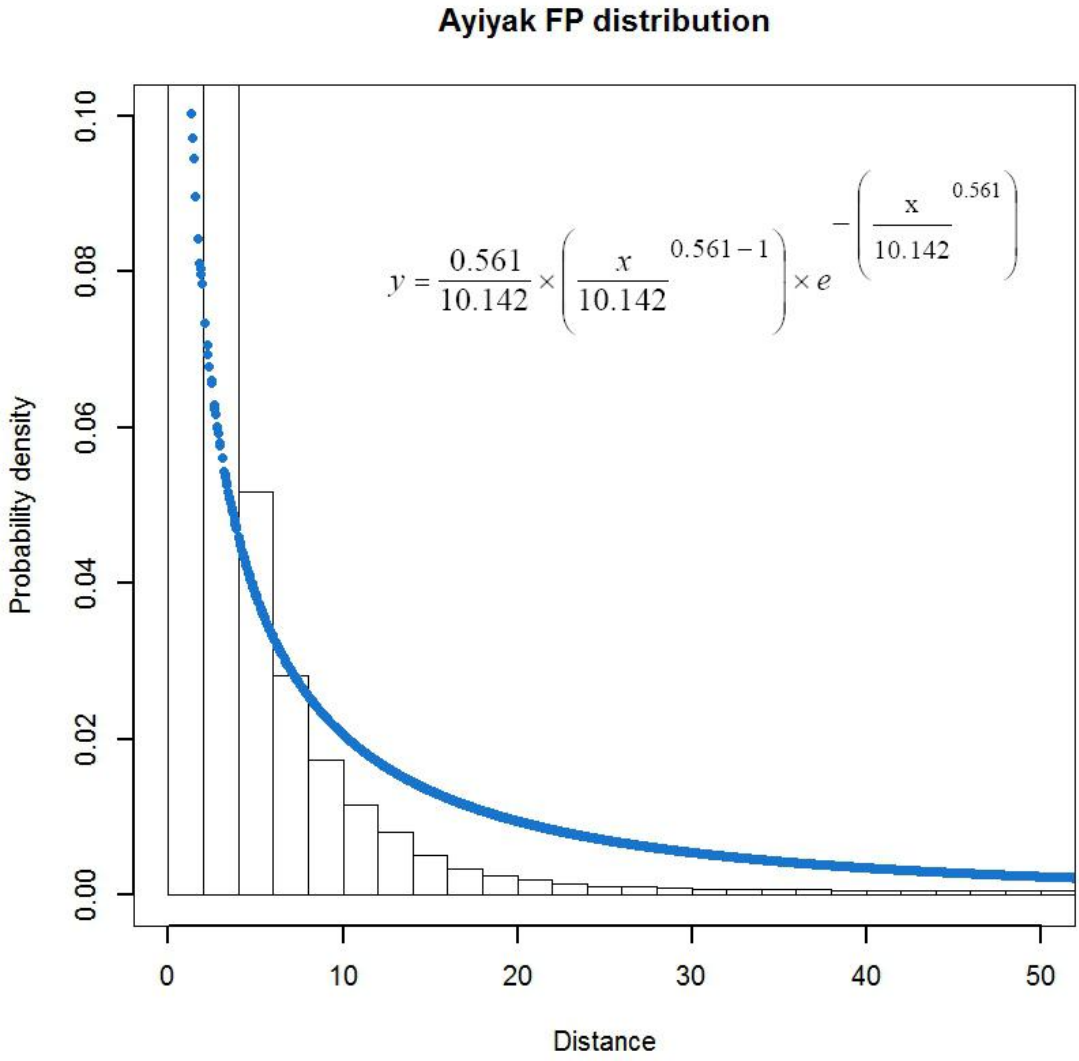

Figure 28: Probability density distribution for the floodplains at the Ayiyak site. This distribution describing the relative likelihood that one encounters a shrub as distance from another shrub increases. Histogram bars represent the density distribution, and the blue line represents the fitted Weibull function that approximates this distribution. The Weibull function serves as the leptokurtic dispersal kernel for the sexual reproduction modes.

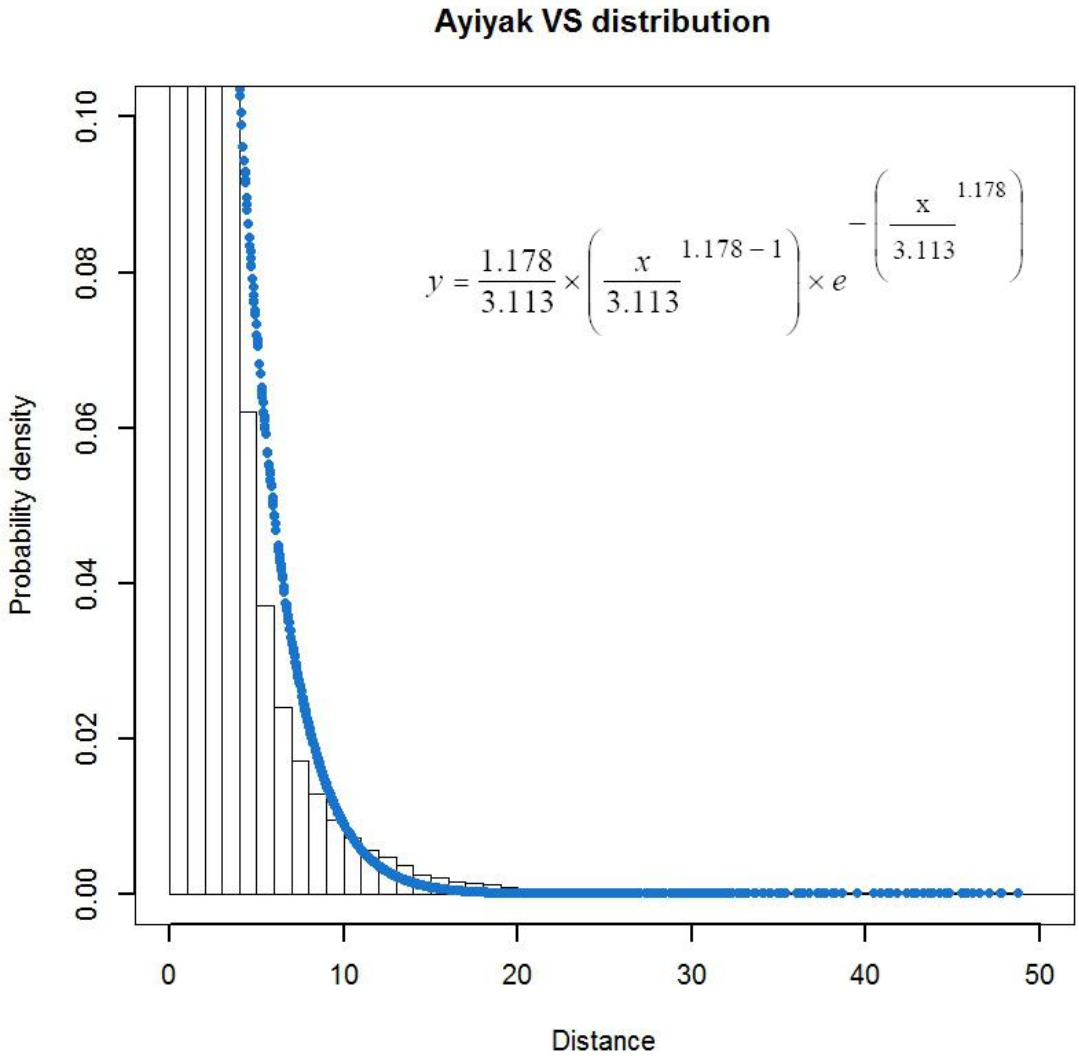

Figure 29: Probability density distribution for the valley slopes at the Ayiyak site.

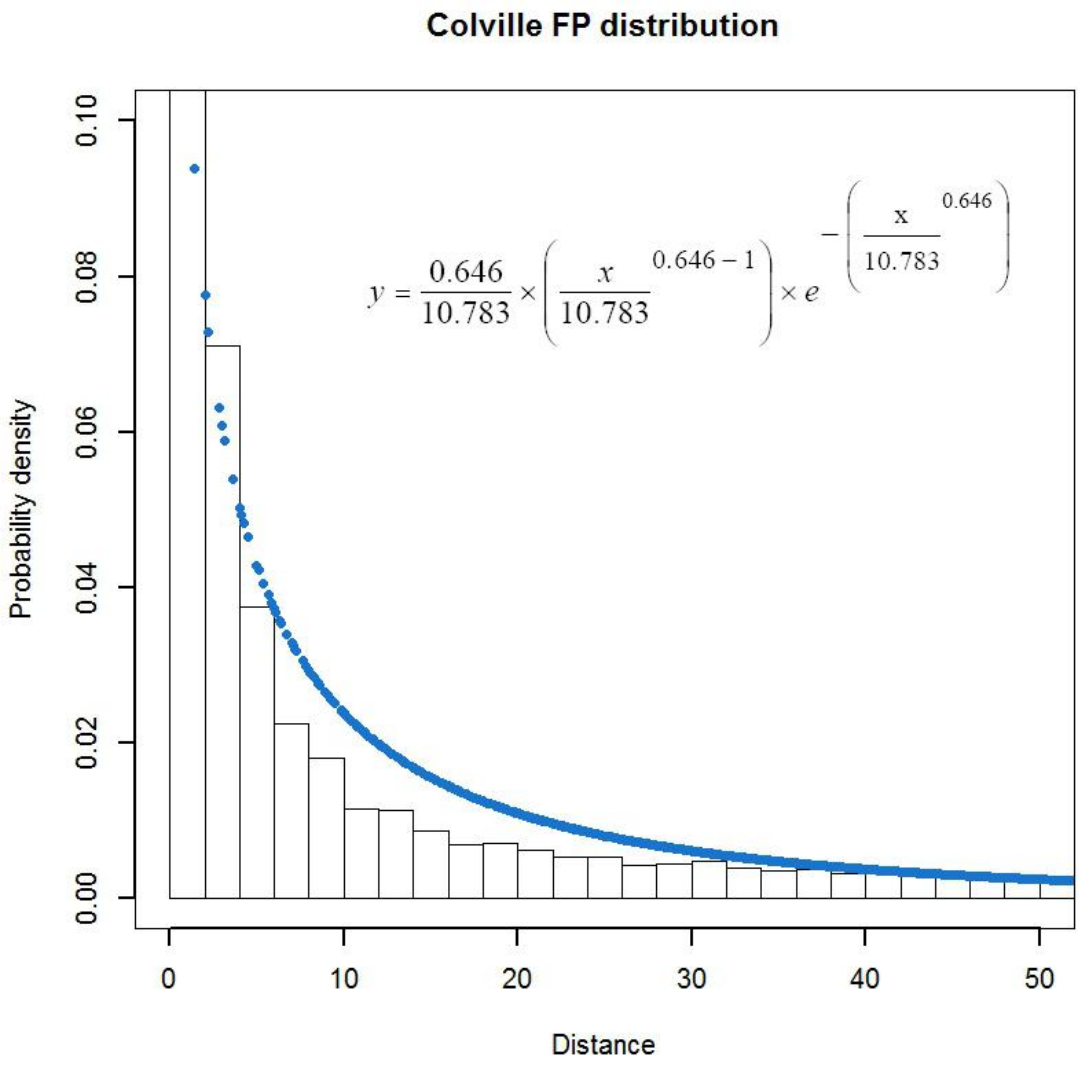

Figure 30: Probability density distribution for the floodplains at the Colville site.

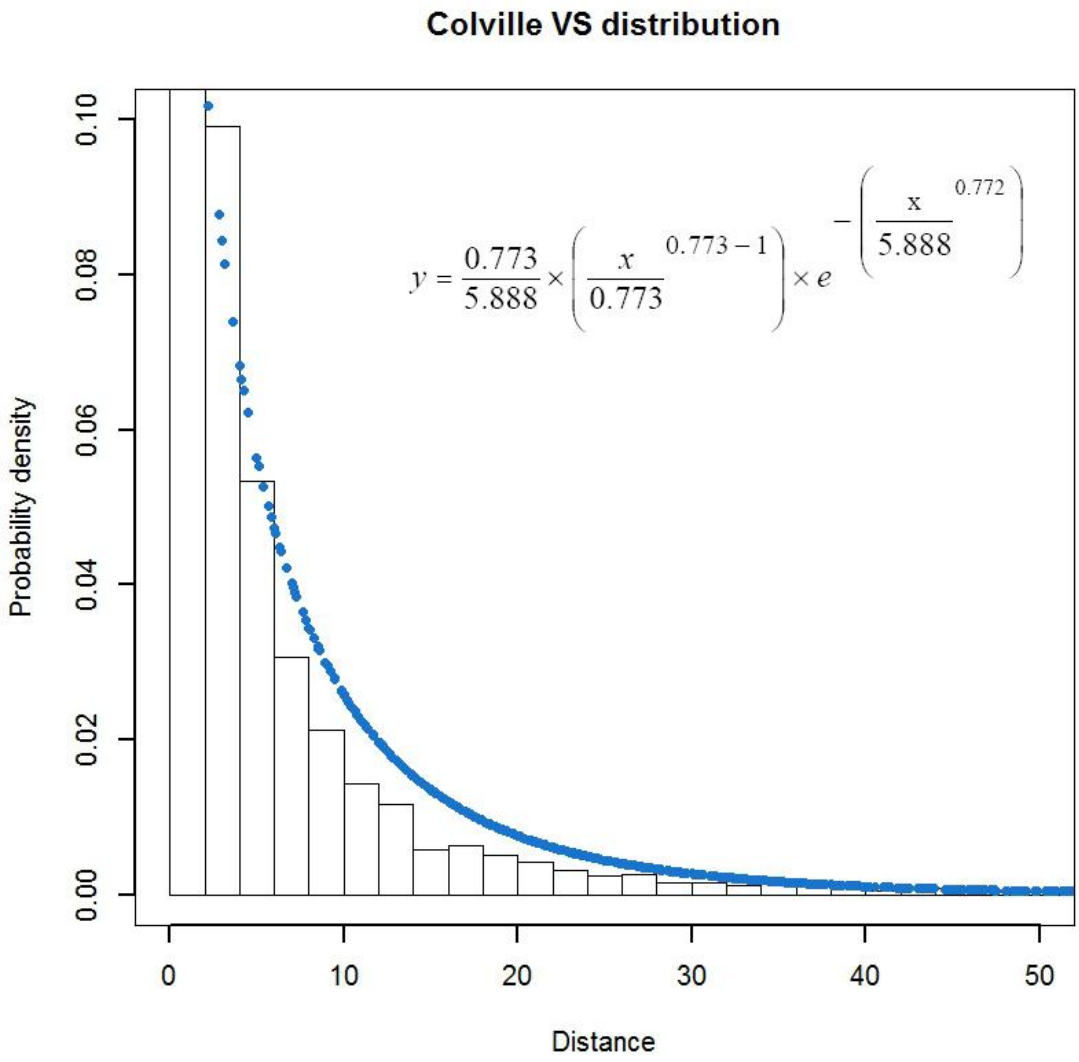

Figure 31: Probability density distribution for the valley slopes at the Colville site.

5.2.4 Data Preparation for Simulations

I assumed that using the entire landscape as the input landscape would introduce too much environmental heterogeneity to identify the potential contribution of reproduction. This would significantly increase both simulation time and computational demands. As a result, I randomly located 3 400 x 400 m map subsets within the floodplain and valley slope geomorphic units within each landscape. These maps then served as the model input (Figure 32-33).

Simulation treatments included clonal reproduction with no "mass effect" (cnm), clonal reproduction with "mass effect" (cme), sexual reproduction using four different maximum distances of 2 m, 5 m, 10 m, and 20 m (s2m, s5m, s10m, and s20m, respectively), and the ubiquitous dispersal. In addition, each of these treatments also involved the consideration of the realized TWI niche. I calculated this by determining the maximum range of TWI values upon which shrubs were found to occur. The range was 3 to 16 for the Ayiyak, and 3 to 17 for Colville. In total, 13 different treatments were simulated.

The model simulated each treatment 30 separate times for the period for which observational data was available (1979 – 2009 for Ayiyak, 1974 – 2008 for Colville). Both the observed landscapes and the 30 landscapes produced during the final year of the simulation from each treatment were quantified using FRAGSTATS. Six pattern metrics were used (Table 2). These metrics have previously been identified as sensitive to pattern at alpine treeline (e.g., Bowersox and Brown 2001; Alftine and Malanson 2004). I averaged these metrics and combined them with the observed results in a

Principal Components Analysis. Results of this analysis were then plotted in two dimensions in ordination space. Simulation results that lie closest to actual conditions in ordination space were considered those that best represent realistic conditions.

Table 2: Description of the pattern metrics used to quantify the spatial pattern of Arctic shrubs.

Abbreviation	Metric	Description
PADENS	Patch density	Density of patches in landscape (patches / ha)
EDENS	Edge density	Number of edge lengths per unit area
CVSIZE	Coefficient of variation of patch size	Standard deviation of patch size divided by mean patch size
SHAPEI	Area-weighted shape index	Average shape index of patches weighted by patch area
FRACTI	Area-weighted fractal dimension index	Average fractal dimension of patches weighted by patch area
MEDIST	Mean Euclidean nearest neighbor distance	Average distance between patches

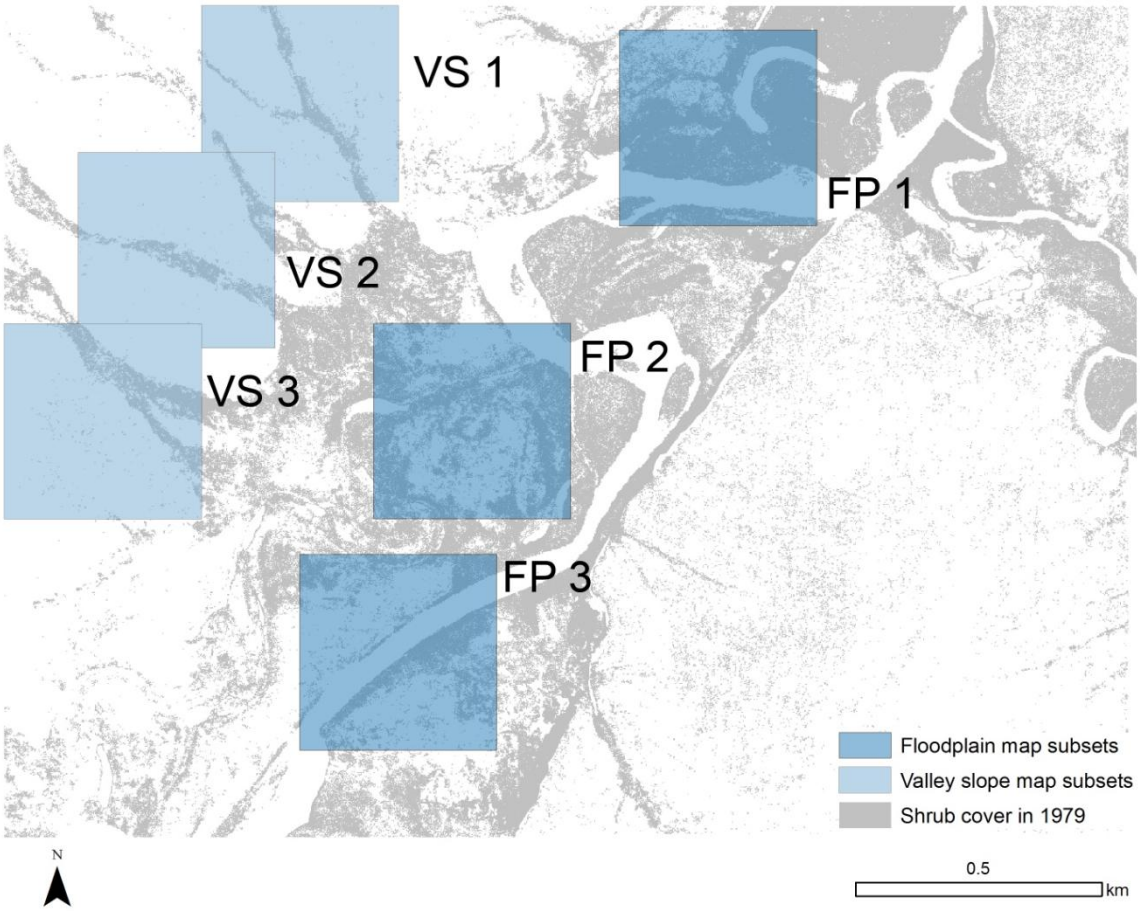

Figure 32: Location of the 400 m x 400 m map subsets at the Ayiyak site overlaid on the full 1979 shrub cover map. FP = Floodplain, VS = Valley Slope

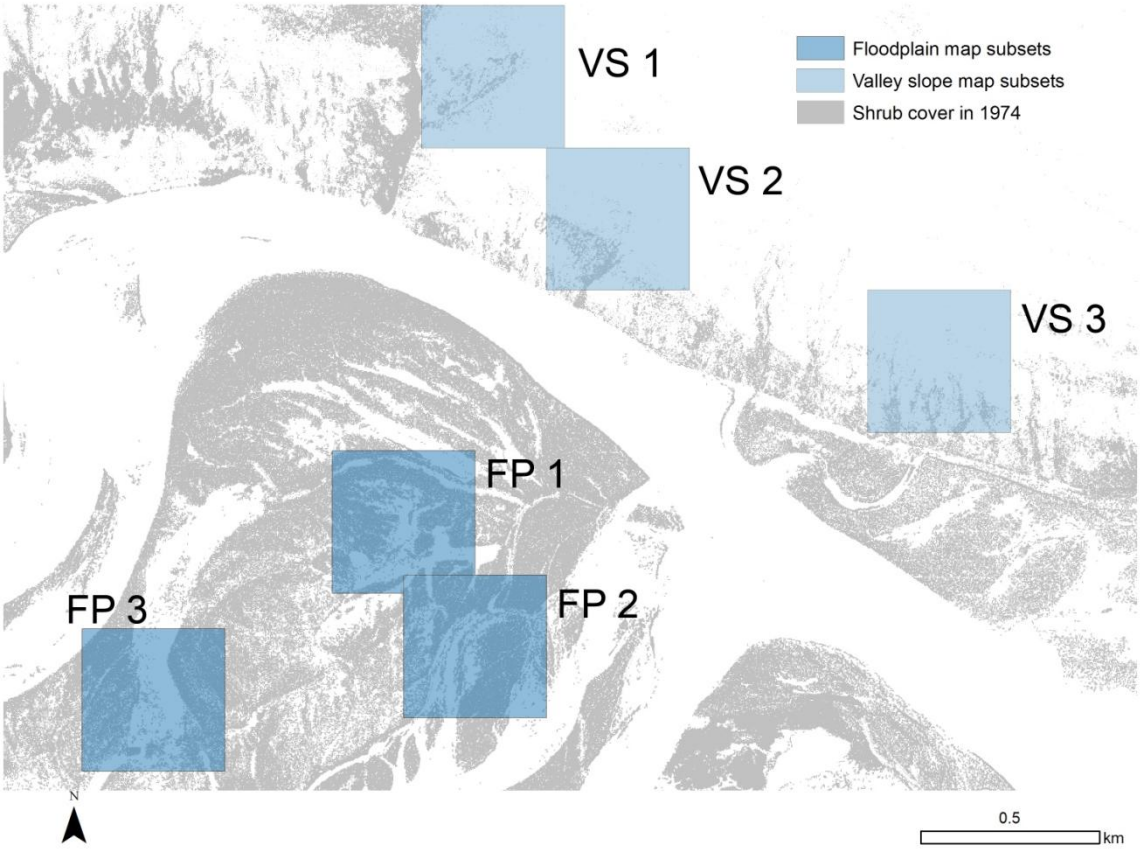

Figure 33: Location of the 400 m x 400 m map subsets at the Colville site overlaid on the full 1979 shrub cover map. FP = Floodplain, VS = Valley Slope

6. RESULTS*

6.1 Pattern Analysis of the Conceptual Landscapes

In the "ecotone" and "phase transition" stages for Case 1, the landscape is highly fragmented for invading shrubs at fine spatial scales (cell sizes ≤ 4 m). At coarser spatial scales, the landscape transitions towards spatial homogeneity. At the coarsest scales, d_I then declines as the irregular distribution of shrubs is sampled (Fig. 34). In the "ecotone" and "phase transition" stages for Case 2, the landscapes are in a state of phase transition at fine spatial scales due to their clumped pattern. At coarser scales, the landscape becomes heterogeneous before transitioning towards spatial homogeneity (Fig. 34). In Case 1, PADENS peaks just before the phase transition period and CVSIZE peaks just after. MEDIST declines throughout the time period, with the greatest decreases occurring between the "fragmented" to "heterogeneous" stages and between the phase transition period and "spatial homogeneity" stages (Fig. 35). In Case 2, PADENS decreases throughout the time period. CVSIZE increases towards the phase transition period and then decreases afterwards. MEDIST also decreases throughout, with the greatest decrease occurring between "fragmented" and "heterogeneous" categories and from "phase transition" to "spatial homogeneity" (Fig. 35). The pattern metrics of the observed landscapes should more closely match that of Case 1.

---

* Part of this section is reprinted with permission from "Relationships between Arctic shrub dynamics and topographically-derived hydrologic characteristics" by Naito, A.T. & Cairns, D.M. 2011. *Environmental Research Letters*, 6(4) : 045506, Copyright [2011] by Institute of Physics. The online abstract is available at http:/iopscience.iop.org/1748-9326/6/4/045506/fulltext/. The Institute of Physics Copyright Policy is available at: http://www.iop.org/copyright/.

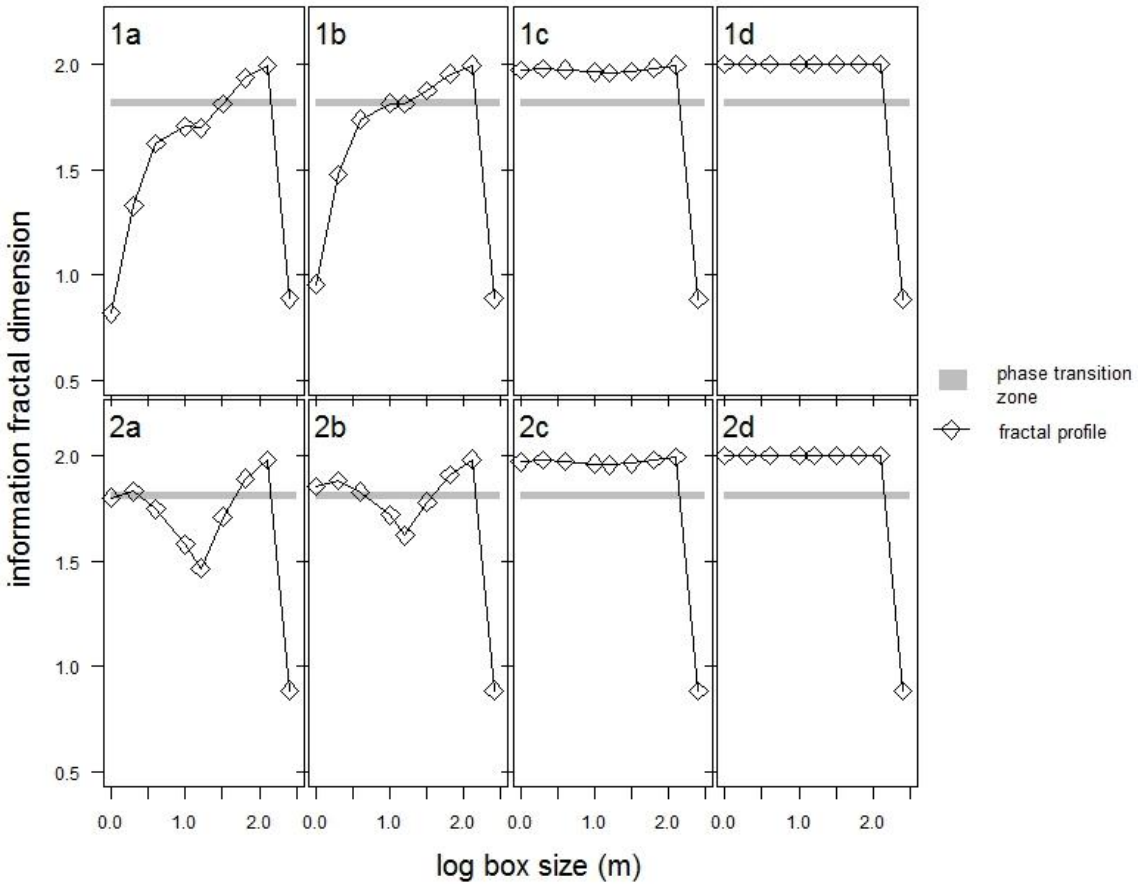

Figure 34: Information fractal dimension (d_I) profiles for the conceptual shrub patch dynamics of landscapes Case 1 and Case 2.

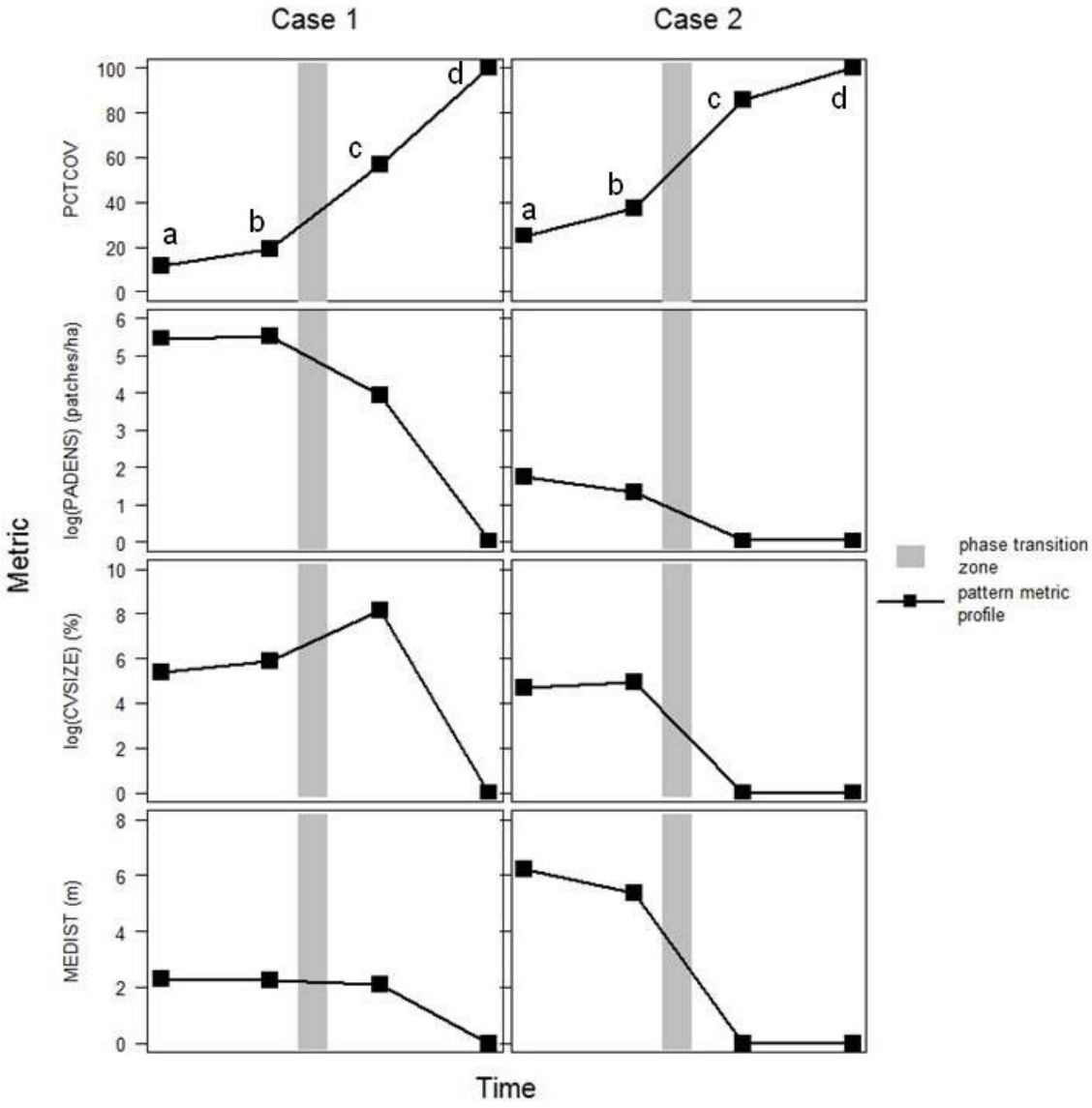

Figure 35: Changes in the pattern metrics of each of the two conceptual landscapes (Case 1 and Case 2) for percent cover (PCTCOV), patch density (PADENS), coefficient of variation of size (CVSIZE), and mean Euclidean nearest neighbor distance between patches (MEDIST). The shaded box approximates a possible phase transition period whereby the d_I ranges from 1.7951 to 1.8286.

6.2 Pattern Analysis of the Observed Landscapes

Net increases in PCTCOV occurred at all nine sites (Table 3 and Figs. 31-33). The average PCTCOV for the two sites in the 1950s was 32.28%. The average PCTCOV in the 1970s was 27.13%, while it was 30.51% in the 1980s. By the 2000s, the average PCTCOV was 34.76%. The greatest percent change in cover for the two landscapes with maps dating from the 1950s onwards occurred at Nanushuk 2 (+79.50%), while the smallest increase occurred at Nanushuk I (+51.08%) The greatest percent change in cover for the seven landscapes with maps dating from the 1970s onwards occurred at Kurupa (+85.03%) while the smallest occurred at Nigu (+22.51%). The average annual percent change in shrub cover for the sites dating from the 1950s was 1.21% /yr. The average annual percent change in shrub cover for the sites dating from the 1970s was 1.29% /yr.

Four sites (Killik, Nanushuk 1 and 2, and Nimiuktuk) exhibited an overall decline in PADENS ranging from -25.00 to -51.70%. The other five sites (Ayiyak, Chandler, Colville, Kurupa, and Nigu) exhibited an increase ranging from 1.75 to 59.72%. Seven (Ayiyak, Chandler, Colville, Killik, Kurupa, Nigu, and Nimiuktuk) exhibited an overall increase in CVSIZE, ranging from 14.75 to 518.28%. In addition, five of the sites (Ayiyak, Chandler, Colville, Killik, Nanushuk 2, and Nigu) exhibited a decrease in MEDIST, ranging from -0.28 to -3.40 m (Table 4 and Figs. 31-33).

With the exception of Colville, the d_I profiles indicate that heterogeneous landscapes are present at fine spatial scales (cell size $\leq$ 2 m). As the cell size increases to

the landscape-scale, the d_I becomes relatively consistent and generally exceeds the critical value for phase transition to occur (Figs. 39-41).

The linear relationship between d_I and PCTCOV is represented in Eq. 12:

$$d_I = 1.785293 + (0.0024580 \times \text{PCTCOV}) \quad (12)$$

$$R^2 = 0.5406, p < 0.001$$

Using the critical d_I values noted by Loehle et al. (1996) and Eq. 12, I calculated the critical PCTCOV for each landscape. (Table 3, Fig. 42). The upper critical d_I value of 1.8286 corresponded to a PCTCOV of 17.62%. Therefore, the PCTCOV value for each landscapes at each observed date exceeded the upper critical value.

Table 3: Median information fractal dimension (d_I) and percent shrub cover (PCTCOV) values for each landscape for each date of observation. By the most recent date of observation, all landscapes have passed through the phase transition zone and are now progressing towards a state of homogeneity.

Site	Year	Median d_I	PCTCOV (%)	TOTAL ΔPCTCOV	TOTAL % ΔPCTCOV
Ayiyak	1979	1.84	27.13	11.21	41.32
	1985	1.85	29.22		
	2009	1.88	38.34		
Chandler	1977	1.84	30.29	9.49	31.33
	1985	1.84	35.68		
	2009	1.96	39.78		
Colville	1975	1.84	24.56	8.56	34.85
	1985	1.86	31.79		
	2008	1.86	33.12		
Killik	1977	1.87	14.11	6.50	46.07
	1982	1.87	13.38		
	2009	1.84	20.61		
Kurupa	1977	1.8	17.30	14.71	85.03
	1985	1.88	32.41		
	2009	1.9	32.01		
Nanushuk 1	1955	1.86	30.66	51.08	51.07
	1978	1.88	38.03		
	2009	1.9	46.32		
Nanushuk 2	1955	1.87	33.9	79.50	79.50
	1978	1.92	50.64		
	2009	1.94	60.85		
Nigu	1977	1.81	25.45	22.51	22.51
	1985	1.81	21.44		
	2008	1.87	31.18		
Nimiuktuk	1977	1.86	27.35	27.09	27.10
	2009	1.91	34.76		
			Median 1950s PCTCOV		**32.28**
			Median 1970s PCTCOV		**27.35**
			Median 1980s PCTCOV		**32.41**
			Median 2000s PCTCOV		**34.76**

Table 4: Changes in pattern metrics PADENS (patches per ha), CVSIZE (coefficient of variation of patch size), and MEDIST (mean Euclidean nearest neighbor distance) at each of the nine sites. Although all sites are progressing from phase transition, the response in pattern metrics is variable from site to site.

Site	Year	PADENS (patches / ha)	CVSIZE (%)	MEDIST (m)
Ayiyak	1979	30.79	4039.17	3.65
	1985	50.47	3081.49	3.03
	2009	37.60	6093.04	3.37
Chandler	1977	27.61	3955.37	3.45
	1985	27.98	5459.91	3.29
	2009	57.79	7652.64	2.65
Colville	1975	11.89	4503.59	4.59
	1985	3.09	2357.68	5.06
	2008	13.64	6269.50	5.38
Killik	1977	66.80	4068.16	3.02
	1982	58.84	3383.77	2.91
	2009	38.95	7008.75	3.54
Kurupa	1977	24.76	5171.26	4.28
	1985	35.47	4912.48	3.36
	2009	30.50	7663.05	3.46
Nanushuk 1	1955	55.40	5421.97	2.67
	1978	77.48	4104.99	2.60
	2009	30.40	4255.65	2.96
Nanushuk 2	1955	76.98	13053.56	2.73
	1978	36.03	4974.07	2.43
	2009	26.53	6173.59	2.50
Nigu	1977	11.52	2366.66	6.18
	1985	33.28	3666.19	3.62
	2008	71.25	6696.34	2.77
Nimiuktuk	1977	148.65	8846.05	2.37
	2009	96.95	9577.23	2.55

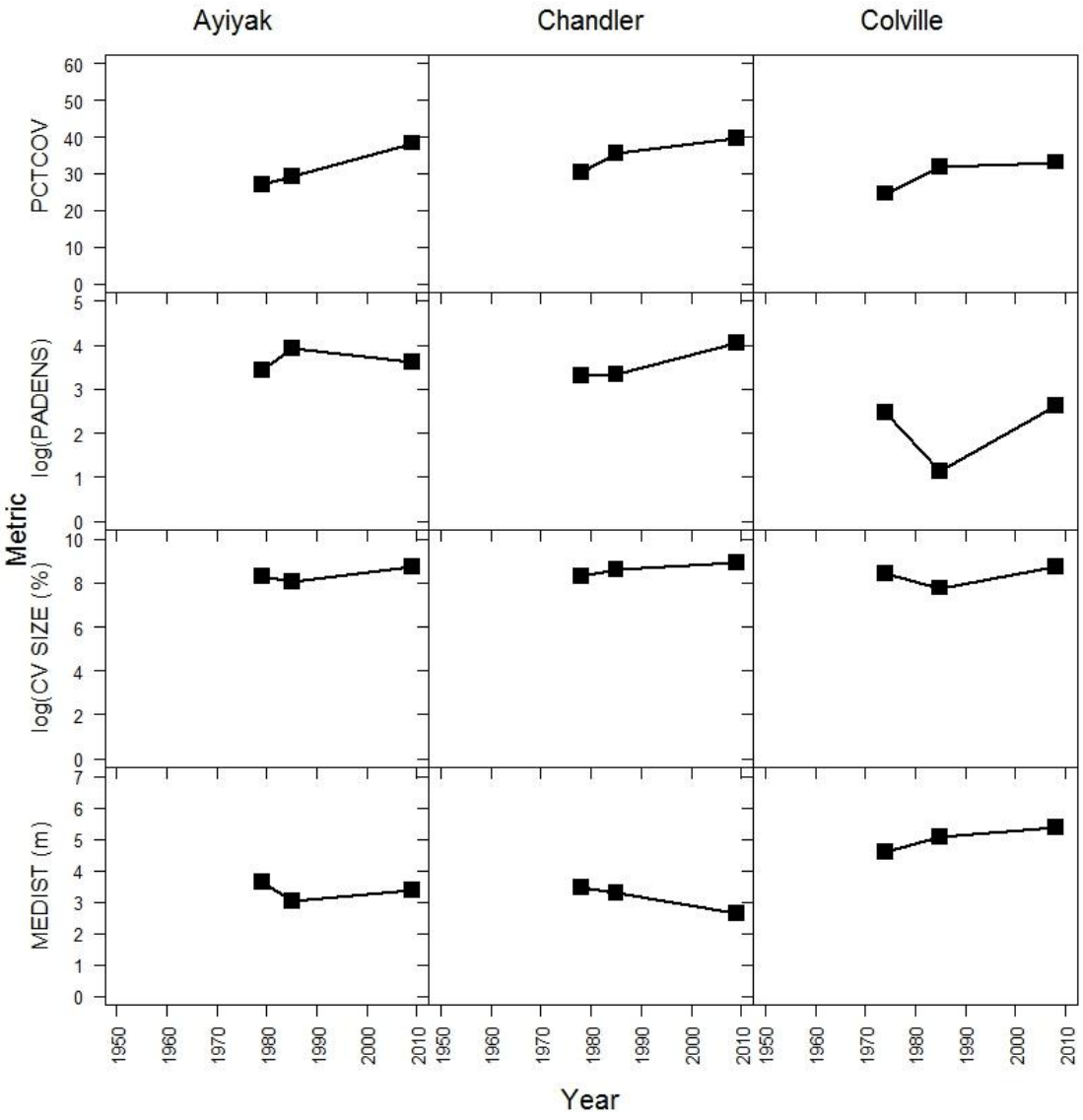

Figure 36: Change in pattern metrics PCTCOV (percent shrub cover), PADENS (patch density), CVSIZE (coefficient of variation of patch size), and MEDIST (mean Euclidean nearest neighbor distance) of the Ayiyak, Chandler, and Colville sites.

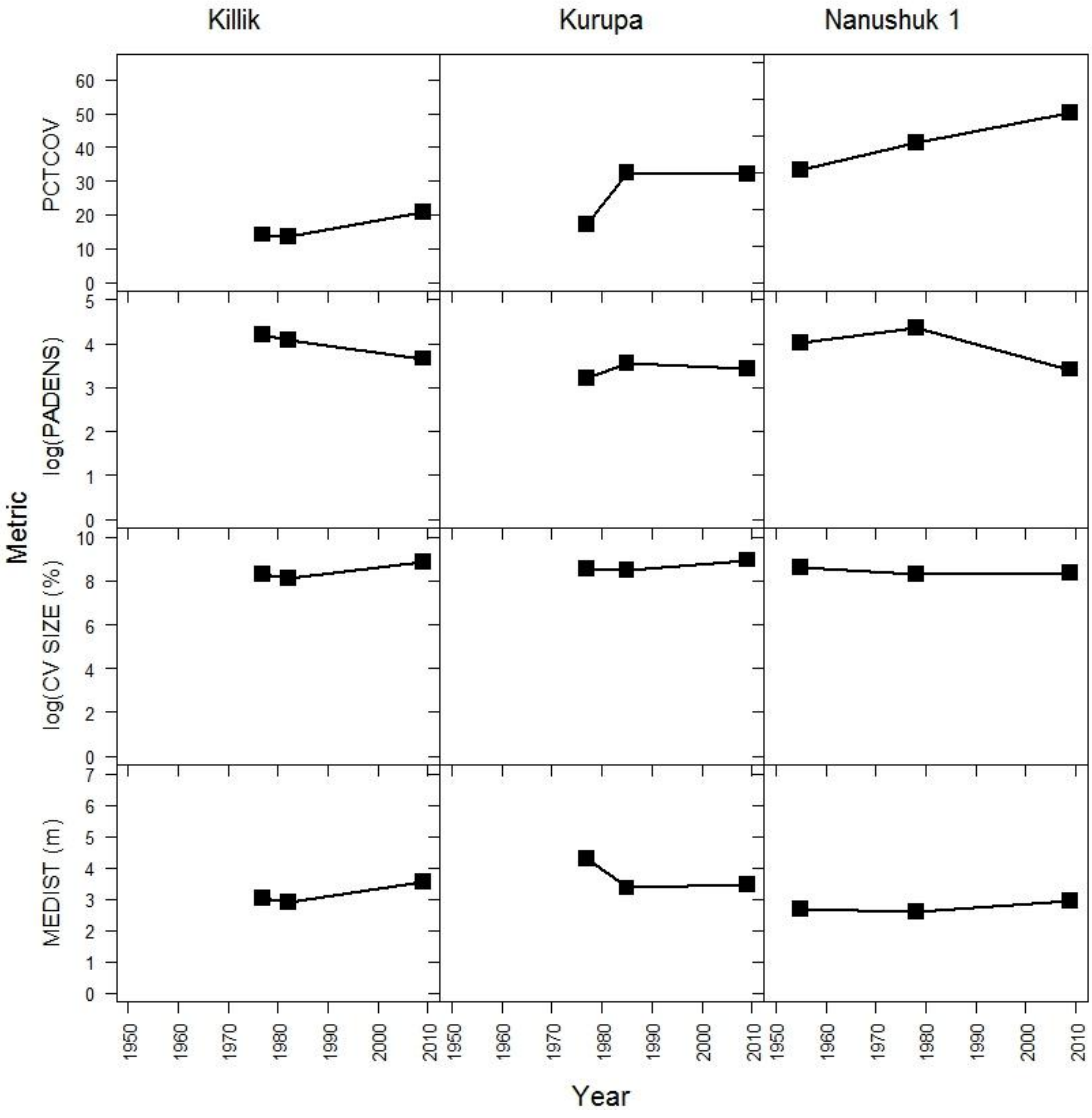

Figure 37: Change in pattern metrics PCTCOV (percent shrub cover), PADENS (patch density), CVSIZE (coefficient of variation of patch size), and MEDIST (mean Euclidean nearest neighbor distance) of the Killik, Kurupa, and Nanushuk 1 sites.

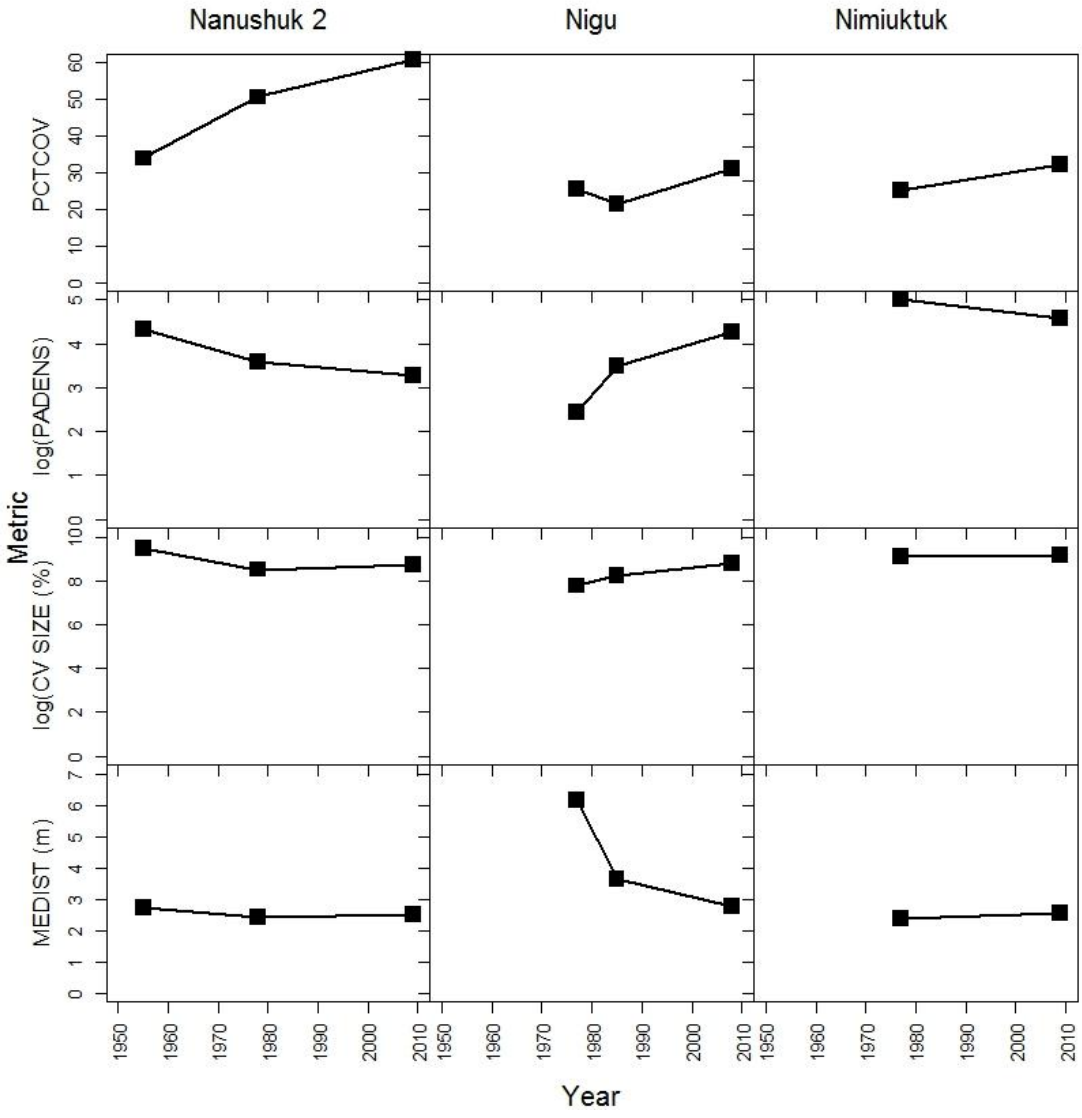

Figure 38: Change in pattern metrics PCTCOV (percent shrub cover), PADENS (patch density), CVSIZE (coefficient of variation of patch size), and MEDIST (mean Euclidean nearest neighbor distance) of the Nanushuk 2, Nigu, and Nimiuktuk sites.

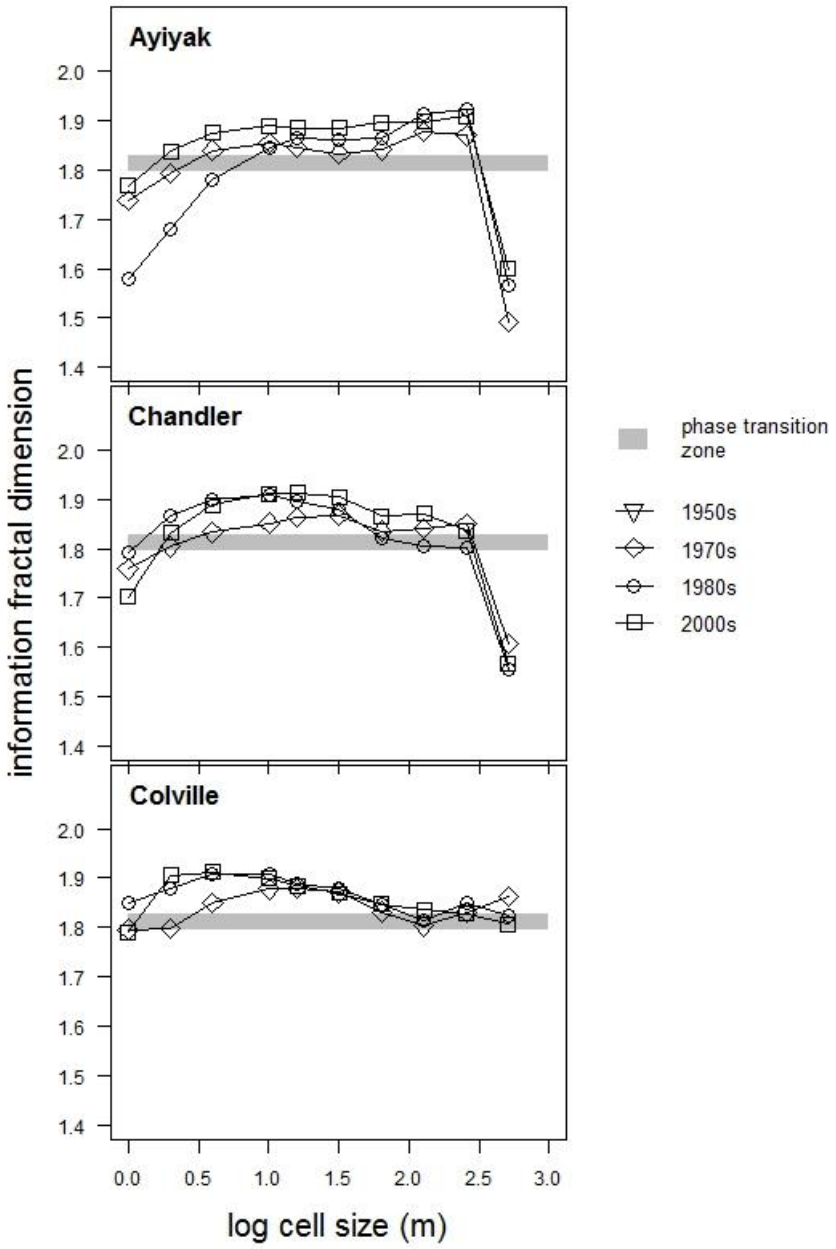

Figure 39: Information fractal dimension (d_I) profiles for Ayiyak, Chandler, and Colville sites.

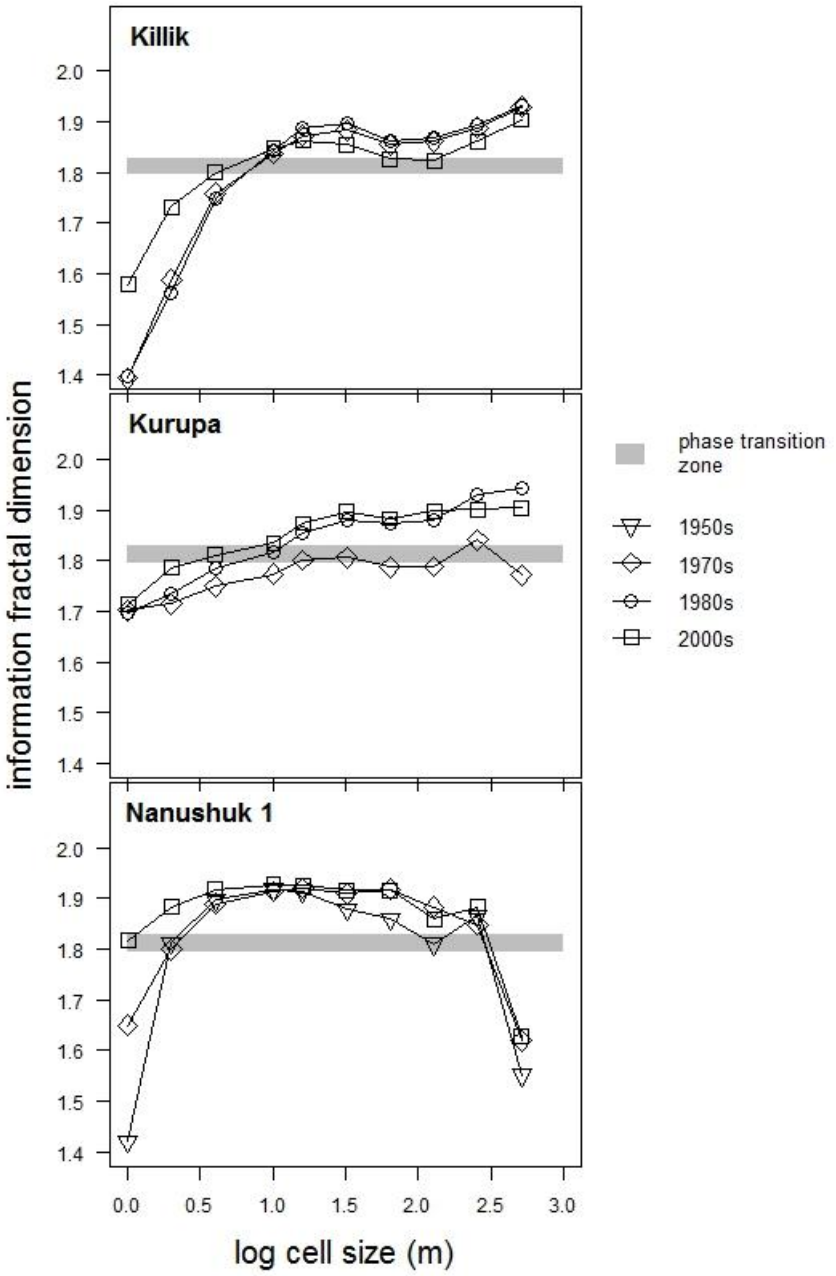

Figure 40: Information fractal dimension (d_I) profiles for Killik, Kurupa, and Nanushuk 1 sites.

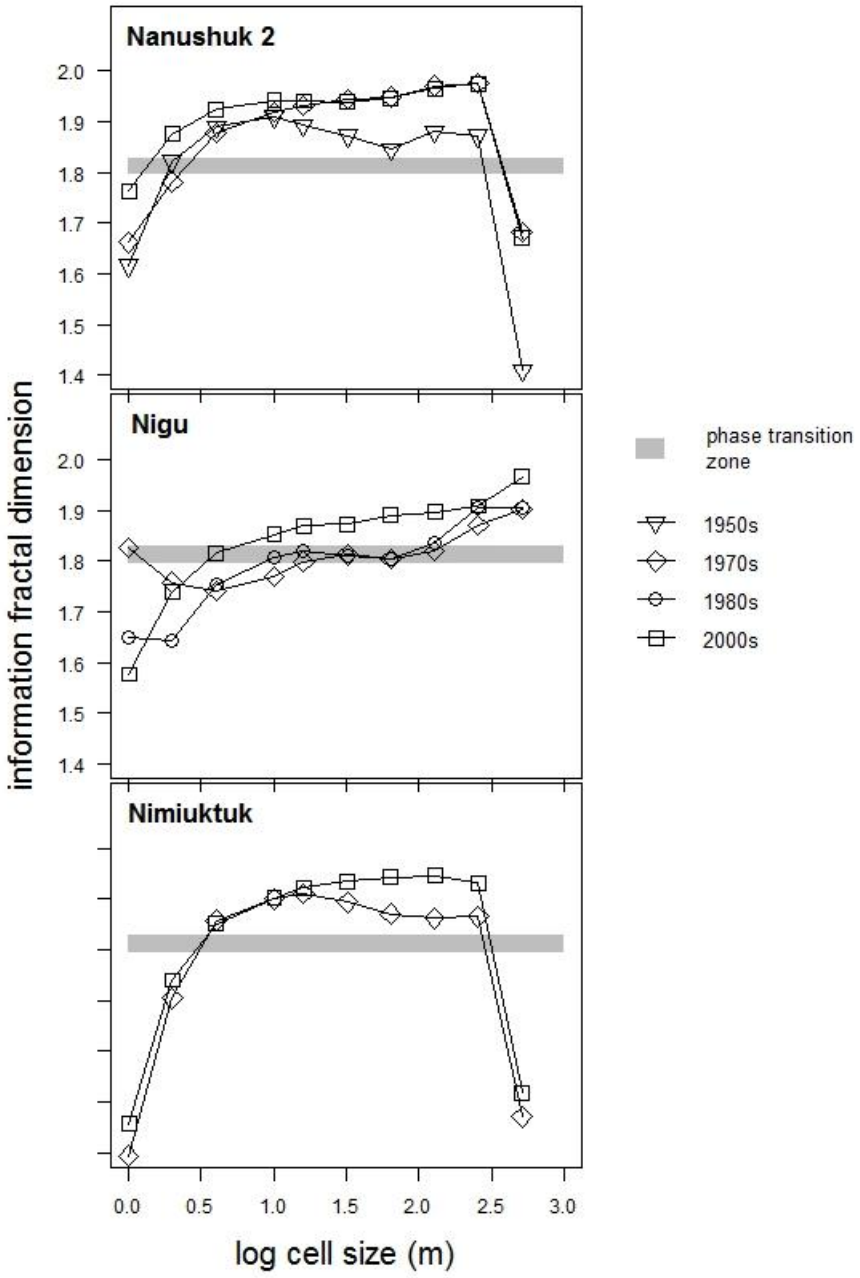

Figure 41: Information fractal dimension (d_I) profiles for Nanushuk 2, Nigu, and Nimiuktuk sites.

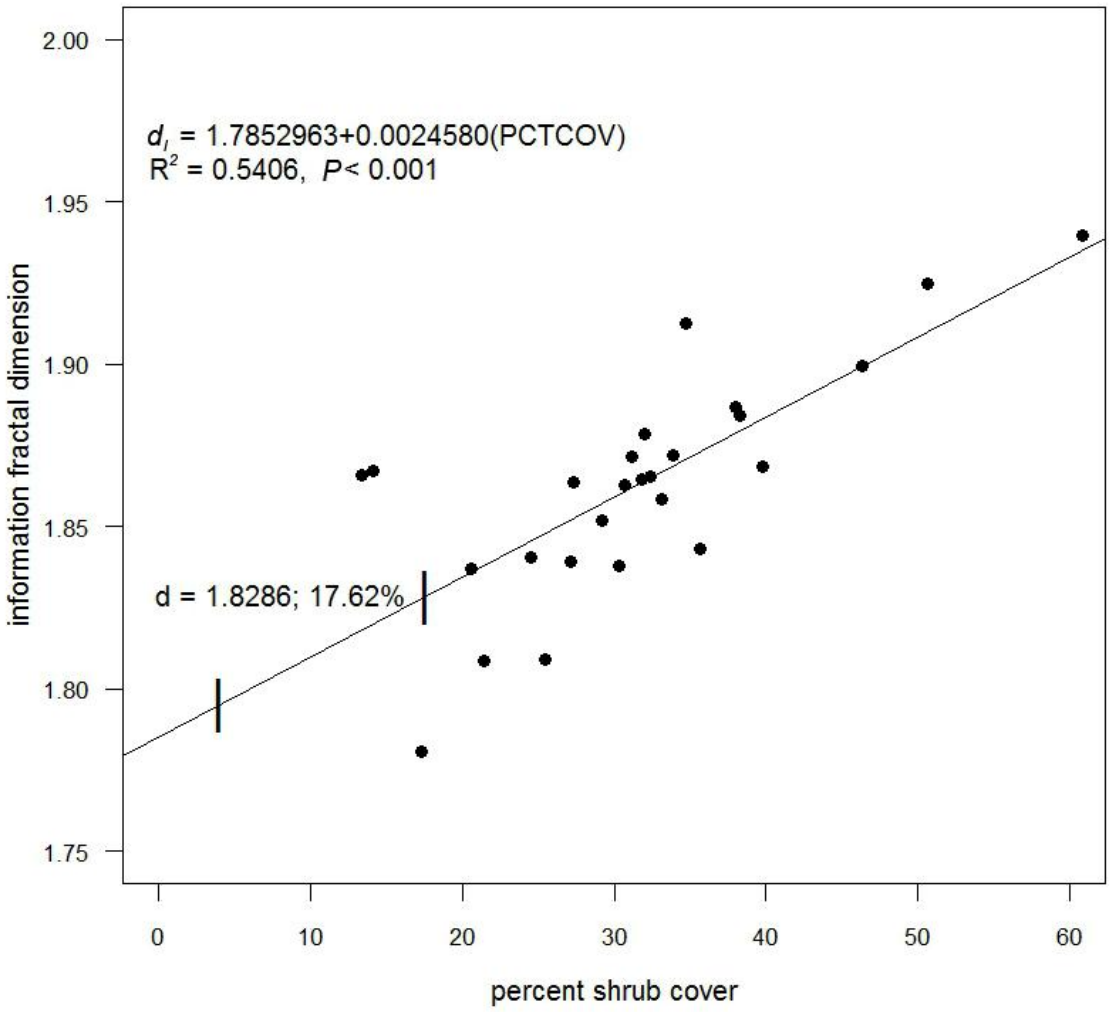

Figure 42: Scatterplot demonstrating the relationship of the information fractal dimension (d_I) for each site at each observed year with their corresponding percent shrub cover (PCTCOV). The regression line equation is d_I =1.7852963+0.0024580(PCTCOV). The vertical lines superimposed on the regression line represent the coordinates of the critical d_I values, with the upper critical value of 1.8286 and its corresponding PCTCOV labeled. All sites at all years meet or exceed this upper critical value.

6.3 Relationships Between Shrub Expansion and Hydrologic Characteristics

6.3.1 Changes in Shrub Cover

Four out of the five sites experienced an increase in shrub cover, while one site experienced a subtle decrease. An increase in shrub cover within floodplains also occurred within all five areas, and ranged from +3.38% (Nanushuk 1) to +76.22% (Nimiuktuk) (Table 4).

6.3.2 Association Between Shrub Cover Changes and TWI

Of the 10,000 total sampled points in the five examined areas, 14.9% underwent an increase in shrub cover (conversion from tundra to shrub), 12.42% underwent a decrease (conversion from shrub to tundra), and 72.68% experienced no change (10.76% in shrub to shrub, and 61.92% tundra to tundra) (Table 5 and Fig. 43). All frequency distributions of TWI values in each study area were non-normally distributed ($Ks = 0.1655$, $p < 0.01$). The Kruskal-Wallis rank-sum test highlighted statistically significant differences among the categories ($\chi^2 = 17.07$, $p = 0.0002$). Post-hoc Wilcoxon rank sum tests determined that TWI frequency distributions for sampled points that gained shrub cover were significantly higher than those that lost cover ($Z = 2.1006$, $p=0.0178$) as well as those experiencing no change ($Z = 4.1085$, $p < 0.01$).

6.3.3 Association Between Floodplain Shrub Dynamics and Fluvial Characteristics

Binomial logistic regression of variables related to shrub cover, TWI values, and river channel characteristics suggests a relationship between the development of floodplain shrubs and migration of the river channel (Table 5). The difference in distance between sampled shrubs and the location of the nearest river bank (Wald χ^2 = 10.12, p = 0.0001) and the TWI value (Wald χ^2 = 6.22, p = 0.005) provide the greatest explanatory power. The floodplain TWI values ranged from 4 to 18, with a median value of 8. The median distance between river bank and shrub cover decreased from 54.47 m in the 1970s to 37.71 m in the late 2000s. Differences in river channel width were not significant.

Table 5: Change in area of shrub patches between years. Percent of change and annual per cent rate of change in cover between years is provided in the bold columns.

Study area	Total area of shrubs (ha)		% change shrub cover	Annual % change
	1970s	2000s		
Colville	274.17	361.59	**31.89**	**0.94**
Killik	241.14	353.43	**46.56**	**1.5**
Nanushuk 1	103.26	102.59	**-0.65**	**-0.02**
Nanushuk 2	129.79	166.65	**28.4**	**0.89**
Nimiuktuk	252.89	287.25	**13.59**	**0.41**
Study area	**Total area of floodplain shrubs (ha)**		**% change shrub cover**	**Annual % change**
	1970s	2000s		
Colville	188.28	224.04	**19**	**0.56**
Killik	29.34	42.89	**46.17**	**1.49**
Nanushuk 1	52.92	54.71	**3.38**	**0.12**
Nanushuk 2	60.8	93.09	**53.1**	**1.66**
Nimiuktuk	62.29	109.77	**76.22**	**2.31**

Table 6: Model statistics for the generalized linear model using logistic regression. The GLM formula is indicated by: GLNC ~ DIFF.DIST + TWI + WIDTH.1970 + DIFF.WID, where GLNC represents the value for shrub cover change (−1, 0, 1), DIFF.DIST represents the difference in the distance between shrubs and the river bank between the 1970s and 2000s, TWI is the topographic wetness index value, WIDTH.1970 is the width of the river bank in 1970, and DIFF.WID is the difference in the width of the river channel between the 1970s and 2000s. SE represets standard error, and *df* represents degrees of freedom.

Coefficients				
Variable	**Value**	**SE**	**t-value**	
DIFF.DIST	0.00	0.00	3.18	
TWI	0.07	0.03	2.49	
WIDTH.1970	0.00	0.00	0.50	
DIFF.WID	0.00	0.00	-0.07	
Analysis of deviance				
Variable	**Deviance**	**Residual df**	**Residual deviance**	**p**
DIFF.DIST	14.60	1044.00	1425.50	0.0001
TWI	7.62	1043.00	1417.88	0.0058
WIDTH.1970	1.66	1042.00	1416.22	0.1974
DIFF.WID	0.00	1041.00	1416.22	0.9474

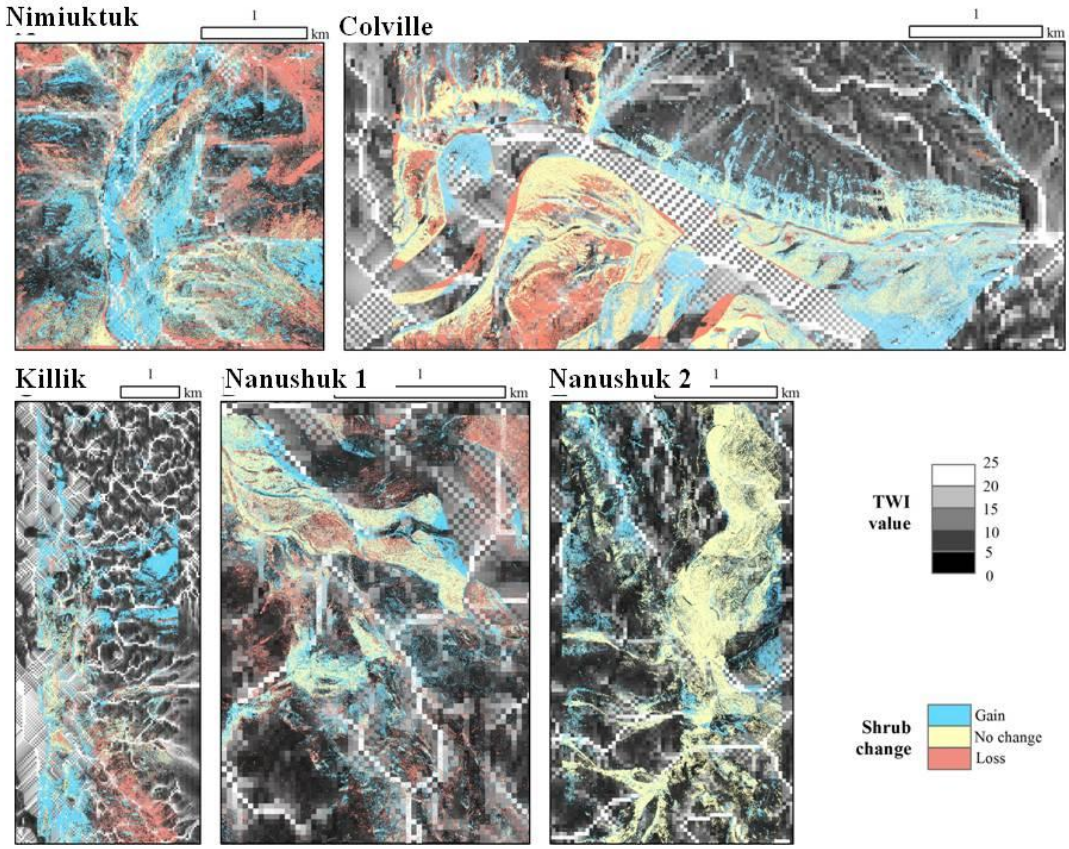

Figure 43: Maps of each of the five study areas detailing TWI values in relation to change in shrub cover between the 1970s and 2000s. Note the areas classified as 'gain' are generally spatially associated with areas of high TWI values. Such values typically occur in drainage channels or flatlands.

6.4 Contribution of Clonal or Sexual Reproduction to Observed Patterns of Expansion

6.4.1 Ayiyak Floodplain Maps

I generated biplots for each PCA analysis on the 3 400 x 400 m subset maps (Fig. 44-46). As I expected, the clonal modes were generally grouped on the opposite side of the biplot as the sexual modes. The metrics calculated from the sexual modes were generally highly clustered at all quadrat sizes In terms of differences in distance in ordination space, the observed results were generally closest to the clonal reproductive modes. While the scores for the clonal parameters are generally similar to the observed on principal components axis 1, they vary considerably with respect to principal components axis 2. There were very little differences in the results between the sexual reproduction modes and the ubiquitous modes, owing to the high degree of clustering in ordination space. Separation only occurred at broader scales. The first eigenvalue for the first principal component explained between 55 and 78% of the variance. There was no clear association with any one specific treatment or pattern metric (Tables 7 and 8).

6.4.2 Ayiyak Valley Slope Maps

I generated biplots for each PCA analysis on the 3 400 x 400 m subset maps (Fig. 47-49). As expected, the clonal modes were generally grouped on the opposite side of the biplot as the sexual modes. The metrics calculated from the sexual modes were generally highly clustered. In terms of differences in distance in ordination space, the observed results were generally much closer to the clonal reproductive modes in

comparison to the floodplain sections. There were very little differences in the results between the sexual reproduction modes and the ubiquitous modes, owing to the high degree of clustering in ordination space. The first eigenvalue for the first principal component explained between 61 and 81% of the variance. With the exception of MEDIST, there was no clear association with any one or two specific pattern metric (Tables 9 and 10)

Based upon the calculation of distances in ordination space between the observed results and the other treatments, clonal or very short distance dispersal appears to create patterns most similar to the observed patterns in the Ayiyak landscape (Table 11).

6.4.3 Colville Floodplain Maps

I generated biplots for each PCA analysis on the 3 400 x 400 m subset maps (Fig. 50-52). In general, the clonal modes maintained a separation from the sexual modes and were closest to the observed results. Again, the sexual modes maintained a high degree of clustering and were not usually associated with the observed results. The first eigenvalue for the first principal component explained between 53 and 83% of the variance. There was no clear association with any one or two specific pattern metric (Tables 12 and 13). MEDIST is the only metric that is consistently positively correlated with the first axis.

6.4.4 Colville Valley Slope Maps

I generated biplots for each PCA analysis on the 3 400 x 400 m subset maps (Fig. 53-55). The clonal modes continued to maintain separation from the sexual modes. The metrics calculated from the sexual modes were generally highly clustered. In terms of differences in distance in ordination space, the observed results were generally much closer to the clonal reproductive modes in comparison to the floodplain sections. There were very little differences in the results between the sexual reproduction modes and the ubiquitous modes, owing to the high degree of clustering in ordination space. The first eigenvalue for the first principal component explained between 49 and 75% of the variance. Once again, there was no clear association with any one or more specific pattern metrics (Tables 14 and 15). MEDIST continues to maintain a relatively high (~50%) correlation with the first principal component.

Based upon the calculation of distances in ordination space between the observed results and the other treatments, clonal or very short distance dispersal appears to create patterns most similar to the observed patterns in the Colville landscape (Table 16).

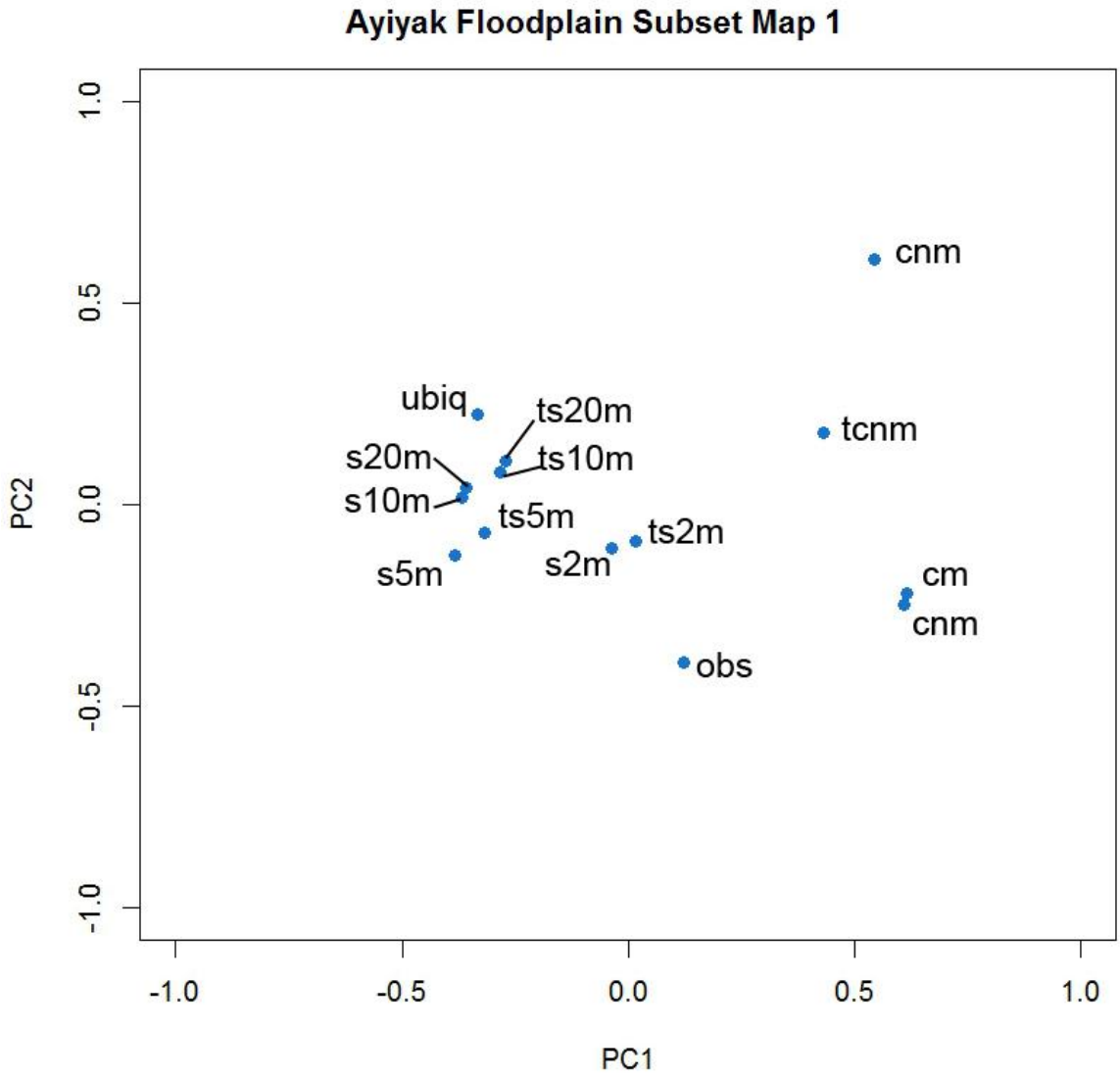

Figure 44: Biplot of the PCA analysis for Ayiyak Floodplain Subset Map 1. In general, the clonal reproductive parameters and sexual reproductive parameters load on opposite ends of principal components axis 1 (PC 1). The observed results scores on PC 1 are also similar to those for the clonal reproductive parameters.

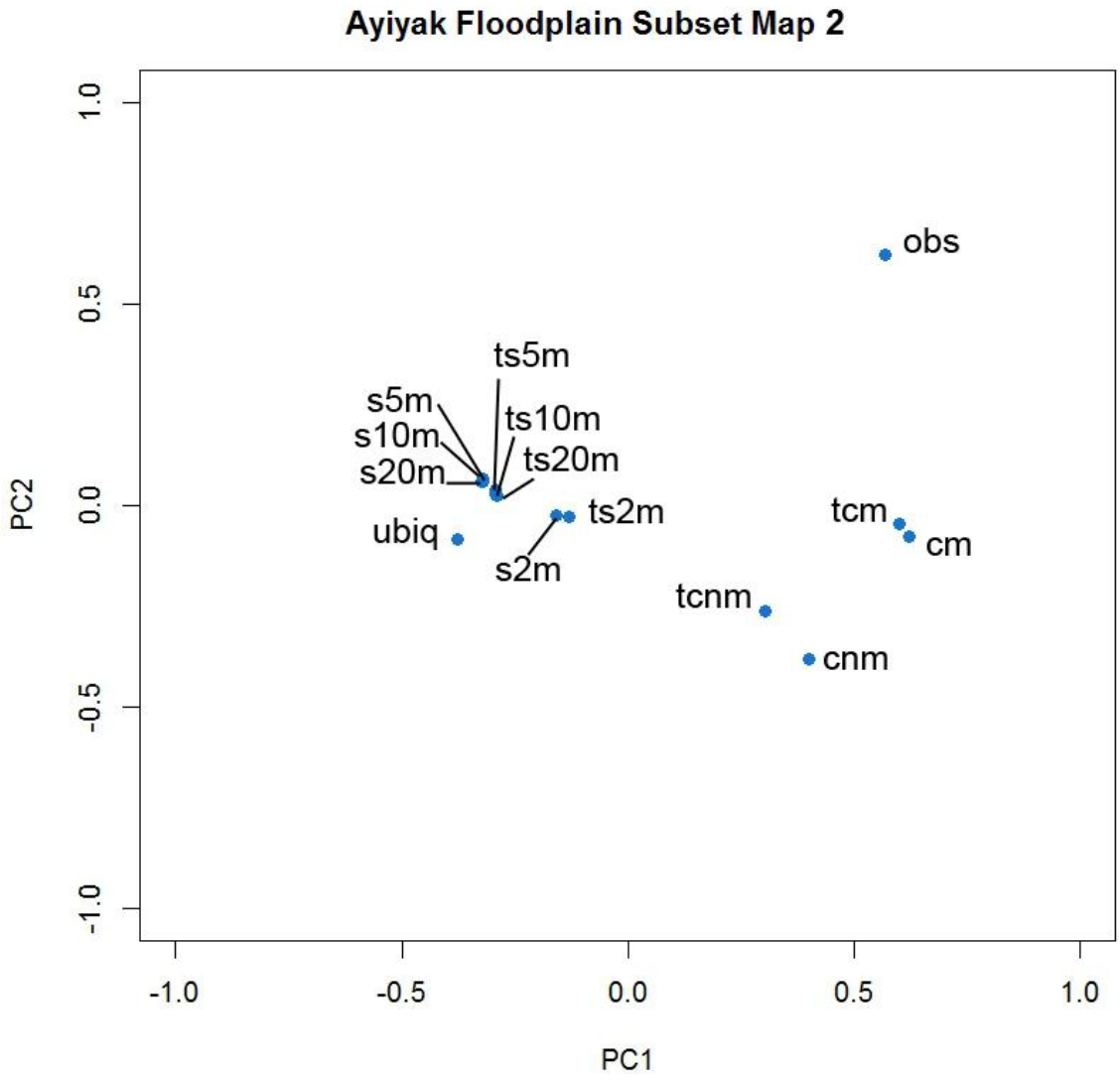

Figure 45: Biplot of the PCA analysis for Ayiyak Floodplain Subset Map 2. In general, the clonal reproductive parameters and sexual reproductive parameters load on opposite ends of principal components axis 1 (PC 1). The observed results scores on PC 1 are also similar to those for the clonal reproductive parameters.

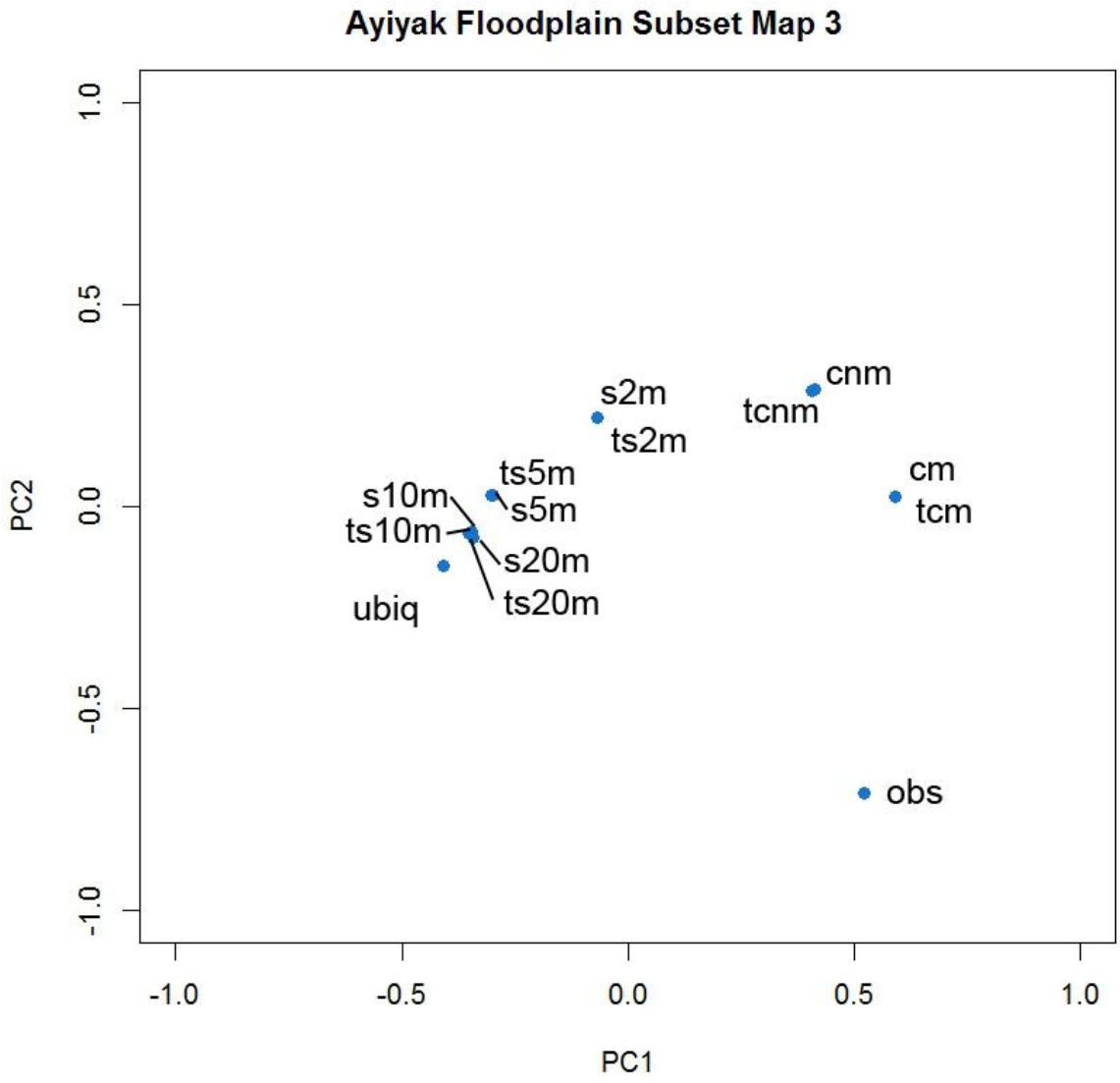

Figure 46: Biplot of the PCA analysis for Ayiyak Floodplain Subset Map 3. In general, the clonal reproductive parameters and sexual reproductive parameters load on opposite ends of principal components axis 1 (PC 1). The observed results scores on PC 1 are also similar to those for the clonal reproductive parameters.

Table 7: Cumulative variance of the first three components of the PCA analyses for the three Ayiyak floodplain maps. FP = Floodplain

	Ayiyak FP 1		**Ayiyak FP 2**		**Ayiyak FP 3**	
Axis	Eigenvalue	Cumulative % of variance	Eigenvalue	Cumulative % of variance	Eigenvalue	Cumulative % of variance
1	4.26	66.24	3.97	66.24	3.83	62.71
2	1.21	94.59	1.70	94.59	1.55	88.05
3	0.48	99.08	0.27	99.08	0.52	97.24

Table 8: First two eigenvectors for the six pattern metrics produced by the PCA analyses for the three Ayiyak floodplain maps. See Table 2 for a description of each of the pattern metrics. FP = Floodplain.

	Ayiyak FP 1		**Ayiyak FP 2**		**Ayiyak FP 3**	
Metric	**V1**	**V2**	**V1**	**V2**	**V1**	**V2**
PADENS	-0.40	-0.37	-0.10	-0.72	-0.42	-0.36
EDENS	-0.47	0.24	-0.48	0.03	-0.50	0.03
CVSIZE	-0.45	-0.28	-0.47	-0.17	-0.49	-0.17
SHAPEI	-0.41	0.40	-0.45	0.35	-0.29	0.60
FRACTI	-0.44	0.36	-0.45	0.33	0.19	-0.67
MEDIST	0.24	0.66	0.37	0.47	0.46	0.17

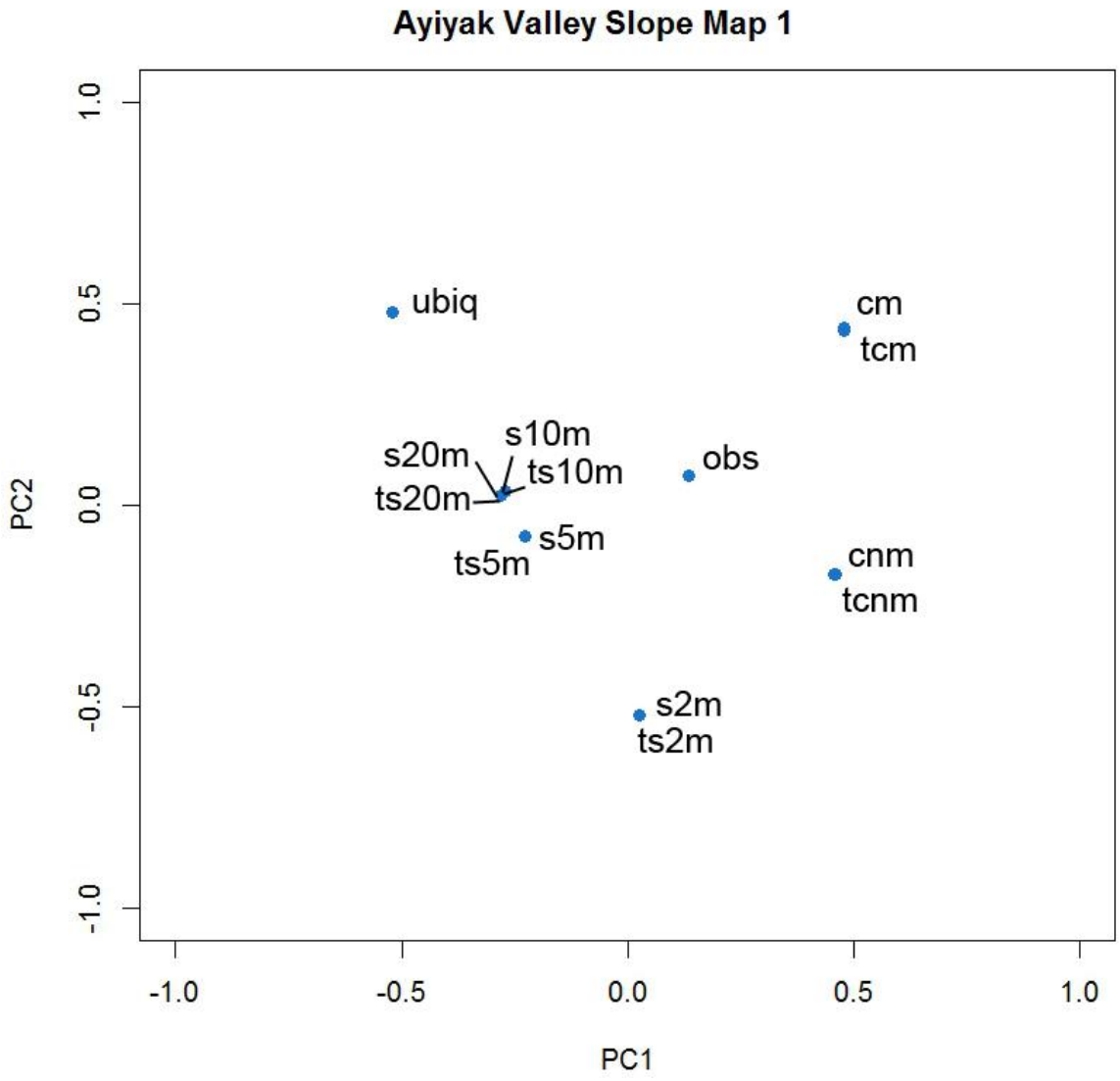

Figure 47: Biplot of the PCA analysis for Ayiyak Valley Slope Subset Map 1. There is now less of a clear separation between clonal and sexual reproductive modes. The scores for the observed results are generally similar to those of the clonal modes and very short distance (2 m) dispersal at small scales. At larger scales, there is greater similarity to the clonal reproductive modes.

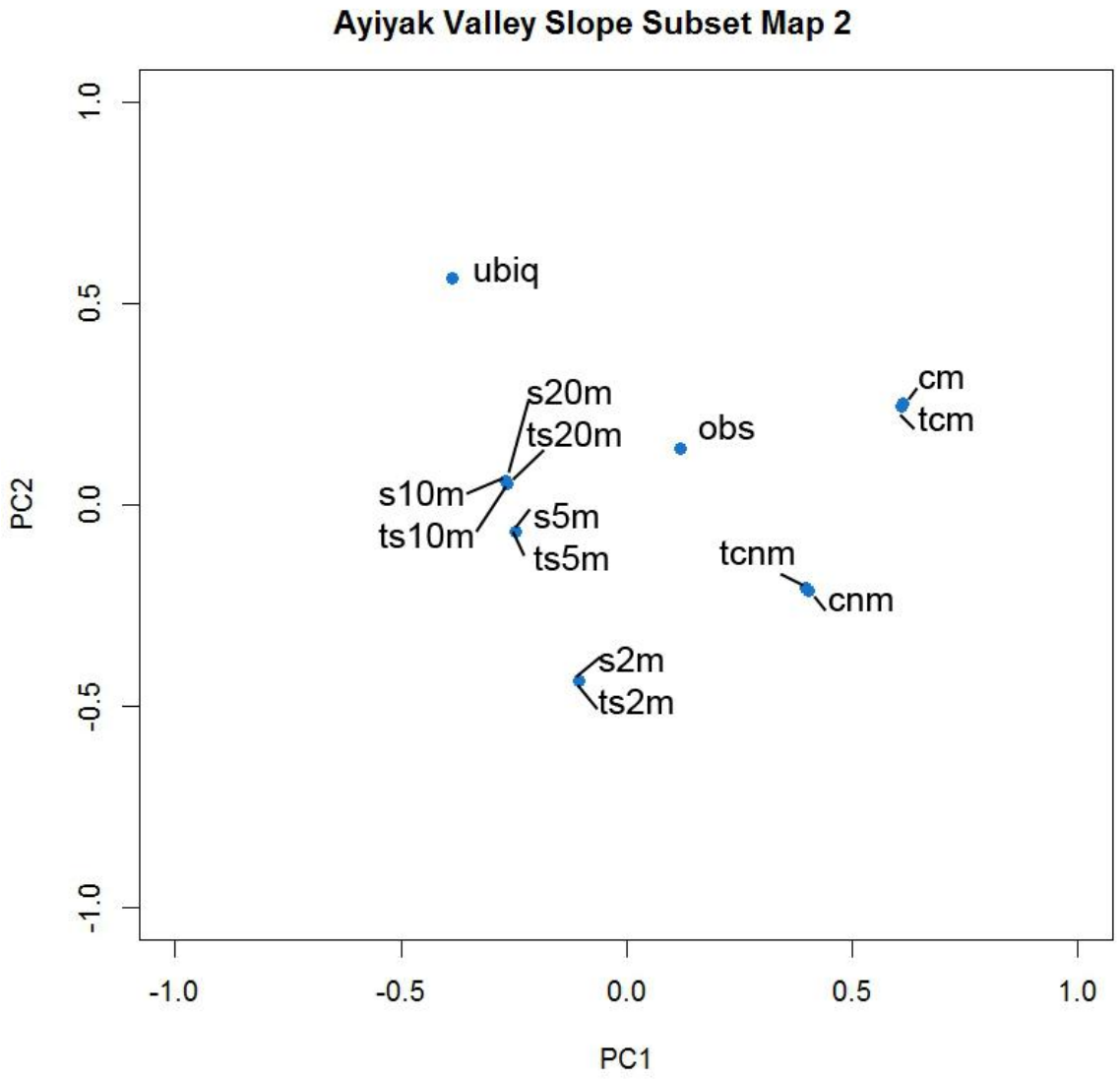

Figure 48: Biplot of the PCA analysis for Ayiyak Valley Slope Subset Map 2. There is now less of a clear separation between clonal and sexual reproductive modes. The scores for the observed results are generally similar to those of the clonal modes and very short distance (2 m) dispersal.

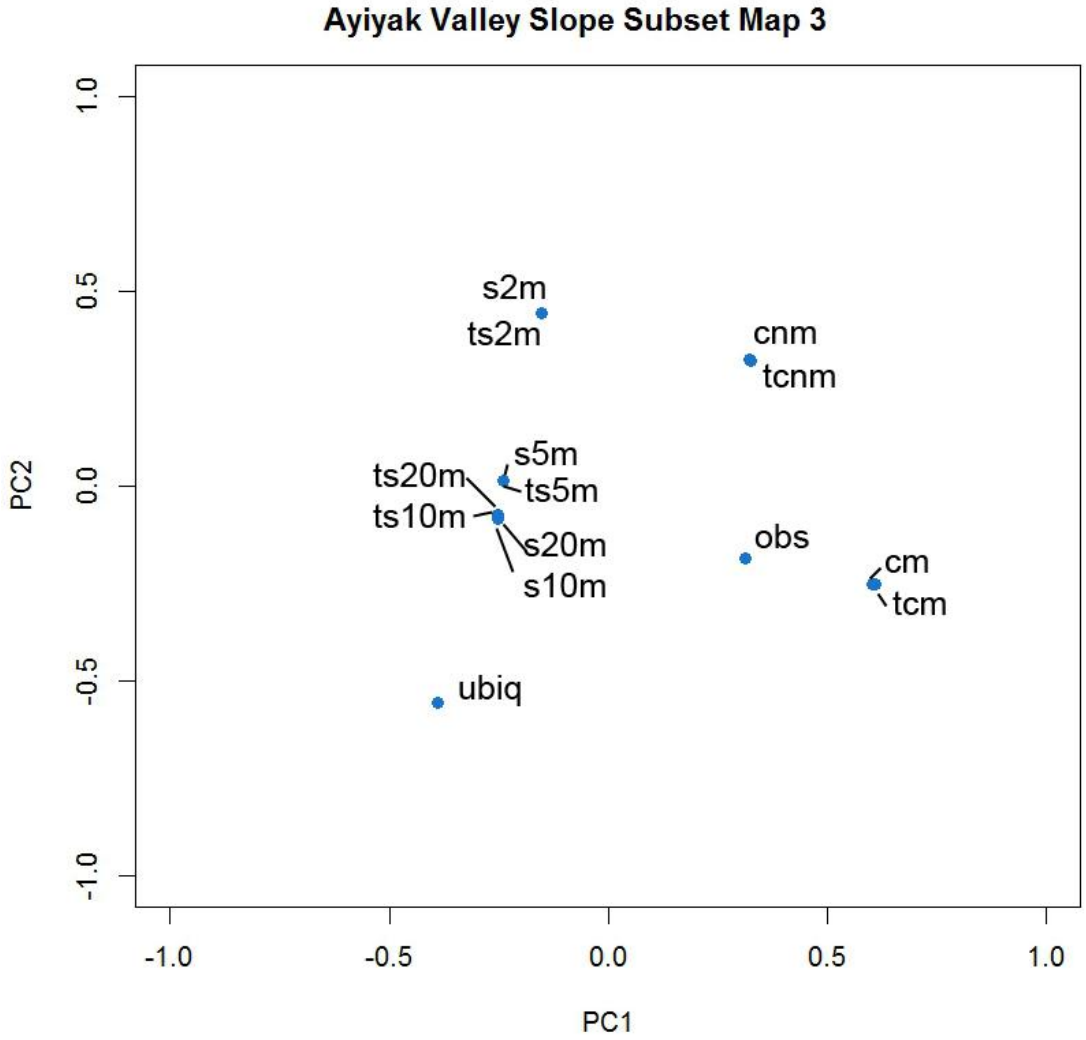

Figure 49: Biplot of the PCA analysis for Ayiyak Valley Slope Subset Map 3. At fine spatial scales, there is little similarity between the observed results and the modeled results. At broader scales, there is closer correspondence with very short distance (2 m) dispersal and clonal modes.

Table 9: Cumulative variance of the first three components of the PCA analyses for the three Ayiyak valley slope maps. See Table 2 for a description of each of the pattern metrics. VS = Valley Slope.

	Ayiyak VS 1		**Ayiyak VS 2**		**Ayiyak VS 3**	
Axis	Eigenvalue	Cumul. % of variance	Eigenvalue	Cumul. % of variance	Eigenvalue	Cumul. % of variance
1	3.18	61.06	3.08	61.45	3.40	66.06
2	2.52	95.24	2.43	93.25	2.26	95.43
3	0.30	98.85	0.46	98.82	0.32	99.35

Table 10: First two eigenvectors for the six pattern metrics produced by the PCA analyses for the three Ayiyak valley slope maps. See Table 2 for a description of each of the pattern metrics. VS = Valley Slope.

	Ayiyak VS 1		**Ayiyak VS2**		**Ayiyak VS 3**	
Metric	V1	V2	V1	V2	V1	V2
PADENS	-0.40	0.42	-0.37	-0.46	-0.34	0.50
EDENS	-0.53	0.11	-0.52	-0.19	-0.51	0.17
CVSIZE	-0.55	0.04	-0.50	-0.18	-0.45	0.34
SHAPEI	-0.09	-0.62	-0.18	0.61	-0.29	-0.56
FRACTI	-0.12	-0.60	-0.24	0.56	-0.32	-0.51
MEDIST	0.48	0.26	0.51	-0.21	0.49	0.17

Table 11: Distances in ordination space between the observed treatment and the other thirteen treatments scaled by the range of PC1 for the six Ayiyak maps. The minimum distance between treatments is highlighted in light gray.

	Ayiyak FP 1	**Ayiyak FP 2**	**Ayiyak FP 3**	**Ayiyak VS 1**	**Ayiyak VS 2**	**Ayiyak VS 3**
obs - cm	0.4924	0.0524	0.0691	0.3442	0.4885	0.2971
obs - cnm	0.4201	0.1674	0.1081	0.3255	0.2839	0.0098
obs - s2m	0.1619	0.7269	0.5910	0.1091	0.2274	0.4652
obs - s5m	0.5076	0.8903	0.8213	0.3614	0.3675	0.5507
obs - s10m	0.4913	0.8925	0.8670	0.4067	0.3872	0.5638
obs - s20m	0.4818	0.8896	0.8737	0.4164	0.3879	0.5660
obs - tcm	0.4847	0.0326	0.0690	0.3424	0.4932	0.2915
obs - tcnm	0.3085	0.2651	0.1148	0.3220	0.2778	0.0145
obs - ts2m	0.1091	0.6976	0.5910	0.1091	0.2274	0.4652
obs - ts5m	0.4418	0.8610	0.8240	0.3614	0.3675	0.5507
obs - ts10m	0.4080	0.8602	0.8670	0.4067	0.3872	0.5651
obs - ts20m	0.3957	0.8595	0.8655	0.4164	0.3879	0.5645
obs - ubiq	0.4575	0.9476	0.9309	0.6558	0.5068	0.7029

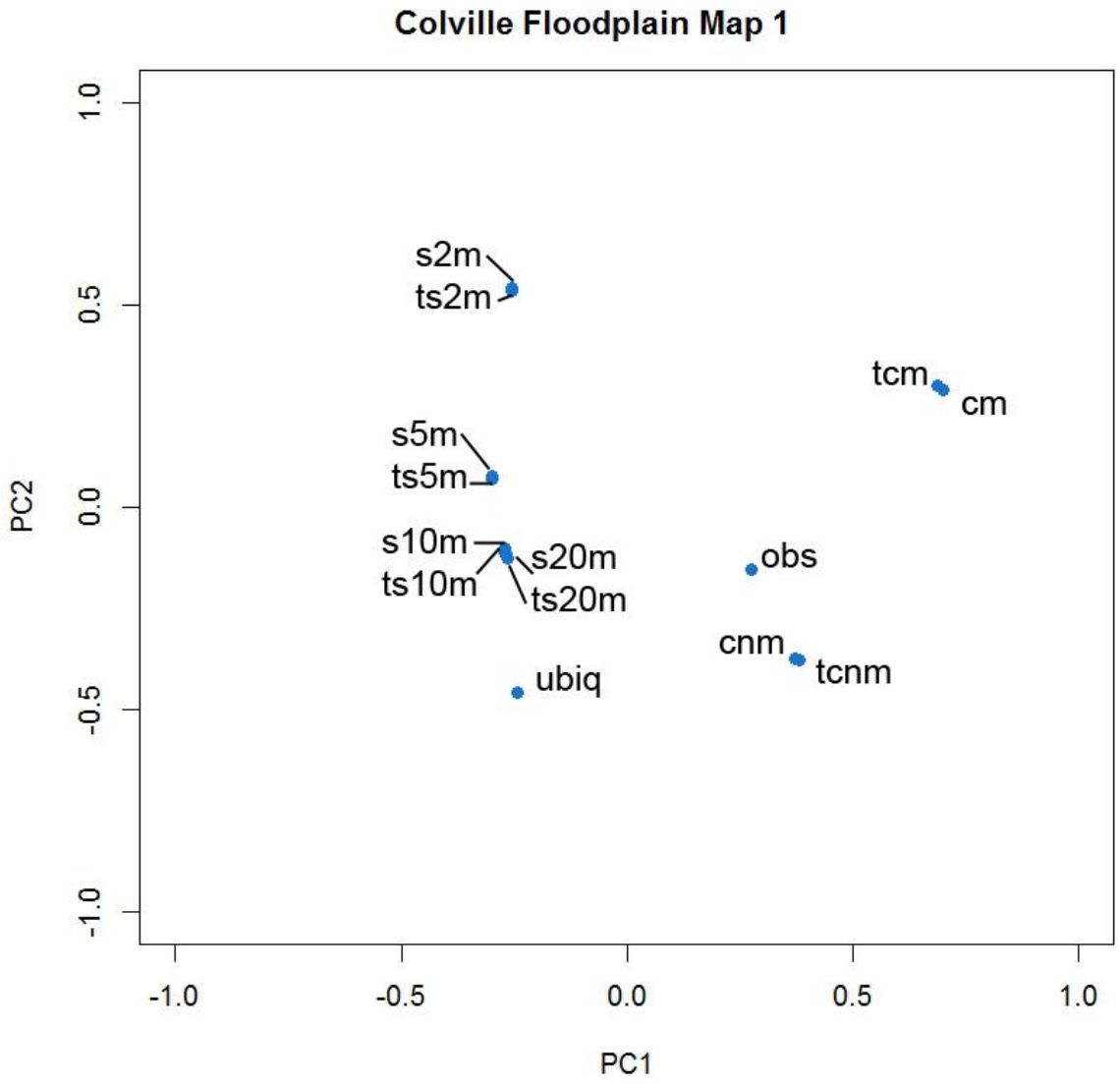

Figure 50: Biplot for the PCA analysis for Colville Floodplain Subset Map 1.

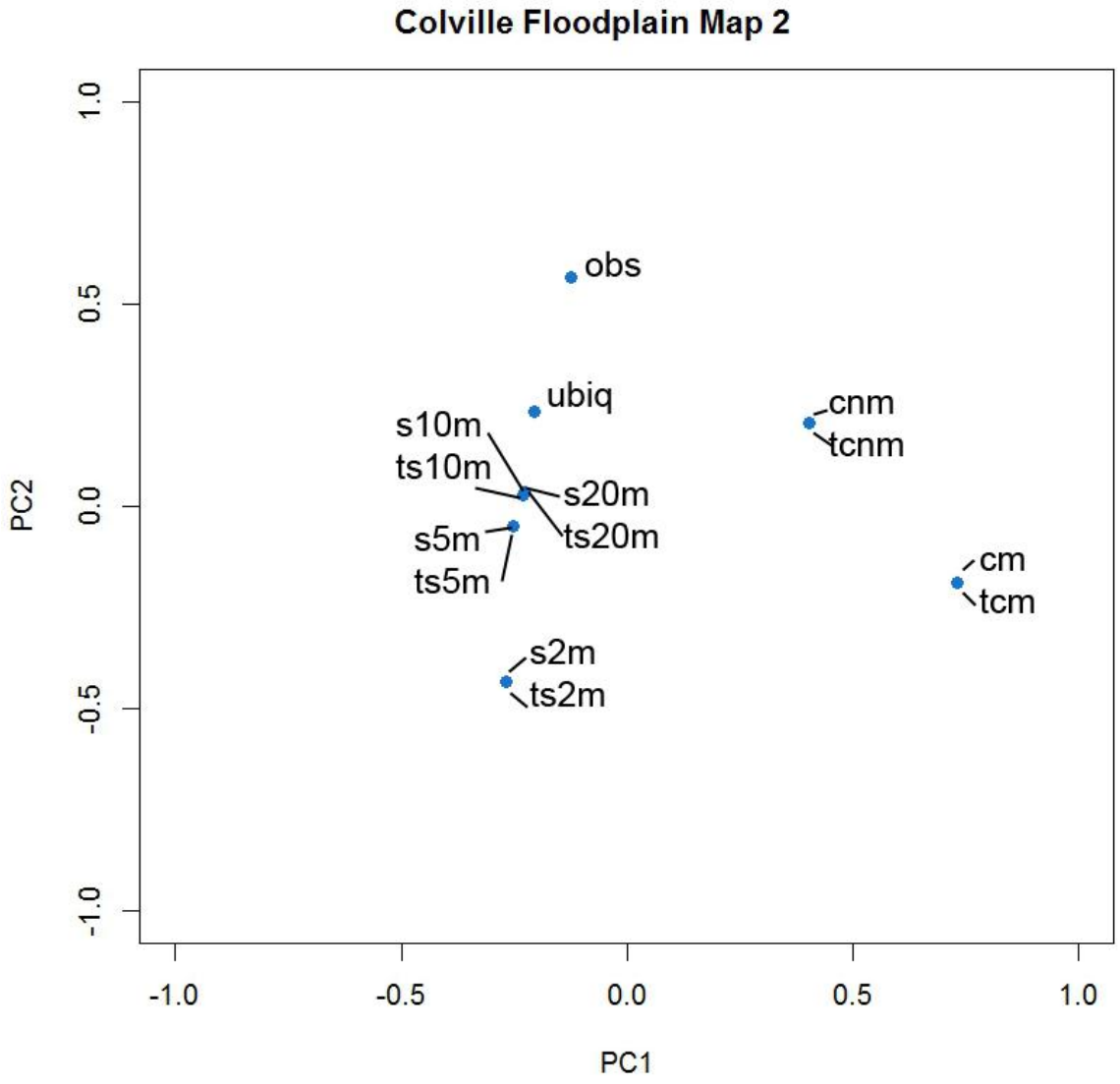

Figure 51: Biplot of the PCA analysis for Colville Floodplain Subset Map 2..

.

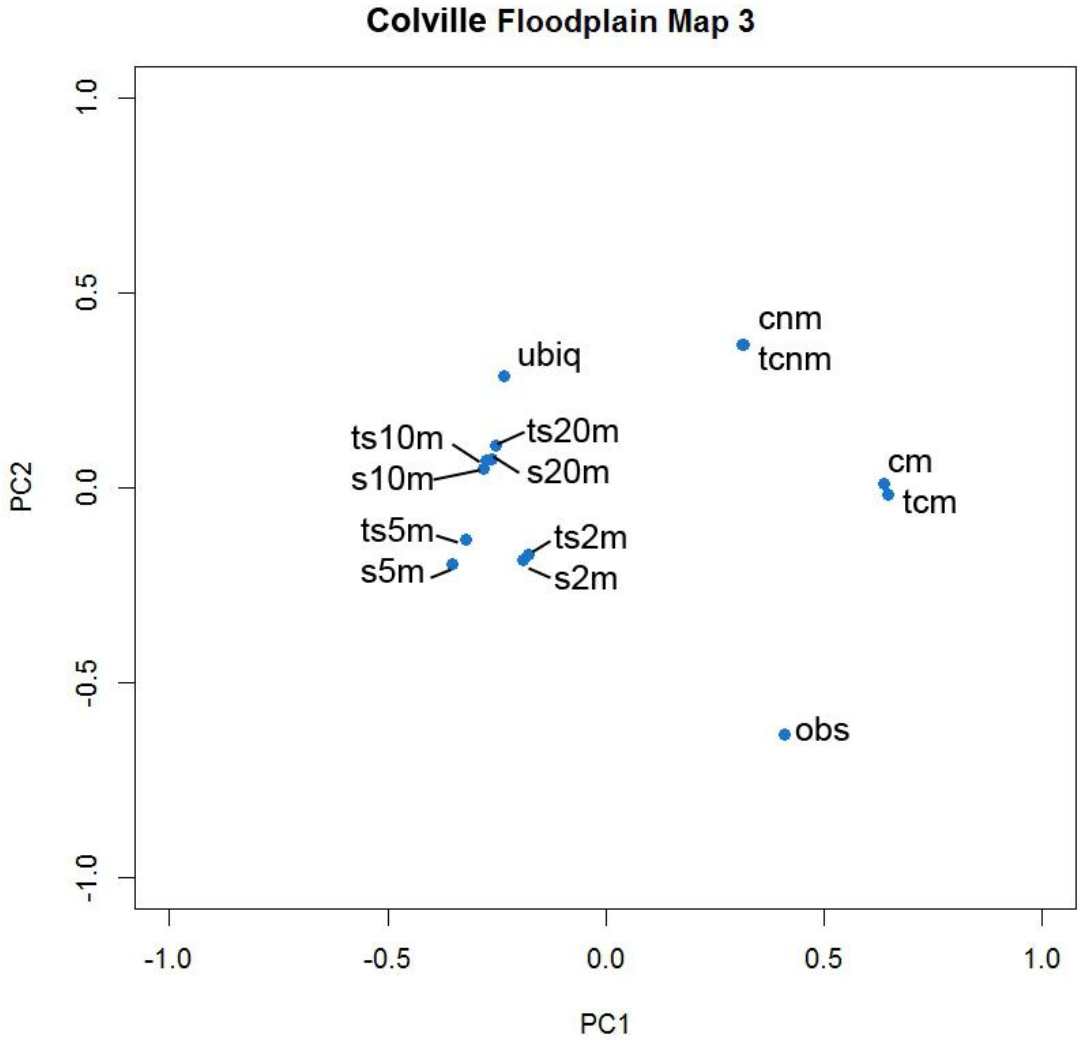

Figure 52: Biplots of the PCA analysis for Colville Floodplain Subset Map 3.

Table 12: Cumulative variance of the first three components of the PCA analyses for the three Colville floodplain maps. FP = Floodplain.

	Colville FP 1		**Colville FP 2**		**Colville FP 3**	
Axis	Eigenvalue	Cumul. % of variance	Eigenvalue	Cumul. % of variance	Eigenvalue	Cumul. % of variance
1	5.28	87.92	4.80	79.92	4.85	80.82
2	0.61	98.02	1.11	98.34	0.64	91.53
3	0.11	99.85	0.09	99.85	0.45	98.98

Table 13: First two eigenvectors for the six pattern metrics produced by the PCA analyses for the three Colville floodplain maps. See Table 2 for a description of each of the pattern metrics. FP = Floodplain.

	Colville FP 1		**Colville FP 2**		**Colville FP 3**	
Metric	V1	V2	V1	V2	V1	V2
PADENS	-0.38	0.62	-0.36	-0.58	-0.39	-0.54
EDENS	-0.42	-0.31	-0.43	0.33	-0.44	0.10
CVSIZE	-0.40	0.47	-0.40	-0.46	-0.42	-0.38
SHAPEI	-0.41	-0.35	-0.42	0.39	-0.44	0.24
FRACTI	-0.40	-0.43	-0.41	0.40	-0.41	-0.04
MEDIST	0.43	-0.05	0.43	0.18	0.34	-0.70

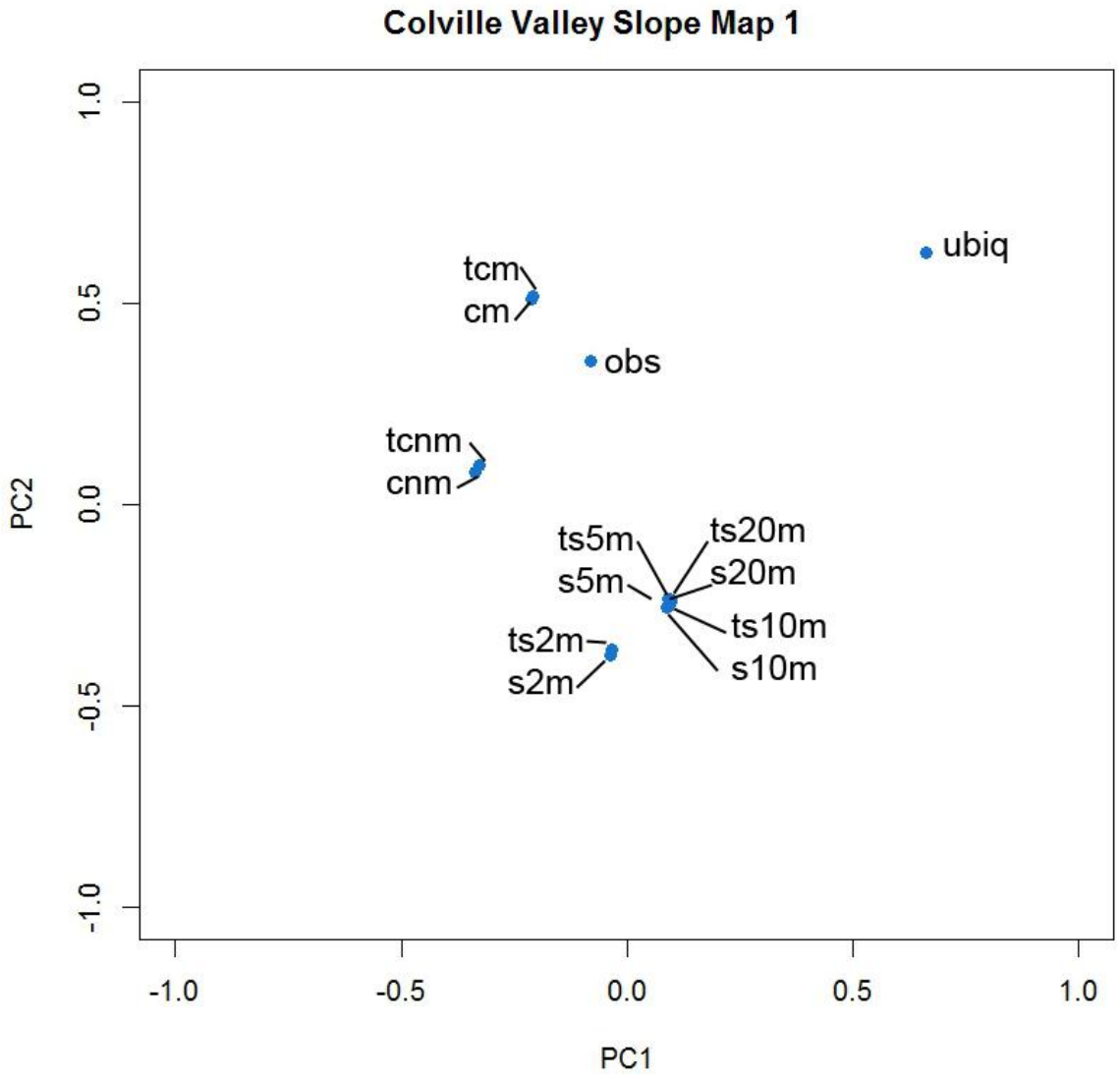

Figure 53: Biplots of the PCA analysis for Colville Valley Slope Subset Map 1.

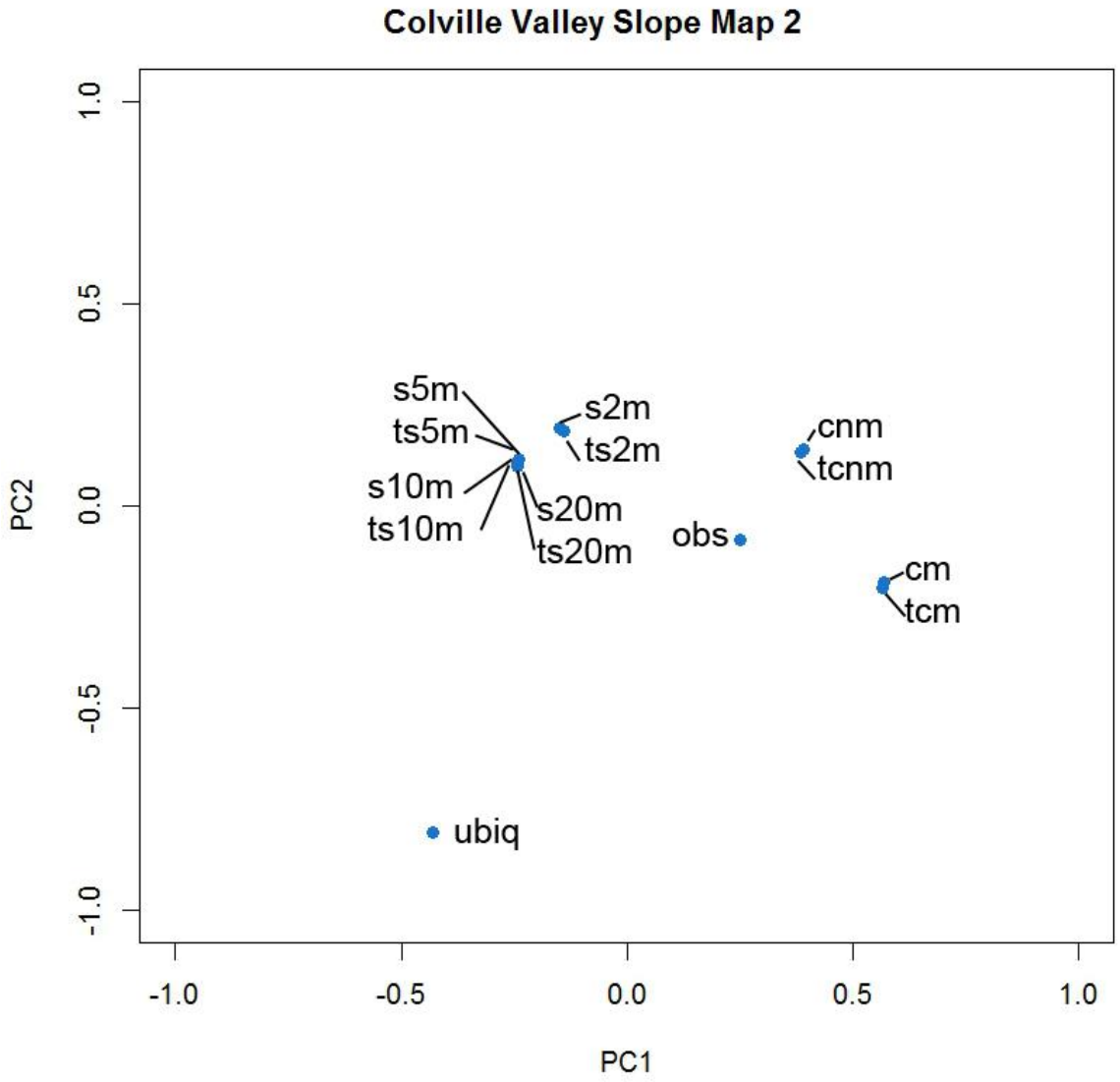

Figure 54: Biplots of the PCA analysis for Colville Valley Slope Subset Map 2.

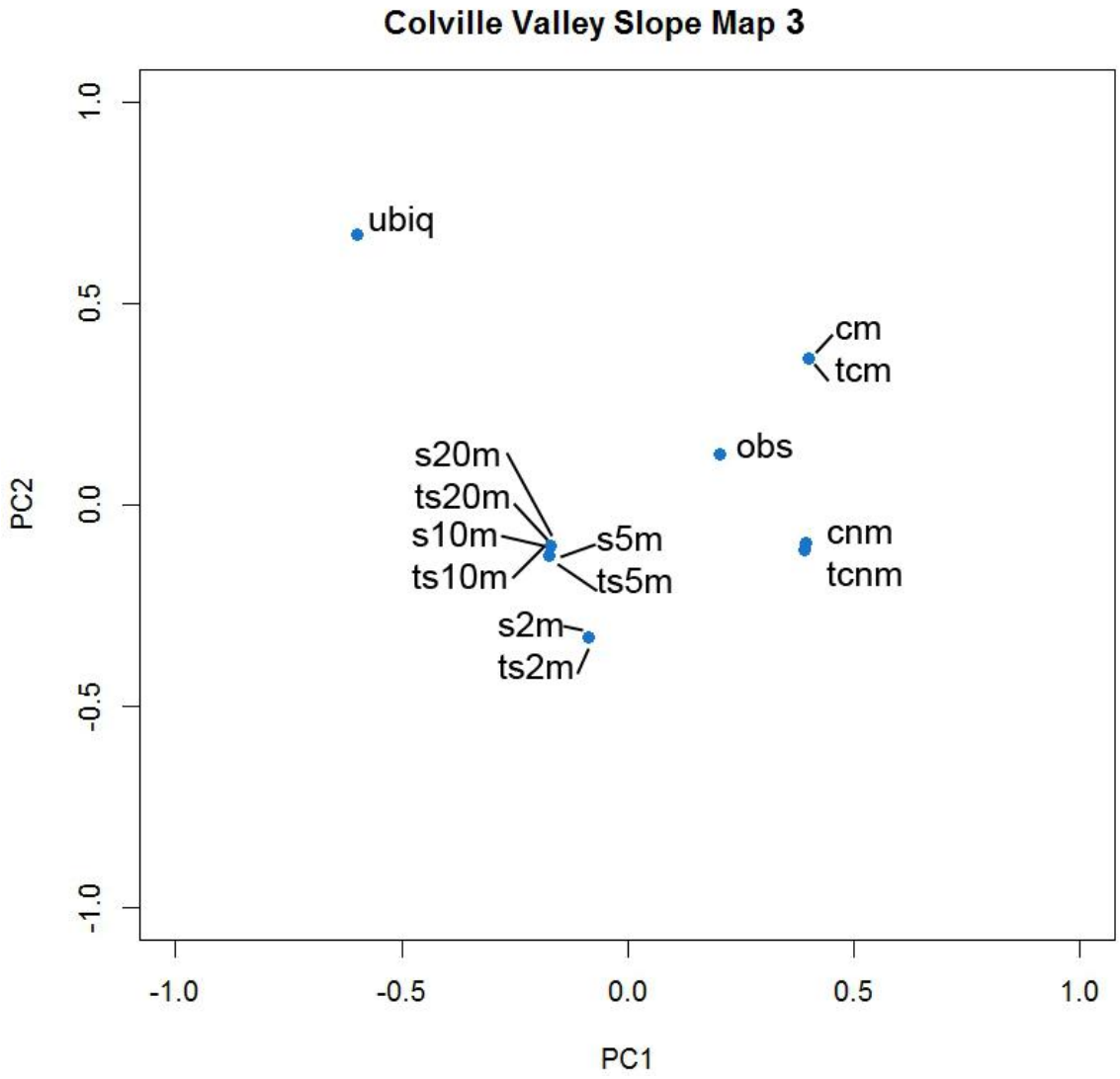

Figure 55: Biplots of the PCA analysis for Colville Valley Slope Subset Map 3.

Table 14: Cumulative variance of the first three components of the PCA analyses for the three Colville valley slope maps. VS = Valley Slope.

	Colville VS 1		**Colville VS 2**		**Colville VS 3**	
Axis	Eigenvalue	Cumul. % of variance	Eigenvalue	Cumul. % of variance	Eigenvalue	Cumul. % of variance
1	2.97	49.47	3.12	52.01	3.01	50.24
2	2.39	89.31	2.47	93.24	2.45	91.08
3	0.58	99.01	0.37	99.46	0.45	98.60

Table 15: First two eigenvectors for the six pattern metrics produced by the PCA analyses for the three Colville valley slope maps. See Table 2 for a description of each of the pattern maps. VS = Valley Slope.

	Colville VS 1		**Colville VS 2**		**Colville VS 3**	
Metric	**V1**	**V2**	**V1**	**V2**	**V1**	**V2**
PADENS	0.53	0.17	-0.30	-0.51	-0.45	0.34
EDENS	0.49	-0.21	-0.51	-0.20	-0.54	0.00
CVSIZE	0.25	-0.52	-0.55	0.03	-0.45	-0.37
SHAPEI	-0.39	-0.43	-0.16	0.60	0.17	-0.57
FRACTI	-0.28	-0.54	-0.21	0.58	0.03	-0.62
MEDIST	-0.43	0.42	0.53	-0.04	0.52	0.20

Table 16: Distances in ordination space between the observed treatment and the other thirteen treatments scaled by the range of PC1 for the six Colville maps. The minimum distance between treatments is highlighted in light gray.

	Colville FP 1	**Colville FP 2**	**Colville FP 3**	**Colville VS 1**	**Colville VS 2**	**Colville VS 3**
obs - cm	0.4397	0.8561	0.2382	0.1591	0.2845	0.1969
obs - cnm	0.0999	0.5280	0.0996	0.3096	0.1271	0.1910
obs - s2m	0.5525	0.1452	0.6202	0.0562	0.3547	0.2886
obs - s5m	0.5985	0.1284	0.7878	0.2080	0.4378	0.3773
obs - s10m	0.5683	0.1046	0.7144	0.2160	0.4391	0.3725
obs - s20m	0.5633	0.1076	0.7078	0.2161	0.4401	0.3725
obs - tcm	0.4270	0.8561	0.2486	0.1563	0.2830	0.1969
obs - tcnm	0.1082	0.5280	0.0970	0.3000	0.1191	0.1879
obs - ts2m	0.5526	0.1452	0.6078	0.0591	0.3470	0.2886
obs - ts5m	0.5964	0.1284	0.7553	0.2103	0.4378	0.3773
obs - ts10m	0.5635	0.1046	0.6946	0.2105	0.4391	0.3725
obs - ts20m	0.5677	0.1076	0.6844	0.2155	0.4401	0.3725
obs - ubiq	0.5393	0.0817	0.6664	0.9065	0.6064	0.8031

7. DISCUSSION *

7.1 Spatial Characteristics of Shrub Expansion in the Context of Ecological Phase Transition Theory

7.1.1 Changes in Shrub Area at the Nine Sites

Net increases in shrub cover occurred at all sites, and this is consistent with previous studies in the region. Loehle et al. (1996) noted that percent cover would increase dramatically during and after the phase transition. Since a transition already appears to have occurred, I expected that continued increases in shrub cover within river corridors will occur as conditions continue to warm (Walker et al. 2006, Lantz et al. 2010). Tape et al. (2006) and Lantz et al. (2010) reported areal increases of shrub patches in the western Arctic between 1 and 6% per decade. The decadal rates are higher likely due to the potential for inadvertent capture of low shrub and our much smaller total areas of investigation. Unusual fluctuations in shrub cover (as exemplified by Killik, Kurupa, and Nigu) between the first and last vertical image available are likely attributable to the larger native resolution values of the images from the 1980s. A consequence of this is the overestimation of area in sites containing large patches, and an underestimation of area in sites containing small patches. These images were also acquired at a higher flight altitude.

Tape et al. (2006) proposed three types of shrub expansion, including an increase in the number and size of patches, and a reduction in the distance between patches. Myers-Smith et al. (2011) additionally proposed that patterns of shrub expansion exhibit an increase in growth potential, as well as latitudinal and altitudinal advance of the shrubline. Therefore, it would be expected that consistent increases in PADENS and CVSIZE, and a reduction in MEDIST would be observed. The conceptual landscape results, however, suggest a reduction in PADENS during or after a phase transition, and an increase followed by a decrease in CVSIZE just after the phase transition. In addition, they do not explicitly contain shrub development as a result of environmental heterogeneity. Upon initial examination, the observed results suggest that the response of PADENS, CVSIZE, and MEDIST are quite variable from site to site. However, these trends do generally conform to those proposed in the conceptual landscape Case 1 (Table 3, Fig. 36-38). Sites for which their median d_I indicated "phase transition" exhibited increases in PADENS and CVSIZE (e.g., Ayiyak, Chandler, and Nigu), suggesting the acceleration of these metrics as shrubs begin to expand across the landscape. For sites with higher d_I values, however, (e.g., Killik and Nimiuktuk), there was better correspondence with Case 1 through reduction in PADENS and CVSIZE. This suggests that the phase transition at these sites is completing, leading to spatial homogeneity. Any other variability in these trends are likely due to the irregular distribution and recruitment of shrubs along the floodplains and valley slope drainage channels in response to local hydrological characteristics (e.g., Naito & Cairns, 2011b). Over the period of analysis, alterations in the stream channel and the creation of sediment banks

that provide new surfaces for shrub recruitment likely introduce additional variability in these trends. Although half the sites exhibited an increase in MEDIST, these increases are very small (< 1 m).

7.1.2 Implications of a Phase Transition

Based upon the median d_I values for each landscape, the results of the linear regression, and the comparison of the historic pattern metric curves with the conceptual metric curves, the shrub-tundra ecotone in each of the landscapes examined exceeds the requirements necessary for shrubs to expand over the entire landscape. Since PCTCOV for every landscape studied since the 1970s exceeds these values, the results suggest that a phase transition has already occurred (Table 3). This is further corroborated by the changes in the median d_I by decade. The median d_I value for each site generally increases over at least the last 30 years, indicating a gradual shift towards spatial homogeneity. An examination of the d_I profiles also provides insights into the pattern-process relationship across spatial scales. At fine spatial scales, the landscapes are highly heterogeneous, corroborating recent findings that shrub expansion patterns maintain a degree of heterogeneity based upon resource availability (e.g., Tape et al., 2012; Raynolds et al. 2013). Otherwise, the general consistency of the d_I values in the fractal profiles (Table 3, Figs. 39-41) suggests that these landscapes can be characterized as approaching spatial homogeneity at all but the finest of scales. There is a reduction in d_I values at the coarsest scales due to the sampling of the upslope areas and interfluves where shrub cover is minimal. Sites that do not demonstrate this trend (e.g., Killik,

Kurupa, and Nigu) are likely due to inadequate imagery coverage of these upslope areas. Interfluves are often dry and exposed to high winds that can limit shrub recruitment and development. One limitation of Loehle et al.'s (1996) approach is that the derivation of a threshold PCTCOV value relies on regression of a single PCTCOV cover and d_I value for each entire landscape rather than these values at multiple spatial scales.

The phase transition occurring in these river corridors have considerable consequences for Arctic ecosystem processes and their associated feedbacks. The target in this work was tall, canopy-forming deciduous shrubs (*Alnus*, *Betula*, and *Salix* spp.). Their recruitment may lead to reductions in surface albedo, as well as broader-scale increases in atmospheric heating, evapotranspiration, ALT, and permafrost degradation (Chapin et al., 2000; Bonfils et al., 2012). There are somewhat contrasting findings regarding nutrient availability and permafrost effects as a result of summer shading under tall shrub canopy (Bokhorst et al., 2010; Blok et al, 2010; Myers-Smith & Hik, 2013; Vankoughnett & Grogan, 2014). This could, in part, help explain the fine-scale heterogeneity indicated by the d_I fractal profile. Climatic warming is thought to be an overriding factor of these finer-scale processes (Lawrence et al., 2011; Bonfils et al., 2012). The expansion of shrubs is also thought to reduce erosion (Tape et al., 2011) and increase the landscape's geomorphic threshold for change (Mann et al., 2010).

7.2 Association Between Shrub Expansion and Hydrologic Characteristics

7.2.1 Changes in Shrub Cover

Results regarding shrub expansion characteristics on the North Slope largely agree with the findings of Tape et al. (2006). Their visual analysis of repeat oblique aerial photographs revealed that shrub cover change across the North Slope between the late 1940s and early 2000s ranged from +3 to +80%. With the exception of Nanushuk 1, total shrub cover change falls well within this range. Total shrub cover figures for the 2000s at Nimiuktuk and Killik are likely to be underestimates. These images were acquired in May, and snow patches were still visible on the ground, particularly on valley slopes and interfluves. Snow covers 2.23% of the 2010 image in Nimiuktuk and 1.3% of the 2009 image at Killik (Table 5).

These values differ somewhat to those presented in the previous subsection. This was due to resizing of the landscape under examination to better accommodate the calculation of the d_I. The d_I requires the use of grids of cells that increase their dimensions geometrically, so the dimensions of the landscape had to be some multiple of a value in that sequence. As a consequence, the landscape area for the d_I calculation was slightly smaller than that used for this part of the study.

7.2.2 Associations Between Shrub Dynamics and Fluvial Characteristics on Valley Slopes

The TWI was useful for inferring relationships between vegetation, hydrology, and geomorphology in the Arctic. The non-parametric statistical testing suggests a

significant association between shrub development and topographically-derived hydrologic characteristics. Since the 1970s, shrubs have generally expanded into areas of greater TWI values. This means that shrubs are preferentially developing in areas that have a greater potential for accumulating moisture. Visual inspection of the aerial images confirms that valley slope shrubs are expanding upslope along hillslope water tracks (*cf.* McNamara et al. 1999). These drainages are typically shallower than the neighboring hillslopes and serve as the primary route for downhill water migration. The TWI captures these features by representing them with higher index values. Future studies incorporating the use of a TWI in conjunction with modeling and field measurements will help to assess potential impacts on the hydrology of the Arctic system. McNamara et al. (1999) suggested that reduced permafrost may lead to hillslope erosion and consequences for the afflicted watersheds. Although an increase in precipitation expected under a warming climate would accelerate hillslope erosion, vegetation responding to wetter environments would likely stabilize the hillslope and reduce erosion potential (Mann et al. 2010; Tape et al. 2012).

7.2.3 Association Between Shrub Expansion/Development and Floodplain Characteristics

The binomial logistic regression shows that positive change in floodplain shrub cover is associated with: 1) a decreasing distance between shrubs and the river bank, and 2) preferential expansion onto areas with high TWI values. Given that net increase in

shrub cover were observed, I concluded that the overall median distance between shrubs and the river banks will continue to decrease as expansion continues (Table 6).

Variability in shrub development patterns within floodplains suggest that river channel dynamics are the dominant driver. Temporary reductions in floodplain shrub cover are likely attributable to the dates of acquisition of the imagery. With the mapping methods used, shrubs are only identifiable in imagery acquired during the growing season in June and July. However, this is also the time when the rivers are at their peak flow. Flooding events can eliminate entire shrub patches through alteration of the channel and floodplain, thereby affecting all three pattern metrics examined. PADENS and CVSIZE generally increased when rivers exhibited a combination of 1) more braided flow (e.g., Chandler), 2) significant channel migration (e.g., Kurupa), or meander changes and narrowing (e.g., Ayiyak). These shifts would create new surfaces for shrub establishment (e.g., Poff et al. 1997, DeWine and Cooper 2007, Konrad et al. 2011, Naito and Cairns 2011b) that would lead to a commensurate decrease in MEDIST. In the case of the Colville site, the river channel only narrowed, allowing present shrubs to expand laterally onto the new surfaces next to the river. The general stability of the Nigu River allowed new patches to form within the floodplain. Studies have suggested that increased floodplain recruitment is attributable to a reduction in erosion and increased warming leading to accelerated evapotranspiration, permafrost thaw, and subsequent infiltration (e.g., Mann et al. 2010, Tape et al. 2011, Naito and Cairns 2011b).

Visual inspection of the aerial photographs suggests that, while unvegetated sediment bars are visible along the river course in the 1970s, many of these have disappeared by the 2000s. This could be attributed to deposits providing a substrate for primary succession of shrubs (e.g., Douglas 1989), erosion of these deposits by the river channels, or channel migration (e.g., Konrad et al. 2011). Since the two mass-wasting events during the Pleistocene-Holocene transition (Mann et al. 2010), rivers in northern Alaska have become increasingly decoupled from valley slope sediment inputs. While deposition and erosion of sediment still occur, the rivers have transported much of the sediment input from those events (Mann et al. 2010). This suggests that overall sediment input has decreased over time, thereby reducing overall sediment loads in the channels. The presence of vegetation can stabilize otherwise ephemeral features like sediment bars, reducing their susceptibility to erosion (Konrad et al. 2011). This has the effect of restricting channel migration.

Warming Arctic temperatures will lead to earlier river ice break up and later freeze-up, thereby increasing evapotranspiration. Prowse et al. (2006) argue that this will lead to diminished surface water and will be compounded by increased infiltration as a result of permafrost loss. The consequence of this will be reduced spring peak flows (Prowse et al. 2006) and potentially less flood-induced disturbance. This would likely improve survivorship of floodplain shrubs.

7.3 Contribution of Clonal Reproduction to Observed Patterns of Expansion

The primary purpose of this component of the work was to develop a working simulation model that could be applied to improve understanding of the contribution of shrub reproductive characteristics to observed patterns of expansion in the BRNS. These processes are currently poorly understood. This can be a potentially important contribution due to the limited number of studies involving analysis of gene flow and seed traps in the Arctic. Studies on dispersal are also somewhat limited. With the exception of Douhovnikoff et al.'s (2010) study in the BRNS, much work on shrub dispersal has been focused in the High Arctic where the dominant growth form are prostrate shrubs. The expansion of these shrubs is more limited and would not pose significant consequences to ecosystem structure and function, unlike the expansion of tall shrubs (> 0.5 m) in the Low Arctic.

In general, the PCA analyses suggest that expansion by clonal reproduction produced spatial patterns similar to those observed in both floodplains and valley slopes. Although floodplains exhibit significant disturbance due to flooding, channel migration, and erosion, these factors did not appear to confound the modeling results. These results are also logical because floodplain tend to be dominated by Salix spp. which are facultative clonal species, and valley slopes tend to be dominated by Alnus spp. which can exhibit either clonal or sexual reproduction. Based upon the results, it is possible to hypothesize that clonal reproduction is a contributor to expansion.

Incorporation of the leptokurtic dispersal kernels derived from spatial pattern improved the model's ability to simulate sexual dispersal. Based upon the results,

however, there was no instance in which the observed closely matched the longest dispersal distance (20 m). This was the case even though the fitted Weibull functions tended to overestimate the probability. The distributions also suggested that the likelihood of finding shrubs 10-20 m was much smaller than the likelihood of finding shrubs within 5 m of each other.

7.4 Limitations of the Study

7.4.1 Imagery and Pattern Analysis

Results are based upon observable tall shrubs from vertical aerial imagery. Vertical imagery affords a more rigorous assessment of shrub cover dynamics than those that can be derived from oblique imagery used in these areas (i.e., Tape et al. 2006). This study, however, only contributes maps from two to three dates for each sites. This still provides only a limited assessment of historic shrub dynamics in the BRNS. I made an effort to obtain the best quality historical imagery (in terms of limited cloud cover and lower flight altitude) . Low shrubs from the maps generated from these imagery were generally omitted because the encroachment of tall shrubs promotes alterations in ecosystem function regarding surface-energy balances and nutrient availability (Cornelissen et al. 2007; Bonfils et al. 2012, Elmendorf et al. 2012, Vankoughnett & Grogan 2014), Both tall and low shrubs are typically visible in the color high-resolution satellite imagery, so exclusion of low shrubs is a relatively simple process. Low shrubs are not immediately apparent in the historical imagery acquired at higher flight altitudes. In color infrared photos, tall shrubs are usually distinguished by dark pink areas, low

shrubs as lighter pink, and prostrate and non-shrub tundra as a pale pink-blue color (Tape et al. 2012). However, it is likely that pixels categorized as tall shrub cover do include some low shrubs. These limitations likely inflate our results for the earlier dates. Some of the best imagery was also panchromatic for some of our areas. Tall shrubs often appears as dark patches, but differentiating low shrub from tussock tundra can be more difficult because only textural characteristics are available. The phase transition theory as proposed by Loehle et al. (1996), however, is predicated on the treatment of landscapes as binary in terms of vegetation composition. Each pixel in each landscape as "shrub" and "not-shrub." The inclusion of low shrubs would therefore be appropriate, considering that Loehle and colleagues did not differentiate different species of trees. This component study should be considered as a preliminary application of phase transition theory to an Arctic ecosystem to determine its applicability and understanding the implications for the local ecosystems.

7.4.2 Elevation Data

The DEMs used in the analysis involving the hydrological constraints on shrub expansion and the model had a resolution of 30.88 m. Given how coarse these data are, it is likely they do not fully capture the topographic variability in river valleys in the BRNS. Because of the nature of the TWI calculation using Tarboton's (2010) method, the resulting raster data exhibits a considerable striping effect. While efforts are being made to develop 5 m resolution DEMs for the entire North Slope of Alaska (Jeremy Hale, i-Cubed, LLC, *pers. comm.*), these data were not available at the time of analysis.

This was one of the main reasons I rigorously sampled each landscape to obtain frequency distributions of TWI values. This ensured that the relationships were less of a chance occurrence.

7.4.3 Simulation Model

The model does recognize the presence of water in the input landscape and will restrict shrub growth to those cells for the duration of the simulation run. However, the ells assigned as river remain static, so the effect of channel migration or erosion is not present. In the present work, input landscapes did not have values for water as the primary objective was to determine the model's usefulness in simulating reproduction. With additional refinements to the calculations for reproduction, additional simulation runs may be executed that include water as a constraining factor.

A number of factors may need to be considered in order to refine the model's utility. For example, the model does not include a maturation lag. As soon as a shrub arrives in a cell, it is capable of reproduction. Species such as *S. glauca* and *A. viridis*, which are common on the North Slope, typically do not reach maturity until approximately 10 years of age, however (Normand et al. 2013). In addition, herbivory by ungulates and rodents is increasingly recognized as a constraint to shrub expansion (Olofsson et al. 2004; den Herder et al. 2008). Rodents and other animals may also reduce the size of the seed bank (Munier et al. 2010). Additional disturbances to the tundra resulting from fire, permafrost degradation, and frost heave may also promote the

presence of tall shrubs. In the current model setup, both factors would have to be integrated as stochastic factors that reduce and increase the value of *p*.

Because shrub expansion is circumpolar in extent, and the processes driving it are likely similar, this model could potentially be applied elsewhere to refine understanding of landscape-scale processes.

8. CONCLUSION

This work has focused on developing an improved understanding of the pattern-process relationship of shrub expansion on the North Slope of Alaska. Through a combination of: 1) historic aerial photographs and high-resolution satellite imagery to generate maps of shrub expansion, 2) pattern metric and multi-scale information fractal dimension analysis of the development of shrub expansion patterns, 3) data products derived from digital elevation models to act as proxies for hydrologic characteristics, and 4) the use of a spatially-explicit simulation model that simulates plausible patterns of expansion via different reproductive modes, several conclusions may be drawn. First, patterns of expansion are highly variable, but they all suggest that a ecological phase transition is either in progress or already has occurred in river valleys. Based upon principles in percolation theory, shrub cover is proceeding towards a state of spatial homogeneity. Second, shrub recruitment is facilitated in areas where the potential for water throughflow or accumulation is greater. Third, through spatially-explicit modeling results, clonal reproduction contributes to the observed patterns of expansion.

Given current understanding of the local-scale implications for hydrology, surface energy balances, and C and nutrient cycling as a result of enhanced shrub cover, continued expansion will likely alter tundra ecosystem structure and function. Such transitions and ecosystem processes are currently being observed in other biomes. The integration of additional field-derived measurements, improved remote sensing products, new remote sensing techniques, and spatially-explicit simulation modeling will be critical for advancing understanding of Arctic ecological interactions and possible

shifts in shrub reproductive characteristics. Refinement of this understanding will also help improve coupling to global-scale climate and atmospheric models. In addition, such studies will also need to focus on better understanding the contribution of the positive and negative feedbacks on ecosystem structure and function that these interacting factors create.

REFERENCES

Abernethy, B. & Rutherfurd, I.D. 2001. The distribution and strength of riparian tree roots in relation to riverbank reinforcement. *Hydrological Processes* 15: 63-79.

Ager, T.A. & Phillips, R.L. 2008. Pollen evidence for late Pleistocene Bering land bridge environments from Norton Sound, northeastern Bering Sea, Alaska. *Arctic Antarctic and Alpine Research* 40: 451-461.

Aguiar, M.R. & Sala, O.E. 1994. Competition, facilitation, seed distribution and the origin of patches in a Patagonian steppe. *Oikos* 70: 26-34.

Aguiar, M.R., Soriano, A. & Sala, O.E. 1992. Competition and facilitation in the recruitment of seedlings in Patagonia steppe. *Functional Ecology* 6: 66-70.

Alados, C.L., Navarro, T., Komac, B., Pascual, V., Martinez, F., Cabezudo, B. & Pueyo, Y. 2009. Do vegetation patch spatial patterns disrupt the spatial organization of plant species? *Ecological Complexity* 6: 197-207.

Alados, C.L., Pueyo, Y., Navas, D., Cabezudo, B., Gonzalez, A. & Freeman, D.C. 2005. Fractal analysis of plant spatial patterns: a monitoring tool for vegetation transition shifts. *Biodiversity and Conservation* 14: 1453-1468.

Alftine, K.J. & Malanson, G.P. 2004. Directional positive feedback and pattern at an alpine tree line. *Journal of Vegetation Science* 15: 3-12.

Alsos, I.G., Eidesen, P.B., Ehrich, D., Skrede, I., Westergaard, K., Jacobsen, G.H., Landvik, J.Y., Taberlet, P. & Brochmann, C. 2007. Frequent long-distance plant colonization in the changing Arctic. *Science* 316: 1606-1609.

Anderson, P.M. 1985. Late quaternary vegetational change in the Kotzebue sound area, northwestern Alaska. *Quaternary Research* 24: 307-321.

Anderson, P.M. & Brubaker, L.B. 1994. Vegetation history of northcentral Alaska: A mapped summary of late-quaternary pollen data. *Quaternary Science Reviews* 13: 71-92.

Anderson, P.M., Lozhkin, A.V. & Brubaker, L.B. 2002. Implications of a 24,000-Yr Palynological Record for a Younger Dryas Cooling and for Boreal Forest Development in Northeastern Siberia. *Quaternary Research* 57: 325-333.

Andreev, A.A., Tarasov, P.E., Siegert, C., Ebel, T., Klimanov, V.A., Melles, M., Bobrov, A.A., Dereviagin, A.Y., Lubinski, D.J. & Hubberten, H.W. 2003. Late Pleistocene and Holocene vegetation and climate on the northern Taymyr Peninsula, Arctic Russia. *Boreas* 32: 484-505.

Anisimov, O.A. & Nelson, F.E. 1996. Permafrost distribution in the Northern Hemisphere under scenarios of climatic change. *Global and Planetary Change* 14: 59-72.

Anisimov, O.A., Shiklomanov, N.I. & Nelson, F.E. 1997. Global warming and active-layer thickness: results from transient general circulation models. *Global and Planetary Change* 15: 61-77.

Ansley, R.J., Ben Wu, X. & Kramp, B.A. 2001. Observation: Long-term increases in mesquite canopy cover in a North Texas savanna. *Journal of Range Management* 54: 171-176.

Archer, S. 1990. Development and stability of grass woody mosaics in a subtropical savanna parkland, Texas, USA. *Journal of Biogeography* 17: 453-462.

Archer, S., Schimel, D.S. & Holland, E.A. 1995. Mechanisms of shrubland expansion: land use, climate or CO2. *Climatic Change* 29: 91-99.

Archer, S., Scifres, C., Bassham, C.R. & Maggio, R. 1988. Autogenic Succession in a Subtropical Savanna: Conversion of Grassland to Thorn Woodland. *Ecological Monographs* 58: 111-127.

Bahre, C.J. & Shelton, M.L. 1993. Historic vegetation change, mesquite increases, and climate in southeastern Arizona. *Journal of Biogeography* 20: 489-504.

Bai, Y.G., Broersma, K., Thompson, D. & Ross, T.J. 2004. Landscape-level dynamics of grassland-forest transitions in British Columbia. *Journal of Range Management* 57: 66-75.

Bai, Y.G., Colberg, T., Romo, J.T., McConkey, B., Pennock, D. & Farrell, R. 2009. Does expansion of western snowberry enhance ecosystem carbon sequestration and storage in Canadian Prairies? *Agriculture Ecosystems & Environment* 134: 269-276.

Bär, A., Brauning, A. & Loffler, J. 2007. Ring-width chronologies of the alpine dwarf shrub *Empetrum hermaphroditum* from the Norwegian mountains. *Iawa Journal* 28: 325-338.

Barnekow, L. 1999. Holocene tree-line dynamics and inferred climatic changes in the Abisko area, northern Sweden, based on macrofossil and pollen records. *Holocene* 9: 253-265.

Barsoum, N. 2001. Relative contributions of sexual and asexual regeneration strategies in Populus nigra and Salix alba during the first years of establishment on a braided gravel bed river. *Evolutionary Ecology* 15: 255-279.

Bartlein, P.J., Anderson, K.H., Anderson, P.M., Edwards, M.E., Mock, C.J., Thompson, R.S., Webb, R.S. & Whitlock, C. 1998. Paleoclimate simulations for North America over the past 21,000 years: Features of the simulated climate and comparisons with paleoenvironmental data. *Quaternary Science Reviews* 17: 549-585.

Beck, P.S.A. & Goetz, S.J. 2011. Satellite observations of high northern latitude vegetation productivity changes between 1982 and 2008: ecological variability and regional differences. *Environmental Research Letters* 6: 045501.

Beck, P.S.A., Horning, N., Goetz, S.J., Loranty, M.M. & Tape, K.D. 2011. Shrub Cover on the North Slope of Alaska: a circa 2000 Baseline Map. *Arctic Antarctic and Alpine Research* 43: 355-363.

Bejarano, M.D., Nilsson, C., Del Tanago, M.G. & Marchamalo, M. 2011. Responses of riparian trees and shrubs to flow regulation along a boreal stream in northern Sweden. *Freshwater Biology* 56: 853-866.

Bell, K.L. & Bliss, L.C. 1980. Plant Reproduction in a High Arctic Environment. *Arctic and Alpine Research* 12: 1-10.

Bendix, J. & Hupp, C.R. 2000. Hydrological and geomorphological impacts on riparian plant communities. *Hydrological Processes* 14: 2977-2990.

Bertiller, M. 1996. Grazing effects on sustainable semiarid rangeiands in Patagonia: The state and dynamics of the soil seed bank. *Environmental Management* 20: 123-132.

Bertiller, M.B., Elissalde, N.O., Rostagno, C.M. & Defossé, G.E. 1995. Environmental patterns and plant distribution along aprecipitation gradient in western Patagonia. *Journal of Arid Environments* 29: 85-97.

Beven, K.J. & Kirkby, M.J. 1979. A physically based, variable contributing area model of basin hydrology. *Hydrological Sciences-Bulletin* 24: 43-69.

Bigelow, N.H., Brubaker, L.B., Edwards, M.E., Harrison, S.P., Prentice, I.C., Anderson, P.M., Andreev, A.A., Bartlein, P.J., Christensen, T.R., Cramer, W., Kaplan, J.O., Lozhkin, A.V., Matveyeva, N.V., Murray, D.F., McGuire, A.D., Razzhivin, V.Y., Ritchie, J.C., Smith, B., Walker, D.A., Gajewski, K., Wolf, V., Holmqvist, B.H., Igarashi, Y., Kremenetskii, K., Paus, A., Pisaric, M.F.J. & Volkova, V.S. 2003. Climate change and Arctic ecosystems: 1. Vegetation changes north of 55 degrees N between the last glacial maximum, mid-Holocene, and present. *Journal of Geophysical Research-Atmospheres* 108: 25.

Bisigato, A.J. & Bertiller, M.B. 2004. Seedling recruitment of perennial grasses in degraded areas of the Patagonian Monte. *Journal of Range Management* 57: 191-196.

Bjune, A., Birks, H.J.B. & Seppa, H. 2004. Holocene vegetation and climate history on a continental-oceanic transect in northern Fennoscandia based on pollen and plant macrofossils. *Boreas* 33: 211-223.

Blok, D., Heijmans, M.M.P.D., Schaepman-Strub, G., Kononov, A.V., Maximov, T.C. & Berendse, F. 2010. Shrub expansion may reduce summer permafrost thaw in Siberian tundra. *Global Change Biology* 16: 1296-1305

Bowersox, M.A. & Brown, D.G. 2001. Measuring the abruptness of patchy ecotones - A simulation-based comparison of landscape pattern statistics. *Plant Ecology* 156: 89-103.

Bragg, T.B. & Hulbert, L.C. 1976. Woody plant invasion of unburned Kansas bluestem prairie. *Journal of Range Management* 29: 19-24.

Bret-Harte, M.S., Shaver, G.R. & Chapin, F.S. 2002. Primary and secondary stem growth in Arctic shrubs: implications for community response to environmental change. *Journal of Ecology* 90: 251-267.

Bret-Harte, M.S., Shaver, G.R., Zoerner, J.P., Johnstone, J.F., Wagner, J.L., Chavez, A.S., Gunkelman, R.F., Lippert, S.C. & Laundre, J.A. 2001. Developmental plasticity allows Betula nana to dominate tundra subjected to an altered environment. *Ecology* 82: 18-32.

Briggs, J.M., Hoch, G.A. & Johnson, L.C. 2002. Assessing the rate, mechanisms, and consequences of the conversion of tallgrass prairie to Juniperus virginiana forest. *Ecosystems* 5: 578-586.

Briggs, J.M., Knapp, A.K., Blair, J.M., Heisler, J.L., Hoch, G.A., Lett, M.S. & McCarron, J.K. 2005. An ecosystem in transition. Causes and consequences of the conversion of mesic grassland to shrubland. *BioScience* 55: 243-254.

Briggs, J.M., Schaafsma, H. & Trenkov, D. 2007. Woody vegetation expansion in a desert grassland: Prehistoric human impact? *Journal of Arid Environments* 69: 458-472.

Brown, J.R. & Archer, S. 1999. Shrub invasion of grassland: recruitment is continuous and not regulated by herbaceous biomass or density. *Ecology* 80: 2385-2396.

Browning, D.M., Archer, S.R., Asner, G.P., McClaran, M.P. & Wessman, C.A. 2008. Woody plants in grasslands: Post-encroachment stand dynamics. *Ecological Applications* 18: 928-944.

Buckeridge, K.M., Zufelt, E., Chu, H.Y. & Grogan, P. 2010. Soil nitrogen cycling rates in low arctic shrub tundra are enhanced by litter feedbacks. *Plant and Soil* 330: 407-421.

Buffington, L.C. & Herbel, C.H. 1965. Vegetational changes on a semidesert grassland range from 1858 to 1963. *Ecological Monographs* 35: 139-&.

Bunn, A.G. & Goetz, S.J. 2006. Trends in satellite-observed circumpolar photosynthetic activity from 1982 to 2003: The influence of seasonality, cover type, and vegetation density. *Earth Interactions* 10.

Burkett, V.R., Wilcox, D.A., Stottlemyer, R., Barrow, W., Fagre, D., Baron, J., Price, J., Nielsen, J.L., Allen, C.D., Peterson, D.L., Ruggerone, G. & Doyle, T. 2005. Nonlinear dynamics in ecosystem response to climatic change: Case studies and policy implications. *Ecological Complexity* 2: 357-394.

Burkinshaw, A.M. & Bork, E.W. 2009. Shrub Encroachment Impacts the Potential for Multiple Use Conflicts on Public Land. *Environmental Management* 44: 493-504.

Butler, L.G., Kielland, K., Rupp, T.S. & Hanley, T.A. 2007. Interactive controls of herbivory and fluvial dynamics on landscape vegetation patterns on the Tanana River floodplain, interior Alaska. *Journal of Biogeography* 34: 1622-1631.

Cairns, D., Lafon, C., Moen, J. & Young, A. 2007. Influences of Animal Activity on Treeline Position and Pattern: Implications for Treeline Responses to Climate Change. *Physical Geography* 28: 419-433.

Cairns, D.M. & Moen, J. 2004. Herbivory influences tree lines. *Journal of Ecology* 92: 1019-1024.

Carlsson, B.A. & Callaghan, T.V. 1991. Positive plant interactions in tundra vegetation and the importance of shelter. *Journal of Ecology* 79: 973-983.

Chapin, F.S., III & Shaver, G.R. 1996. Physiological and Growth Responses of Arctic Plants to a Field Experiment Simulating Climatic Change. *Ecology* 77: 822-840.

Chapin, F.S., Shaver, G.R., Giblin, A.E., Nadelhoffer, K.J. & Laundre, J.A. 1995. Responses of Arctic tundra to experimental and observed changes in climate. *Ecology* 76: 694-711.

Chapin, F.S., Sturm, M., Serreze, M.C., McFadden, J.P., Key, J.R., Lloyd, A.H., McGuire, A.D., Rupp, T.S., Lynch, A.H., Schimel, J.P., Beringer, J., Chapman, W.L., Epstein, H.E., Euskirchen, E.S., Hinzman, L.D., Jia, G., Ping, C.L., Tape,

K.D., Thompson, C.D.C., Walker, D.A. & Welker, J.M. 2005. Role of land-surface changes in Arctic summer warming. *Science* 310: 657-660.

Chen, J.S., Lei, N.F., Yu, D. & Dong, M. 2006. Differential effects of clonal integration on performance in the stoloniferous herb Duchesnea indica, as growing at two sites with different altitude. *Plant Ecology* 183: 147-156.

Clark, J.S., Fastie, C., Hurtt, G., Jackson, S.T., Johnson, C., King, G.A., Lewis, M., Lynch, J., Pacala, S., Prentice, C., Schupp, E.W., Webb, T. & Wyckoff, P. 1998. Reid's paradox of rapid plant migration - Dispersal theory and interpretation of paleoecological records. *BioScience* 48: 13-24.

Clark, J.S., Silman, M., Kern, R., Macklin, E. & HilleRisLambers, J. 1999. Seed Dispersal near and Far: Patterns across Temperate and Tropical Forests. *Ecology* 80: 1475-1494.

Colinvaux, P.A. 1964. The environment of the Bering land bridge. *Ecological Monographs* 34: 297-329.

Cooper, E.J., Alsos, I.G., Hagen, D., Smith, F.M., Coulson, S.J. & Hodkinson, I.D. 2004. Plant recruitment in the High Arctic: Seed bank and seedling emergence on Svalbard. *Journal of Vegetation Science* 15: 115-124.

Corenblit, D., Tabacchi, E., Steiger, J. & Gurnell, A.M. 2007. Reciprocal interactions and adjustments between fluvial landforms and vegetation dynamics in river corridors: A review of complementary approaches. *Earth-Science Reviews* 84: 56-86.

Costello, D.A., Lunt, I.D. & Williams, J.E. 2000. Effects of invasion by the indigenous shrub Acacia sophorae on plant composition of coastal grasslands in south-eastern Australia. *Biological Conservation* 96: 113-121.

Craine, J.M., Towne, E.G. & Nippert, J.B. 2010. Climate controls on grass culm production over a quarter century in a tallgrass prairie. *Ecology* 91: 2132-2140.

Craine, J.M.E.G.T. & Nippert, J.B. 2010. Climate controls on grass culm production over a quarter century in a tallgrass prairie. 91.

Danby, R.K. & Hik, D.S. 2007. Variability, contingency and rapid change in recent subarctic alpine tree line dynamics. *Journal of Ecology* 95: 352-363.

Darby, S.E. 1999. Effect of riparian vegetation on flow resistance and flood potential. *Journal of Hydraulic Engineering-Asce* 125: 443-454.

de Groot, W.J., Thomas, P.A. & Wein, R.W. 1997. *Betula nana* L. and *Betula glandulosa* Michx. *Journal of Ecology* 85: 241-264.

de Groot, W.J. & Wein, R.W. 2004. Effects of fire severity and season of burn on Betula glandulosa growth dynamics. *International Journal of Wildland Fire* 13: 287-295.

de Molenaar, J.G. 1987. An ecohydrological approach to floral and vegetational patterns in Arctic lanadscape ecology. *Arctic and Alpine Research* 19: 414-424.

de Witte, L.C. & Stocklin, J. 2010. Longevity of clonal plants: why it matters and how to measure it. *Annals of Botany* 106: 859-870.

den Herder, M., Virtanen, R. & Roininen, H. 2008. Reindeer herbivory reduces willow growth and grouse forage in a forest-tundra ecotone. *Basic and Applied Ecology* 9: 324-331.

DeWine, J.M. & Cooper, D.J. 2007. Effects of river regulation on riparian box elder (Acer negundo) forests in canyons of the upper Colorado River Basin, USA. *Wetlands* 27: 278-289.

Douglas, D.A. 1989. Clonal growth of *Salix setchelliana* on glacier river gravel bars in Alaska. *Journal of Ecology* 77: 112-126.

Douhovnikoff, V., Goldsmith, G.R., Tape, K.D., Huang, C., Sur, N. & Bret-Harte, M.S. 2010. Clonal Diversity in an Expanding Community of Arctic Salix spp. and a Model for Recruitment Modes of Arctic Plants. *Arctic Antarctic and Alpine Research* 42: 406-411.

Dullinger, S., Dirnbock, T. & Grabherr, G. 2004. Modelling climate change-driven treeline shifts: relative effects of temperature increase, dispersal and invasibility. *Journal of Ecology* 92: 241-252.

Dutta, K., Schuur, E.A.G., Neff, J.C. & Zimov, S.A. 2006. Potential carbon release from permafrost soils of Northeastern Siberia. *Global Change Biology* 12: 2336-2351.

Elmendorf, S.C., Henry, G.H.R., Hollister, R.D., Bjork, R.G., Boulanger-Lapointe, N., Cooper, E.J., Cornelissen, J.H.C., Day, T.A., Dorrepaal, E., Elumeeva, T.G., Gill, M., Gould, W.A., Harte, J., Hik, D.S., Hofgaard, A., Johnson, D.R., Johnstone, J.F., Jonsdottir, I.S., Jorgenson, J.C., Klanderud, K., Klein, J.A., Koh, S., Kudo, G., Lara, M., Levesque, E., Magnusson, B., May, J.L., Mercado-Diaz, J.A.,

Michelsen, A., Molau, U., Myers-Smith, I.H., Oberbauer, S.F., Onipchenko, V.G., Rixen, C., Martin Schmidt, N., Shaver, G.R., Spasojevic, M.J., orhallsdottir, o.E., Tolvanen, A., Troxler, T., Tweedie, C.E., Villareal, S., Wahren, C.-H., Walker, X., Webber, P.J., Welker, J.M. & Wipf, S. 2012. Plot-scale evidence of tundra vegetation change and links to recent summer warming. *Nature Clim. Change* 2: 453-457.

Epstein, H.E., Beringer, J., Gould, W.A., Lloyd, A.H., Thompson, C.D., Chapin, F.S., Michaelson, G.J., Ping, C.L., Rupp, T.S. & Walker, D.A. 2004. The nature of spatial transitions in the Arctic. *Journal of Biogeography* 31: 1917-1933.

Epstein, H.E., Walker, M.D., Chapin, F.S. & Starfield, A.M. 2000. A transient, nutrient-based model of Arctic plant community response to climatic warming. *Ecological Applications* 10: 824-841.

Fensham, R.J., Fairfax, R.J. & Archer, S.R. 2005. Rainfall, land use and woody vegetation cover change in semi-arid Australian savanna. *Journal of Ecology* 93: 596-606.

Forbes, B.C., Fauria, M.M. & Zetterberg, P. 2010. Russian Arctic warming and 'greening' are closely tracked by tundra shrub willows. *Global Change Biology* 16: 1542-1554.

Friedman, J.M., Auble, G.T., Andrews, E.D., Kittel, G., Madole, R.F., Griffin, E.R. & Allred, T.M. 2006. Transverse and longitudinal variation in woody riparian vegetation along a montane river. *Western North American Naturalist* 66: 78-91.

Frost, G.V., Epstein, H.E., Walker, D.A., Matyshak, G. & Ermokhina, K. 2013. Patterned-ground facilitates shrub expansion in Low Arctic tundra. *Environmental Research Letters* 8.

Fujiwara, M., Anderson, K.E., Neubert, M.G. & Caswell, H. 2006. On the estimation of dispersal kernels from individual mark-recapture data. *Environmental and Ecological Statistics* 13: 183-197.

Ghersa, C.M., de la Fuente, E., Suarez, S. & Leon, R.J.C. 2002. Woody species invasion in the Rolling Pampa grasslands, Argentina. *Agriculture Ecosystems & Environment* 88: 271-278.

Gibbens, R.P., McNeely, R.P., Havstad, K.M., Beck, R.F. & Nolen, B. 2005. Vegetation changes in the Jornada Basin from 1858 to 1998. *Journal of Arid Environments* 61: 651-668.

Gillson, L. & Ekblom, A. 2009. Resilience and Thresholds in Savannas: Nitrogen and Fire as Drivers and Responders of Vegetation Transition. *Ecosystems* 12: 1189-1203.

Glenz, C., Schlaepfer, R., Iorgulescu, I. & Kienast, F. 2006. Flooding tolerance of Central European tree and shrub species. *Forest Ecology and Management* 235: 1-13.

Goetz, S.J., Bunn, A.G., Fiske, G.J. & Houghton, R.A. 2005. Satellite-observed photosynthetic trends across boreal North America associated with climate and fire disturbance. *Proceedings of the National Academy of Sciences of the United States of America* 102: 13521-13525.

Gonzalez, V.T., Brathen, K.A., Ravolainen, V.T., Iversen, M. & Hagen, S.B. 2010. Large-scale grazing history effects on Arctic-alpine germinable seed banks. *Plant Ecology* 207: 321-331.

Gordon, C., Wynn, J.M. & Woodin, S.J. 2001. Impacts of increased nitrogen supply on high Arctic heath: the importance of bryophytes and phosphorus availability. *New Phytologist* 149: 461-471.

Gorham, E. 1991. Northern peatlands - role in the carbon-cycle and probable responses to climatic warming. *Ecological Applications* 1: 182-195.

Gough, L. 2006. Neighbor effects on germination, survival, and growth in two arctic tundra plant communities. *Ecography* 29: 44-56.

Gould, W.A., Raynolds, M. & Walker, D.A. 2003. Vegetation, plant biomass, and net primary productivity patterns in the Canadian Arctic. *Journal of Geophysical Research-Atmospheres* 108.

Graae, B.J., Alsos, I.G. & Ejrnaes, R. 2008. The impact of temperature regimes on development, dormancy breaking and germination of dwarf shrub seeds from arctic, alpine and boreal sites. *Plant Ecology* 198: 275-284.

Green, D.R., Cummins, R., Wright, R. & Miles, J. 1993. A methodology for acquiring informaiton on vegetation succession from remotely sensed imagery. In: Haines-Young, R., Green, D.R. & Cousins, S.H. (eds.) *Landscape Ecology and GIS*, pp. 111-128. Taylor and Francis, London.

Guilloy-Froget, H., Muller, E., Barsoum, N. & Hughes, F.M.R. 2002. Dispersal, germination, and survival of Populus nigra L. (Salicaceae) in changing hydrologic conditions. *Wetlands* 22: 478-488.

Guthrie, R.D. 2001. Origin and causes of the mammoth steppe: a story of cloud cover, woolly mammal tooth pits, buckles, and inside-out Beringia. *Quaternary Science Reviews* 20: 549-574.

Hallinger, M., Manthey, M. & Wilmking, M. 2010. Establishing a missing link: warm summers and winter snow cover promote shrub expansion into alpine tundra in Scandinavia. *New Phytologist* 186: 890-899.

Heisler, J.L., Briggs, J.M., Knapp, A.K., Blair, J.M. & Seery, A. 2004. Direct and indirect effects of fire on shrub density and aboveground productivity in a mesic grassland. *Ecology* 85: 2245-2257.

Hinzman, L.D., Bettez, N.D., Bolton, W.R., Chapin, F.S., Dyurgerov, M.B., Fastie, C.L., Griffith, B., Hollister, R.D., Hope, A., Huntington, H.P., Jensen, A.M., Jia, G.J., Jorgenson, T., Kane, D.L., Klein, D.R., Kofinas, G., Lynch, A.H., Lloyd, A.H., McGuire, A.D., Nelson, F.E., Oechel, W.C., Osterkamp, T.E., Racine, C.H., Romanovsky, V.E., Stone, R.S., Stow, D.A., Sturm, M., Tweedie, C.E., Vourlitis, G.L., Walker, M.D., Walker, D.A., Webber, P.J., Welker, J.M., Winker, K. & Yoshikawa, K. 2005. Evidence and implications of recent climate change in northern Alaska and other arctic regions. *Climatic Change* 72: 251-298.

Hobbie, S.E. 1996. Temperature and Plant Species Control Over Litter Decomposition in Alaskan Tundra. *Ecological Monographs* 66: 503-522.

Hobbie, S.E., Nadelhoffer, K.J. & Hogberg, P. 2002. A synthesis: The role of nutrients as constraints on carbon balances in boreal and arctic regions. *Plant and Soil* 242: 163-170.

Hoffman, M.T. & Rohde, R.F. 2011. Rivers Through Time: Historical Changes in the Riparian Vegetation of the Semi-Arid, Winter Rainfall Region of South Africa in Response to Climate and Land Use. *Journal of the History of Biology* 44: 59-80.

Hudson, J.M.G. & Henry, G.H.R. 2009. Increased plant biomass in a High Arctic heath community from 1981 to 2008. *Ecology* 90: 2657-2663.

Hupp, C.R. 1992. Riparian vegetation recovery patterns following stream channelization - a geomorphic perspective. *Ecology* 73: 1209-1226.

Illeris, L., Michelsen, A. & Jonasson, S. 2003. Soil Plus Root Respiration and Microbial Biomass Following Water, Nitrogen, and Phosphorus Application at a High Arctic Semi Desert. *Biogeochemistry* 65: 15-29.

Jackson, R.B., Banner, J.L., Jobbagy, E.G., Pockman, W.T. & Wall, D.H. 2002. Ecosystem carbon loss with woody plant invasion of grasslands. *Nature* 418: 623-626.

Jeltsch, F., Milton, S.J., Dean, W.R.J. & Rooyen, N. 1997. Simulated pattern formation around artificial waterholes in the semi-arid Kalahari. *Journal of Vegetation Science* 8: 177-188.

Jia, G.J., Epstein, H.E. & Walker, D.A. 2003. Greening of arctic Alaska, 1981-2001. *Geophysical Research Letters* 30: 3-1 - 3-4.

Jia, G.S., Epstein, H.E. & Walker, D.A. 2006. Spatial heterogeneity of tundra vegetation response to recent temperature changes. *Global Change Biology* 12: 42-55.

Johnson, D.D. & Miller, R.F. 2006. Structure and development of expanding western juniper woodlands as influenced by two topographic variables. *Forest Ecology and Management* 229: 7-15.

Johnson, W.C. 1998. Adjustment of riparian vegetation to river regulation in the great plains, USA. *Wetlands* 18: 608-618.

Johnson, W.C. 2000. Tree recruitment and survival in rivers: influence of hydrological processes. *Hydrological Processes* 14: 3051-+.

Jonasson, S., Michelsen, A., Schmidt, I.K. & Nielsen, E.V. 1999. Responses in microbes and plants to changed temperature, nutrient, and light regimes in the Arctic. *Ecology* 80: 1828-1843.

Junk, W.J. 1999. The flood pulse concept of large rivers: learning from the tropics. *Archiv Fur Hydrobiologie*: 261-280.

Kaplan, J.O., Bigelow, N.H., Prentice, I.C., Harrison, S.P., Bartlein, P.J., Christensen, T.R., Cramer, W., Matveyeva, N.V., McGuire, A.D., Murray, D.F., Razzhivin, V.Y., Smith, B., Walker, D.A., Anderson, P.M., Andreev, A.A., Brubaker, L.B., Edwards, M.E. & Lozhkin, A.V. 2003. Climate change and Arctic ecosystems: 2. Modeling, paleodata-model comparisons, and future projections. *Journal of Geophysical Research-Atmospheres* 108: 17.

Kjolner, S., Sastad, S.M. & Brochmann, C. 2006. Clonality and recombination in the arctic plant Saxifraga cernua. *Botanical Journal of the Linnean Society* 152: 209-217.

Klady, R.A., Henry, G.H.R. & Lemay, V. 2011. Changes in high arctic tundra plant reproduction in response to long-term experimental warming. *Global Change Biology* 17: 1611-1624.

Knoop, W.T. & Walker, B.H. 1985. Interactions of woody and herbaceous vegetation in a southern African savanna. *Journal of Ecology* 73: 235-253.

Konrad, C., Berge, H., Fuerstenberg, R., Steff, K., Olsen, T. & Guyenet, J. 2011. Channel Dynamics in the Middle Green River, Washington, from 1936 to 2002. *Northwest Science* 85: 1-14.

rner , C. 2003. *Alpine plant life : functional plant ecology of high mountain ecosystems*.2nd ed. Springer, New York.

Kremenetski, C.V., Sulerzhitsky, L.D. & Hantemirov, R. 1998. Holocene History of the Northern Range Limits of Some Trees and Shrubs in Russia. *Arctic and Alpine Research* 30: 317-333.

Kremenetski, K.V., MacDonald, G.M., Gervais, B.R., Borisova, O.K. & Snyder, J.A. 2004. Holocene vegetation history and climate change on the northern Kola Peninsula, Russia: a case study from a small tundra lake. *Quaternary International* 122: 57-68.

Lachenbruch, A.H. & Marshall, B.V. 1986. Changing climate - geothermal evidenc from permafrost in the Alaskan Arctic. *Science* 234: 689-696.

Lantz, T.C., Gergel, S.E. & Kokelj, S.V. 2010. Spatial Heterogeneity in the Shrub Tundra Ecotone in the Mackenzie Delta Region, Northwest Territories: Implications for Arctic Environmental Change. *Ecosystems* 13: 194-204.

Lawrence, D., M. & Swenson, S., C. 2011. Permafrost response to increasing Arctic shrub abundance depends on the relative influence of shrubs on local soil cooling versus large-scale climate warming. *Environmental Research Letters* 6: 045504.

Lawrence, D.M. & Slater, A.G. 2005. A projection of severe near-surface permafrost degradation during the 21st century. *Geophysical Research Letters* 32: L24401.

Lett, M.S. & Knapp, A.K. 2003. Consequences of shrub expansion in mesic grassland: Resource alterations and graminoid responses. *Journal of Vegetation Science* 14: 487-496.

Lett, M.S. & Knapp, A.K. 2005. Woody Plant Encroachment and Removal in Mesic Grassland: Production and Composition Responses of Herbaceous Vegetation. *American Midland Naturalist* 153: 217-231.

Lett, M.S., Knapp, A.K., Briggs, J.M. & Blair, J.M. 2004. Influence of shrub encroachment on aboveground net primary productivity and carbon and nitrogen pools in a mesic grassland. *Canadian Journal of Botany-Revue Canadienne De Botanique* 82: 1363-1370.

Li, B.L. 2002. A theoretical framework of ecological phase transitions for characterizing tree-grass dynamics. *Acta Biotheoretica* 50: 141-154.

Liston, G.E., McFadden, J.P., Sturm, M. & Pielke, R.A. 2002. Modelled changes in arctic tundra snow, energy and moisture fluxes due to increased shrubs. *Global Change Biology* 8: 17-32.

Livingstone, D.A. 1957. Pollen analysis of a valley fill near Umiat, Alaska. *American Journal of Science* 255: 254-260.

Livingstone, D.A. 1955. Some pollen profiles from arctic Alaska. *Ecology* 36: 587-600.

Lloyd, A.H., Rupp, T.S., Fastie, C.L. & Starfield, A.M. 2002. Patterns and dynamics of treeline advance on the Seward Peninsula, Alaska. *Journal of Geophysical Research-Atmospheres* 108.

Loehle, C. & Li, B.L. 1996. Statistical properties of ecological and geologic fractals. *Ecological Modelling* 85: 271-284.

Loehle, C., Li, B.L. & Sundell, R.C. 1996. Forest spread and phase transitions at forest-prairie ecotones in Kansas, USA. *Landscape Ecology* 11: 225-235.

Lozhkin, A., Anderson, P., Matrosova, T. & Minyuk, P. 2007. The pollen record from El'gygytgyn Lake: implications for vegetation and climate histories of northern Chukotka since the late middle Pleistocene. *Journal of Paleolimnology* 37: 135-153.

Lunt, I.D., Winsemius, L.M., McDonald, S.P., Morgan, J.W. & Dehaan, R.L. 2010. How widespread is woody plant encroachment in temperate Australia? Changes in woody vegetation cover in lowland woodland and coastal ecosystems in Victoria from 1989 to 2005. *Journal of Biogeography* 37: 722-732.

Mack, M.C., Schuur, E.A.G., Bret-Harte, M.S., Shaver, G.R. & Chapin, F.S. 2004. Ecosystem carbon storage in arctic tundra reduced by long-term nutrient fertilization. *Nature* 431: 440-443.

Malanson, G.P. 1993. *Riparian landscapes*. Cambridge New York : Cambridge University Press, Cambridge New York.

Malanson, G.P. & Cairns, D.M. 1997. Effects of dispersal, population delays, and forest fragmentation on tree migration rates. *Plant Ecology* 131: 67-79.

Mandre, M., Pärn, H., lõšei ko, J., Ingerslev, M., Stupak, I., rt, M . & Paasrand, . 2010. Use of biofuel ashes for fertilisation of Betula pendula seedlings on nutrient-poor peat soil. *Biomass and Bioenergy* 34: 1384-1392.

Mann, D.H., Groves, P., Reanier, R.E. & Kunz, M.L. 2010. Floodplains, permafrost, cottonwood trees, and peat: What happened the last time climate warmed suddenly in arctic Alaska? *Quaternary Science Reviews* 29: 3812-3830.

Mann, D.H., Peteet, D.M., Reanier, R.E. & Kunz, M.L. 2002. Responses of an arctic landscape to Lateglacial and early Holocene climatic changes: the importance of moisture. *Quaternary Science Reviews* 21: 997-1021.

McAuliffe, J.R. 1994. Landscape Evolution, Soil Formation, and Ecological Patterns and Processes in Sonoran Desert Bajadas. *Ecological Monographs* 64: 112-148.

McGarigal, K. & Marks, B.J. 1995. FRAGSTATS: spatial pattern program for quantifying landscape structure, PNW-GTR-351. In, Portland, Oregon.

McGuire, A.D., Chapin, F.S., Walsh, J.E. & Wirth, C. 2006. Integrated regional changes in arctic climate feedbacks: Implications for the global climate system. *Annual Review of Environment and Resources* 31: 61-91.

McKane, R.B., Rastetter, E.B., Shaver, G.R., Nadelhoffer, K.J., Giblin, A.E., Laundre, J.A. & Chapin, F.S. 1997. Reconstruction and Analysis of Historical Changes in Carbon Storage in Arctic Tundra. *Ecology* 78: 1188-1198.

Miller, G.H., Brigham-Grette, J., Alley, R.B., Anderson, L., Bauch, H.A., Douglas, M.S.V., Edwards, M.E., Elias, S.A., Finney, B.P., Fitzpatrick, J.J., Funder, S.V., Herbert, T.D., Hinzman, L.D., Kaufman, D.S., MacDonald, G.M., Polyak, L., Robock, A., Serreze, M.C., Smol, J.P., Spielhagen, R., White, J.W.C., Wolfe, A.P. & Wolff, E.W. 2010. Temperature and precipitation history of the Arctic. *Quaternary Science Reviews* 29: 1679-1715.

Milne, B.T., Johnson, A.R., Keitt, T.H., Hatfield, C.A., David, J. & Hraber, P.T. 1996. Detection of critical densities associated with pinon-juniper woodland ecotones. *Ecology* 77: 805-821.

Moen, J., Cairns, D.M. & Lafon, C.W. 2008. Factors structuring the treeline ecotone in Fennoscandia. *Plant Ecology & Diversity* 1: 77 - 87.

Morgan, J.A., Milchunas, D.G., LeCain, D.R., West, M. & Mosier, A.R. 2007. Carbon dioxide enrichment alters plant community structure and accelerates shrub growth in the shortgrass steppe. *Proceedings of the National Academy of Sciences of the United States of America* 104: 14724-14729.

Mulholland, P.J., Roberts, B.J., Hill, W.R. & Smith, J.G. 2009. Stream ecosystem responses to the 2007 spring freeze in the southeastern United States: unexpected effects of climate change. *Global Change Biology* 15: 1767-1776.

Munier, A., Hermanutz, L., Jacobs, J.D. & Lewis, K. 2010. The interacting effects of temperature, ground disturbance, and herbivory on seedling establishment: implications for treeline advance with climate warming. *Plant Ecology* 210: 19-30.

Myers-Smith, I.H., Forbes, B.C., Wilmking, M., Hallinger, M., Lantz, T., Blok, D., Tape, K.D., Macias-Fauria, M., Sass-Klaassen, U., Levesque, E., Boudreau, S., Ropars, P., Hermanutz, L., Trant, A., Collier, L.S., Weijers, S., Rozema, J., Rayback, S.A., Schmidt, N.M., Schaepman-Strub, G., Wipf, S., Rixen, C., Menard, C.B., Venn, S., Goetz, S., Andreu-Hayles, L., Elmendorf, S., Ravolainen, V., Welker, J., Grogan, P., Epstein, H.E. & Hik, D.S. 2011a. Shrub expansion in tundra ecosystems: dynamics, impacts and research priorities. *Environmental Research Letters* 6.

Myers-Smith, I.H., Forbes, B.C., Wilmking, M., Hallinger, M., Lantz, T., Blok, D., Tape, K.D., Macias-Fauria, M., Sass-Klaassen, U., Lévesque, E., Boudreau, S., Ropars, P., Hermanutz, L., Trant, A., Collier, L.S., Weijers, S., Rozema, J., Rayback, S.A., Schmidt, N.M., Schaepman-Strub, G., Wipf, S., Rixen, C., Ménard, C.B., Venn, S., Goetz, S., Andreu-Hayles, L., Elmendorf, S., Ravolainen, V., Welker, J., Grogan, P., Epstein, H.E. & Hik, D.S. 2011b. Shrub

expansion in tundra ecosystems: dynamics, impacts and research priorities. *Environmental Research Letters* 6: 045509.

Myers-Smith, I.H. & Hik, D.S. 2013. Shrub canopies influence soil temperatures but not nutrient dynamics: An experimental test of tundra snow–shrub interactions. *Ecology and Evolution* 3: 3683-3700.

Myneni, R.B., Keeling, C.D., Tucker, C.J., Asrar, G. & Nemani, R.R. 1997. Increased plant growth in the northern high latitudes from 1981 to 1991. *Nature* 386: 698-701.

Naiman, R.J., Elliott, S.R., Helfield, J.M. & O'Keefe, T.C. 1999. Biophysical interactions and the structure and dynamics of riverine ecosystems: the importance of biotic feedbacks. *Hydrobiologia* 410: 79-86.

Naito, A.T. & Cairns, D.M. 2011a. Patterns and processes of global shrub expansion. *Progress in Physical Geography* 35: 423-442.

Naito, A.T. & Cairns, D.M. 2011b. Relationships between Arctic shrub dynamics and topographically derived hydrologic characteristics. *Environmental Research Letters* 6: 045506.

Neary, D.G. & Medina, A.L. 1996. Geomorphic response of a montane riparian habitat to interactions of ungulates, vegetation, and hydrology. *Desired Future Conditions for Southwestern Riparian Ecosystems: Bringing Interests and Concerns Together* 272: 143-147.

Normand, S., Randin, C., Ohlemuller, R., Bay, C., Hoye, T.T., Kjaer, E.D., Korner, C., Lischke, H., Maiorano, L., Paulsen, J., Pearman, P.B., Psomas, A., Treier, U.A.,

Zimmermann, N.E. & Svenning, J.C. 2013. A greener Greenland? Climatic potential and long-term constraints on future expansions of trees and shrubs. *Philosophical Transactions of the Royal Society B-Biological Sciences* 368.

O'Connor, T.G. 1995. *Acacia karroo* invasion of grassland - environmental and biotic effects influencing seedling emergence and establishment. *Oecologia* 103: 214-223.

Oksanen, P.O., Kuhry, P. & Alekseeva, R.N. 2001. Holocene development of the Rogovaya River peat plateau, European Russian Arctic. *Holocene* 11: 25-40.

Olofsson, J., Kitti, H., Rautiainen, P., Stark, S. & Oksanen, L. 2001. Effects of summer grazing by reindeer on composition of vegetation, productivity and nitrogen cycling. *Ecography* 24: 13-24.

Olofsson, J., Oksanen, L., Callaghan, T., Hulme, P.E., Oksanen, T. & Suominen, O. 2009. Herbivores inhibt climate-driven shrub expansion on the tundra. *Global Change Biology* 15: 2681-2693.

Olofsson, J., Stark, S. & Oksanen, L. 2004. Reindeer influence on ecosystem processes in the tundra. *Oikos* 105: 386-396.

Osterkamp, T.E. & Romanovsky, V.E. 1999. Evidence for warming and thawing of discontinuous permafrost in Alaska. *Permafrost and Periglacial Processes* 10: 17-37.

Oswald, W.W., Brubaker, L.B. & Anderson, P.M. 1999. Late Quaternary vegetational history of the Howard Pass area, northwestern Alaska. *Canadian Journal of Botany-Revue Canadienne De Botanique* 77: 570-581.

Overpeck, J., Hughen, K., Hardy, D., Bradley, R., Case, R., Douglas, M., Finney, B., Gajewski, K., Jacoby, G., Jennings, A., Lamoureux, S., Lasca, A., MacDonald, G., Moore, J., Retelle, M., Smith, S., Wolfe, A. & Zielinski, G. 1997. Arctic environmental change of the last four centuries. *Science* 278: 1251-1256.

Pajunen, A.M. 2009. Environmental and Biotic Determinants of Growth and Height of Arctic Willow Shrubs along a Latitudinal Gradient. *Arctic Antarctic and Alpine Research* 41: 478-485.

Paruelo, J.M. & Sala, O.E. 1995. Water Losses in the Patagonian Steppe: A Modelling Approach. *Ecology* 76: 510-520.

Paulsen, H.A., Jr. 1953. A Comparison of Surface Soil Properties Under Mesquite and Perennial Grass. *Ecology* 34: 727-732.

Peters, D.P.C., Yao, J. & Gosz, J.R. 2006. Woody plant invasion at a semi-arid/arid transition zone: importance of ecosystem type to colonization and patch expansion. *Journal of Vegetation Science* 17: 389-396.

Poff, B., Koestner, K.A., Neary, D.G. & Henderson, V. 2011. Threats to Riparian Ecosystems in Western North America: An Analysis of Existing Literature. *Journal of the American Water Resources Association* 47: 1241-1254.

Poff, N.L., Allan, J.D., Bain, M.B., Karr, J.R., Prestegaard, K.L., Richter, B.D., Sparks, R.E. & Stromberg, J.C. 1997. The natural flow regime. *BioScience* 47: 769-784.

Pouliot, D., Latifovic, R. & Olthof, I. 2008. Trends in vegetation NDVI from 1 km AVHRR data over Canada for the period 1985–2006. *International Journal of Remote Sensing* 30: 149-168.

Press, M.C., Potter, J.A., Burke, M.J.W., Callaghan, T.V. & Lee, J.A. 1998. Responses of a Subarctic Dwarf Shrub Heath Community to Simulated Environmental Change. *Journal of Ecology* 86: 315-327.

Price, J.N. & Morgan, J.W. 2008. Woody plant encroachment reduces species richness of herb-rich woodlands in southern Australia. *Austral Ecology* 33: 278-289.

Rastetter, E.B., Perakis, S.S., Shaver, G.R. & Agren, G.I. 2005. Terrestrial C sequestration at elevated-CO2 and temperature: The role of dissolved organic N loss. *Ecological Applications* 15: 71-86.

Raynolds, M.K., Walker, D.A., Verbyla, D. & Munger, C.A. 2013. Patterns of Change within a Tundra Landscape: 22-year Landsat NDVI Trends in an Area of the Northern Foothills of the Brooks Range, Alaska. *Arctic, Antarctic, and Alpine Research* 45: 249-260.

Reynolds, J.F., Virginia, R.A., Kemp, P.R., de Soyza, A.G. & Tremmel, D.C. 1999. Impact of drought on desert shrubs: Effects of seasonality and degree of resource island development. *Ecological Monographs* 69: 69-106.

Risser, P.G. 1995. The status of the science examining ecotones: a dynamic aspect of landscape is the area of steep gradient between more homogenous vegetation associations. *BioScience* 45: 318-325.

Robinson, T.P., van Klinken, R.D. & Metternicht, G. 2008. Spatial and temporal rates and patterns of mesquite (Prosopis species) invasion in Western Australia. *Journal of Arid Environments* 72: 175-188.

Robledo-Arnuncio, J.J. & Garcia, C. 2007. Estimation of the seed dispersal kernel from exact identification of source plants. *Molecular Ecology* 16: 5098-5109.

Rocchini, D., Perry, G.L.W., Salerno, M., Maccherini, S. & Chiarucci, A. 2006. Landscape change and the dynamics of open formations in a natural reserve. *Landscape and Urban Planning* 77: 167-177.

Roques, K.G., O'Connor, T.G. & Watkinson, A.R. 2001. Dynamics of shrub encroachment in an African savanna: relative influences of fire, herbivory, rainfall and density dependence. *Journal of Applied Ecology* 38: 268-280.

Ruhland, K., St Jacques, J.M., Beierle, B.D., Lamoureux, S.F., Dyke, A.S. & Smol, J.P. 2009. Lateglacial and Holocene paleoenvironmental changes recorded in lake sediments, Brock Plateau (Melville Hills), Northwest Territories, Canada. *Holocene* 19: 1005-1016.

Rupp, T.S., Starfield, A.M. & Chapin, F.S. 2000. A frame-based spatially explicit model of subarctic vegetation response to climatic change: comparison with a point model. *Landscape Ecology* 15: 383-400.

Scheffer, M., Hirota, M., Holmgren, M., Van Nes, E.H. & Chapin, F.S. 2012. Thresholds for boreal biome transitions. *Proceedings of the National Academy of Sciences of the United States of America* 109: 21384-21389.

Schlesinger, W.H., Abrahams, A.D., Parsons, A.J. & Wainwright, J. 1999. Nutrient losses in runoff from grassland and shrubland habitats in Southern New Mexico: I. rainfall simulation experiments. *Biogeochemistry* 45: 21-34.

Schlesinger, W.H., Raikes, J.A., Hartley, A.E. & Cross, A.E. 1996. On the spatial pattern of soil nutrients in desert ecosystems. *Ecology* 77: 364-374.

Schlesinger, W.H., Reynolds, J.F., Cunningham, G.L., Huenneke, L.F., Jarrell, W.M., Virginia, R.A. & Whitford, W.G. 1990. Biological feedbacks in global desertification. *Science* 247: 1043-1048.

Schlesinger, W.H., Ward, T.J. & Anderson, J. 2000. Nutrient losses in runoff from grassland and shrubland habitats in southern New Mexico: II. Field plots. *Biogeochemistry* 49: 69-86.

Schuur, E.A.G., Bockheim, J., Canadell, J.G., Euskirchen, E., Field, C.B., Goryachkin, S.V., Hagemann, S., Kuhry, P., Lafleur, P.M., Lee, H., Mazhitova, G., Nelson, F.E., Rinke, A., Romanovsky, V.E., Shiklomanov, N., Tarnocai, C., Venevsky, S., Vogel, J.G. & Zimov, S.A. 2008. Vulnerability of permafrost carbon to climate change: Implications for the global carbon cycle. *BioScience* 58: 701-714.

Seppä, H., Nyman, M., Korhola, A. & Weckström, J. 2002. Changes of treelines and alpine vegetation in relation to post-glacial climate dynamics in northern Fennoscandia based on pollen and chironomid records. *Journal of Quaternary Science* 17: 287-301.

Serreze, M.C., Walsh, J.E., Chapin, F.S., Osterkamp, T., Dyurgerov, M., Romanovsky, V., Oechel, W.C., Morison, J., Zhang, T. & Barry, R.G. 2000. Observational Evidence of Recent Change in the Northern High-Latitude Environment. *Climatic Change* 46: 159-207.

Seyfried, M.S. & Wilcox, B.P. 2006. Soil water storage and rooting depth: key factors controlling recharge on rangelands. *Hydrological Processes* 20: 3261-3275.

Shevtsova, A., Ojala, A., Neuvonen, S., Vieno, M. & Haukioja, E. 1995. Growth and Reproduction of Dwarf Shrubs in a Subarctic Plant Community: Annual Variation and Above-Ground Interactions with Neighbours. *Journal of Ecology* 83: 263-275.

Skarpe, C. 1991. Spatial patterns and dynamics of woody vegetation in an arid savanna. *Journal of Vegetation Science* 2: 565-572.

Sorensen, R., Zinko, U. & Seibert, J. 2006. On the calculation of the topographic wetness index: evaluation of different methods based on field observations. *Hydrology and Earth System Sciences* 10: 101-112.

Steltzer, H., Hufbauer, R.A., Welker, J.M., Casalis, M., Sullivan, P.F. & Chimner, R. 2008. Frequent sexual reproduction and high intraspecific variation in Salix arctica: Implications for a terrestrial feedback to climate change in the High Arctic. *Journal of Geophysical Research-Biogeosciences* 113.

Stephens, J.M.C., Molan, P.C. & Clarkson, B.D. 2005. A review of *Leptospermum scoparium* (*Myrtaceae*) in New Zealand. *New Zealand Journal of Botany* 43: 431-449.

Stieglitz, M., Déry, S.J., Romanovsky, V.E. & Osterkamp, T.E. 2003. The role of snow cover in the warming of arctic permafrost. *Geophysical Research Letters* 30: 1721.

Stieglitz, M., McKane, R.B. & Klausmeier, C.A. 2006. A simple model for analyzing climatic effects on terrestrial carbon and nitrogen dynamics: An arctic case study. *Global Biogeochemical Cycles* 20.

Strom, L., Jansson, R., Nilsson, C., Johansson, M.E. & Xiong, S.J. 2011. Hydrologic effects on riparian vegetation in a boreal river: an experiment testing climate change predictions. *Global Change Biology* 17: 254-267.

Stromberg, J.C., Lite, S.J. & Dixon, M.D. 2010a. Effects of stream flow patterns on riparian vegetation of a semiarid river: implications for a changing climate. *River Research and Applications* 26: 712-729.

Stromberg, J.C., Tluczek, M.G.F., Hazelton, A.F. & Ajami, H. 2010b. A century of riparian forest expansion following extreme disturbance: Spatio-temporal change in Populus/Salix/Tamarix forests along the Upper San Pedro River, Arizona, USA. *Forest Ecology and Management* 259: 1181-1189.

Sturm, M., McFadden, J.P., Liston, G.E., Chapin, F.S., III, Racine, C.H. & Holmgren, J. 2001a. Snow-Shrub Interactions in Arctic Tundra: A Hypothesis with Climatic Implications. *Journal of Climate* 14: 336.

Sturm, M., Racine, C. & Tape, K. 2001b. Climate change - Increasing shrub abundance in the Arctic. *Nature* 411: 546-547.

Sturm, M., Schimel, J., Michaelson, G., Welker, J.M., Oberbauer, S.F., Liston, G.E., Fahnestock, J. & Romanovsky, V.E. 2005. Winter Biological Processes Could Help Convert Arctic Tundra to Shrubland. *BioScience* 55: 17-26.

Tape, K., Hallinger, M., Welker, J. & Ruess, R. 2012. Landscape heterogeneity of shrub expansion in Arctic Alaska. *Ecosystems*: 1-14.

Tape, K., Sturm, M. & Racine, C. 2006. The evidence for shrub expansion in Northern Alaska and the Pan-Arctic. *Global Change Biology* 12: 686-702.

Tarboton, D.G. 1997. A new method for the determination of flow directions and upslope areas in grid digital elevation models. *Water Resources Research* 33: 309-319.

Tews, J., Esther, A., Milton, S.J. & Jeltsch, F. 2006. Linking a population model with an ecosystem model: Assessing the impact of land use and climate change on savanna shrub cover dynamics. *Ecological Modelling* 195: 219-228.

Tews, J., Schurr, F. & Jeltsch, F. 2004. Seed dispersal by cattle may cause shrub encroachment of Grewia lava on southern Kalahari rangelands. *Applied Vegetation Science* 7: 89-102.

Tockner, K. & Stanford, J.A. 2002. Riverine flood plains: present state and future trends. *Environmental Conservation* 29: 308-330.

Uzunov, D.I. 1993. *Introduction to the Theory of Critical Phenomena: Mean Field, Fluctuations and Renormalization.* World Scientific, Singapore.

Valiranta, M., Kultti, S. & Seppa, H. 2006. Vegetation dynamics during the Younger Dryas-Holocene transition in the extreme northern taiga zone, northeastern European Russia. *Boreas* 35: 202-212.

Van Auken, O.W. 2009. Causes and consequences of woody plant encroachment into western North American grasslands. *Journal of Environmental Management* 90: 2931-2942.

Van Auken, O.W. 2000. Shrub invasions of Norht American semiarid grasslands. *Annual Review of Ecology and Systematics* 31: 197-215.

van der Wal, R. 2006. Do herbivores cause habitat degradation or vegetation state transition? Evidence from the tundra. *Oikos* 114: 177-186.

van Klinken, R.D., Graham, J. & Flack, L.K. 2006. Population ecology of hybrid mesquite (Prosopis species) in Western Australia: how does it differ from native range invasions and what are the implications for impacts and management? *Biological Invasions* 8: 727-741.

van Vegten, J.A. 1984. Thornbush Invasion in a Savanna Ecosystem in Eastern Botswana. *Vegetatio* 56: 3-7.

Verbyla, D. 2008. The greening and browning of Alaska based on 1982-2003 satellite data. *Global Ecology and Biogeography* 17: 547-555.

Waelbroeck, C., Monfray, P., Oechel, W.C., Hastings, S. & Vourlitis, G. 1997. The impact of permafrost thawing on the carbon dynamics of tundra. *Geophysical Research Letters* 24: 229-232.

Wahren, C.H.A., Walker, M.D. & Bret-Harte, M.S. 2005. Vegetation responses in Alaskan arctic tundra after 8 years of a summer warming and winter snow manipulation experiment. *Global Change Biology* 11: 537-552.

Walck, J.L., Hidayati, S.N., Dixon, K.W., Thompson, K. & Poschlod, P. 2011. Climate change and plant regeneration from seed. *Global Change Biology* 17: 2145-2161.

Walker, D.A. 2000. Hierarchical subdivision of Arctic tundra based on vegetation response to climate, parent material and topography. *Global Change Biology* 6: 19-34.

Walker, D.A., Bay, C., Daniels, F.J.A., Einarsson, E., Elvebakk, A., Johansen, B.E., Kapitsa, A., Kholod, S.S., Murray, D.F., Talbot, S.S., Yurtsev, B.A. & Zoltai, S.C. 1995. Toward a new Arctic vegetation map - a review of existing maps. *Journal of Vegetation Science* 6: 427-436.

Walker, D.A., Epstein, H.E., Jia, G.J., Balser, A., Copass, C., Edwards, E.J., Gould, W.A., Hollingsworth, J., Knudson, J., Maier, H.A., Moody, A. & Raynolds, M.K. 2003a. Phytomass, LAI, and NDVI in northern Alaska: Relationships to summer warmth, soil pH, plant functional types, and extrapolation to the circumpolar Arctic. *Journal of Geophysical Research-Atmospheres* 108.

Walker, D.A., Epstein, H.E., Raynolds, M.K., Kuss, P., Kopecky, M.A., Frost, G.V., Daniëls, F.J.A., Leibman, M.O., Moskalenko, N.G., Matyshak, G.V., Khitun, O.V., Khomutov, A.V., Forbes, B.C., Bhatt, U.S., Kade, A.N., Vonlanthen, C.M. & Tichý, L. 2012. Environment, vegetation and greenness (NDVI) along the North America and Eurasia Arctic transects. *Environmental Research Letters* 7: 015504.

Walker, D.A., Jia, G.J., Epstein, H.E., Raynolds, M.K., Chapin, F.S., Copass, C., Hinzman, L.D., Knudson, J.A., Maier, H.A., Michaelson, G.J., Nelson, F., Ping,

C.L., Romanovsky, V.E. & Shiklomanov, N. 2003b. Vegetation-soil-thaw-depth relationships along a Low-Arctic bioclimate gradient, Alaska: Synthesis of information from the ATLAS studies. *Permafrost and Periglacial Processes* 14: 103-123.

Walker, D.A., Raynolds, M.K., Daniels, F.J.A., Einarsson, E., Elvebakk, A., Gould, W.A., Katenin, A.E., Kholod, S.S., Markon, C.J., Melnikov, E.S., Moskalenko, N.G., Talbot, S.S., Yurtsev, B.A. & Team, C. 2005. The Circumpolar Arctic vegetation map. *Journal of Vegetation Science* 16: 267-282.

Walker, M.D., Wahren, C.H., Hollister, R.D., Henry, G.H.R., Ahlquist, L.E., Alatalo, J.M., Bret-Harte, M.S., Calef, M.P., Callaghan, T.V., Carroll, A.B., Epstein, H.E., Jonsdottir, I.S., Klein, J.A., Magnusson, B., Molau, U., Oberbauer, S.F., Rewa, S.P., Robinson, C.H., Shaver, G.R., Suding, K.N., Thompson, C.C., Tolvanen, A., Totland, O., Turner, P.L., Tweedie, C.E., Webber, P.J. & Wookey, P.A. 2006. Plant community responses to experimental warming across the tundra biome. *Proceedings of the National Academy of Sciences of the United States of America* 103: 1342-1346.

Werner, K., Tarasov, P.E., Andreev, A.A., Muller, S., Kienast, F., Zech, M., Zech, W. & Diekmann, B. 2010. A 12.5-kyr history of vegetation dynamics and mire development with evidence of Younger Dryas larch presence in the Verkhoyansk Mountains, East Siberia, Russia. *Boreas* 39: 56-68.

Willson, M.F. 1993. Dispersal mode, seed shadows, and colonization patterns. *Vegetatio* 108: 261-280.

Woo, M.K., Lewkowicz, A.G. & Rouse, W.R. 1992. Response to the Canadian permafrost environment to climatic-change. *Physical Geography* 13: 287-317.

Wu, X. & Archer, S. 2005. Scale-Dependent Influence of Topography-Based Hydrologic Features on Patterns of Woody Plant Encroachment in Savanna Landscapes. *Landscape Ecology* 20: 733-742.

Yahdjian, L. & Sala, O. 2010. Size of Precipitation Pulses Controls Nitrogen Transformation and Losses in an Arid Patagonian Ecosystem. *Ecosystems* 13: 575-585.

Yu, Q., Epstein, H. & Walker, D. 2009. Simulating the effects of soil organic nitrogen and grazing on arctic tundra vegetation dynamics on the Yamal Peninsula, Russia. *Environmental Research Letters* 4.

Yurtsev, B.A. 2001. The Pleistocene "Tundra-Steppe" and the productivity paradox: the landscape approach. *Quaternary Science Reviews* 20: 165-174.

Zeng, Y. & Malanson, G.P. 2006. Endogenous fractal dynamics at alpine treeline ecotones. *Geographical Analysis* 38: 271-287.

Zhang, T., Osterkamp, T.E. & Stamnes, K. 1997. Effects of climate on the active layer and permafrost on the north slope of Alaska, USA. *Permafrost and Periglacial Processes* 8: 45-67.

Zhang, T.J., Frauenfeld, O.W., Serreze, M.C., Etringer, A., Oelke, C., McCreight, J., Barry, R.G., Gilichinsky, D., Yang, D.Q., Ye, H.C., Ling, F. & Chudinova, S. 2005. Spatial and temporal variability in active layer thickness over the Russian Arctic drainage basin. *Journal of Geophysical Research-Atmospheres* 110.

Zimov, S.A., Schuur, E.A.G. & Chapin, F.S. 2006. Permafrost and the global carbon budget. *Science* 312: 1612-1613.

Zinko, U., Seibert, J., Dynesius, M. & Nilsson, C. 2005. Plant species numbers predicted by a topography-based groundwater flow index. *Ecosystems* 8: 430-441.

APPENDIX

A.1: Introduction

The following pages contain a series of tables and figures providing information about the major available datasets acquired or developed and processed for this study. These include metadata for the historical vertical aerial images from the Arctic National Wildlife Refuge (acquired from the U.S. Fish and Wildlife Service), BRNS (acquired from the USGS), and the Noatak National Preserve (acquired from the National Park Service). In addition, there are metadata for the satellite image, as well as the major GIS datasets, including shrub cover maps, geomorphic unit boundaries, and river and lake polygons and associated digitized centerlines. Each general dataset has its own dedicated subsection. Each subsection includes a text description, examples of the imagery if necessary, a map or map series noting the geographic locations of the data, and tables that include the image metadata.

A.2: Source locations from Tape et al.'s (2006) study

The selection for study sites presented in this dissertation were based on areas originally selected for analysis in the study by Tape et al. (2006). Tape et al. (2006) acquired black and white oblique aerial photographs of a number of river corridors across the North Slope of Alaska from the United States military in the 1950s. Approximately 50 years later, these areas were located and rephotographed using helicopter. This led to the development of a dataset comprising approximately 200 pairs of oblique photographs taken approximately 50 years apart and allowed for high-quality estimates of the changes in shrub cover over that time period. Ken Tape and Matthew Sturm generously loaned a copy of their oblique aerial photographs for use as ground validation for the classification of the imagery. A map of the locations of these photo pairs is included in Figure A-1.

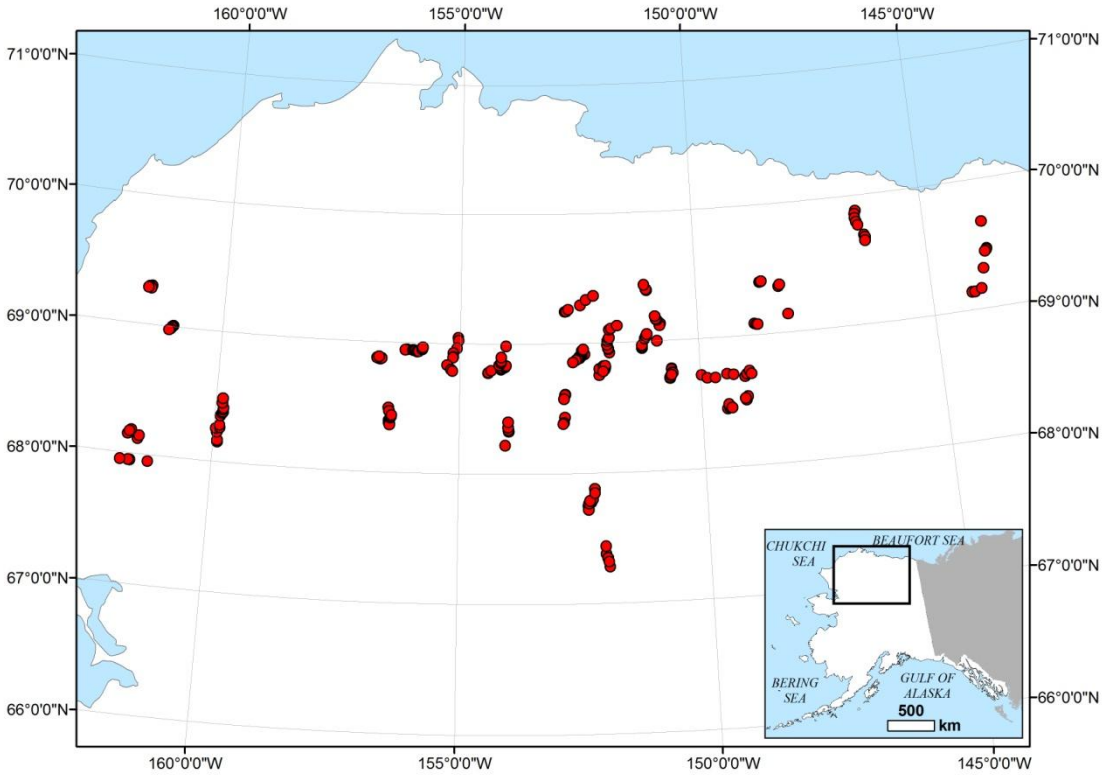

Figure A-1: Location of the repeat photo pairs analyzed in Tape et al. (2006).

A.3: Footprints for the USGS images collected in this study

This work has relied on the acquisition of historic vertical aerial photographs of northern Alaska. These data were acquired on a series of reconaissance missions by federal agenices including the U.S. Fish and Wildlife Service, the U.S. Navy, the U.S. Air Force, the NASA Ames Research Center, and the Department of Homeland Security. Many of the best images dating from the late 1970s and 1980s were acquired by U-2 and ER-2 aircraft operated primarily by NASA for the Alaska High-Altitude Aerial Photography Program (AHAP). The AHAP set is considered to be the last successful and comprehensive effort to photograph and map much of Northern Alaska.

These imagery are primarily black and white or color infrared. The general purpose of the black and white imagery was to facilitate production of topographic maps. The color infrared images were acquired to facilitate accurate mapping of water bodies and assess vegetation health. However, these imagery do vary in scale, ranging from 1:20,000 to 1:136,000. Much of the AHAP imagery was acquired at 1:60,000 to 1:70,000 scale. For the purposes of this work, these imagery were used to map historic shrub cover from the 1950s, 1970s, and 1980s.

I purchased much of these imagery for the BRNS and Arctic National Wildlife Refuge (ANWR) from the United States Geological Survey. These were purchased on NSF grants ARC-0806506 and 1203444.

I would like to thank Dr. David Swanson at the National Park Service for loaning us a copy of the USGS images he acquired for the Noatak National Preserve and Gates

of the Arctic National Park and Preserve (the series of images in central and western Alaska in the succeeding map series).

Figures A-2 through A-24 note the location of the footprints of these imagery acquired for this study. They have been categorized by scale, date of acquisition, and whether they have been processed (co-registered to available satellite imagery, since these photos are not geographically referenced).

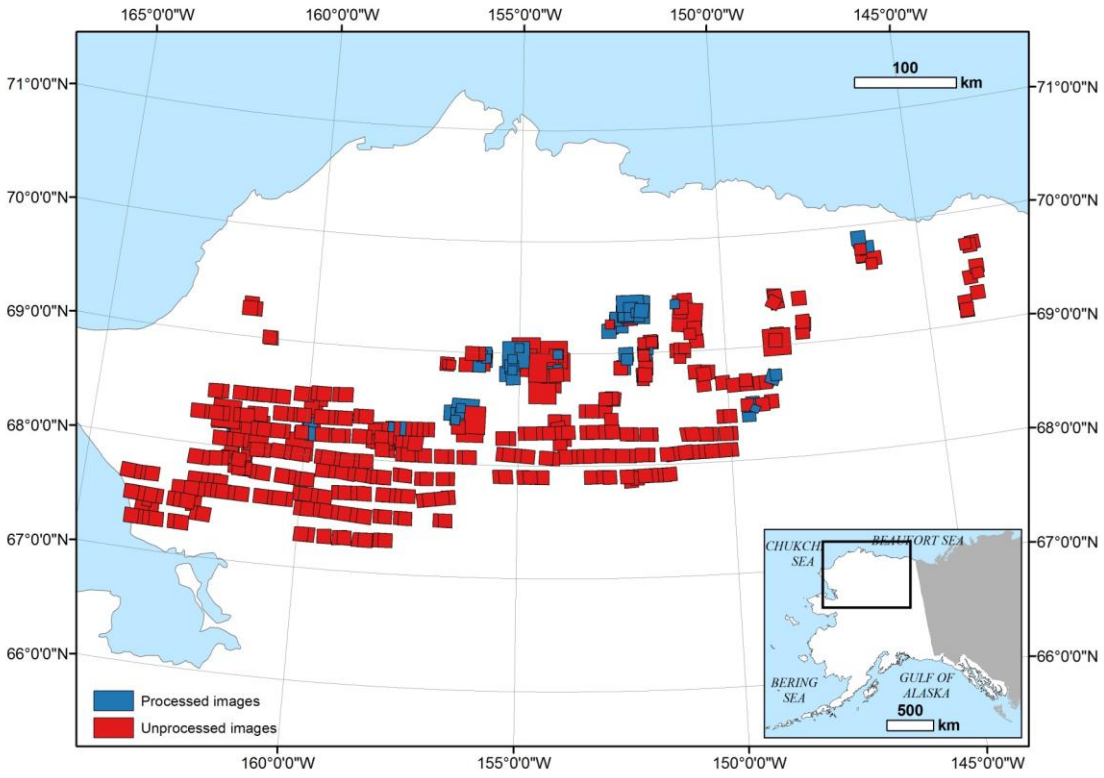

Figure A-2: Footprints of processed and unprocessed USGS images from the North Slope of Alaska acquired for this study. Processed = co-registered to available satellite imagery. Unprocessed = not yet co-registered to available satellite imagery.

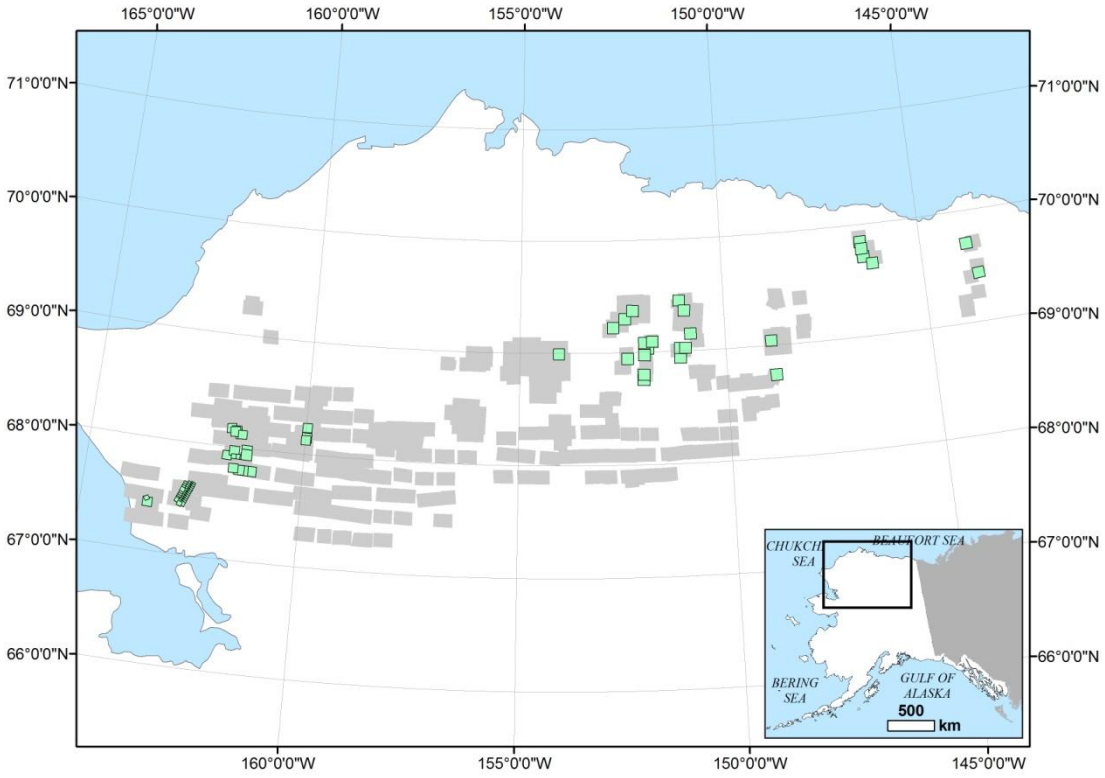

Figure A-3: Footprints of USGS images from the North Slope of Alaska acquired for this study, with the footprints for the 1950s highlighted in color. These include both processed and unprocessed images.

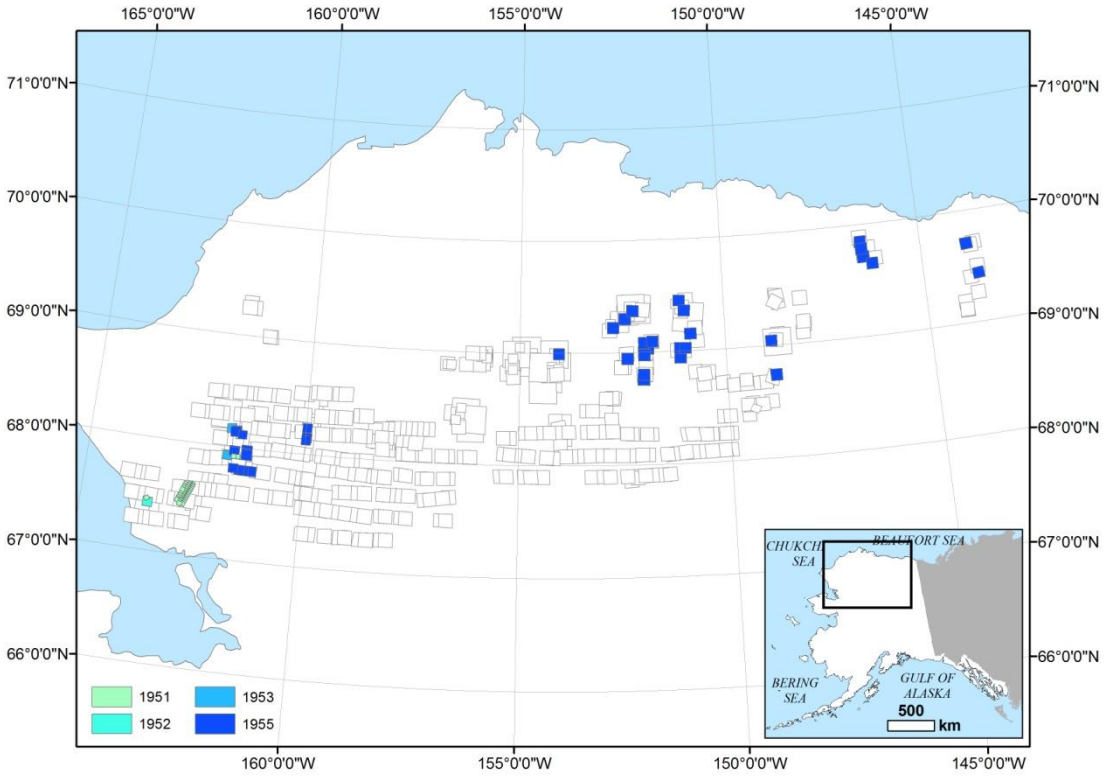

Figure A-4: Footprints of the 1950s USGS images from the North Slope of Alaska acquired for this study, color-coded by year.

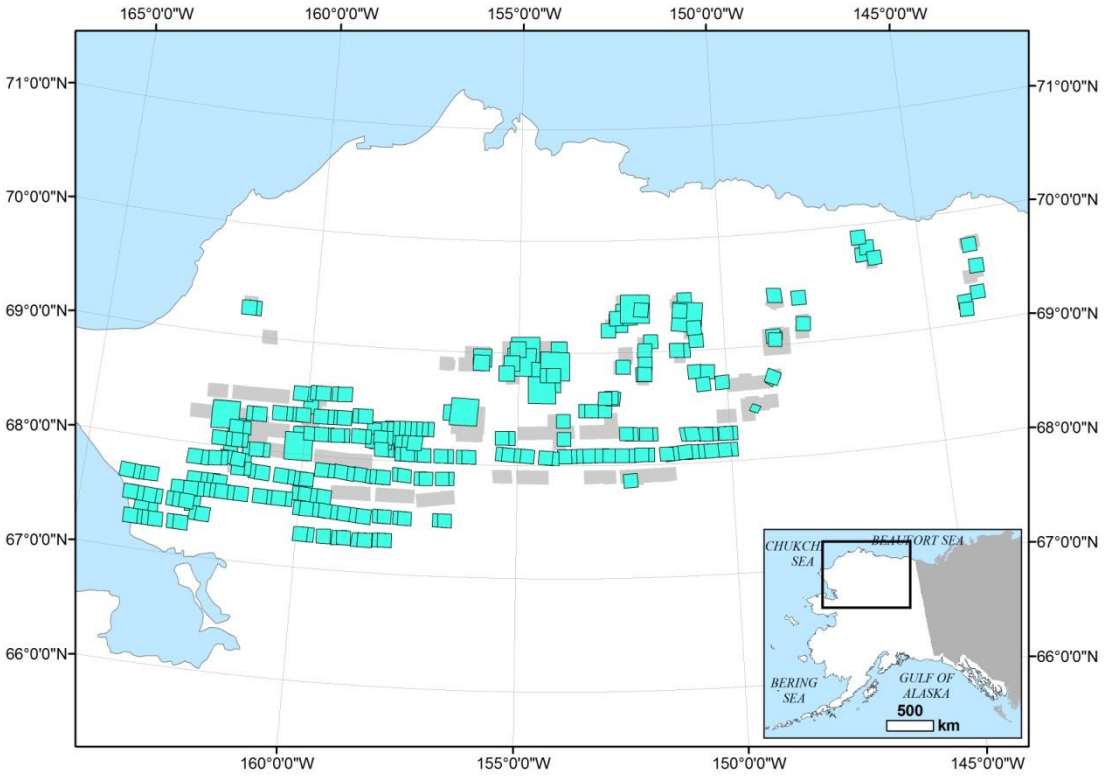

Figure A-5: Footprints of USGS images from the North Slope of Alaska acquired for this study, with the footprints for the 1970s highlighted in color. These include both processed and unprocessed images.

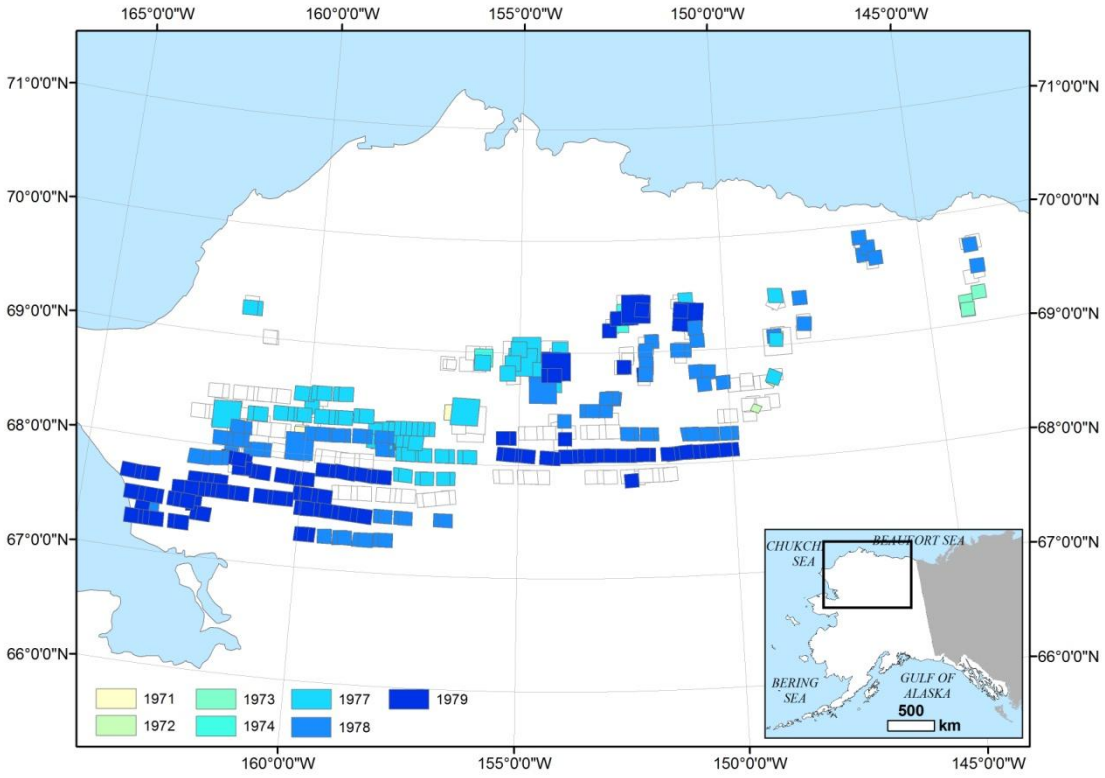

Figure A-6: Footprints of the 1970s USGS images from the North Slope of Alaska acquired for this study, color-coded by year.

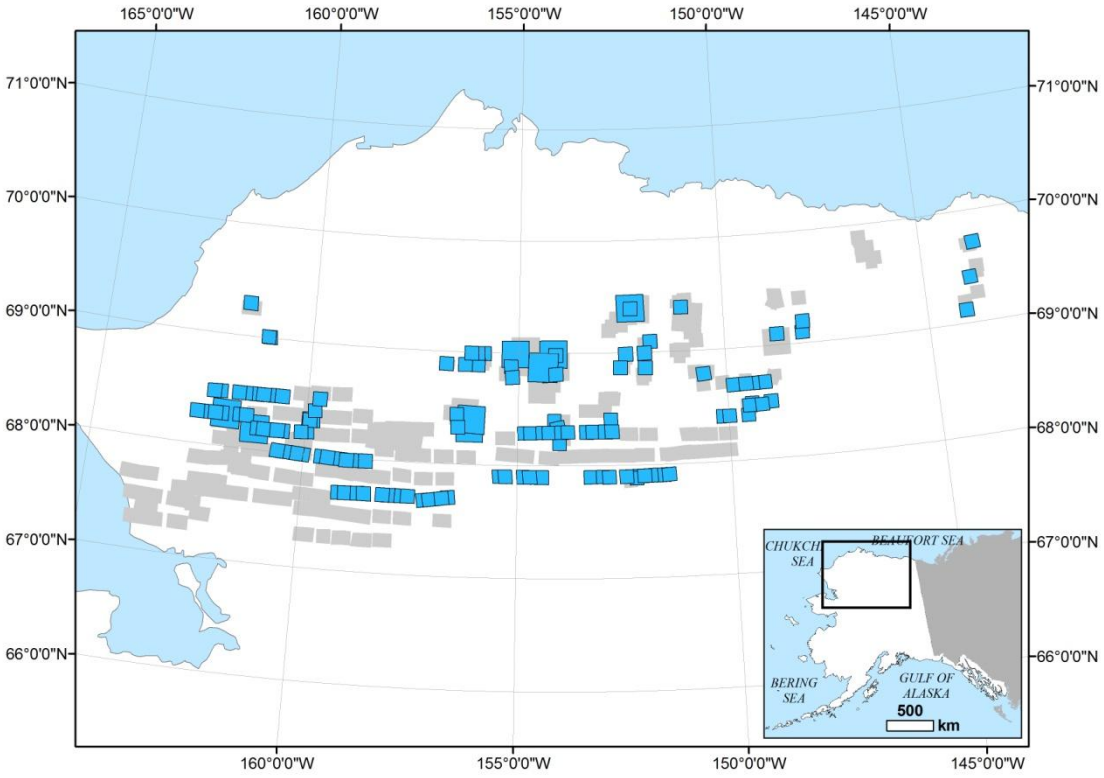

Figure A-7: Footprints of USGS images from the North Slope of Alaska acquired for this study, with the footprints for the 1980s highlighted in color. These include both processed and unprocessed images.

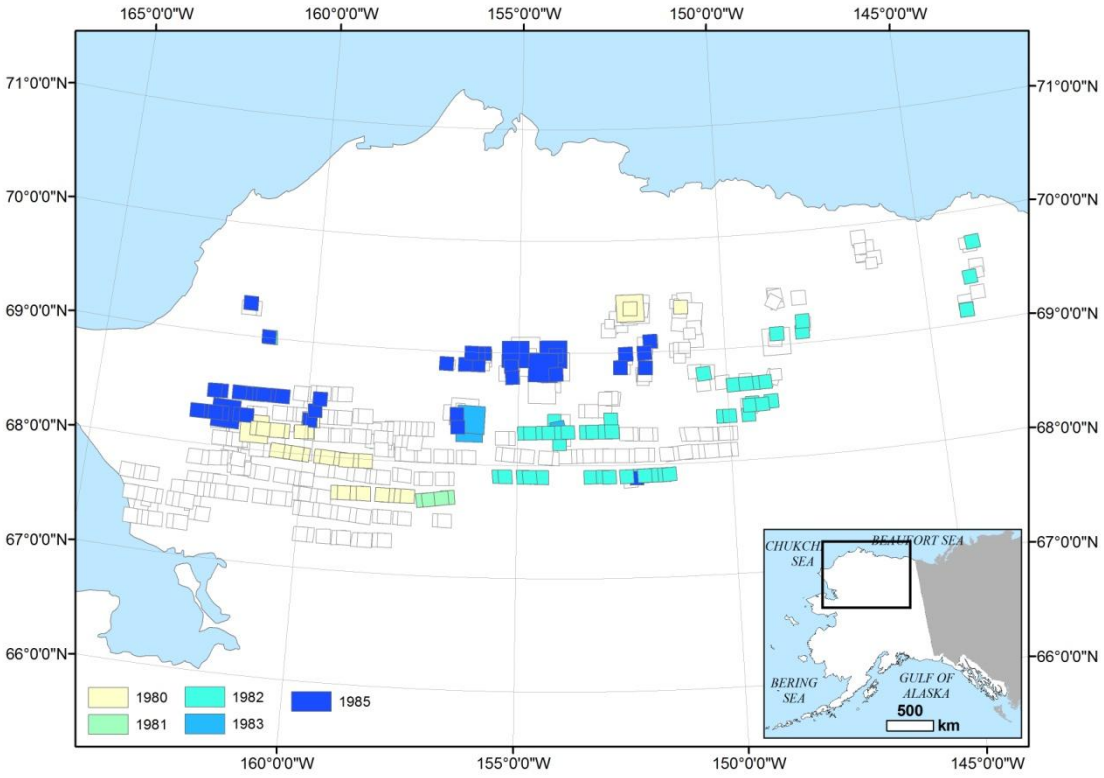

Figure A-8: Footprints of the 1980s USGS images from the North Slope of Alaska acquired for this study, color-coded by year.

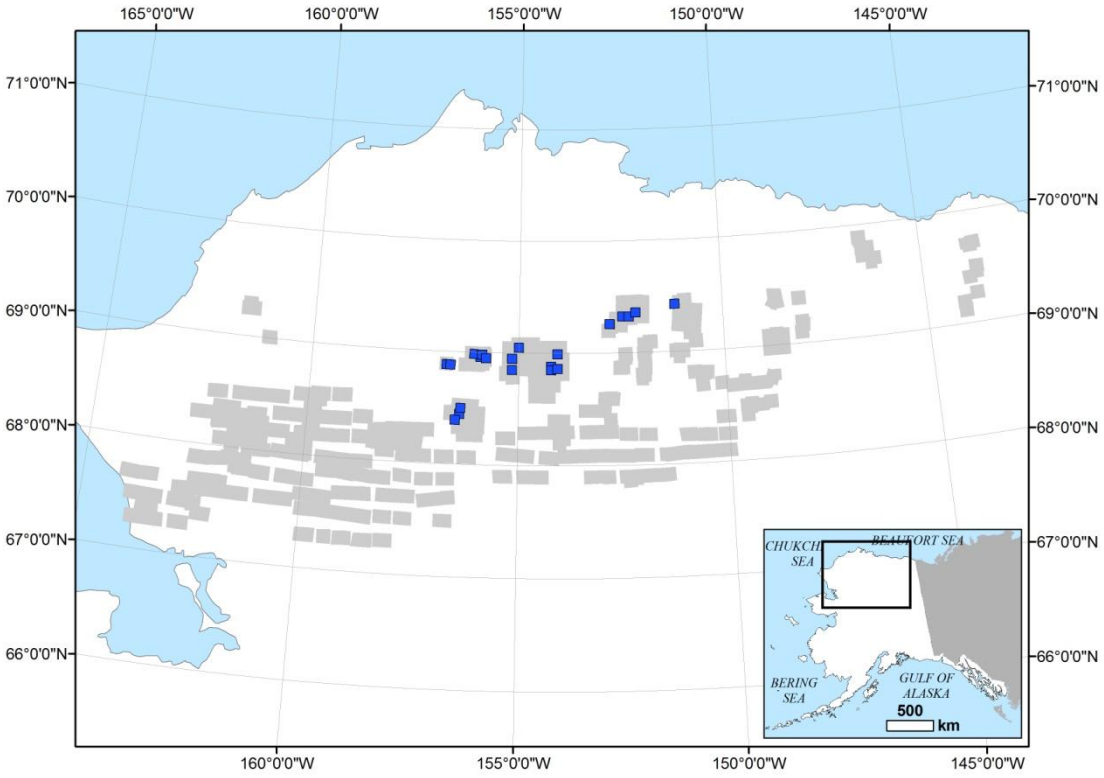

Figure A-9: Footprints of USGS images from the North Slope of Alaska acquired for this study, with the footprints for the 2000s highlighted in color. These include both processed and unprocessed images.

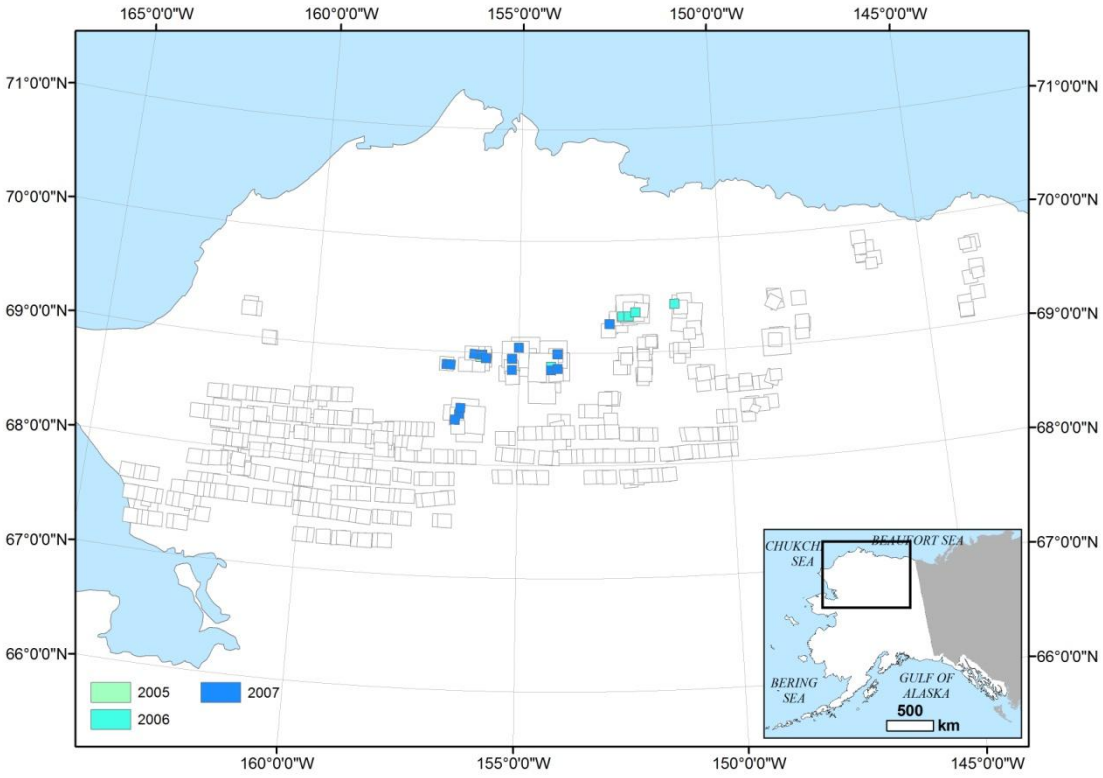

Figure A-10: Footprints of the 2000s USGS images from the North Slope of Alaska acquired for this study, color-coded by year.

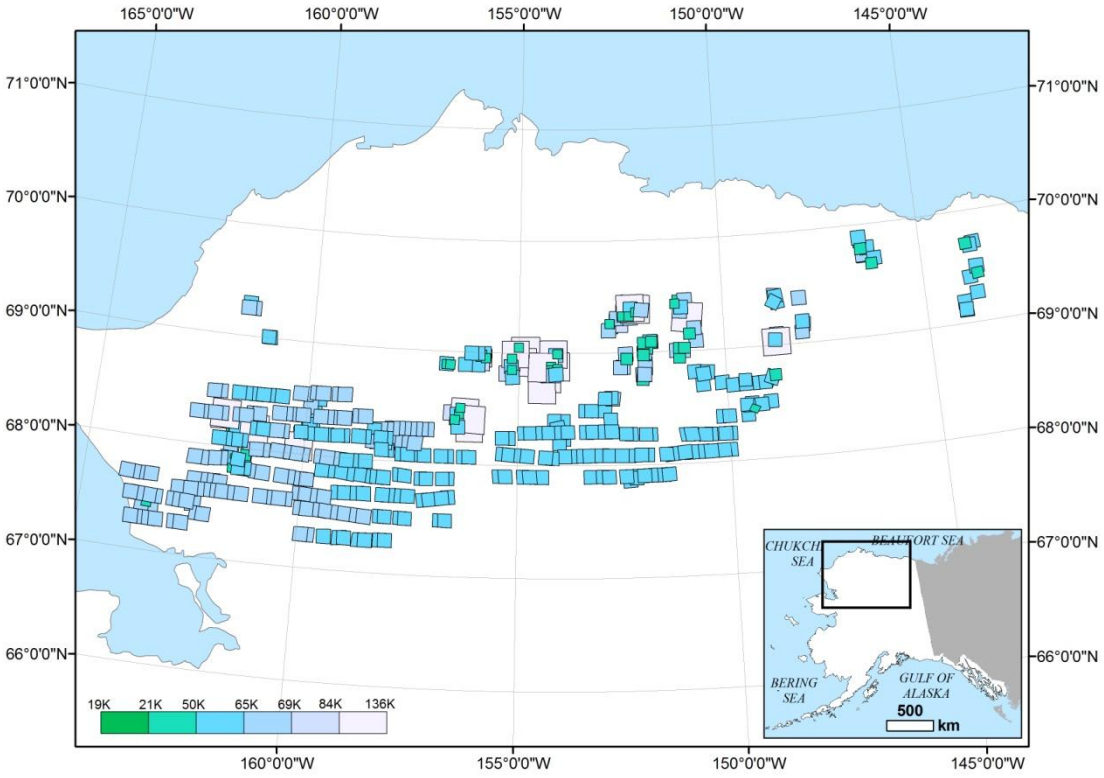

Figure A-11: Footprints of the USGS images from the North Slope of Alaska acquired for this study, with the footprints symbolized by scale.

Figure A-12: Footprints of the 1951, 1952, and 1953 USGS images from the North Slope of Alaska acquired for this study.

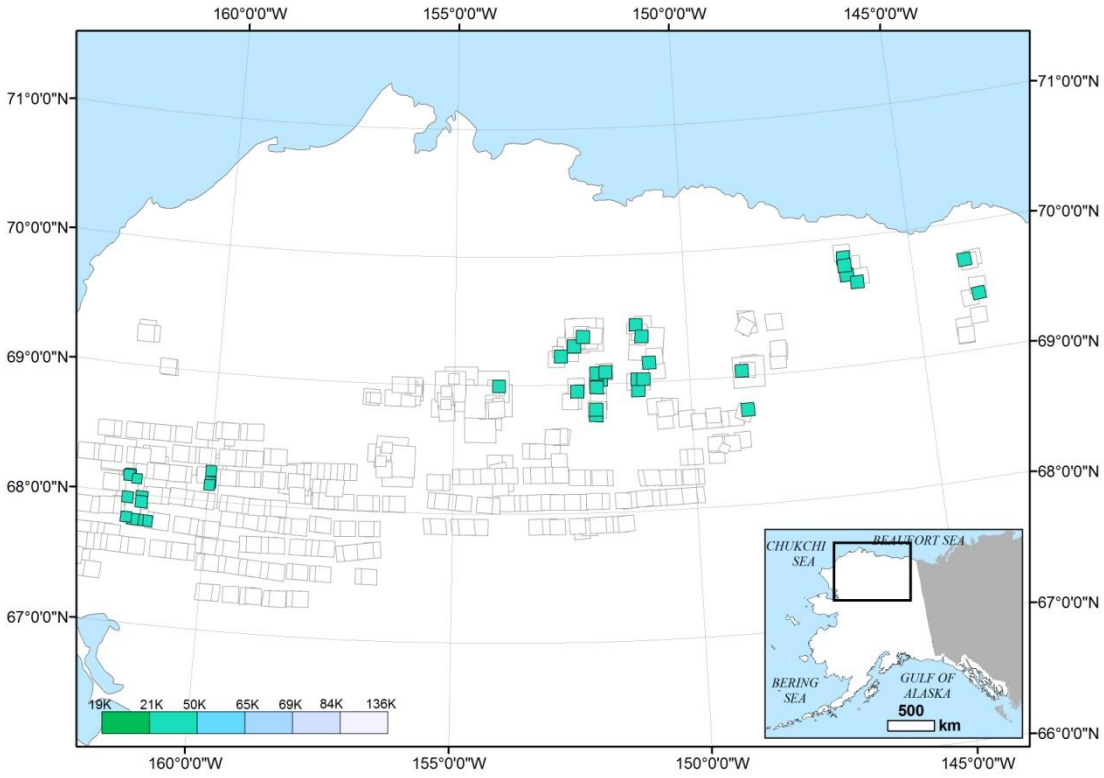

Figure A-13: Footprints of the 1955 USGS images from the North Slope of Alaska acquired for this study.

Figure A-14: Footprints of the 1971 USGS images from the North Slope of Alaska acquired for this study.

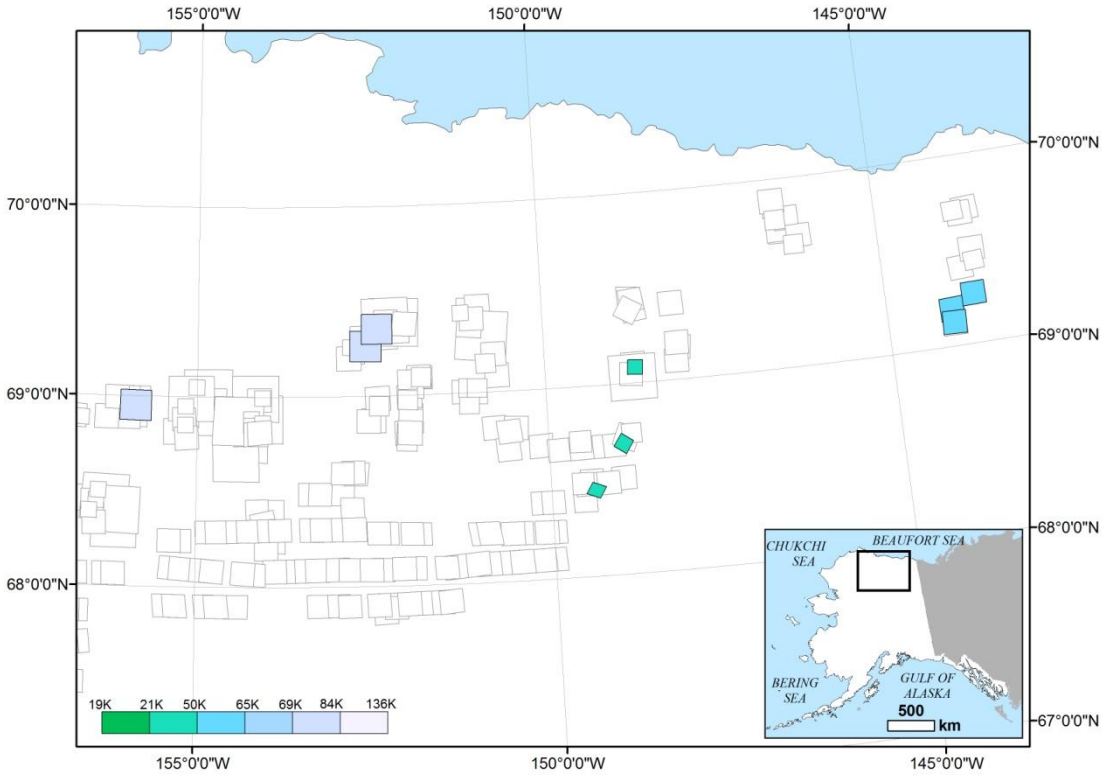

Figure A-15: Footprints of the 1972, 1973, and 1974 USGS images from the North Slope of Alaska acquired for this study.

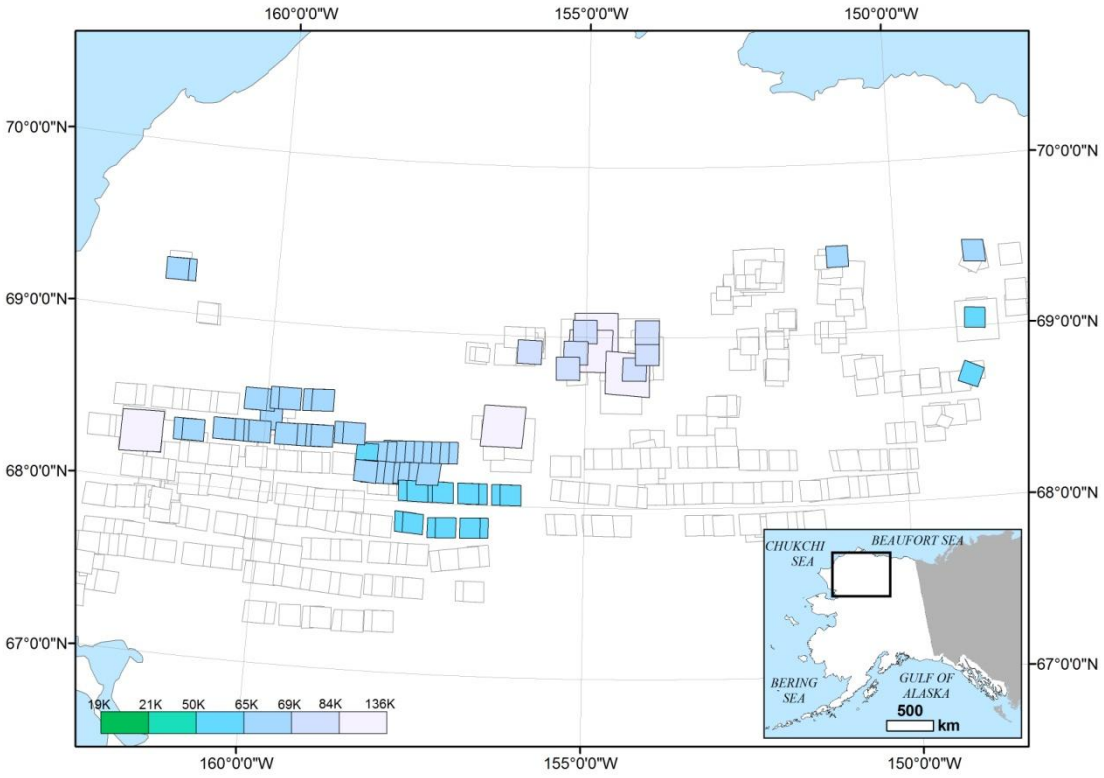

Figure A-16: Footprints of the 1977 USGS images from the North Slope of Alaska acquired for this study.

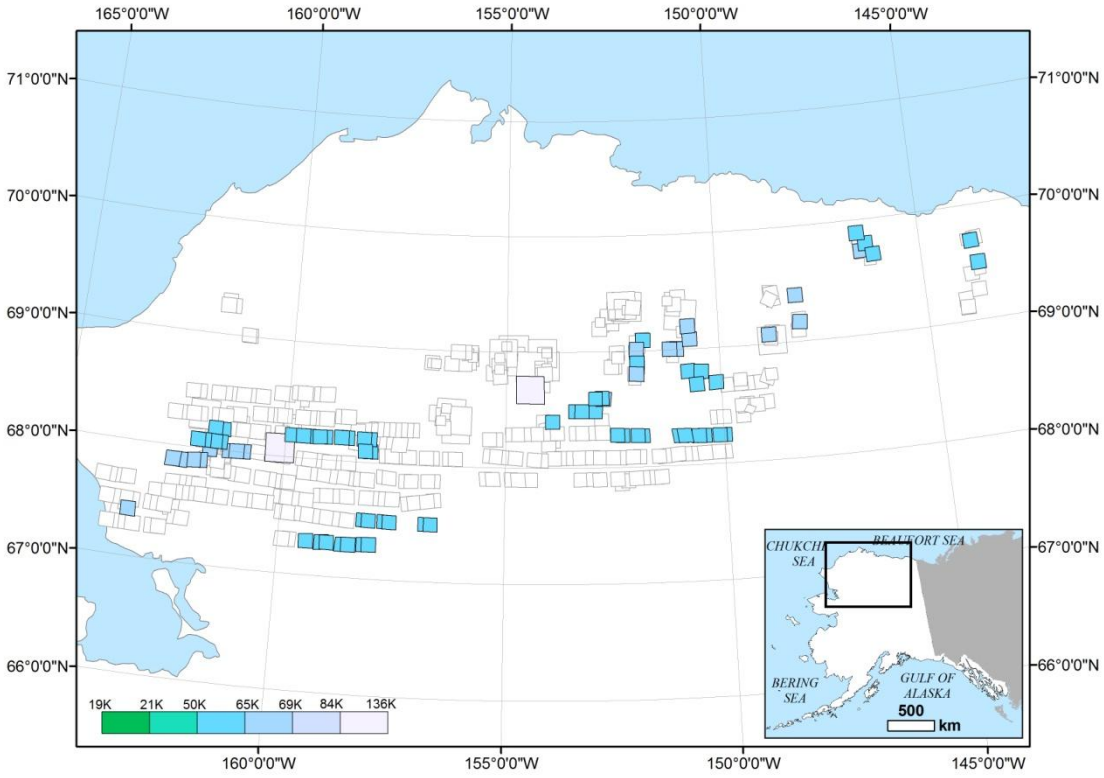

Figure A-17: Footprints of the 1978 USGS images from the North Slope of Alaska acquired for this study.

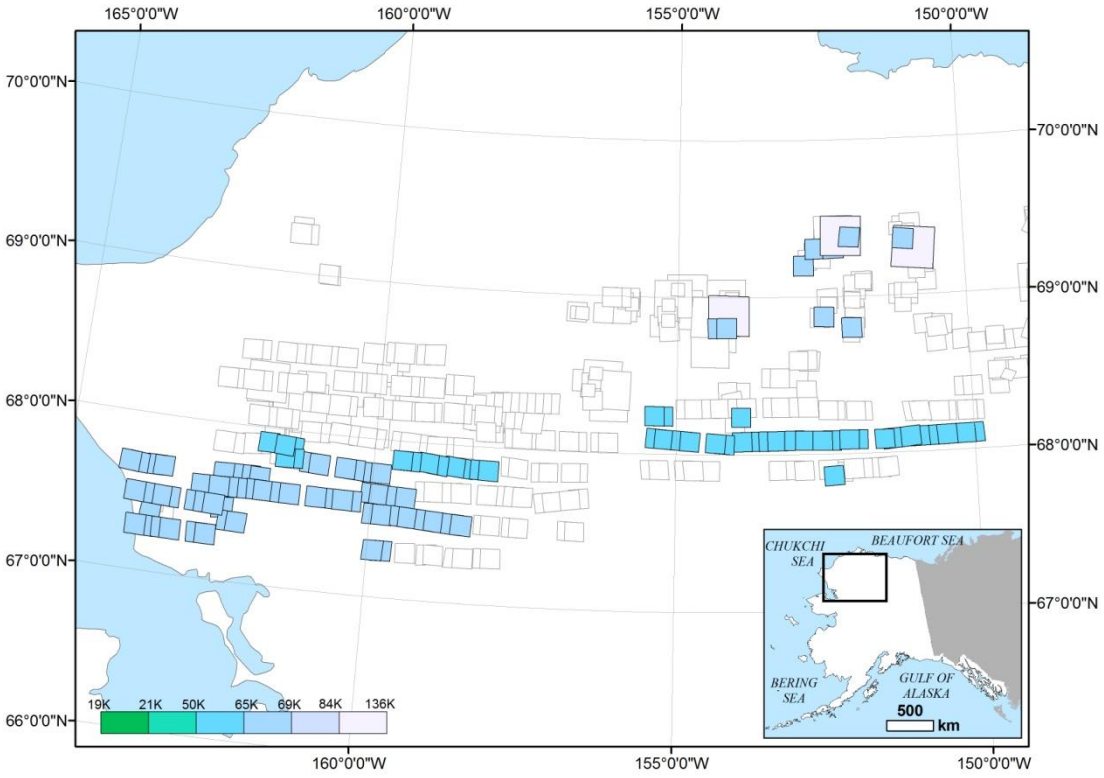

Figure A-18: Footprints of the 1979 USGS images from the North Slope of Alaska acquired for this study.

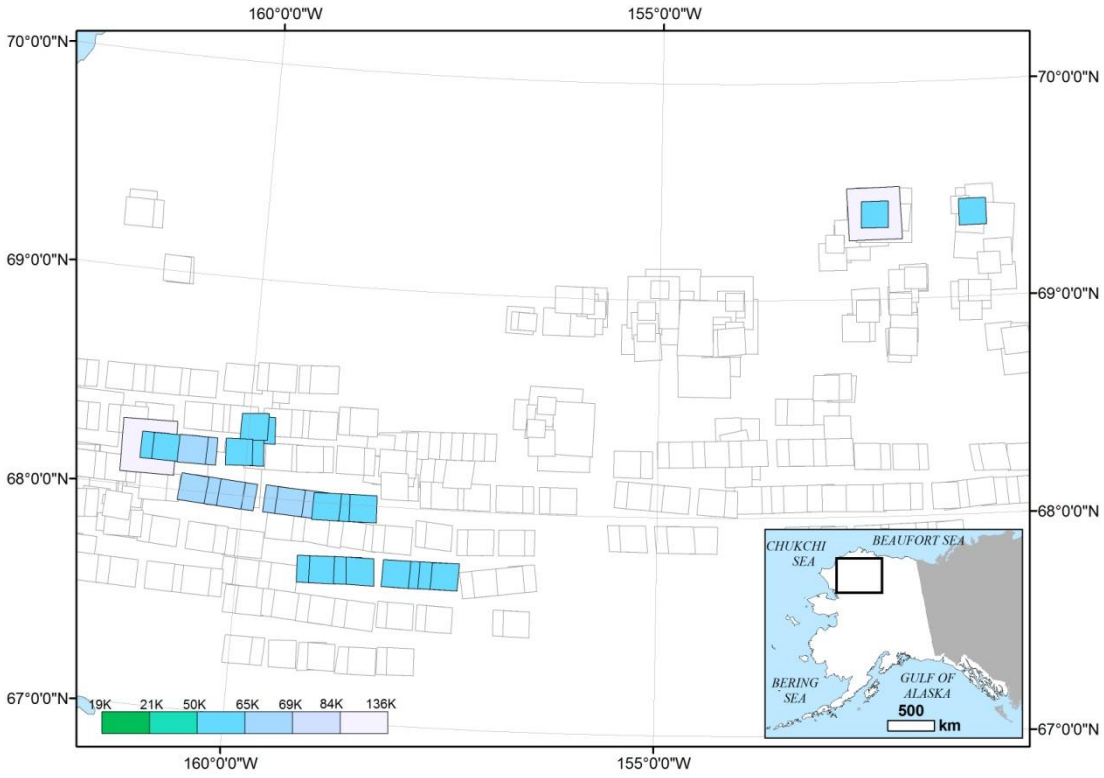

Figure A-19: Footprints of the 1980 USGS images from the North Slope of Alaska acquired for this study.

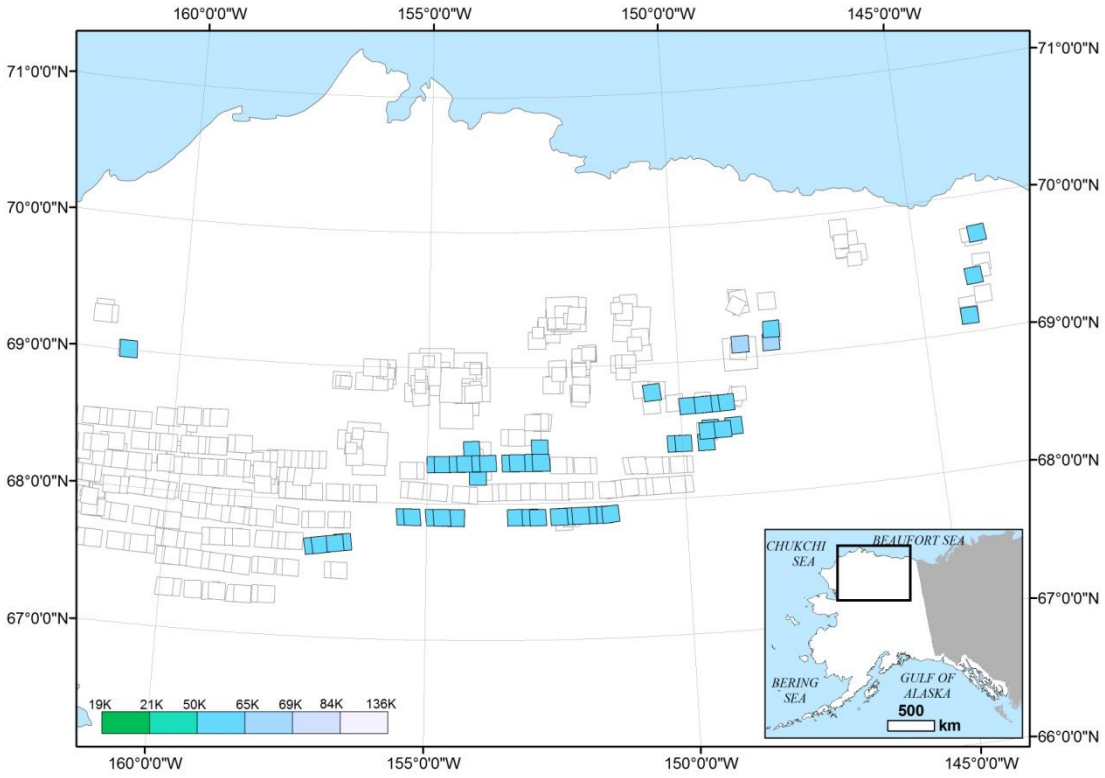

Figure A-20: Footprints of the 1981 and 1982 USGS images from the North Slope of Alaska acquired for this study.

Figure A-21: Footprints of the 1983 and 1984 USGS images from the North Slope of Alaska acquired for this study.

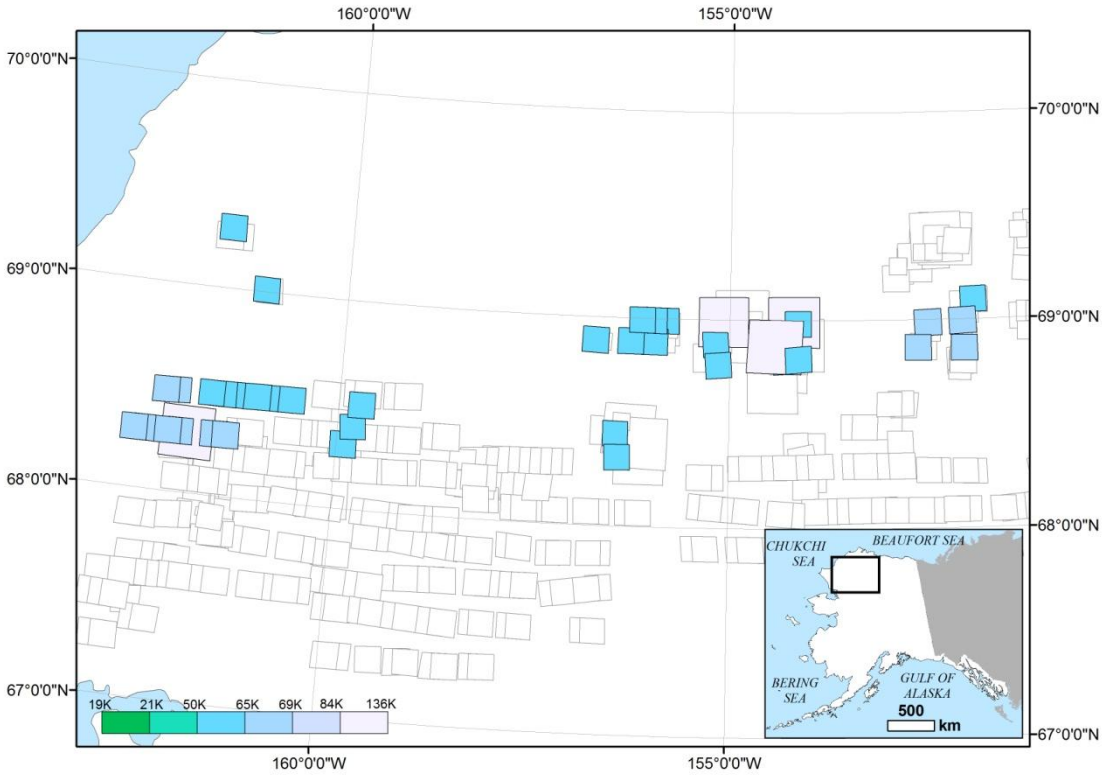

Figure A-22: Footprints of the 1985 USGS images from the North Slope of Alaska acquired for this study.

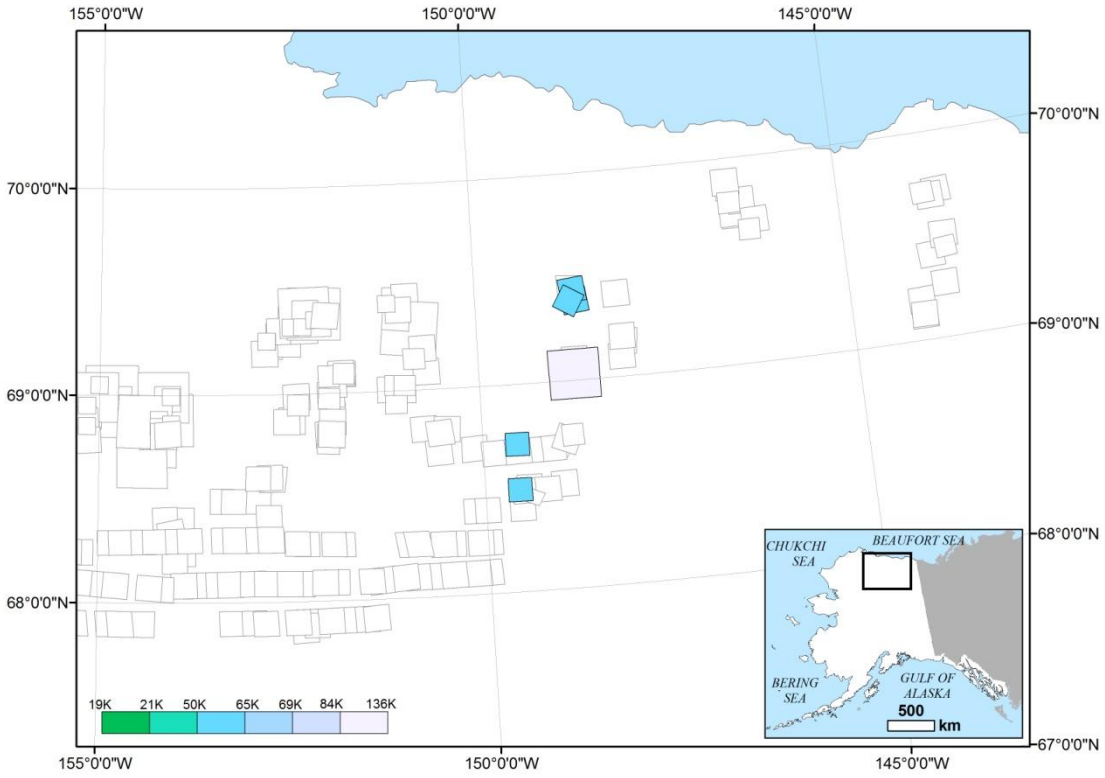

Figure A-23: Footprints of the 1995 USGS images from the North Slope of Alaska acquired for this study.

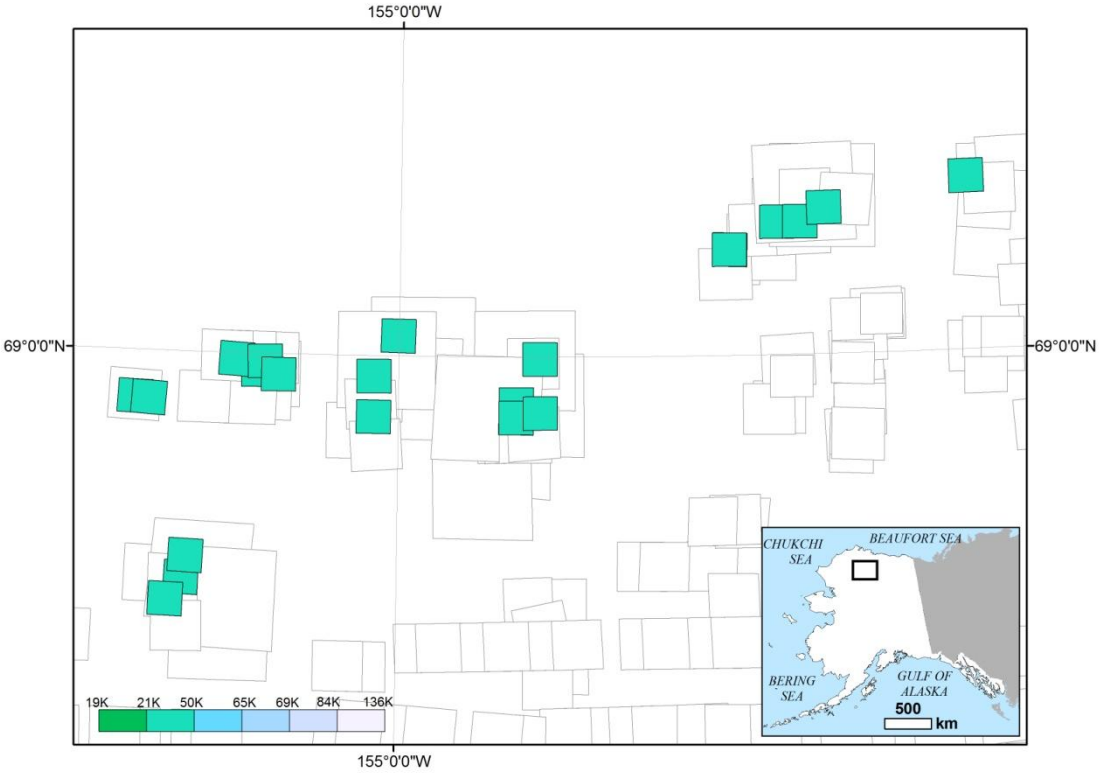

Figure A-24: Footprints of the 2005, 2006, and 2007 USGS images from the North Slope of Alaska acquired for this study.

Table A-1: USGS Image metadata part 1

Area	Center latitude	Center longitude	Acq. Date	Type	Scale	Image Name	Processed?
Atigun	68.40	-149.54	8/6/82	CIR	63529	AR5820031140662	Y
Atigun	68.50	-149.43	8/6/82	CIR	64176	AR5820031140684	Y
Atigun	68.49	-149.50	8/7/82	CIR	63166	AR5820031161025	Y
Atigun	68.49	-149.19	8/7/82	CIR	63166	AR5820031161027	N
Atigun	68.49	-149.55	6/13/95	BW	59000	AR5950049366445	N
Atigun	68.45	-149.37	7/13/72	Color	39347	AR6209000700072	Y
Ayiyak	68.87	-152.48	7/13/79	CIR	65500	AR5790027862147	Y
Ayiyak	68.99	-152.41	8/2/85	CIR	66200	AR5850034708536	Y
Ayiyak	68.87	-152.55	8/19/85	CIR	65636	AR5850034769381	N
Ayiyak	68.95	-152.39	6/26/55	BW	49597	ARHM04908911490	Y
--	68.27	-151.86	7/17/78	CIR	57865	AR6386003100124	N
--	68.27	-151.98	7/17/78	CIR	57865	AR6386003100123	N
--	68.28	-152.32	7/17/78	CIR	57865	AR6386003100120	N
--	68.28	-152.44	7/17/78	CIR	57865	AR6386003100119	N
--	68.25	-149.98	7/17/78	CIR	59762	AR6386003100141	N
--	68.25	-150.10	7/17/78	CIR	59762	AR6386003100140	N
--	68.25	-150.45	7/17/78	CIR	59762	AR6386003100137	N
--	68.25	-150.57	7/17/78	CIR	59762	AR6386003100136	N
--	68.26	-151.01	7/17/78	CIR	58972	AR6386003100132	N
--	68.26	-150.89	7/17/78	CIR	58972	AR6386003100133	N
--	68.10	-150.00	7/12/79	CIR	63333	AR5790027842042	N
--	68.10	-150.15	7/12/79	CIR	63333	AR5790027842041	N
--	68.09	-151.95	7/12/79	CIR	64500	AR5790027842029	N
--	68.09	-152.40	7/12/79	CIR	64000	AR5790027842026	N
--	68.09	-152.10	7/12/79	CIR	64500	AR5790027842028	N
--	68.09	-151.37	7/12/79	CIR	63666	AR5790027842033	N
--	68.09	-151.51	7/12/79	CIR	64500	AR5790027842032	N
--	68.10	-150.61	7/12/79	CIR	63333	AR5790027842038	N
--	68.10	-150.92	7/12/79	CIR	63333	AR5790027842036	N
--	68.10	-151.07	7/12/79	CIR	63666	AR5790027842035	N
--	68.10	-150.46	7/12/79	CIR	63333	AR5790027842039	N
--	68.40	-150.14	8/6/82	CIR	63529	AR5820031140658	N
--	68.40	-149.99	8/6/82	CIR	63529	AR5820031140659	N
--	68.49	-153.40	6/28/78	CIR	63583	AR5780026225457	N
--	68.49	-153.25	6/28/78	CIR	63583	AR5780026225458	N
--	68.60	-152.93	7/13/78	CIR	58782	AR6386002700041	N
--	68.08	-153.75	7/12/79	CIR	64125	AR5790027842017	N
--	68.08	-153.90	7/12/79	CIR	64125	AR5790027842016	N

Table A-2: USGS Image metadata part 2

Area	Center latitude	Center longitude	Acq. Date	Type	Scale	Image Name	Processed?
--	68.07	-154.19	7/12/79	CIR	63818	AR5790027842014	N
--	68.09	-153.45	7/12/79	CIR	64125	AR5790027842019	N
--	68.09	-153.31	7/12/79	CIR	64125	AR5790027842020	N
--	68.07	-154.34	7/12/79	CIR	63818	AR5790027842013	N
--	68.09	-153.02	7/12/79	CIR	64125	AR5790027842022	N
--	68.10	-155.35	7/12/79	CIR	63818	AR5790027842006	N
--	68.10	-155.20	7/12/79	CIR	63818	AR5790027842007	N
--	68.09	-154.92	7/12/79	CIR	63818	AR5790027842009	N
--	68.08	-154.77	7/12/79	CIR	63818	AR5790027842010	N
--	68.24	-155.22	7/12/79	CIR	63500	AR5790027842098	N
--	68.24	-155.37	7/12/79	CIR	63500	AR5790027842099	N
--	68.09	-152.84	7/12/79	CIR	64000	AR5790027842023	N
--	68.09	-152.55	7/12/79	CIR	64000	AR5790027842025	N
--	68.29	-154.85	8/6/82	CIR	62555	AR5820031140711	N
--	68.29	-154.71	8/6/82	CIR	62555	AR5820031140712	N
--	68.29	-154.42	8/6/82	CIR	62555	AR5820031140714	N
--	68.30	-153.38	8/6/82	CIR	63500	AR5820031140721	N
--	68.30	-153.23	8/6/82	CIR	63500	AR5820031140722	N
--	68.30	-152.93	8/6/82	CIR	63500	AR5820031140724	N
--	68.30	-152.78	8/6/82	CIR	63500	AR5820031140725	N
--	67.90	-154.43	8/28/82	CIR	64625	AR5820031302776	N
--	67.90	-154.85	8/28/82	CIR	64625	AR5820031302773	N
--	67.90	-154.71	8/28/82	CIR	64625	AR5820031302774	N
--	67.91	-151.60	8/28/82	CIR	63800	AR5820031302796	N
--	67.90	-153.29	8/28/82	CIR	64142	AR5820031302784	N
--	67.90	-155.42	8/28/82	CIR	64625	AR5820031302769	N
--	67.90	-155.28	8/28/82	CIR	64625	AR5820031302770	N
--	67.90	-153.01	8/28/82	CIR	64142	AR5820031302786	N
--	67.90	-152.86	8/28/82	CIR	63800	AR5820031302787	N
--	67.90	-152.45	8/28/82	CIR	63800	AR5820031302790	N
--	67.91	-151.89	8/28/82	CIR	63800	AR5820031302794	N
--	67.90	-152.04	8/28/82	CIR	63800	AR5820031302793	N
--	67.91	-151.46	8/28/82	CIR	63500	AR5820031302797	N
--	67.29	-159.03	7/14/78	CIR	62389	AR6386002900232	N
--	67.29	-158.92	7/14/78	CIR	61018	AR6386002900233	N
--	67.29	-159.37	7/14/78	CIR	60703	AR6386002900229	N
Canning	69.85	-146.49	6/21/55	BW	40000	ARBM00340587034	Y
Canning	69.71	-146.44	6/21/55	BW	40000	ARBM00340576808	Y

Table A-3: USGS Image metadata part 3

Area	Center latitude	Center longitude	Acq. Date	Type	Scale	Image Name	Processed?
Canning	69.73	-146.43	6/28/78	CIR	65500	AR5780026225779	N
Canning	69.79	-146.31	7/8/78	CIR	61171	AR6386001900289	Y
Canning	69.69	-146.15	7/8/78	CIR	59486	AR6386001900209	N
Canning	69.89	-146.50	7/8/78	CIR	60727	AR6386001900320	Y
Canning	69.79	-146.47	6/21/55	BW	50000	ARBM00380657913	N
Chandler	69.09	-151.80	6/28/78	CIR	65000	AR5780026225576	N
Chandler	69.02	-151.95	6/28/78	CIR	65375	AR5780026225573	Y
Chandler	68.90	-151.95	6/28/78	CIR	65000	AR5780026225535	N
Chandler	68.80	-152.01	7/13/79	CIR	65375	AR5790027862117	N
Chandler	69.10	-151.82	8/2/85	CIR	64166	AR5850034708546	N
Chandler	68.99	-151.96	8/2/85	CIR	66200	AR5850034708539	Y
Chandler	68.86	-151.95	8/19/85	CIR	65636	AR5850034769385	N
Chandler	69.03	-151.89	6/26/55	BW	50000	ARHM04908911519	Y
Chandler	68.76	-152.01	6/26/55	BW	50000	ARHM04909011675	N
Chandler	68.98	-151.98	6/26/55	BW	50000	ARHM04909011680	N
Chandler	69.08	-151.98	6/26/55	BW	50000	ARHM04909011682	N
Chandler	69.09	-151.78	6/26/55	BW	50000	ARHM04908911543	N
Chandler	68.80	-152.01	6/26/55	BW	50000	ARHM04909011676	N
Chandler	68.80	-151.97	6/28/78	CIR	66000	AR5780026225533	N
Colville 1	68.95	-155.88	6/22/74	BW	84000	AR1VECX00G70042	Y
Colville 1	68.91	-155.90	7/26/77	CIR	73266	AR6364001500166	N
Colville 1	68.99	-155.84	8/2/85	CIR	64769	AR5850034708514	Y
Colville 1	68.89	-155.98	8/19/85	CIR	65000	AR5850034769366	Y
Colville 1	68.96	-155.93	8/2/05	CIR	40000	ARUNPRA00060249	Y
Colville 1	68.99	-156.08	7/6/07	CIR	40000	ARUNPRA00150122	N
Colville 1	68.98	-155.89	7/6/07	CIR	40000	ARUNPRA00150120	Y
Colville 1	68.95	-155.80	7/6/07	CIR	40000	ARUNPRA00130167	Y
Colville 1	68.99	-155.99	8/2/85	CIR	64769	AR5850034708513	N
Colville 1	68.89	-156.29	8/19/85	CIR	65000	AR5850034769364	N
Colville 1	68.99	-156.14	8/2/85	CIR	64769	AR5850034708512	N
Colville 2,3,4	69.22	-152.73	6/26/55	BW	50000	ARHM04908911605	Y
Colville 2,3,4	69.30	-152.44	6/26/55	BW	50000	ARHM04908911625	Y
Colville 2,3,4	69.37	-152.24	6/26/55	BW	50000	ARHM04909011660	Y
Colville 2,3,4	69.26	-152.58	6/22/74	BW	84000	AR1VECX00F10048	Y
Colville 2,3,4	69.35	-152.41	6/22/74	BW	84000	AR1VECX00F20048	Y
Colville 2,3,4	69.20	-152.82	7/13/79	CIR	66125	AR5790027862155	Y
Colville 2,3,4	69.31	-152.61	7/13/79	CIR	67200	AR5790027862190	Y
Colville 2,3,4	69.31	-152.30	7/13/79	CIR	67200	AR5790027862192	N

Table A-4: USGS Image metadata part 4

Area	Center latitude	Center longitude	Acq. Date	Type	Scale	Image Name	Processed?
Colville 2,3,4	69.39	-152.16	7/13/79	BW	133666	AR5790027875581	Y
Colville 2,3,4	69.40	-152.28	8/2/80	BW	126833	AR5800029266009	Y
Colville 2,3,4	69.39	-152.28	8/2/80	CIR	63750	AR5800029258322	Y
Colville 2,3,4	69.26	-152.79	8/28/06	CIR	40000	ARUNPRA00080065	Y
Colville 2,3,4	69.33	-152.47	8/28/06	CIR	40000	ARUNPRA00080026	Y
Colville 2,3,4	69.32	-152.32	8/28/06	CIR	40000	ARUNPRA00080008	Y
Colville 2,3,4	69.36	-152.15	8/28/06	CIR	40000	ARUNPRA00080159	Y
Colville 2,3,4	69.26	-152.79	7/4/07	CIR	40000	ARUNPRA00110070	N
Colville 2,3,4	69.38	-152.01	7/13/79	CIR	66125	AR5790027862219	Y
Killik	68.40	-153.92	6/28/78	CIR	63090	AR5780026225440	N
Killik	68.24	-153.91	7/12/79	CIR	63666	AR5790027842089	N
Killik	68.20	-154.01	8/6/82	CIR	63800	AR5820031140619	N
Killik	68.40	-154.14	8/6/82	CIR	63857	AR5820031140631	N
Killik	68.30	-154.12	8/6/82	CIR	62555	AR5820031140716	N
Killik	68.33	-154.05	7/31/83	CIR	65000	AR5830032594973	N
Killik	68.29	-154.27	8/6/82	CIR	62555	AR5820031140715	N
Killik	68.30	-153.97	8/6/82	CIR	62555	AR5820031140717	N
Killik	68.30	-153.82	8/6/82	CIR	62555	AR5820031140718	N
Kurupa	69.02	-154.84	7/1/77	CIR	131719	AR6364001400141	N
Kurupa	68.92	-154.94	7/1/77	CIR	131390	AR6364001400083	N
Kurupa	69.03	-155.02	7/26/77	CIR	73265	AR6364001500269	Y
Kurupa	68.91	-155.17	7/26/77	CIR	73185	AR6364001500161	Y
Kurupa	68.82	-155.29	7/26/77	CIR	71873	AR6364001500108	Y
Kurupa	68.99	-155.06	8/2/85	CIR	64769	AR5850034708519	Y
Kurupa	68.99	-155.08	8/2/85	BW	125000	AR5850034710714	Y
Kurupa	68.88	-155.18	8/19/85	CIR	64600	AR5850034769371	Y
Kurupa	68.78	-155.15	8/19/85	CIR	64000	AR5850034769309	Y
Kurupa	69.05	-155.01	7/6/07	CIR	40000	ARUNPRA00130080	Y
Kurupa	68.95	-155.17	7/6/07	CIR	40000	ARUNPRA00130090	Y
Kurupa	68.85	-155.17	7/6/07	CIR	40000	ARUNPRA00130087	Y
Nanushuk 1,2	69.30	-150.89	7/13/79	BW	136750	AR5790027875571	N
Nanushuk 1,2	69.09	-150.69	6/28/78	CIR	65615	AR5780026225583	N
Nanushuk 1,2	69.20	-150.73	6/28/78	CIR	65750	AR5780026225617	N
Nanushuk 1,2	69.15	-150.85	6/26/55	BW	50000	ARHM04908911582	N
Nigu	68.46	-156.59	8/14/71	CIR	73216	ARB071400122084	Y
Nigu	68.47	-156.28	7/19/77	CIR	127824	AR6364000600140	Y
Nigu	68.32	-156.14	7/31/83	BW	123000	AR5830032605652	N
Nigu	68.40	-156.11	7/31/83	BW	127000	AR5830032605669	N

Table A-5: USGS Image metadata part 5

Area	Center latitude	Center longitude	Acq. Date	Type	Scale	Image Name	Processed?
Nigu	68.44	-156.45	8/19/85	CIR	64166	AR5850034769099	Y
Nigu	68.33	-156.42	8/19/85	CIR	62111	AR5850034769072	N
Nigu	68.45	-156.40	7/6/07	CIR	40000	ARUNPRA00120183	Y
Nigu	68.40	-156.50	7/6/07	CIR	40000	ARUNPRA00120169	Y
Nigu	68.50	-156.38	8/8/07	CIR	40000	ARUNPRA00160010	Y
Nimiuktuk 1,2	68.31	-159.84	7/30/80	CIR	63285	AR5800029217620	N
Nimiuktuk 1,2	68.32	-159.93	7/31/80	CIR	65000	AR5800029238215	N
Nimiuktuk 1,2	68.31	-159.91	8/2/85	CIR	64687	AR5850034708450	Y
Nimiuktuk 1,2	68.40	-159.81	8/19/85	CIR	63875	AR5850034769122	N
Nimiuktuk 1,2	68.50	-159.71	8/19/85	CIR	64153	AR5850034769227	N
Nimiuktuk 1,2	68.43	-159.92	7/19/77	CIR	67371	AR6364000700230	N
Nimiuktuk 1,2	68.35	-159.52	7/19/77	CIR	67889	AR6364000700192	N
Nimiuktuk 1,2	68.35	-159.66	7/19/77	CIR	67889	AR6364000700193	N
Nimiuktuk 1,2	68.35	-160.07	7/19/77	CIR	66740	AR6364000700196	N
Noatak 1	68.29	-157.69	7/19/77	CIR	66685	AR6364000700141	N
Noatak 1	68.29	-157.83	7/19/77	CIR	66685	AR6364000700140	Y
Noatak 1	68.16	-157.98	7/19/77	CIR	68706	AR6364000700119	N
Noatak 1	68.17	-157.84	7/19/77	CIR	68244	AR6364000700118	N
Noatak 1	68.29	-157.96	7/19/77	CIR	66685	AR6364000700139	N
Noatak 1	68.28	-158.10	7/19/77	CIR	66532	AR6364000700138	Y
Noatak 1	68.28	-158.25	7/19/77	CIR	66532	AR6364000700137	N
Noatak 1	68.27	-158.38	7/19/77	CIR	64962	AR6364000700136	N
Noatak 1	68.17	-158.12	7/19/77	CIR	68706	AR6364000700120	N
Noatak 1	68.17	-158.27	7/19/77	CIR	68706	AR6364000700121	N
Noatak 1	68.17	-158.38	7/19/77	CIR	66793	AR6364000700122	N
Noatak 1	68.20	-158.10	7/5/78	CIR	59522	AR6386001500009	N
Noatak 1	68.20	-158.22	7/5/78	CIR	59522	AR6386001500010	N
Noatak 2	67.63	-162.56	7/14/51	BW	19849	ARCNAV000020094	N
Noatak 2	67.61	-162.50	7/14/51	BW	19780	ARCNAV000020068	N
Noatak 2	67.63	-162.65	7/14/51	BW	19509	ARCNAV000020116	N
Noatak 2	67.61	-162.57	7/14/51	BW	19849	ARCNAV000020093	N
Noatak 2	67.60	-162.52	7/14/51	BW	19780	ARCNAV000020069	N
Noatak 2	67.61	-162.67	7/14/51	BW	19509	ARCNAV000020117	N
Noatak 2	67.60	-162.59	7/14/51	BW	19849	ARCNAV000020092	N
Noatak 2	67.58	-162.53	7/14/51	BW	19780	ARCNAV000020070	N
Noatak 2	67.59	-162.69	7/14/51	BW	19509	ARCNAV000020118	N
Noatak 2	67.58	-162.60	7/14/51	BW	19849	ARCNAV000020091	N
Noatak 2	67.57	-162.55	7/14/51	BW	19780	ARCNAV000020071	N

Table A-6: USGS Image metadata part 6

Area	Center latitude	Center longitude	Acq. Date	Type	Scale	Image Name	Processed?
Noatak 2	67.56	-162.62	7/14/51	BW	19849	ARCNAV000020090	N
Noatak 2	67.55	-162.56	7/14/51	BW	19780	ARCNAV000020072	N
Noatak 2	67.55	-162.64	7/14/51	BW	19849	ARCNAV000020089	N
Noatak 2	67.53	-162.58	7/14/51	BW	19780	ARCNAV000020073	N
Noatak 2	67.53	-162.65	7/14/51	BW	19849	ARCNAV000020088	N
Noatak 2	67.52	-162.60	7/14/51	BW	19780	ARCNAV000020074	N
Noatak 2	67.51	-162.67	7/14/51	BW	19849	ARCNAV000020087	N
Noatak 2	67.50	-162.61	7/14/51	BW	19780	ARCNAV000020075	N
Noatak 2	67.51	-162.77	7/14/51	BW	19474	ARCNAV000020123	N
Noatak 2	67.50	-162.68	7/14/51	BW	19849	ARCNAV000020086	N
Noatak 2	67.48	-162.63	7/14/51	BW	19780	ARCNAV000020076	N
Noatak 2	67.49	-162.78	7/14/51	BW	19474	ARCNAV000020124	N
Noatak 2	67.48	-162.70	7/14/51	BW	19849	ARCNAV000020085	N
Noatak 2	67.47	-162.64	7/14/51	BW	19780	ARCNAV000020077	N
Noatak 2	67.48	-162.80	7/14/51	BW	19474	ARCNAV000020125	N
Noatak 2	67.46	-162.72	7/14/51	BW	19849	ARCNAV000020084	N
Noatak 2	67.45	-162.66	7/14/51	BW	19780	ARCNAV000020078	N
Noatak 2	67.45	-162.73	7/14/51	BW	19849	ARCNAV000020083	N
Noatak 2	67.53	-162.75	7/14/51	BW	19474	ARCNAV000020122	N
Noatak 2	67.54	-162.74	7/14/51	BW	19509	ARCNAV000020121	N
Noatak 2	67.56	-162.72	7/14/51	BW	19509	ARCNAV000020120	N
Noatak 2	67.58	-162.70	7/14/51	BW	19509	ARCNAV000020119	N
Noatak 2	67.69	-162.31	7/14/79	CIR	66083	AR5790027882800	Y
Noatak 2	67.69	-162.45	7/14/79	CIR	66083	AR5790027882799	Y
Noatak 2	67.60	-162.64	7/14/79	CIR	66769	AR5790027882772	Y
Noatak 2	67.59	-162.79	7/14/79	CIR	66769	AR5790027882773	Y
Noatak 2	67.48	-162.85	7/14/79	CIR	66818	AR5790027882864	Y
Noatak 2	67.48	-162.70	7/14/79	CIR	66818	AR5790027882863	Y
Noatak 2	67.46	-162.41	7/14/79	CIR	66250	AR5790027882861	Y
Noatak 2	67.60	-162.36	7/14/79	CIR	66769	AR5790027882770	Y
Noatak 2	67.48	-162.56	7/14/79	CIR	66818	AR5790027882862	N
Noatak 3	67.97	-161.65	7/15/53	BW	44000	ARCKTZ000140089	N
Noatak 3	67.93	-161.78	7/15/53	BW	44000	ARCKTZ000140043	N
Noatak 3	67.97	-161.62	6/21/55	BW	40000	ARBM00390688290	N
Noatak 3	67.98	-161.33	6/26/55	BW	40000	ARHM04307809973	N
Noatak 3	68.00	-161.69	7/3/78	CIR	66000	AR5780026245810	N
Noatak 3	68.00	-161.24	7/3/78	CIR	66000	AR5780026245807	N
Noatak 3	67.91	-161.77	7/12/79	CIR	64500	AR5790027841873	N

Table A-7: USGS Image metadata part 7

Area	Center latitude	Center longitude	Acq. Date	Type	Scale	Image Name	Processed?
Noatak 3	67.90	-161.35	7/12/79	CIR	63750	AR5790027841876	N
Noatak 3	67.92	-161.44	7/14/51	BW	20392	ARCNAV000080142	N
Noatak 3	67.92	-161.53	7/14/51	BW	20392	ARCNAV000080140	N
Noatak 3	67.92	-161.63	7/14/51	BW	20392	ARCNAV000080138	N
Noatak 3	67.95	-161.33	6/26/55	BW	40000	ARHM04307809974	N
Noatak 3	67.80	-161.19	6/21/55	BW	40000	ARBM00390678229	Y
Noatak 3	67.80	-161.37	6/21/55	BW	40000	ARBM00390678227	N
Noatak 3	67.80	-161.47	6/21/55	BW	40000	ARBM00390678226	N
Noatak 3	67.82	-161.61	6/21/55	BW	40000	ARBM00390688294	N
Noatak 3	68.01	-161.09	7/3/78	CIR	66000	AR5780026245806	N
Noatak 3	67.81	-161.05	7/12/79	CIR	65285	AR5790027841867	N
Noatak 3	67.82	-161.33	7/12/79	CIR	63000	AR5790027841869	N
Noatak 3	67.82	-161.47	7/12/79	CIR	63000	AR5790027841870	N
Noatak 3	67.90	-161.49	7/12/79	CIR	63750	AR5790027841875	N
Noatak 4	68.07	-157.31	7/19/77	CIR	63665	AR6364000700072	N
Noatak 4	68.17	-157.70	7/19/77	CIR	68244	AR6364000700117	Y
Noatak 4	68.07	-157.70	7/19/77	CIR	63665	AR6364000700069	Y
Noatak 4	68.17	-157.54	7/19/77	CIR	67980	AR6364000700116	N
Noatak 4	68.07	-157.57	7/19/77	CIR	63665	AR6364000700070	N
Noatak 4	68.17	-157.41	7/19/77	CIR	67980	AR6364000700115	N
Noatak 4	68.10	-158.06	7/5/78	CIR	59425	AR6386001500060	N
--	68.07	-156.66	7/19/77	CIR	63665	AR6364000700077	N
--	68.07	-156.79	7/19/77	CIR	63665	AR6364000700076	N
--	68.07	-156.26	7/19/77	CIR	63665	AR6364000700080	N
--	68.07	-156.13	7/19/77	CIR	63665	AR6364000700081	N
--	68.07	-157.18	7/19/77	CIR	63665	AR6364000700073	N
--	68.30	-157.15	7/19/77	CIR	66685	AR6364000700145	N
--	68.30	-157.28	7/19/77	CIR	66685	AR6364000700144	N
--	68.30	-157.42	7/19/77	CIR	66685	AR6364000700143	N
--	68.30	-157.56	7/19/77	CIR	66685	AR6364000700142	N
--	68.35	-160.21	7/19/77	CIR	66740	AR6364000700197	N
--	68.35	-159.24	7/19/77	CIR	67889	AR6364000700190	N
--	68.56	-159.27	7/19/77	CIR	67357	AR6364000700299	N
--	68.56	-159.13	7/19/77	CIR	67357	AR6364000700298	N
--	68.54	-160.05	7/19/77	CIR	67844	AR6364000700305	N
--	68.56	-159.77	7/19/77	CIR	67572	AR6364000700303	N
--	68.56	-159.65	7/19/77	CIR	67572	AR6364000700302	N
--	68.54	-160.18	7/19/77	CIR	67844	AR6364000700306	N

Table A-8: USGS Image metadata part 8

Area	Center latitude	Center longitude	Acq. Date	Type	Scale	Image Name	Processed?
--	68.38	-158.74	7/19/77	CIR	66980	AR6364000700186	N
--	68.35	-159.10	7/19/77	CIR	67889	AR6364000700189	N
--	68.38	-158.61	7/19/77	CIR	66980	AR6364000700185	N
--	68.19	-159.48	7/5/78	CIR	59775	AR6386001500020	N
--	68.19	-159.61	7/5/78	CIR	59775	AR6386001500021	N
--	68.20	-158.61	7/5/78	CIR	59522	AR6386001500013	N
--	68.20	-158.74	7/5/78	CIR	59522	AR6386001500014	N
--	68.10	-158.18	7/5/78	CIR	59425	AR6386001500059	N
--	68.20	-159.11	7/5/78	CIR	59059	AR6386001500017	N
--	68.20	-159.23	7/5/78	CIR	59059	AR6386001500018	N
--	68.20	-160.09	7/31/80	CIR	64500	AR5800029238226	N
--	68.32	-161.24	7/19/77	CIR	66937	AR6364000700205	N
--	68.32	-161.11	7/19/77	CIR	66937	AR6364000700204	N
--	68.07	-161.48	6/24/78	CIR	60522	AR6386000500229	N
--	68.07	-161.60	6/24/78	CIR	60522	AR6386000500228	N
--	68.07	-161.85	6/24/78	CIR	60522	AR6386000500226	N
--	68.07	-161.99	6/24/78	CIR	60522	AR6386000500225	N
--	68.01	-160.94	7/3/78	CIR	66000	AR5780026245805	N
--	67.90	-161.90	7/3/78	CIR	66666	AR5780026245854	N
--	67.89	-162.05	7/3/78	CIR	66666	AR5780026245853	N
--	67.88	-162.34	7/3/78	CIR	67000	AR5780026245851	N
--	67.79	-160.02	7/12/79	CIR	65333	AR5790027841860	N
--	67.79	-160.31	7/12/79	CIR	65285	AR5790027841862	N
--	67.80	-160.46	7/12/79	CIR	65285	AR5790027841863	N
--	67.81	-160.90	7/12/79	CIR	65285	AR5790027841866	N
--	67.86	-158.52	7/12/79	CIR	63666	AR5790027841896	N
--	67.86	-158.66	7/12/79	CIR	63666	AR5790027841895	N
--	67.87	-158.94	7/12/79	CIR	65000	AR5790027841893	N
--	67.87	-159.10	7/12/79	CIR	65000	AR5790027841892	N
--	67.88	-159.39	7/12/79	CIR	64083	AR5790027841890	N
--	67.88	-159.53	7/12/79	CIR	64083	AR5790027841889	N
--	67.63	-162.48	7/14/51	BW	19780	ARCNAV000020067	N
--	68.35	-160.49	7/19/77	CIR	66740	AR6364000700199	N
--	68.35	-160.63	7/19/77	CIR	66740	AR6364000700200	N
Oolamnagavik	68.99	-154.05	6/26/55	BW	50000	ARHM04908911503	N
Oolamnagavik	68.83	-154.35	7/23/71	BW	72733	ARB071400091532	N
Oolamnagavik	68.79	-154.34	7/1/77	CIR	132845	AR6364001400059	N
Oolamnagavik	68.82	-154.23	7/26/77	CIR	71803	AR6364001500116	N

Table A-9: USGS Image metadata part 9

Area	Center latitude	Center longitude	Acq. Date	Type	Scale	Image Name	Processed?
Oolamnagavik	68.91	-154.03	7/26/77	CIR	73185	AR6364001500153	N
Oolamnagavik	69.03	-154.03	7/26/77	CIR	73265	AR6364001500276	N
Oolamnagavik	68.67	-154.44	6/28/78	BW	126571	AR5780026236367	N
Oolamnagavik	68.88	-154.12	7/13/79	BW	130571	AR5790027875537	N
Oolamnagavik	68.80	-154.31	7/13/79	CIR	65444	AR5790027862132	N
Oolamnagavik	68.99	-154.16	8/2/85	BW	125000	AR5850034710717	N
Oolamnagavik	68.98	-154.11	8/2/85	CIR	64857	AR5850034708525	N
Oolamnagavik	68.81	-154.26	8/19/85	CIR	64000	AR5850034769303	Y
Oolamnagavik	68.87	-154.41	8/19/85	BW	132571	AR5850034751178	N
Oolamnagavik	68.85	-154.22	8/14/06	CIR	40000	ARUNPRA00070037	Y
Oolamnagavik	68.88	-154.22	8/14/06	CIR	40000	ARUNPRA00070038	N
Oolamnagavik	68.85	-154.22	7/4/07	CIR	40000	ARUNPRA00120029	Y
Oolamnagavik	68.86	-154.06	7/4/07	CIR	40000	ARUNPRA00120028	Y
Oolamnagavik	69.00	-154.06	7/4/07	CIR	40000	ARUNPRA00120024	Y
Oolamnagavik	68.80	-154.16	7/13/79	CIR	65444	AR5790027862131	N
Oolamnagavik	68.81	-154.10	8/19/85	CIR	64750	AR5850034769301	N
--	68.10	-161.57	9/2/51	BW	20312	ARCNAV000160158	Y
--	68.17	-159.97	9/2/51	BW	20696	ARCNAV000160193	Y
--	68.17	-161.74	7/15/53	BW	44000	ARCKTZ000140050	Y
--	68.15	-159.97	6/21/55	BW	40000	ARHM05510113082	Y
--	68.15	-161.61	6/21/55	BW	40000	ARBM00390678280	Y
--	68.14	-161.64	6/21/55	BW	40000	ARHM05510113064	Y
--	69.45	-151.10	6/21/55	BW	50000	ARBM00350617418	N
--	69.04	-148.89	6/21/55	BW	50000	ARBM00360627465	N
--	68.24	-159.97	6/26/55	BW	39573	ARHM04307910133	Y
--	68.13	-159.98	6/26/55	BW	39619	ARHM04307910130	Y
--	68.12	-161.47	6/26/55	BW	40000	ARHM04307810018	Y
--	69.36	-150.98	6/26/55	BW	50000	ARHM04909011650	N
--	68.19	-161.60	8/14/71	CIR	72276	ARB071400122043	N
--	68.17	-160.07	9/8/71	CIR	78050	ARB071400142648	Y
--	69.08	-148.70	7/13/72	Color	41086	AR6209000700085	Y
--	68.69	-148.95	7/13/72	Color	39721	AR6209000700080	Y
--	68.28	-161.90	7/19/77	CIR	127252	AR6364000600113	N
--	69.45	-150.93	8/1/77	CIR	65524	AR6364002500194	N
--	68.07	-160.12	6/24/78	BW	121764	AR6386000400129	N
--	68.18	-161.43	6/24/78	CIR	59256	AR6386000500155	N
--	68.19	-161.61	6/24/78	CIR	58778	AR6386000500157	N
--	69.08	-148.81	6/28/78	CIR	65400	AR5780026225595	N

Table A-10: USGS Image metadata part 10

Area	Center latitude	Center longitude	Acq. Date	Type	Scale	Image Name	Processed?
--	69.36	-151.06	7/13/79	CIR	66571	AR5790027862213	N
--	68.19	-161.19	7/31/80	BW	126000	AR5800029245951	N
--	69.39	-151.03	8/2/80	CIR	64416	AR5800029258330	N
--	68.68	-149.10	8/7/82	CIR	63900	AR5820031161272	N
--	69.10	-148.72	8/7/82	CIR	65200	AR5820031161406	N
--	68.29	-161.90	8/2/85	BW	126500	AR5850034710687	N
--	69.03	-148.74	4/3/95	BW	126857	AR5950049018808	N
--	69.42	-151.18	8/28/06	CIR	40000	ARUNPRA00080099	Y
--	69.44	-148.71	6/17/77	CIR	65500	AR5770025041660	N
--	68.49	-152.94	6/28/78	CIR	64500	AR5780026225460	N
--	68.81	-150.76	6/28/78	CIR	65000	AR5780026225525	N
--	68.80	-150.45	6/28/78	CIR	64000	AR5780026225523	N
--	68.59	-152.74	6/28/78	CIR	65166	AR5780026225466	N
--	68.69	-150.57	6/28/78	CIR	64200	AR5780026225514	N
--	68.70	-150.12	6/28/78	CIR	64200	AR5780026225517	N
--	69.05	-148.77	6/17/77	CIR	62400	AR5770025041613	N
--	68.72	-148.90	6/17/77	CIR	64000	AR5770025041605	Y
--	69.01	-151.02	6/28/78	CIR	65375	AR5780026225567	N
--	69.01	-151.17	6/28/78	CIR	65375	AR5780026225568	N
--	69.40	-148.12	6/28/78	CIR	65384	AR5780026225670	N
--	69.17	-148.06	6/28/78	CIR	65166	AR5780026225600	N
--	67.41	-163.35	7/3/78	CIR	66285	AR5780026245934	N
--	67.86	-152.37	7/12/79	CIR	63666	AR5790027841929	N
--	67.40	-163.56	7/14/79	CIR	66166	AR5790027882877	N
--	68.20	-159.96	7/31/80	CIR	64500	AR5800029238225	Y
--	68.51	-148.97	8/6/82	CIR	64111	AR5820031140681	N
--	68.41	-152.80	8/6/82	CIR	63000	AR5820031140640	N
--	69.01	-161.04	8/6/82	CIR	65000	AR5820031140808	N
--	69.12	-144.05	8/7/82	CIR	63500	AR5820031161376	N
--	68.68	-149.85	8/7/82	CIR	63900	AR5820031161277	N
--	68.79	-150.55	8/7/82	CIR	65000	AR5820031161147	N
--	68.68	-149.40	8/7/82	CIR	63900	AR5820031161274	N
--	68.68	-149.55	8/7/82	CIR	63900	AR5820031161275	N
--	69.10	-148.10	8/7/82	CIR	65200	AR5820031161402	N
--	69.71	-143.66	8/24/82	CIR	64800	AR5820031262472	N
--	69.41	-143.86	8/24/82	CIR	63555	AR5820031262408	N
--	67.90	-152.32	8/28/82	CIR	63800	AR5820031302791	N
--	69.19	-148.08	8/24/82	CIR	64250	AR5820031262296	N

Table A-11: USGS Image metadata part 11

Area	Center latitude	Center longitude	Acq. Date	Type	Scale	Image Name	Processed?
--	69.01	-161.08	8/2/85	CIR	63250	AR5850034708480	N
--	67.89	-152.22	8/2/85	CIR	63818	AR5850034708413	N
--	69.29	-161.60	8/2/85	CIR	65000	AR5850034708695	N
--	68.89	-156.75	8/19/85	CIR	64000	AR5850034769361	N
--	69.39	-148.67	6/7/95	CIR	62000	AR5950049325405	N
--	69.44	-148.69	6/11/95	CIR	62000	AR5950049345830	N
--	68.71	-149.56	6/13/95	BW	59000	AR5950049366449	N
--	69.25	-161.51	8/1/77	CIR	67539	AR6364002500045	N
--	69.25	-161.63	8/1/77	CIR	67539	AR6364002500044	N
--	69.39	-148.75	6/13/95	BW	59000	AR5950049366455	N
--	68.19	-159.87	7/5/78	CIR	59775	AR6386001500023	Y
--	69.69	-143.76	7/8/78	CIR	60669	AR6386001900228	N
--	69.50	-143.66	7/8/78	CIR	60714	AR6386001900143	N
--	69.20	-144.06	8/3/73	BW	63857	ARB071400355588	N
--	69.26	-143.72	8/3/73	BW	63943	ARB071400355498	N
--	69.13	-144.05	8/8/73	BW	63710	ARB071400345437	N
--	68.60	-152.79	7/13/78	CIR	58800	AR6386002700040	N
--	67.43	-163.47	7/20/52	BW	42000	ARCKTZ000120054	N
--	69.44	-143.65	6/21/55	BW	50000	ARBM00350607211	N
--	68.74	-148.82	6/21/55	BW	50000	ARBM00360627457	Y
--	69.71	-143.85	6/21/55	BW	50000	ARBM00360627556	N
--	67.46	-163.49	7/14/51	BW	19936	ARCNAV000040156	N
--	68.94	-151.10	6/26/55	BW	49597	ARHM04908911480	N
--	68.89	-156.74	7/6/07	CIR	40000	ARUNPRA00150101	N
--	68.88	-156.65	7/6/07	CIR	40000	ARUNPRA00150100	N
--	69.65	-146.23	6/21/55	BW	48329	ARHM06011214579	N
--	69.03	-151.11	6/26/55	BW	50000	ARHM04908911525	N
--	69.03	-150.98	6/26/55	BW	50000	ARHM04908911526	N
--	68.50	-160.76	8/19/85	CIR	64153	AR5850034769234	N
--	68.50	-160.61	8/19/85	CIR	64153	AR5850034769233	N
--	68.49	-161.20	8/19/85	CIR	64153	AR5850034769237	N
--	68.49	-161.49	8/19/85	CIR	64153	AR5850034769239	N
--	68.50	-161.05	8/19/85	CIR	64153	AR5850034769236	N
--	68.49	-162.08	8/19/85	CIR	65200	AR5850034769243	N
--	68.49	-161.64	8/19/85	CIR	64000	AR5850034769240	N
--	68.49	-162.22	8/19/85	CIR	65200	AR5850034769244	N
--	68.29	-162.00	8/2/85	CIR	66000	AR5850034708464	N
--	68.29	-162.43	8/2/85	CIR	66000	AR5850034708467	N

Table A-12: USGS Image metadata part 12

Area	Center latitude	Center longitude	Acq. Date	Type	Scale	Image Name	Processed?
--	68.29	-162.15	8/2/85	CIR	66000	AR5850034708465	N
--	68.29	-162.58	8/2/85	CIR	66000	AR5850034708468	N
--	68.30	-161.56	8/2/85	CIR	66000	AR5850034708461	N
--	68.30	-161.41	8/2/85	CIR	66000	AR5850034708460	N
--	67.67	-157.16	8/5/81	CIR	64500	AR5810030083098	N
--	67.68	-157.02	8/5/81	CIR	64500	AR5810030083099	N
--	67.70	-156.60	8/5/81	CIR	64333	AR5810030083102	N
--	67.69	-156.74	8/5/81	CIR	64500	AR5810030083101	N
--	68.00	-160.01	7/31/80	CIR	65142	AR5800029238173	N
--	68.00	-160.16	7/31/80	CIR	65142	AR5800029238174	N
--	68.19	-161.13	7/31/80	CIR	64666	AR5800029238233	N
--	68.19	-160.98	7/31/80	CIR	64666	AR5800029238232	N
--	67.99	-159.14	7/31/80	CIR	65200	AR5800029238167	N
--	68.19	-160.54	7/31/80	CIR	66500	AR5800029238229	N
--	68.19	-160.66	7/31/80	CIR	66500	AR5800029238230	N
--	68.01	-160.46	7/31/80	CIR	65142	AR5800029238176	N
--	68.01	-160.61	7/31/80	CIR	65142	AR5800029238177	N
--	67.99	-158.69	7/31/80	CIR	64571	AR5800029238164	N
--	67.99	-158.54	7/31/80	CIR	64571	AR5800029238163	N
--	67.69	-159.12	7/31/80	CIR	64250	AR5800029238125	N
--	67.69	-158.98	7/31/80	CIR	64250	AR5800029238124	N
--	67.70	-157.95	7/31/80	CIR	64600	AR5800029238117	N
--	67.70	-157.66	7/31/80	CIR	64600	AR5800029238115	N
--	67.70	-157.52	7/31/80	CIR	64600	AR5800029238114	N
--	67.98	-158.98	7/31/80	CIR	64571	AR5800029238166	N
--	68.00	-159.58	7/31/80	CIR	65200	AR5800029238170	N
--	67.99	-159.43	7/31/80	CIR	65200	AR5800029238169	N
--	67.70	-158.68	7/31/80	CIR	64250	AR5800029238122	N
--	67.70	-158.53	7/31/80	CIR	64600	AR5800029238121	N
--	67.70	-158.10	7/31/80	CIR	64600	AR5800029238118	N
--	67.68	-163.58	7/14/79	CIR	66083	AR5790027882791	N
--	67.68	-163.86	7/14/79	CIR	66285	AR5790027882789	N
--	67.68	-164.00	7/14/79	CIR	66285	AR5790027882788	N
--	67.68	-163.44	7/14/79	CIR	66083	AR5790027882792	N
--	67.69	-162.01	7/14/79	CIR	66083	AR5790027882802	N
--	67.68	-161.86	7/14/79	CIR	65333	AR5790027882803	N
--	67.60	-161.90	7/14/79	CIR	66000	AR5790027882767	N
--	67.60	-161.77	7/14/79	CIR	66000	AR5790027882766	N

Table A-13: USGS Image metadata part 13

Area	Center latitude	Center longitude	Acq. Date	Type	Scale	Image Name	Processed?
--	67.49	-163.28	7/14/79	CIR	66818	AR5790027882867	N
--	67.60	-161.48	7/14/79	CIR	66000	AR5790027882764	N
--	67.60	-161.34	7/14/79	CIR	66000	AR5790027882763	N
--	67.38	-162.30	7/14/79	CIR	65384	AR5790027882886	N
--	67.38	-162.16	7/14/79	CIR	65384	AR5790027882887	N
--	67.49	-163.43	7/14/79	CIR	66818	AR5790027882868	N
--	67.60	-162.21	7/14/79	CIR	66769	AR5790027882769	N
--	67.29	-163.63	7/14/79	CIR	66818	AR5790027882942	N
--	67.29	-163.78	7/14/79	CIR	66818	AR5790027882943	N
--	67.29	-163.35	7/14/79	CIR	66818	AR5790027882940	N
--	67.29	-163.21	7/14/79	CIR	66818	AR5790027882939	N
--	67.29	-162.78	7/14/79	CIR	66818	AR5790027882936	N
--	67.29	-162.64	7/14/79	CIR	66818	AR5790027882935	N
--	67.49	-163.71	7/14/79	CIR	66818	AR5790027882870	N
--	67.50	-163.85	7/14/79	CIR	66818	AR5790027882871	N
--	67.60	-160.76	7/14/79	CIR	66000	AR5790027882759	N
--	67.60	-160.90	7/14/79	CIR	66000	AR5790027882760	N
--	67.30	-159.76	7/14/79	CIR	66187	AR5790027882915	N
--	67.30	-159.91	7/14/79	CIR	66187	AR5790027882916	N
--	67.65	-160.01	7/14/79	CIR	65562	AR5790027882816	N
--	67.65	-159.87	7/14/79	CIR	65562	AR5790027882817	N
--	67.53	-159.95	7/14/79	CIR	66285	AR5790027882844	N
--	67.52	-159.80	7/14/79	CIR	66285	AR5790027882843	N
--	67.65	-159.58	7/14/79	CIR	65562	AR5790027882819	N
--	67.64	-159.44	7/14/79	CIR	65562	AR5790027882820	N
--	67.52	-159.50	7/14/79	CIR	66875	AR5790027882841	N
--	67.52	-159.37	7/14/79	CIR	66875	AR5790027882840	N
--	67.59	-160.32	7/14/79	CIR	66000	AR5790027882756	N
--	67.59	-160.47	7/14/79	CIR	66000	AR5790027882757	N
--	67.51	-159.08	7/14/79	CIR	66875	AR5790027882838	N
--	67.51	-158.94	7/14/79	CIR	66875	AR5790027882837	N
--	67.50	-158.65	7/14/79	CIR	66875	AR5790027882835	N
--	67.50	-158.50	7/14/79	CIR	66875	AR5790027882834	N
--	67.85	-158.24	7/12/79	CIR	65000	AR5790027841898	N
--	67.85	-158.10	7/12/79	CIR	65000	AR5790027841899	N
--	67.78	-159.88	7/12/79	CIR	65333	AR5790027841859	N
--	67.29	-158.58	7/14/78	CIR	60777	AR6386002900236	N
--	67.29	-158.44	7/14/78	CIR	60777	AR6386002900237	N

Table A-14: USGS Image metadata part 14

Area	Center latitude	Center longitude	Acq. Date	Type	Scale	Image Name	Processed?
--	67.30	-158.11	7/14/78	CIR	60519	AR6386002900240	N
--	67.30	-157.99	7/14/78	CIR	60519	AR6386002900241	N
--	67.51	-158.14	7/14/78	CIR	59047	AR6386002900089	N
--	67.50	-158.02	7/14/78	CIR	59047	AR6386002900090	N
--	67.50	-157.68	7/14/78	CIR	59047	AR6386002900093	N
--	67.50	-157.56	7/14/78	CIR	59047	AR6386002900094	N
--	67.50	-156.77	7/14/78	CIR	58917	AR6386002900101	N
--	67.50	-156.65	7/14/78	CIR	58917	AR6386002900102	N
--	67.88	-162.50	7/3/78	CIR	67000	AR5780026245850	N
--	67.87	-156.62	7/19/77	CIR	62104	AR6364000700026	N
--	67.88	-157.73	7/19/77	CIR	63163	AR6364000700017	N
--	67.88	-157.61	7/19/77	CIR	63163	AR6364000700018	N
--	67.86	-157.24	7/19/77	CIR	62104	AR6364000700021	N
--	67.86	-157.11	7/19/77	CIR	62104	AR6364000700022	N
--	67.87	-156.74	7/19/77	CIR	62104	AR6364000700025	N

A.4: Footprints for the satellite images acquired in this study

This work has relied on the acquisition of relatively recent satellite imagery (2008-2012) to characterize contemporary shrub cover in northern Alaska. These data were acquired by various satellite platforms, including Quick Bird, WorldView, IKONOS, and GeoEye. These imagery are useful because they are geographically referenced and are of high resolution (0.5 – 2.4 m) to allow for detailed mapping of shrub cover. I made an effort to acquire the best possible imagery available for the study sites, but sometimes this meant that only panchromatic (black and white) imagery was available. If multispectral imagery was acquired along with panchromatic imagery, I pan-sharpened the imagery myself using the Gram-Schmidt transformation algorithm in ENVI 4.7. All necessary mosaicking was also conducted in ENVI 4.7.

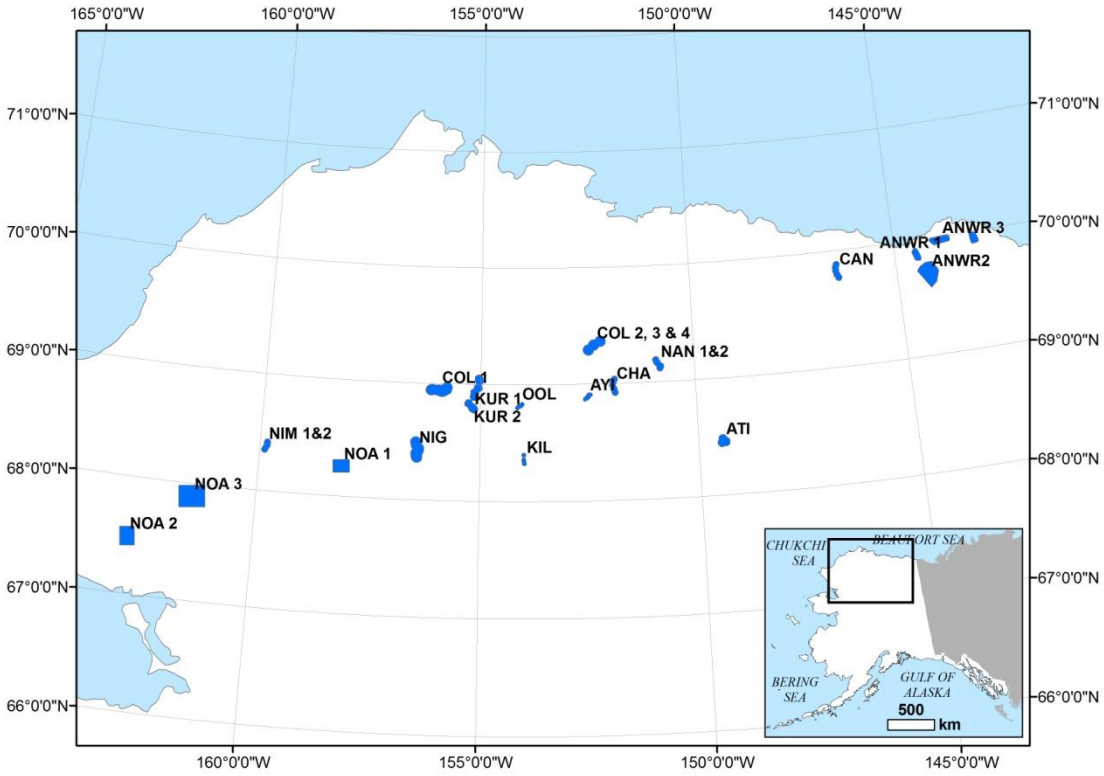

Figure A-25: Generalized footprints for the satellite images acquired for this study.

Table A-15: Satellite image metadata

Area	Satellite	Acq. Date	Type	Resolution (m)	Center latitude	Center longitude
ANWR 1	QuickBird	07/2012	Pan MS	0.5 /2 .4	69.90	-144.99
ANWR 2	QuickBird	07/2012	Pan MS	0.5 / 2.4	69.88	-144.48
ANWR 3	QuickBird	07/2012	Pan MS	0.5 / 2.4	69.97	-143.87
ANWR 4	QuickBird	07/2012	Pan MS	0.5 / 2.4	69.95	-143.05
Atigun	QuickBird	09/2010	Pan MS	0.5 / 2.4	68.46	-149.44
Ayiyak	WorldView	07/2010	Pan	0.5	68.89	-152.51
Canning	QuickBird	06/2010	Pan MS	0.5 / 2.4	69.82	-146.44
Chandler	QuickBird	07/2010	Pan MS	0.5 / 2.4	68.98	-151.90
Colville 1	QuickBird	08/2008	Pan MS	0.5 / 2.4	68.95	-155.95
Colville 2,3,4	QuickBird	08/2004	Pan	0.5	69.33	-152.34
Itagnik	WorldView	08/2008	Pan	0.5	68.73	-150.10
Killik	Ikonos	05/2008	Pan MS	0.8 / 4	68.36	-153.99
Kurupa 1	WorldView	08/2008	Pan	0.5	68.97	-155.09
Kurupa 2	WorldView	08/2008	Pan	0.5	68.81	-155.21
Nanushuk 1,2	GeoEye	08/2009	Pan MS	0.5 / 1.5	69.15	-150.85
Nigu	QuickBird	08/2009	Pan MS	0.5 / 2.4	68.43	-156.44
Nimiuktuk 1,2	WorldView	08/2009	Pan	0.5	68.38	-159.86
Noatak 1	Ikonos	06/2008	Pan MS	0.8 / 2.4	68.26	-158.13
Noatak 2	GeoEye	06/2010	Pan MS	0.5 / 2.4	67.49	-162.73
Noatak 3	GeoEye	06/2010	Pan MS	0.5 / 2.4	67.89	-161.41
Oolamnagavik	WorldView	05/2008	Pan	0.5	68.82	-154.09

A.5: Balser and George photographs from the Noatak National Preserve and Gates of the Arctic National Park and Preserve

Thanks to Dr. David Swanson at the National Park Service, I have access to a series of high-resolution aerial photographs photographed by Tom George and others of the Noatak National Preserve and Gates of the Arctic National Park and Preserve in western Alaska. These were photographed at an altitude of approximately 2 km and provide relatively high-resolution coverage of small areas at 20 km intervals. From my understanding, Mr. Tom George photographed most of these images. A selection of them were used by Mr. Andrew Balser to investigate thermokarst features on the landscape. The National Park Service is currently using them to assess vegetation changes at these 20 km intervals. It is for these reasons that images cover relatively small areas. I suspect that once these images are co-registered to satellite imagery that they can be useful for better characterizing annual rates of shrub cover change.

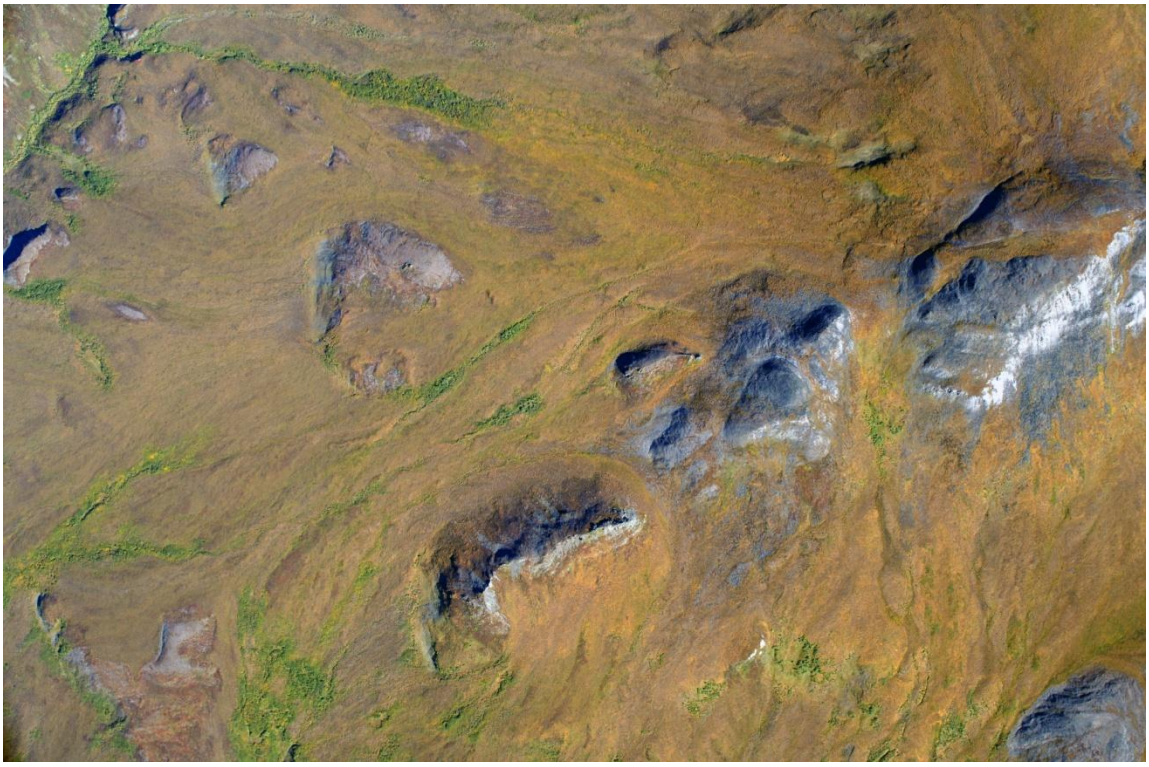

Figure A-26: An example of one of the Balser and George images (TT0_2418).

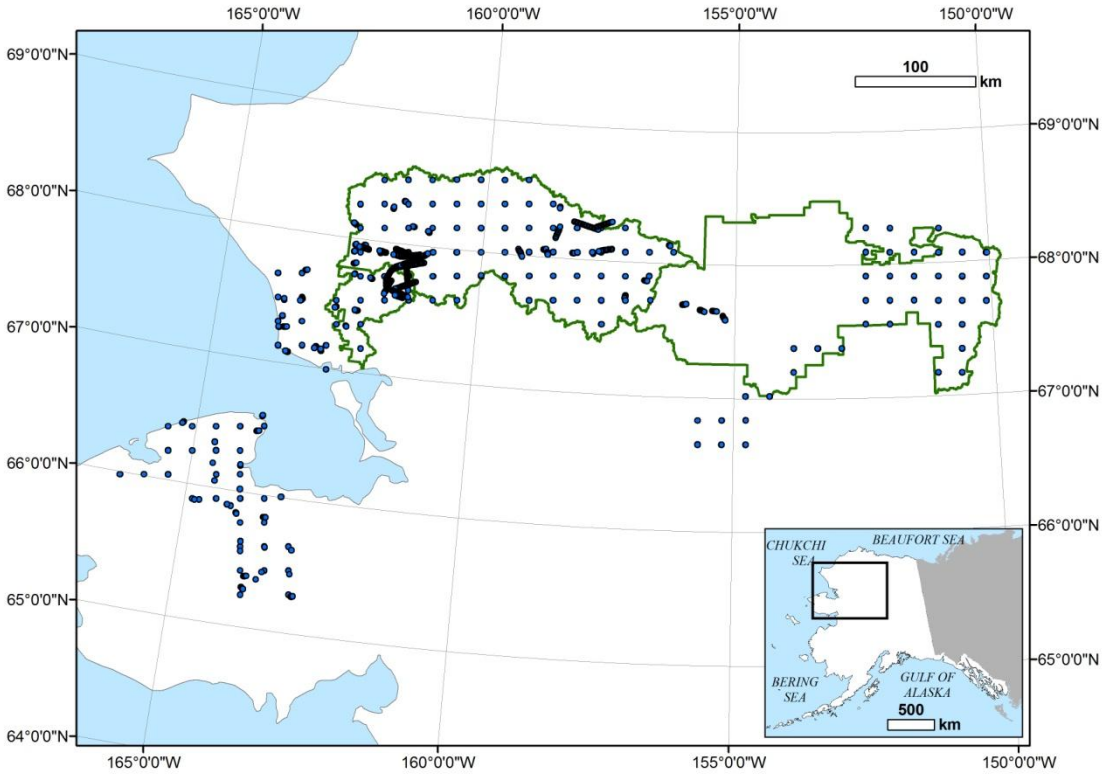

Figure A-27: Location of the Balser and George photographs in the Noatak National Preserve (western green polygon), the Gates of the Arctic National Park (eastern green polygon), and surrounding area. Points indicate the center coordinates for each image.

Table A-16: Balser and George image metadata part 1

Image name	Altitude	Year	Center latitude	Center longitude	Processed?
BELA_GP01-1_20080820.JPG	1822 m	2008	65.29	-162.89	N
BELA_GP01-2_20080820.JPG	1820 m	2008	65.29	-162.89	N
BELA_GP02-1_20080820.JPG	1444 m	2008	65.42	-163.80	N
BELA_GP02-2_20080820.JPG	1442 m	2008	65.42	-163.80	N
BELA_GP03-1_20080820.JPG	1592 m	2008	65.44	-163.38	N
BELA_GP03-2_20080820.JPG	1591 m	2008	65.44	-163.38	N
BELA_GP04-1_20080820.JPG	1721 m	2008	65.47	-162.95	N
BELA_GP04-2_20080820.JPG	1721 m	2008	65.47	-162.95	N
BELA_GP05-1_20080820.JPG	1460 m	2008	65.60	-163.87	N
BELA_GP05-2_20080820.JPG	1461 m	2008	65.59	-163.87	N
BELA_GP06-1_20080820.JPG	1571 m	2008	65.62	-163.44	N
BELA_GP06-2_20080820.JPG	1568 m	2008	65.62	-163.44	N
BELA_GP07-1_20080820.JPG	1626 m	2008	65.65	-163.01	N
BELA_GP07-2_20080820.JPG	1626 m	2008	65.65	-163.01	N
BELA_GP08-1_20080820.JPG	1503 m	2008	65.77	-163.93	N
BELA_GP08-2_20080820.JPG	1502 m	2008	65.77	-163.93	N
BELA_GP09-1_20080820.JPG	1522 m	2008	65.80	-163.50	N
BELA_GP09-2_20080820.JPG	1521 m	2008	65.80	-163.50	N
BELA_GP11-1_20080820.JPG	1210 m	2008	66.04	-165.37	N
BELA_GP11-2_20080820.JPG	1210 m	2008	66.04	-165.37	N
BELA_GP12-1_20080820.JPG	1194 m	2008	66.22	-165.45	N
BELA_GP12-2_20080820.JPG	1193 m	2008	66.22	-165.44	N
BELA_GP13-1_20080820.JPG	1219 m	2008	66.40	-165.52	N
BELA_GP13-2_20080820.JPG	1218 m	2008	66.40	-165.52	N
BELA_GP14-1_20080820.JPG	1255 m	2008	65.98	-166.23	N
BELA_GP14-2_20080820.JPG	1252 m	2008	65.98	-166.24	N
BELA_GP16-1_20080820.JPG	1330 m	2008	65.89	-164.86	N
BELA_GP16-2_20080820.JPG	1329 m	2008	65.89	-164.86	N
BELA_GP17-1_20080820.JPG	1356 m	2008	65.92	-164.43	N
BELA_GP17-2_20080820.JPG	1356 m	2008	65.92	-164.43	N
BELA_GP18-1_20080820.JPG	1394 m	2008	65.95	-163.99	N
BELA_GP18-2_20080820.JPG	1391 m	2008	65.95	-164.00	N
BELA_GP19-1_20080820.JPG	1478 m	2008	65.98	-163.56	N
BELA_GP19-2_20080820.JPG	1480 m	2008	65.98	-163.57	N
BELA_GP22-1_20080820.JPG	1194 m	2008	66.01	-165.80	N
BELA_GP22-2_20080820.JPG	1194 m	2008	66.01	-165.81	N
BELA_GP23-1_20080820.JPG	1231 m	2008	66.10	-164.50	N
BELA_GP23-2_20080820.JPG	1229 m	2008	66.10	-164.50	N

Table A-17: Balser and George image metadata part 2

Image name	Altitude	Year	Center latitude	Center longitude	Processed?
BELA_GP24-2_20080820.JPG	1293 m	8/20/08	66.13	-164.06	N
BELA_GP25-1_20080820.JPG	1202 m	8/20/08	66.25	-165.01	N
BELA_GP25-2_20080820.JPG	1201 m	8/20/08	66.25	-165.01	N
BELA_GP26-1_20080820.JPG	1198 m	8/20/08	66.28	-164.57	N
BELA_GP26-2_20080820.JPG	1196 m	8/20/08	66.28	-164.57	N
BELA_GP27-1_20080820.JPG	1318 m	8/20/08	66.30	-164.13	N
BELA_GP27-2_20080820.JPG	1316 m	8/20/08	66.31	-164.13	N
BELA_GP28-1_20080820.JPG	1200 m	8/20/08	66.43	-165.08	N
BELA_GP28-2_20080820.JPG	1200 m	8/20/08	66.43	-165.08	N
BELA_GP29-1_20080820.JPG	1213 m	8/20/08	66.46	-164.64	N
BELA_GP29-2_20080820.JPG	1214 m	8/20/08	66.46	-164.64	N
BELA_GP30-1_20080820.JPG	1195 m	8/20/08	66.48	-164.20	N
BELA_GP30-2_20080820.JPG	1192 m	8/20/08	66.48	-164.20	N
BELA_GP31-1_20080820.JPG	1232 m	8/20/08	66.51	-163.75	N
BELA_GP31-2_20080820.JPG	1230 m	8/20/08	66.51	-163.75	N
BELA_GP32-1_20080820.JPG	1940 m	8/20/08	65.24	-163.74	N
BELA_GP32-2_20080820.JPG	1936 m	8/20/08	65.24	-163.74	N
BELA_LP01-1_20080820.jpg	1868 m	8/20/08	65.37	-163.51	N
BELA_LP01-2_20080820.jpg	1866 m	8/20/08	65.37	-163.51	N
BELA_LP02-1_20080820.JPG	1743 m	8/20/08	65.43	-163.42	N
BELA_LP02-2_20080820.JPG	1744 m	8/20/08	65.43	-163.42	N
BELA_LP07-1_20080820.JPG	1763 m	8/20/08	65.44	-162.93	N
BELA_LP07-2_20080820.JPG	1764 m	8/20/08	65.44	-162.92	N
BELA_LP15-1_20080820.JPG	1462 m	8/20/08	65.56	-163.86	N
BELA_LP15-2_20080820.JPG	1464 m	8/20/08	65.56	-163.86	N
BELA_LP22-1_20080820.JPG	1604 m	8/20/08	65.62	-162.95	N
BELA_LP22-2_20080820.JPG	1603 m	8/20/08	65.62	-162.95	N
BELA_LP28-1_20080820.JPG	1525 m	8/20/08	65.62	-163.43	N
BELA_LP28-2_20080820.JPG	1524 m	8/20/08	65.62	-163.43	N
BELA_LP31-1_20080820.JPG	1453 m	8/20/08	65.64	-163.88	N
BELA_LP31-2_20080820.JPG	1454 m	8/20/08	65.63	-163.88	N
BELA_LP45-1_20080820.JPG	1409 m	8/20/08	66.01	-163.26	N
BELA_LP45-2_20080820.JPG	1409 m	8/20/08	66.01	-163.27	N
BELA_LP49-1_20080820.JPG	1469 m	8/20/08	65.89	-164.15	N
BELA_LP49-2_20080820.JPG	1467 m	8/20/08	65.89	-164.15	N
BELA_LP51-1_20080820.JPG	1453 m	8/20/08	65.89	-164.22	N
BELA_LP51-2_20080820.JPG	1453 m	8/20/08	65.89	-164.22	N
BELA_LP53-1_20080820.JPG	1326 m	8/20/08	65.90	-164.73	N

Table A-18: Balser and George image metadata part 3

Image name	Altitude	Year	Center latitude	Center longitude	Processed?
BELA_LP54-1_20080820.JPG	1318 m	08/20/08	65.89	-164.82	N
BELA_LP54-2_20080820.JPG	1318 m	08/20/08	65.89	-164.82	N
BELA_LP59-1_20080822.JPG	1334 m	08/20/08	66.02	-164.03	N
BELA_LP59-2_20080822.JPG	1331 m	08/20/08	66.02	-164.03	N
BELA_LP65-1_20080820.JPG	1218 m	08/20/08	66.05	-164.51	N
BELA_LP65-2_20080820.JPG	1219 m	08/20/08	66.05	-164.51	N
BELA_LP73-1_20080820.JPG	1196 m	08/20/08	66.34	-164.62	N
BELA_LP73-2_20080820.JPG	1194 m	08/20/08	66.34	-164.62	N
BELA_LP74-1_20080820.JPG	1251 m	08/20/08	66.18	-164.60	N
BELA_LP74-2_20080820.JPG	1251 m	08/20/08	66.18	-164.60	N
BELA_T04_air20080820_01.JPG	1497 m	08/20/08	65.38	-163.73	N
BELA_T04_air20080820_02.JPG	1496 m	08/20/08	65.38	-163.73	N
BELA_T04_air20080820_03.JPG	1495 m	08/20/08	65.38	-163.73	N
BELA_T04_air20080820_04.JPG	1495 m	08/20/08	65.38	-163.73	N
BELA_T04_air20080820_05.JPG	1496 m	08/20/08	65.38	-163.72	N
BELA_T04_air20080820_06.JPG	1496 m	08/20/08	65.38	-163.72	N
BELA_T04_air20080820_07.JPG	1496 m	08/20/08	65.38	-163.72	N
BELA_T04_air20080820_08.JPG	1496 m	08/20/08	65.38	-163.72	N
BELA_T04_air20080820_09.JPG	1497 m	08/20/08	65.38	-163.71	N
BELA_T04_air20080820_10.JPG	1498 m	08/20/08	65.38	-163.71	N
BELA_T04_air20080820_11.JPG	1498 m	08/20/08	65.38	-163.71	N
BELA_T04_air20080820_12.JPG	1499 m	08/20/08	65.38	-163.71	N
BELA_T04_air20080820_13.JPG	1499 m	08/20/08	65.38	-163.70	N
BELA_T04_air20080820_14.JPG	1499 m	08/20/08	65.38	-163.70	N
BELA_T04_air20080820_15.JPG	1499 m	08/20/08	65.38	-163.70	N
BELA_T04_air20080820_16.JPG	1498 m	08/20/08	65.38	-163.70	N
BELA_T04_air20080820_17.JPG	1497 m	08/20/08	65.38	-163.70	N
BELA_T04_air20080820_18.JPG	1496 m	08/20/08	65.38	-163.69	N
BELA_T04_air20080820_19.JPG	1494 m	08/20/08	65.38	-163.69	N
BELA_T04_air20080820_20.JPG	1492 m	08/20/08	65.38	-163.69	N
BELA_T04_air20080820_21.JPG	1491 m	08/20/08	65.38	-163.69	N
BELA_T04_air20080820_22.JPG	1491 m	08/20/08	65.38	-163.68	N
BELA_T05_air20080820_01.JPG	1978 m	08/20/08	65.30	-163.75	N
BELA_T05_air20080820_02.JPG	1978 m	08/20/08	65.30	-163.75	N
BELA_T05_air20080820_03.JPG	1980 m	08/20/08	65.30	-163.75	N
BELA_T05_air20080820_04.JPG	1979 m	08/20/08	65.29	-163.74	N
BELA_T05_air20080820_05.JPG	1977 m	08/20/08	65.29	-163.74	N
BELA_T05_air20080820_06.JPG	1975 m	08/20/08	65.29	-163.74	N

Table A-19: Balser and George image metadata part 4

Image name	Altitude	Year	Center latitude	Center longitude	Processed?
BELA_T05_air20080820_08.JPG	1976 m	08/20/08	65.29	-163.74	N
BELA_T05_air20080820_09.JPG	1978 m	08/20/08	65.29	-163.73	N
BELA_T05_air20080820_10.JPG	1980 m	08/20/08	65.29	-163.73	N
BELA_T05_air20080820_11.JPG	1982 m	08/20/08	65.29	-163.73	N
BELA_T05_air20080820_12.JPG	1984 m	08/20/08	65.29	-163.73	N
BELA_T05_air20080820_13.JPG	1984 m	08/20/08	65.29	-163.73	N
BELA_T05_air20080820_14.JPG	1983 m	08/20/08	65.29	-163.73	N
BELA_T05_air20080820_15.JPG	1983 m	08/20/08	65.29	-163.72	N
BELA_T05_air20080820_16.JPG	1982 m	08/20/08	65.29	-163.72	N
BELA_T05_air20080820_17.JPG	1981 m	08/20/08	65.29	-163.72	N
BELA_T05_air20080820_18.JPG	1981 m	08/20/08	65.29	-163.72	N
BELA_T05_air20080820_19.JPG	1982 m	08/20/08	65.29	-163.72	N
BELA_T05_air20080820_20.JPG	1983 m	08/20/08	65.29	-163.72	N
BELA_T05_air20080820_21.JPG	1983 m	08/20/08	65.29	-163.71	N
BELA_T05_air20080820_22.JPG	1982 m	08/20/08	65.28	-163.71	N
BELA_T06_air20080820_01.JPG	1729 m	08/20/08	65.28	-162.85	N
BELA_T06_air20080820_02.JPG	1736 m	08/20/08	65.28	-162.85	N
BELA_T06_air20080820_03.JPG	1741 m	08/20/08	65.28	-162.84	N
BELA_T06_air20080820_04.JPG	1745 m	08/20/08	65.28	-162.84	N
BELA_T06_air20080820_05.JPG	1747 m	08/20/08	65.28	-162.84	N
BELA_T06_air20080820_06.JPG	1748 m	08/20/08	65.28	-162.84	N
BELA_T06_air20080820_07.JPG	1747 m	08/20/08	65.28	-162.84	N
BELA_T06_air20080820_08.JPG	1746 m	08/20/08	65.28	-162.83	N
BELA_T06_air20080820_09.JPG	1743 m	08/20/08	65.28	-162.83	N
BELA_T06_air20080820_10.JPG	1742 m	08/20/08	65.28	-162.83	N
BELA_T06_air20080820_11.JPG	1740 m	08/20/08	65.28	-162.83	N
BELA_T06_air20080820_12.JPG	1739 m	08/20/08	65.28	-162.82	N
BELA_T06_air20080820_13.JPG	1738 m	08/20/08	65.28	-162.82	N
BELA_T06_air20080820_14.JPG	1738 m	08/20/08	65.28	-162.82	N
BELA_T06_air20080820_15.JPG	1738 m	08/20/08	65.28	-162.82	N
BELA_T06_air20080820_16.JPG	1737 m	08/20/08	65.28	-162.82	N
BELA_T06_air20080820_17.JPG	1736 m	08/20/08	65.28	-162.81	N
BELA_T10_air_20080820_01.JPG	1487 m	08/20/08	65.84	-164.04	N
BELA_T10_air_20080820_02.JPG	1487 m	08/20/08	65.84	-164.04	N
BELA_T10_air_20080820_03.JPG	1488 m	08/20/08	65.84	-164.04	N
BELA_T10_air_20080820_04.JPG	1488 m	08/20/08	65.84	-164.04	N
BELA_T10_air_20080820_05.JPG	1488 m	08/20/08	65.84	-164.04	N
BELA_T10_air_20080820_06.JPG	1488 m	08/20/08	65.84	-164.03	N

Table A-20: Balser and George image metadata part 5

Image name	Altitude	Year	Center latitude	Center longitude	Processed?
BELA_T10_air_20080820_08.JPG	1484 m	08/20/08	65.84	-164.03	N
BELA_T10_air_20080820_09.JPG	1481 m	08/20/08	65.84	-164.03	N
BELA_T10_air_20080820_10.JPG	1479 m	08/20/08	65.84	-164.03	N
BELA_T10_air_20080820_11.JPG	1475 m	08/20/08	65.84	-164.03	N
BELA_T10_air_20080820_12.JPG	1474 m	08/20/08	65.83	-164.02	N
BELA_T11_air_20080820_01.JPG	1575 m	08/20/08	65.84	-163.54	N
BELA_T11_air_20080820_02.JPG	1576 m	08/20/08	65.84	-163.53	N
BELA_T11_air_20080820_03.JPG	1577 m	08/20/08	65.84	-163.53	N
BELA_T11_air_20080820_04.JPG	1574 m	08/20/08	65.84	-163.53	N
BELA_T11_air_20080820_05.JPG	1571 m	08/20/08	65.84	-163.53	N
BELA_T11_air_20080820_06.JPG	1567 m	08/20/08	65.84	-163.52	N
BELA_T11_air_20080820_07.JPG	1562 m	08/20/08	65.84	-163.52	N
BELA_T11_air_20080820_08.JPG	1558 m	08/20/08	65.84	-163.52	N
BELA_T11_air_20080820_09.JPG	1556 m	08/20/08	65.84	-163.52	N
BELA_T11_air_20080820_10.JPG	1556 m	08/20/08	65.84	-163.51	N
BELA_T11_air_20080820_11.JPG	1557 m	08/20/08	65.84	-163.51	N
BELA_T11_air_20080820_12.JPG	1558 m	08/20/08	65.84	-163.51	N
BELA_T11_air_20080820_13.JPG	1561 m	08/20/08	65.84	-163.51	N
BELA_T11_air_20080820_14.JPG	1564 m	08/20/08	65.84	-163.50	N
BELA_T11_air_20080820_15.JPG	1566 m	08/20/08	65.84	-163.50	N
BELA_T11_air_20080820_16.JPG	1566 m	08/20/08	65.84	-163.50	N
BELA_T11_air_20080820_17.JPG	1566 m	08/20/08	65.84	-163.50	N
BELA_T11_air_20080820_18.JPG	1567 m	08/20/08	65.84	-163.49	N
BELA_T11_air_20080820_19.JPG	1569 m	08/20/08	65.84	-163.49	N
BELA_T11_air_20080820_20.JPG	1571 m	08/20/08	65.84	-163.49	N
BELA_T17_air_20080820_01.JPG	1295 m	08/20/08	66.19	-164.08	N
BELA_T17_air_20080820_02.JPG	1296 m	08/20/08	66.19	-164.08	N
BELA_T17_air_20080820_03.JPG	1296 m	08/20/08	66.19	-164.09	N
BELA_T17_air_20080820_04.JPG	1296 m	08/20/08	66.20	-164.09	N
BELA_T17_air_20080820_05.JPG	1296 m	08/20/08	66.20	-164.09	N
BELA_T17_air_20080820_06.JPG	1295 m	08/20/08	66.20	-164.09	N
BELA_T17_air_20080820_07.JPG	1295 m	08/20/08	66.20	-164.09	N
BELA_T17_air_20080820_08.JPG	1295 m	08/20/08	66.20	-164.09	N
BELA_T17_air_20080820_09.JPG	1296 m	08/20/08	66.20	-164.09	N
BELA_T17_air_20080820_10.JPG	1296 m	08/20/08	66.20	-164.09	N
BELA_T18_air_20080820_01.JPG	1280 m	08/20/08	66.58	-163.82	N
BELA_T18_air_20080820_02.JPG	1274 m	08/20/08	66.58	-163.82	N
BELA_T18_air_20080820_03.JPG	1273 m	08/20/08	66.59	-163.82	N

Table A-21: Balser and George image metadata part 6

Image name	Altitude	Year	Center latitude	Center longitude	Processed?
BELA_T18_air_20080820_05.JPG	1273 m	08/20/08	66.59	-163.82	N
BELA_T18_air_20080820_06.JPG	1276 m	08/20/08	66.59	-163.81	N
BELA_T19_air_20080820_01.JPG	1226 m	08/20/08	66.47	-163.88	N
BELA_T19_air_20080820_02.JPG	1225 m	08/20/08	66.47	-163.88	N
BELA_T19_air_20080820_03.JPG	1224 m	08/20/08	66.47	-163.88	N
BELA_T19_air_20080820_04.JPG	1223 m	08/20/08	66.47	-163.87	N
BELA_T19_air_20080820_05.JPG	1223 m	08/20/08	66.47	-163.87	N
BELA_T19_air_20080820_06.JPG	1222 m	08/20/08	66.47	-163.87	N
BELA_T19_air_20080820_07.JPG	1222 m	08/20/08	66.47	-163.86	N
BELA_T19_air_20080820_08.JPG	1223 m	08/20/08	66.47	-163.86	N
BELA_T19_air_20080820_09.JPG	1223 m	08/20/08	66.47	-163.85	N
BELA_T19_air_20080820_10.JPG	1224 m	08/20/08	66.47	-163.85	N
BELA_T19_air_20080820_11.JPG	1223 m	08/20/08	66.47	-163.85	N
BELA_T19_air_20080820_12.JPG	1222 m	08/20/08	66.47	-163.85	N
BELA_T19_air_20080820_13.JPG	1221 m	08/20/08	66.47	-163.84	N
BELA_T21_air_20080820_01.JPG	1258 m	08/20/08	66.45	-165.25	N
BELA_T21_air_20080820_02.JPG	1258 m	08/20/08	66.45	-165.25	N
BELA_T21_air_20080820_03.JPG	1259 m	08/20/08	66.45	-165.25	N
BELA_T21_air_20080820_04.JPG	1260 m	08/20/08	66.45	-165.25	N
BELA_T21_air_20080820_05.JPG	1261 m	08/20/08	66.45	-165.26	N
BELA_T21_air_20080820_06.JPG	1261 m	08/20/08	66.45	-165.26	N
BELA_T21_air_20080820_07.JPG	1260 m	08/20/08	66.44	-165.26	N
BELA_T21_air_20080820_08.JPG	1258 m	08/20/08	66.44	-165.26	N
BELA_T21_air_20080820_09.JPG	1257 m	08/20/08	66.44	-165.27	N
BELA_T21_air_20080820_10.JPG	1257 m	08/20/08	66.44	-165.27	N
CAKR_GP01-1_20080821.JPG	1209 m	8/21/08	67.00	-162.75	N
CAKR_GP01-2_20080821.JPG	1205 m	8/21/08	67.00	-162.76	N
CAKR_GP02-1_20080821.JPG	1232 m	8/21/08	67.13	-163.72	N
CAKR_GP02-2_20080821.JPG	1233 m	8/21/08	67.13	-163.73	N
CAKR_GP03-1_20080821.JPG	1345 m	8/21/08	67.15	-163.27	N
CAKR_GP03-2_20080821.JPG	1346 m	8/21/08	67.15	-163.27	N
CAKR_GP04-1_20080821.JPG	1386 m	8/21/08	67.18	-162.82	N
CAKR_GP04-2_20080821.JPG	1384 m	8/21/08	67.18	-162.81	N
CAKR_GP05-1_20080821.JPG	1165 m	8/21/08	67.30	-163.79	N
CAKR_GP05-2_20080821.JPG	1165 m	8/21/08	67.30	-163.79	N
CAKR_GP06-1_20080821.JPG	1299 m	8/21/08	67.33	-163.34	N
CAKR_GP06-2_20080821.JPG	1298 m	8/21/08	67.33	-163.33	N
CAKR_GP07-1_20080821.JPG	1256 m	8/21/08	67.48	-163.86	N

Table A-22: Balser and George image metadata part 7

Image name	Altitude	Year	Center latitude	Center longitude	Processed?
CAKR_GP08-1_20080821.JPG	1392 m	8/21/08	67.51	-163.40	N
CAKR_GP08-2_20080821.JPG	1390 m	8/21/08	67.51	-163.40	N
CAKR_GP09-1_20080821.JPG	1268 m	8/21/08	67.66	-163.93	N
CAKR_GP09-2_20080821.JPG	1267 m	8/21/08	67.66	-163.93	N
CAKR_GP10-1_20080821.JPG	1460 m	8/21/08	67.69	-163.47	N
CAKR_GP10-2_20080821.JPG	1460 m	8/21/08	67.69	-163.47	N
CK_T01_air_20080821_01.JPG	1359 m	8/21/08	67.13	-162.90	N
CK_T01_air_20080821_02.JPG	1359 m	8/21/08	67.13	-162.90	N
CK_T01_air_20080821_03.JPG	1358 m	8/21/08	67.13	-162.90	N
CK_T01_air_20080821_04.JPG	1357 m	8/21/08	67.13	-162.91	N
CK_T01_air_20080821_05.JPG	1357 m	8/21/08	67.13	-162.91	N
CK_T01_air_20080821_06.JPG	1356 m	8/21/08	67.14	-162.91	N
CK_T01_air_20080821_07.JPG	1355 m	8/21/08	67.14	-162.91	N
CK_T01_air_20080821_08.JPG	1354 m	8/21/08	67.14	-162.91	N
CK_T01_air_20080821_09.JPG	1353 m	8/21/08	67.14	-162.91	N
CK_T01_air_20080821_10.JPG	1352 m	8/21/08	67.14	-162.91	N
CK_T01_air_20080821_11.JPG	1351 m	8/21/08	67.14	-162.91	N
CK_T01_air_20080821_12.JPG	1350 m	8/21/08	67.14	-162.91	N
CK_T01_air_20080821_13.JPG	1349 m	8/21/08	67.14	-162.91	N
CK_T02_air_20080821_01.JPG	1366 m	8/21/08	67.16	-163.01	N
CK_T02_air_20080821_02.JPG	1367 m	8/21/08	67.16	-163.01	N
CK_T02_air_20080821_03.JPG	1367 m	8/21/08	67.16	-163.01	N
CK_T02_air_20080821_04.JPG	1368 m	8/21/08	67.16	-163.01	N
CK_T02_air_20080821_05.JPG	1368 m	8/21/08	67.15	-163.01	N
CK_T02_air_20080821_06.JPG	1368 m	8/21/08	67.15	-163.02	N
CK_T02_air_20080821_07.JPG	1368 m	8/21/08	67.15	-163.02	N
CK_T02_air_20080821_08.JPG	1367 m	8/21/08	67.15	-163.02	N
CK_T02_air_20080821_09.JPG	1366 m	8/21/08	67.15	-163.02	N
CK_T02_air_20080821_10.JPG	1366 m	8/21/08	67.15	-163.02	N
CK_T02_air_20080821_11.JPG	1365 m	8/21/08	67.15	-163.03	N
CK_T02_air_20080821_12.JPG	1364 m	8/21/08	67.15	-163.03	N
CK_T02_air_20080821_13.JPG	1362 m	8/21/08	67.15	-163.03	N
CK_T02_air_20080821_14.JPG	1362 m	8/21/08	67.15	-163.03	N
CK_T02_air_20080821_15.JPG	1361 m	8/21/08	67.15	-163.03	N
CK_T05_air_20080821_01.JPG	1256 m	8/21/08	67.09	-163.53	N
CK_T05_air_20080821_02.JPG	1259 m	8/21/08	67.09	-163.53	N
CK_T05_air_20080821_03.JPG	1261 m	8/21/08	67.09	-163.53	N
CK_T05_air_20080821_04.JPG	1263 m	8/21/08	67.09	-163.53	N

Table A-23: Balser and George image metadata part 8

Image name	Altitude	Year	Center latitude	Center longitude	Processed?
CK_T05_air_20080821_06.JPG	1264 m	8/21/08	67.09	-163.54	N
CK_T05_air_20080821_07.JPG	1264 m	8/21/08	67.09	-163.54	N
CK_T05_air_20080821_08.JPG	1264 m	8/21/08	67.09	-163.55	N
CK_T05_air_20080821_09.JPG	1263 m	8/21/08	67.09	-163.55	N
CK_T05_air_20080821_10.JPG	1263 m	8/21/08	67.09	-163.55	N
CK_T05_air_20080821_11.JPG	1263 m	8/21/08	67.09	-163.55	N
CK_T05_air_20080821_12.JPG	1262 m	8/21/08	67.09	-163.56	N
CK_T05_air_20080821_13.JPG	1262 m	8/21/08	67.09	-163.56	N
CK_T05_air_20080821_14.JPG	1262 m	8/21/08	67.09	-163.56	N
CK_T05_air_20080821_15.JPG	1262 m	8/21/08	67.09	-163.56	N
CK_T05_air_20080821_16.JPG	1263 m	8/21/08	67.09	-163.57	N
CK_T05_air_20080821_17.JPG	1263 m	8/21/08	67.09	-163.57	N
CK_T07_air_20080821_01.JPG	1257 m	8/21/08	67.27	-163.67	N
CK_T07_air_20080821_02.JPG	1257 m	8/21/08	67.27	-163.67	N
CK_T07_air_20080821_03.JPG	1258 m	8/21/08	67.27	-163.67	N
CK_T07_air_20080821_04.JPG	1258 m	8/21/08	67.27	-163.66	N
CK_T07_air_20080821_05.JPG	1258 m	8/21/08	67.27	-163.66	N
CK_T07_air_20080821_06.JPG	1258 m	8/21/08	67.27	-163.66	N
CK_T07_air_20080821_07.JPG	1258 m	8/21/08	67.27	-163.66	N
CK_T07_air_20080821_08.JPG	1258 m	8/21/08	67.27	-163.65	N
CK_T07_air_20080821_09.JPG	1257 m	8/21/08	67.27	-163.65	N
CK_T07_air_20080821_10.JPG	1257 m	8/21/08	67.27	-163.65	N
CK_T07_air_20080821_11.JPG	1256 m	8/21/08	67.27	-163.65	N
CK_T07_air_20080821_12.JPG	1256 m	8/21/08	67.27	-163.64	N
CK_T07_air_20080821_13.JPG	1256 m	8/21/08	67.27	-163.64	N
CK_T07_air_20080821_14.JPG	1256 m	8/21/08	67.27	-163.64	N
CK_T07_air_20080821_15.JPG	1257 m	8/21/08	67.27	-163.63	N
CK_T07_air_20080821_16.JPG	1258 m	8/21/08	67.27	-163.63	N
CK_T07_air_20080821_17.JPG	1259 m	8/21/08	67.27	-163.63	N
CK_T07_air_20080821_18.JPG	1259 m	8/21/08	67.27	-163.63	N
CK_T07_air_20080821_19.JPG	1259 m	8/21/08	67.27	-163.62	N
CK_T07_air_20080821_20.JPG	1259 m	8/21/08	67.27	-163.62	N
CK_T07_air_20080821_21.JPG	1259 m	8/21/08	67.27	-163.62	N
CK_T07_air_20080821_22.JPG	1259 m	8/21/08	67.27	-163.62	N
CK_T07_air_20080821_23.JPG	1259 m	8/21/08	67.27	-163.61	N
CK_T08_air_20080821_01.JPG	1296 m	8/21/08	67.35	-163.72	N
CK_T08_air_20080821_02.JPG	1294 m	8/21/08	67.35	-163.72	N
CK_T08_air_20080821_03.JPG	1293 m	8/21/08	67.35	-163.72	N

Table A-24: Balser and George image metadata part 9

Image name	Altitude	Year	Center latitude	Center longitude	Processed?
CK_T08_air_20080821_05.JPG	1290 m	8/21/08	67.35	-163.72	N
CK_T08_air_20080821_06.JPG	1288 m	8/21/08	67.35	-163.72	N
CK_T10_air_20080821_01.JPG	1486 m	8/21/08	67.50	-163.38	N
CK_T10_air_20080821_02.JPG	1484 m	8/21/08	67.50	-163.39	N
CK_T10_air_20080821_03.JPG	1482 m	8/21/08	67.50	-163.39	N
CK_T10_air_20080821_04.JPG	1481 m	8/21/08	67.50	-163.39	N
CK_T10_air_20080821_05.JPG	1479 m	8/21/08	67.49	-163.39	N
CK_T10_air_20080821_06.JPG	1479 m	8/21/08	67.49	-163.39	N
CK_T10_air_20080821_07.JPG	1479 m	8/21/08	67.49	-163.40	N
CK_T10_air_20080821_08.JPG	1479 m	8/21/08	67.49	-163.40	N
CK_T10_air_20080821_09.JPG	1479 m	8/21/08	67.49	-163.40	N
CK_T10_air_20080821_10.JPG	1478 m	8/21/08	67.49	-163.40	N
CK_T10_air_20080821_11.JPG	1476 m	8/21/08	67.49	-163.41	N
CK_T10_air_20080821_12.JPG	1474 m	8/21/08	67.49	-163.41	N
CK_T10_air_20080821_13.JPG	1472 m	8/21/08	67.49	-163.41	N
CK_T10_air_20080821_14.JPG	1470 m	8/21/08	67.49	-163.41	N
CK_T10_air_20080821_15.JPG	1468 m	8/21/08	67.49	-163.41	N
CK_T10_air_20080821_16.JPG	1466 m	8/21/08	67.49	-163.42	N
CK_T10_air_20080821_17.JPG	1465 m	8/21/08	67.48	-163.42	N
CK_T10_air_20080821_18.JPG	1466 m	8/21/08	67.48	-163.42	N
CK_T10_air_20080821_19.JPG	1468 m	8/21/08	67.48	-163.42	N
CK_T11_air_20080821_01.JPG	1254 m	8/21/08	67.47	-163.73	N
CK_T11_air_20080821_02.JPG	1254 m	8/21/08	67.47	-163.73	N
CK_T11_air_20080821_03.JPG	1255 m	8/21/08	67.47	-163.73	N
CK_T11_air_20080821_04.JPG	1256 m	8/21/08	67.47	-163.73	N
CK_T11_air_20080821_05.JPG	1257 m	8/21/08	67.47	-163.73	N
CK_T11_air_20080821_06.JPG	1260 m	8/21/08	67.48	-163.73	N
CK_T11_air_20080821_07.JPG	1261 m	8/21/08	67.48	-163.73	N
CK_T11_air_20080821_08.JPG	1262 m	8/21/08	67.48	-163.73	N
CK_T11_air_20080821_09.JPG	1263 m	8/21/08	67.48	-163.73	N
CK_T11_air_20080821_10.JPG	1263 m	8/21/08	67.48	-163.73	N
CK_T13_air_20080821_01.JPG	1420 m	8/21/08	67.71	-163.41	N
CK_T13_air_20080821_02.JPG	1419 m	8/21/08	67.71	-163.40	N
CK_T13_air_20080821_03.JPG	1418 m	8/21/08	67.71	-163.40	N
CK_T13_air_20080821_04.JPG	1418 m	8/21/08	67.71	-163.40	N
CK_T13_air_20080821_05.JPG	1418 m	8/21/08	67.71	-163.40	N
CK_T13_air_20080821_06.JPG	1418 m	8/21/08	67.72	-163.39	N
CK_T13_air_20080821_07.JPG	1418 m	8/21/08	67.72	-163.39	N

Table A-25: Balser and George image metadata part 10

Image name	Altitude	Year	Center latitude	Center longitude	Processed?
CK_T13_air_20080821_09.JPG	1417 m	8/21/08	67.72	-163.38	N
CK_T13_air_20080821_10.JPG	1416 m	8/21/08	67.72	-163.38	N
CK_T13_air_20080821_11.JPG	1414 m	8/21/08	67.72	-163.38	N
CK_T13_air_20080821_12.JPG	1412 m	8/21/08	67.72	-163.38	N
CK_T13_air_20080821_13.JPG	1412 m	8/21/08	67.72	-163.37	N
CK_T13_air_20080821_14.JPG	1413 m	8/21/08	67.72	-163.37	N
CK_T13_air_20080821_15.JPG	1414 m	8/21/08	67.72	-163.37	N
CK_T15_air_20080821_01.JPG	1188 m	8/21/08	67.26	-163.75	N
CK_T15_air_20080821_02.JPG	1186 m	8/21/08	67.26	-163.76	N
CK_T15_air_20080821_03.JPG	1183 m	8/21/08	67.26	-163.76	N
CK_T15_air_20080821_04.JPG	1180 m	8/21/08	67.26	-163.76	N
CK_T15_air_20080821_05.JPG	1178 m	8/21/08	67.27	-163.76	N
CK_T15_air_20080821_06.JPG	1176 m	8/21/08	67.27	-163.76	N
CK_T15_air_20080821_07.JPG	1174 m	8/21/08	67.27	-163.77	N
NO_T02_air_20080821_01.JPG	1253 m	8/21/08	67.34	-162.49	N
NO_T02_air_20080821_02.JPG	1254 m	8/21/08	67.34	-162.49	N
NO_T02_air_20080821_03.JPG	1256 m	8/21/08	67.34	-162.49	N
NO_T02_air_20080821_04.JPG	1257 m	8/21/08	67.34	-162.49	N
NO_T02_air_20080821_05.JPG	1257 m	8/21/08	67.34	-162.48	N
NO_T02_air_20080821_06.JPG	1258 m	8/21/08	67.34	-162.48	N
NO_T02_air_20080821_07.JPG	1258 m	8/21/08	67.34	-162.48	N
NO_T02_air_20080821_08.JPG	1258 m	8/21/08	67.33	-162.48	N
NO_T02_air_20080821_09.JPG	1258 m	8/21/08	67.33	-162.48	N
NO_T03_air_20080821_01.JPG	1675 m	8/21/08	67.46	-162.30	N
NO_T03_air_20080821_02.JPG	1675 m	8/21/08	67.46	-162.30	N
NO_T03_air_20080821_03.JPG	1675 m	8/21/08	67.46	-162.31	N
NO_T03_air_20080821_04.JPG	1674 m	8/21/08	67.46	-162.31	N
NO_T03_air_20080821_05.JPG	1673 m	8/21/08	67.46	-162.31	N
NO_T03_air_20080821_06.JPG	1673 m	8/21/08	67.46	-162.32	N
NO_T03_air_20080821_07.JPG	1673 m	8/21/08	67.46	-162.32	N
NO_T03_air_20080821_08.JPG	1672 m	8/21/08	67.46	-162.32	N
NO_T03_air_20080821_09.JPG	1671 m	8/21/08	67.46	-162.32	N
NO_T03_air_20080821_10.JPG	1670 m	8/21/08	67.46	-162.33	N
NO_T03_air_20080821_11.JPG	1669 m	8/21/08	67.46	-162.33	N
NO_T03_air_20080821_12.JPG	1669 m	8/21/08	67.46	-162.33	N
NO_T03_air_20080821_13.JPG	1669 m	8/21/08	67.47	-162.34	N
NO_T03_air_20080821_14.JPG	1669 m	8/21/08	67.47	-162.34	N
NO_T03_air_20080821_15.JPG	1670 m	8/21/08	67.47	-162.34	N

Table A-26: Balser and George image metadata part 11

Image name	Altitude	Year	Center latitude	Center longitude	Processed?
NO_T03_air_20080821_17.JPG	1671 m	8/21/08	67.47	-162.35	N
NO_T03_air_20080821_18.JPG	1672 m	8/21/08	67.47	-162.35	N
NO_T03_air_20080821_19.JPG	1673 m	8/21/08	67.47	-162.35	N
NO_T03_air_20080821_20.JPG	1674 m	8/21/08	67.47	-162.36	N
NO_T04_air_20080821_01.JPG	1408 m	8/21/08	67.47	-162.72	N
NO_T04_air_20080821_02.JPG	1406 m	8/21/08	67.47	-162.72	N
NO_T04_air_20080821_03.JPG	1404 m	8/21/08	67.47	-162.72	N
NO_T04_air_20080821_04.JPG	1402 m	8/21/08	67.47	-162.73	N
NO_T04_air_20080821_05.JPG	1399 m	8/21/08	67.47	-162.73	N
NO_T04_air_20080821_06.JPG	1397 m	8/21/08	67.47	-162.73	N
NO_T04_air_20080821_07.JPG	1394 m	8/21/08	67.47	-162.74	N
NO_T04_air_20080821_08.JPG	1392 m	8/21/08	67.47	-162.74	N
NO_T04_air_20080821_09.JPG	1389 m	8/21/08	67.47	-162.74	N
NO_T04_air_20080821_10.JPG	1386 m	8/21/08	67.47	-162.74	N
NO_T07_air_20080821_01.JPG	1280 m	8/21/08	67.74	-162.44	N
NO_T07_air_20080821_02.JPG	1279 m	8/21/08	67.74	-162.44	N
NO_T07_air_20080821_03.JPG	1279 m	8/21/08	67.74	-162.44	N
NO_T07_air_20080821_04.JPG	1277 m	8/21/08	67.73	-162.44	N
NO_T07_air_20080821_05.JPG	1275 m	8/21/08	67.73	-162.44	N
NO_T07_air_20080821_06.JPG	1274 m	8/21/08	67.73	-162.45	N
NO_T07_air_20080821_07.JPG	1272 m	8/21/08	67.73	-162.45	N
NO_T07_air_20080821_08.JPG	1271 m	8/21/08	67.73	-162.45	N
NO_T08_air_20080821_01.JPG	1335 m	8/21/08	67.81	-162.49	N
NO_T08_air_20080821_02.JPG	1335 m	8/21/08	67.81	-162.48	N
NO_T08_air_20080821_03.JPG	1335 m	8/21/08	67.81	-162.48	N
NO_T08_air_20080821_04.JPG	1335 m	8/21/08	67.81	-162.48	N
NO_T08_air_20080821_05.JPG	1335 m	8/21/08	67.81	-162.48	N
NO_T08_air_20080821_06.JPG	1336 m	8/21/08	67.81	-162.47	N
NO_T08_air_20080821_07.JPG	1336 m	8/21/08	67.81	-162.47	N
NO_T08_air_20080821_08.JPG	1337 m	8/21/08	67.81	-162.47	N
NO_T08_air_20080821_09.JPG	1337 m	8/21/08	67.81	-162.47	N
NO_T08_air_20080821_10.JPG	1338 m	8/21/08	67.82	-162.46	N
NO_T08_air_20080821_11.JPG	1338 m	8/21/08	67.82	-162.46	N
NO_T08_air_20080821_12.JPG	1339 m	8/21/08	67.82	-162.46	N
NO_T08_air_20080821_13.JPG	1339 m	8/21/08	67.82	-162.46	N
NO_T08_air_20080821_14.JPG	1340 m	8/21/08	67.82	-162.45	N
NO_T08_air_20080821_15.JPG	1340 m	8/21/08	67.82	-162.45	N
NO_T08_air_20080821_16.JPG	1340 m	8/21/08	67.82	-162.45	N

Table A-27: Balser and George image metadata part 12

Image name	Altitude	Year	Center latitude	Center longitude	Processed?
NO_T08_air_20080821_18.JPG	1337 m	8/21/08	67.82	-162.45	N
NO_T08_air_20080821_19.JPG	1335 m	8/21/08	67.82	-162.44	N
NO_T08_air_20080821_20.JPG	1333 m	8/21/08	67.82	-162.44	N
NO_T08_air_20080821_21.JPG	1331 m	8/21/08	67.82	-162.44	N
NO_T09_air_20080821_01.JPG	1769 m	8/21/08	67.71	-162.10	N
NO_T09_air_20080821_02.JPG	1768 m	8/21/08	67.71	-162.10	N
NO_T09_air_20080821_03.JPG	1766 m	8/21/08	67.71	-162.11	N
NO_T09_air_20080821_04.JPG	1764 m	8/21/08	67.71	-162.11	N
NO_T09_air_20080821_05.JPG	1760 m	8/21/08	67.72	-162.11	N
NO_T09_air_20080821_06.JPG	1755 m	8/21/08	67.72	-162.11	N
NO_T09_air_20080821_07.JPG	1751 m	8/21/08	67.72	-162.12	N
NO_T09_air_20080821_08.JPG	1748 m	8/21/08	67.72	-162.12	N
NO_T09_air_20080821_09.JPG	1745 m	8/21/08	67.72	-162.12	N
NO_T09_air_20080821_10.JPG	1743 m	8/21/08	67.72	-162.12	N
NO_T09_air_20080821_11.JPG	1741 m	8/21/08	67.72	-162.13	N
NO_T09_air_20080821_12.JPG	1738 m	8/21/08	67.72	-162.13	N
NO_T09_air_20080821_13.JPG	1734 m	8/21/08	67.72	-162.13	N
NO_T10_air_20080821_01.JPG	1244 m	8/21/08	67.90	-162.51	N
NO_T10_air_20080821_02.JPG	1243 m	8/21/08	67.90	-162.51	N
NO_T10_air_20080821_03.JPG	1241 m	8/21/08	67.90	-162.51	N
NO_T10_air_20080821_04.JPG	1240 m	8/21/08	67.90	-162.51	N
NO_T10_air_20080821_05.JPG	1239 m	8/21/08	67.90	-162.50	N
NO_T10_air_20080821_06.JPG	1238 m	8/21/08	67.90	-162.50	N
NO_T10_air_20080821_07.JPG	1237 m	8/21/08	67.90	-162.50	N
NO_T10_air_20080821_08.JPG	1235 m	8/21/08	67.91	-162.50	N
NO_T12_air_20080821_01.JPG	1327 m	8/21/08	67.92	-161.99	N
NO_T12_air_20080821_02.JPG	1326 m	8/21/08	67.92	-161.99	N
NO_T12_air_20080821_03.JPG	1325 m	8/21/08	67.92	-161.99	N
NO_T12_air_20080821_04.JPG	1324 m	8/21/08	67.92	-161.99	N
NO_T12_air_20080821_05.JPG	1322 m	8/21/08	67.92	-161.99	N
NO_T12_air_20080821_06.JPG	1322 m	8/21/08	67.92	-161.99	N
NO_T12_air_20080821_07.JPG	1322 m	8/21/08	67.92	-162.00	N
NO_T12_air_20080821_08.JPG	1323 m	8/21/08	67.92	-162.00	N
NO_T12_air_20080821_09.JPG	1322 m	8/21/08	67.92	-162.00	N
NO_T12_air_20080821_10.JPG	1322 m	8/21/08	67.92	-162.00	N
NO_T12_air_20080821_11.JPG	1322 m	8/21/08	67.93	-162.00	N
NO_T12_air_20080821_12.JPG	1322 m	8/21/08	67.93	-162.00	N
NO_T12_air_20080821_13.JPG	1321 m	8/21/08	67.93	-162.00	N
NO_T13_air_20080821_01.JPG	1287 m	8/21/08	67.95	-162.51	N

Table A-28: Balser and George image metadata part 13

Image name	Altitude	Year	Center latitude	Center longitude	Processed?
NO_T13_air_20080821_02.JPG	1291 m	8/21/08	67.95	-162.50	N
NO_T13_air_20080821_03.JPG	1295 m	8/21/08	67.95	-162.50	N
NO_T13_air_20080821_04.JPG	1298 m	8/21/08	67.95	-162.50	N
NO_T13_air_20080821_05.JPG	1301 m	8/21/08	67.95	-162.50	N
NO_T13_air_20080821_06.JPG	1304 m	8/21/08	67.96	-162.50	N
NO_T13_air_20080821_07.JPG	1307 m	8/21/08	67.96	-162.49	N
NO_T13_air_20080821_08.JPG	1309 m	8/21/08	67.96	-162.49	N
NO_T13_air_20080821_09.JPG	1309 m	8/21/08	67.96	-162.49	N
NO_T13_air_20080821_10.JPG	1310 m	8/21/08	67.96	-162.49	N
NO_T13_air_20080821_11.JPG	1310 m	8/21/08	67.96	-162.49	N
NO_T13_air_20080821_12.JPG	1310 m	8/21/08	67.96	-162.49	N
NO_T15_air_20080821_01.JPG	1317 m	8/21/08	67.96	-162.32	N
NO_T15_air_20080821_02.JPG	1316 m	8/21/08	67.96	-162.32	N
NO_T15_air_20080821_03.JPG	1314 m	8/21/08	67.96	-162.32	N
NO_T15_air_20080821_04.JPG	1314 m	8/21/08	67.96	-162.31	N
NO_T15_air_20080821_05.JPG	1315 m	8/21/08	67.96	-162.31	N
NO_T15_air_20080821_06.JPG	1316 m	8/21/08	67.96	-162.31	N
NO_T15_air_20080821_07.JPG	1317 m	8/21/08	67.96	-162.31	N
NO_T15_air_20080821_08.JPG	1318 m	8/21/08	67.96	-162.30	N
NO_T15_air_20080821_09.JPG	1319 m	8/21/08	67.96	-162.30	N
NO_T15_air_20080821_10.JPG	1319 m	8/21/08	67.96	-162.30	N
NO_T15_air_20080821_11.JPG	1319 m	8/21/08	67.96	-162.30	N
NO_T18_air_20080821_01.JPG	1670 m	8/21/08	68.11	-162.54	N
NO_T18_air_20080821_02.JPG	1671 m	8/21/08	68.11	-162.55	N
NO_T18_air_20080821_03.JPG	1672 m	8/21/08	68.11	-162.55	N
NO_T18_air_20080821_04.JPG	1673 m	8/21/08	68.11	-162.55	N
NO_T18_air_20080821_05.JPG	1675 m	8/21/08	68.11	-162.56	N
NO_T18_air_20080821_06.JPG	1677 m	8/21/08	68.11	-162.56	N
NO_T18_air_20080821_07.JPG	1678 m	8/21/08	68.11	-162.56	N
NO_T18_air_20080821_08.JPG	1679 m	8/21/08	68.11	-162.56	N
NO_T18_air_20080821_09.JPG	1679 m	8/21/08	68.11	-162.57	N
NO_T18_air_20080821_10.JPG	1678 m	8/21/08	68.11	-162.57	N
NO_T18_air_20080821_11.JPG	1678 m	8/21/08	68.11	-162.57	N
NO_T18_air_20080821_12.JPG	1677 m	8/21/08	68.11	-162.57	N
NO_T18_air_20080821_13.JPG	1677 m	8/21/08	68.11	-162.58	N
NO_T18_air_20080821_14.JPG	1676 m	8/21/08	68.11	-162.58	N
NO_T18_air_20080821_15.JPG	1674 m	8/21/08	68.11	-162.58	N
NO_T18_air_20080821_16.JPG	1674 m	8/21/08	68.11	-162.59	N

Table A-29: Balser and George image metadata part 14

Image name	Altitude	Year	Center latitude	Center longitude	Processed?
NO_T20_air_20080821_02.JPG	1934 m	8/22/08	68.26	-161.84	N
NO_T20_air_20080821_03.JPG	1937 m	8/22/08	68.26	-161.84	N
NO_T20_air_20080821_04.JPG	1940 m	8/22/08	68.26	-161.84	N
NO_T20_air_20080821_05.JPG	1943 m	8/22/08	68.26	-161.84	N
NO_T20_air_20080821_06.JPG	1947 m	8/22/08	68.26	-161.84	N
NO_T20_air_20080821_07.JPG	1947 m	8/22/08	68.26	-161.84	N
NO_T20_air_20080821_08.JPG	1949 m	8/22/08	68.27	-161.84	N
NO_T20_air_20080821_09.JPG	1953 m	8/22/08	68.27	-161.84	N
NO_T20_air_20080821_10.JPG	1957 m	8/22/08	68.27	-161.84	N
NO_T20_air_20080821_11.JPG	1961 m	8/22/08	68.27	-161.84	N
NO_T20_air_20080821_12.JPG	1964 m	8/22/08	68.27	-161.84	N
NO_T21_air_20080821_01.JPG	1962 m	8/22/08	68.32	-161.63	N
NO_T21_air_20080821_02.JPG	1962 m	8/22/08	68.32	-161.63	N
NO_T21_air_20080821_03.JPG	1963 m	8/22/08	68.32	-161.63	N
NO_T21_air_20080821_04.JPG	1965 m	8/22/08	68.32	-161.63	N
NO_T21_air_20080821_05.JPG	1965 m	8/22/08	68.32	-161.62	N
NO_T21_air_20080821_06.JPG	1964 m	8/22/08	68.32	-161.62	N
NO_T21_air_20080821_07.JPG	1962 m	8/22/08	68.32	-161.62	N
NO_T21_air_20080821_08.JPG	1961 m	8/22/08	68.32	-161.62	N
NO_T21_air_20080821_09.JPG	1960 m	8/22/08	68.32	-161.61	N
NO_T21_air_20080821_10.JPG	1959 m	8/22/08	68.32	-161.61	N
NO_T23_air_20080821_01.JPG	1710 m	8/22/08	68.14	-161.39	N
NO_T23_air_20080821_02.JPG	1708 m	8/22/08	68.14	-161.40	N
NO_T23_air_20080821_03.JPG	1707 m	8/22/08	68.14	-161.40	N
NO_T23_air_20080821_04.JPG	1706 m	8/22/08	68.14	-161.40	N
NO_T23_air_20080821_05.JPG	1703 m	8/22/08	68.14	-161.40	N
NO_T23_air_20080821_06.JPG	1699 m	8/22/08	68.14	-161.41	N
NO_T23_air_20080821_07.JPG	1695 m	8/22/08	68.14	-161.41	N
NO_T23_air_20080821_08.JPG	1691 m	8/22/08	68.14	-161.41	N
NO_T23_air_20080821_09.JPG	1686 m	8/22/08	68.14	-161.41	N
NO_T23_air_20080821_10.JPG	1682 m	8/22/08	68.14	-161.42	N
NO_T23_air_20080821_11.JPG	1679 m	8/22/08	68.14	-161.42	N
NO_T25_air_20080821_01.JPG	1930 m	8/22/08	68.11	-161.08	N
NO_T25_air_20080821_02.JPG	1931 m	8/22/08	68.11	-161.09	N
NO_T25_air_20080821_03.JPG	1933 m	8/22/08	68.11	-161.09	N
NO_T25_air_20080821_04.JPG	1933 m	8/22/08	68.11	-161.09	N
NO_T25_air_20080821_05.JPG	1934 m	8/22/08	68.11	-161.09	N
NO_T25_air_20080821_06.JPG	1935 m	8/22/08	68.11	-161.09	N

Table A-30: Balser and George image metadata part 15

Image name	Altitude	Year	Center latitude	Center longitude	Processed?
NO_T25_air_20080821_08.JPG	1937 m	8/22/08	68.11	-161.10	N
NO_T25_air_20080821_09.JPG	1939 m	8/22/08	68.11	-161.10	N
NO_T25_air_20080821_10.JPG	1942 m	8/22/08	68.11	-161.10	N
NO_T25_air_20080821_11.JPG	1943 m	8/22/08	68.11	-161.10	N
NO_T25_air_20080821_12.JPG	1944 m	8/22/08	68.11	-161.10	N
NO_T25_air_20080821_13.JPG	1945 m	8/22/08	68.12	-161.11	N
NO_T25_air_20080821_14.JPG	1946 m	8/22/08	68.12	-161.11	N
NO_T43_air_20080822_01.JPG	1829 m	8/22/08	68.39	-158.53	N
NO_T43_air_20080822_02.JPG	1825 m	8/22/08	68.39	-158.53	N
NO_T43_air_20080822_03.JPG	1820 m	8/22/08	68.39	-158.53	N
NO_T43_air_20080822_04.JPG	1814 m	8/22/08	68.38	-158.53	N
NO_T43_air_20080822_05.JPG	1809 m	8/22/08	68.38	-158.53	N
NO_T43_air_20080822_06.JPG	1805 m	8/22/08	68.38	-158.53	N
NO_T43_air_20080822_07.JPG	1800 m	8/22/08	68.38	-158.53	N
NO_T43_air_20080822_08.JPG	1794 m	8/22/08	68.38	-158.53	N
NO_T43_air_20080822_09.JPG	1788 m	8/22/08	68.38	-158.53	N
NO_T43_air_20080822_10.JPG	1782 m	8/22/08	68.38	-158.53	N
NO_T43_air_20080822_11.JPG	1775 m	8/22/08	68.38	-158.53	N
NO_T43_air_20080822_12.JPG	1768 m	8/22/08	68.38	-158.53	N
NO_T47_air_20080822_01.JPG	1522 m	8/22/08	68.06	-158.80	N
NO_T47_air_20080822_02.JPG	1516 m	8/22/08	68.06	-158.80	N
NO_T47_air_20080822_03.JPG	1511 m	8/22/08	68.06	-158.80	N
NO_T47_air_20080822_04.JPG	1507 m	8/22/08	68.06	-158.80	N
NO_T47_air_20080822_05.JPG	1502 m	8/22/08	68.06	-158.79	N
NO_T47_air_20080822_06.JPG	1496 m	8/22/08	68.06	-158.79	N
NO_T47_air_20080822_07.JPG	1491 m	8/22/08	68.06	-158.79	N
NO_T47_air_20080822_08.JPG	1486 m	8/22/08	68.06	-158.79	N
NO_T47_air_20080822_09.JPG	1483 m	8/22/08	68.06	-158.79	N
NO_T47_air_20080822_10.JPG	1483 m	8/22/08	68.06	-158.78	N
NO_T47_air_20080822_11.JPG	1484 m	8/22/08	68.06	-158.78	N
NO_T47_air_20080822_12.JPG	1485 m	8/22/08	68.06	-158.78	N
NO_T47_air_20080822_13.JPG	1485 m	8/22/08	68.06	-158.78	N
NO_T47_air_20080822_14.JPG	1485 m	8/22/08	68.06	-158.77	N
NO_T47_air_20080822_15.JPG	1485 m	8/22/08	68.06	-158.77	N
NO_T47_air_20080822_16.JPG	1484 m	8/22/08	68.06	-158.77	N
NO_T47_air_20080822_17.JPG	1482 m	8/22/08	68.06	-158.77	N
NO_T47_air_20080822_18.JPG	1482 m	8/22/08	68.06	-158.77	N
NO_T47_air_20080822_19.JPG	1481 m	8/22/08	68.06	-158.76	N

Table A-31: Balser and George image metadata part 16

Image name	Altitude	Year	Center latitude	Center longitude	Processed?
NO_T47_air_20080822_21.jpg	1481 m	8/22/08	68.06	-158.76	N
NO_T47_air_20080822_22.JPG	1481 m	8/22/08	68.06	-158.76	N
NO_T47_air_20080822_23.JPG	1481 m	8/22/08	68.06	-158.76	N
NO_T47_air_20080822_24.JPG	1481 m	8/22/08	68.06	-158.75	N
NO_T47_air_20080822_25.JPG	1481 m	8/22/08	68.06	-158.75	N
NO_T47_air_20080822_26.JPG	1482 m	8/22/08	68.06	-158.75	N
NO_T48_air_20080822_01.JPG	1513 m	8/22/08	68.04	-158.72	N
NO_T48_air_20080822_02.JPG	1514 m	8/22/08	68.04	-158.72	N
NO_T48_air_20080822_03.JPG	1515 m	8/22/08	68.04	-158.72	N
NO_T48_air_20080822_04.JPG	1516 m	8/22/08	68.04	-158.72	N
NO_T48_air_20080822_05.jpg	1518 m	8/22/08	68.03	-158.72	N
NO_T48_air_20080822_06.JPG	1518 m	8/22/08	68.03	-158.72	N
NO_T48_air_20080822_07.JPG	1519 m	8/22/08	68.03	-158.72	N
NO_T48_air_20080822_08.JPG	1520 m	8/22/08	68.03	-158.72	N
NO_T48_air_20080822_09.JPG	1522 m	8/22/08	68.03	-158.72	N
NO_T48_air_20080822_10.JPG	1524 m	8/22/08	68.03	-158.72	N
NO_T48_air_20080822_11.JPG	1527 m	8/22/08	68.03	-158.72	N
NO_T48_air_20080822_12.JPG	1530 m	8/22/08	68.03	-158.72	N
NO_T48_air_20080822_13.JPG	1533 m	8/22/08	68.03	-158.72	N
NO_T48_air_20080822_14.JPG	1537 m	8/22/08	68.03	-158.72	N
NO_T48_air_20080822_15.JPG	1540 m	8/22/08	68.02	-158.72	N
NO_T48_air_20080822_16.JPG	1542 m	8/22/08	68.02	-158.72	N
NO_T48_air_20080822_17.JPG	1544 m	8/22/08	68.02	-158.71	N
NO_T48_air_20080822_18.JPG	1546 m	8/22/08	68.02	-158.71	N
NO_T49_air_20080822_01.jpg	1652 m	8/22/08	68.05	-158.23	N
NO_T49_air_20080822_02.JPG	1653 m	8/22/08	68.05	-158.22	N
NO_T49_air_20080822_03.jpg	1654 m	8/22/08	68.05	-158.22	N
NO_T49_air_20080822_04.jpg	1656 m	8/22/08	68.05	-158.22	N
NO_T49_air_20080822_05.jpg	1658 m	8/22/08	68.05	-158.22	N
NO_T49_air_20080822_06.jpg	1661 m	8/22/08	68.05	-158.21	N
NO_T49_air_20080822_07.jpg	1664 m	8/22/08	68.05	-158.21	N
NO_T49_air_20080822_08.JPG	1666 m	8/22/08	68.05	-158.21	N
NO_T49_air_20080822_09.jpg	1666 m	8/22/08	68.05	-158.21	N
NO_T49_air_20080822_10.JPG	1668 m	8/22/08	68.05	-158.21	N
NO_T49_air_20080822_11.JPG	1670 m	8/22/08	68.05	-158.20	N
NO_T49_air_20080822_12.JPG	1671 m	8/22/08	68.05	-158.20	N
NO_T49_air_20080822_13.JPG	1673 m	8/22/08	68.05	-158.20	N
NO_T49_air_20080822_14.JPG	1675 m	8/22/08	68.05	-158.20	N

Table A-32: Balser and George image metadata part 17

Image name	Altitude	Year	Center latitude	Center longitude	Processed?
NO_T50_air_20080822_01.JPG	1601 m	8/23/08	68.05	-157.82	N
NO_T50_air_20080822_02.JPG	1601 m	8/23/08	68.05	-157.82	N
NO_T50_air_20080822_03.JPG	1600 m	8/23/08	68.05	-157.82	N
NO_T50_air_20080822_04.JPG	1598 m	8/23/08	68.06	-157.83	N
NO_T50_air_20080822_05.jpg	1596 m	8/23/08	68.06	-157.83	N
NO_T50_air_20080822_06.JPG	1594 m	8/23/08	68.06	-157.83	N
NO_T50_air_20080822_07.JPG	1592 m	8/23/08	68.06	-157.83	N
NO_T50_air_20080822_08.JPG	1590 m	8/23/08	68.06	-157.83	N
NO_T50_air_20080822_09.JPG	1588 m	8/23/08	68.06	-157.83	N
NO_T50_air_20080822_10.JPG	1586 m	8/23/08	68.06	-157.84	N
NO_T50_air_20080822_11.JPG	1585 m	8/23/08	68.06	-157.84	N
NO_T52_air_20080822_01.JPG	1879 m	8/23/08	68.14	-156.33	N
NO_T52_air_20080822_02.JPG	1879 m	8/23/08	68.14	-156.33	N
NO_T52_air_20080822_03.JPG	1879 m	8/23/08	68.14	-156.33	N
NO_T52_air_20080822_04.JPG	1879 m	8/23/08	68.14	-156.32	N
NO_T52_air_20080822_05.JPG	1878 m	8/23/08	68.14	-156.32	N
NO_T52_air_20080822_06.JPG	1878 m	8/23/08	68.14	-156.32	N
NO_T52_air_20080822_07.jpg	1878 m	8/23/08	68.14	-156.32	N
NO_T52_air_20080822_08.JPG	1877 m	8/23/08	68.14	-156.32	N
NO_T52_air_20080822_09.JPG	1875 m	8/23/08	68.14	-156.31	N
NO_T52_air_20080822_10.JPG	1874 m	8/23/08	68.14	-156.31	N
NO_T52_air_20080822_11.JPG	1874 m	8/23/08	68.14	-156.31	N
NO_T52_air_20080822_12.JPG	1873 m	8/23/08	68.14	-156.31	N
NO_T52_air_20080822_13.JPG	1873 m	8/23/08	68.14	-156.31	N
NO_T52_air_20080822_14.JPG	1873 m	8/23/08	68.14	-156.30	N
NO_T52_air_20080822_15.JPG	1875 m	8/23/08	68.14	-156.30	N
NO_T52_air_20080822_16.JPG	1878 m	8/23/08	68.14	-156.30	N
NO_T53_air_20080822_01.JPG	1936 m	8/23/08	67.75	-157.15	N
NO_T53_air_20080822_02.JPG	1936 m	8/23/08	67.75	-157.15	N
NO_T53_air_20080822_03.JPG	1936 m	8/23/08	67.75	-157.15	N
NO_T53_air_20080822_04.JPG	1937 m	8/23/08	67.75	-157.15	N
NO_T53_air_20080822_05.JPG	1939 m	8/23/08	67.75	-157.15	N
NO_T53_air_20080822_06.JPG	1940 m	8/23/08	67.75	-157.15	N
NO_T53_air_20080822_07.JPG	1941 m	8/23/08	67.74	-157.15	N
NO_T53_air_20080822_08.JPG	1941 m	8/23/08	67.74	-157.15	N
NO_T53_air_20080822_09.JPG	1941 m	8/23/08	67.74	-157.15	N
NO_T53_air_20080822_10.JPG	1941 m	8/23/08	67.74	-157.15	N
NO_T53_air_20080822_11.JPG	1941 m	8/23/08	67.74	-157.15	N

Table A-33: Balser and George image metadata part 18

Image name	Altitude	Year	Center latitude	Center longitude	Processed?
NO_T53_air_20080822_13.JPG	1945 m	8/23/08	67.74	-157.15	N
NO_T53_air_20080822_14.JPG	1947 m	8/23/08	67.74	-157.15	N
NO_T53_air_20080822_15.JPG	1949 m	8/23/08	67.74	-157.16	N
NO_T53_air_20080822_16.JPG	1952 m	8/23/08	67.74	-157.16	N
NO_T53_air_20080822_17.JPG	1954 m	8/23/08	67.73	-157.16	N
NO_T53_air_20080822_18.JPG	1956 m	8/23/08	67.73	-157.16	N
NO_T53_air_20080822_19.JPG	1959 m	8/23/08	67.73	-157.16	N
NO_T53_air_20080822_20.JPG	1960 m	8/23/08	67.73	-157.16	N
NO_T53_air_20080822_21.jpg	1961 m	8/23/08	67.73	-157.16	N
NO_T53_air_20080822_22.JPG	1962 m	8/23/08	67.73	-157.16	N
NOAT_GP01-1_20080821.JPG	1228 m	8/21/08	67.19	-162.15	N
NOAT_GP01-2_20080821.JPG	1225 m	8/21/08	67.18	-162.15	N
NOAT_GP02-1_20080821.JPG	1327 m	8/21/08	67.34	-162.67	N
NOAT_GP02-2_20080821.JPG	1327 m	8/21/08	67.34	-162.67	N
NOAT_GP03-1_20080821.JPG	1507 m	8/21/08	67.52	-162.73	N
NOAT_GP03-2_20080821.JPG	1504 m	8/21/08	67.52	-162.73	N
NOAT_GP04-1_20080821.JPG	1366 m	8/21/08	67.36	-162.21	N
NOAT_GP04-2_20080821.JPG	1365 m	8/21/08	67.36	-162.21	N
NOAT_GP05-1_20080821.JPG	1540 m	8/21/08	67.54	-162.27	N
NOAT_GP05-2_20080821.JPG	1543 m	8/21/08	67.54	-162.27	N
NOAT_GP06-1_20080821.JPG	1276 m	8/21/08	67.72	-162.33	N
NOAT_GP06-2_20080821.JPG	1277 m	8/21/08	67.72	-162.33	N
NOAT_GP07-1_20080821.JPG	1347 m	8/21/08	67.90	-162.39	N
NOAT_GP07-2_20080821.JPG	1346 m	8/21/08	67.90	-162.39	N
NOAT_GP08-1_20080821.JPG	1646 m	8/21/08	68.08	-162.45	N
NOAT_GP08-2_20080821.JPG	1647 m	8/21/08	68.08	-162.45	N
NOAT_GP09-1_20080821.JPG	2083 m	8/22/08	68.26	-162.51	N
NOAT_GP09-2_20080821.JPG	2083 m	8/22/08	68.26	-162.51	N
NOAT_GP10-1_20080821.JPG	1557 m	8/21/08	67.57	-161.81	N
NOAT_GP10-2_20080821.JPG	1556 m	8/21/08	67.57	-161.81	N
NOAT_GP11-1_20080821.JPG	1804 m	8/21/08	67.74	-161.86	N
NOAT_GP11-2_20080821.JPG	1805 m	8/21/08	67.74	-161.86	N
NOAT_GP12-1_20080821.JPG	1376 m	8/21/08	67.92	-161.92	N
NOAT_GP12-2_20080821.JPG	1376 m	8/21/08	67.92	-161.92	N
NOAT_GP13-1_20080821.JPG	1597 m	8/22/08	68.10	-161.97	N
NOAT_GP13-2_20080821.JPG	1600 m	8/22/08	68.10	-161.97	N
NOAT_GP14-1_20080821.JPG	1770 m	8/22/08	68.28	-162.03	N
NOAT_GP14-2_20080821.JPG	1770 m	8/22/08	68.28	-162.03	N

Table A-34: Balser and George image metadata part 19

Image name	Altitude	Year	Center latitude	Center longitude	Processed?
NOAT_GP15-2_20080821.JPG	1879 m	8/22/08	68.46	-162.09	N
NOAT_GP16-1_20080821.JPG	2094 m	8/21/08	67.59	-161.34	N
NOAT_GP16-2_20080821.JPG	2092 m	8/21/08	67.59	-161.34	N
NOAT_GP17-1_20080821.JPG	1974 m	8/21/08	67.77	-161.39	N
NOAT_GP17-2_20080821.JPG	1972 m	8/21/08	67.77	-161.40	N
NOAT_GP18-1_20080821.JPG	1578 m	8/21/08	67.94	-161.45	N
NOAT_GP18-2_20080821.JPG	1577 m	8/21/08	67.94	-161.45	N
NOAT_GP19-1_20080821.JPG	1622 m	8/22/08	68.12	-161.50	N
NOAT_GP19-2_20080821.JPG	1617 m	8/22/08	68.12	-161.50	N
NOAT_GP20-1_20080821.JPG	1929 m	8/22/08	68.30	-161.56	N
NOAT_GP20-2_20080821.JPG	1926 m	8/22/08	68.30	-161.55	N
NOAT_GP21-1_20080821.JPG	2072 m	8/22/08	68.48	-161.61	N
NOAT_GP21-2_20080821.JPG	2066 m	8/22/08	68.48	-161.61	N
NOAT_GP22-1_20080821.JPG	1889 m	8/21/08	67.61	-160.88	N
NOAT_GP22-2_20080821.JPG	1889 m	8/21/08	67.61	-160.88	N
NOAT_GP23-1_20080821.JPG	1680 m	8/21/08	67.78	-160.92	N
NOAT_GP23-2_20080821.JPG	1677 m	8/21/08	67.78	-160.93	N
NOAT_GP24-1_20080821.JPG	1629 m	8/22/08	67.96	-160.98	N
NOAT_GP24-2_20080821.JPG	1631 m	8/22/08	67.96	-160.97	N
NOAT_GP25-1_20080821.JPG	1973 m	8/22/08	68.14	-161.03	N
NOAT_GP25-2_20080821.JPG	1973 m	8/22/08	68.14	-161.03	N
NOAT_GP26-1_20080821.JPG	1750 m	8/22/08	68.32	-161.08	N
NOAT_GP26-2_20080821.JPG	1748 m	8/22/08	68.32	-161.08	N
NOAT_GP27-1_20080821.JPG	2175 m	8/22/08	68.50	-161.13	N
NOAT_GP27-2_20080821.JPG	2174 m	8/22/08	68.50	-161.13	N
NOAT_GP28-1_20080821.JPG	1880 m	8/21/08	67.62	-160.42	N
NOAT_GP28-2_20080821.JPG	1881 m	8/21/08	67.62	-160.41	N
NOAT_GP29-1_20080821.JPG	1673 m	8/21/08	67.80	-160.46	N
NOAT_GP29-2_20080821.JPG	1670 m	8/21/08	67.80	-160.46	N
NOAT_GP30-1_20080821.JPG	1784 m	8/22/08	67.98	-160.51	N
NOAT_GP30-2_20080821.JPG	1784 m	8/22/08	67.98	-160.51	N
NOAT_GP31-1_20080821.JPG	1961 m	8/22/08	68.16	-160.55	N
NOAT_GP31-2_20080821.JPG	1965 m	8/22/08	68.16	-160.55	N
NOAT_GP32-1_20080821.JPG	2132 m	8/22/08	68.34	-160.60	N
NOAT_GP32-2_20080821.JPG	2133 m	8/22/08	68.34	-160.60	N
NOAT_GP33-1_20080821.JPG	2188 m	8/22/08	68.52	-160.65	N
NOAT_GP33-2_20080821.JPG	2186 m	8/22/08	68.52	-160.65	N
NOAT_GP34-1_20080822.JPG	1830 m	8/22/08	67.82	-159.99	N

Table A-35: Balser and George image metadata part 20

Image name	Altitude	Year	Center latitude	Center longitude	Processed?
NOAT_GP35-1_20080821.JPG	1859 m	8/22/08	68.00	-160.03	N
NOAT_GP35-2_20080821.JPG	1861 m	8/22/08	68.00	-160.03	N
NOAT_GP36-1_20080821.JPG	1983 m	8/22/08	68.18	-160.08	N
NOAT_GP36-2_20080821.JPG	1982 m	8/22/08	68.18	-160.08	N
NOAT_GP37-1_20080821.JPG	2026 m	8/22/08	68.36	-160.12	N
NOAT_GP37-2_20080821.JPG	2024 m	8/22/08	68.36	-160.12	N
NOAT_GP38-1_20080821.JPG	2006 m	8/22/08	68.54	-160.16	N
NOAT_GP38-2_20080821.JPG	2008 m	8/22/08	68.54	-160.16	N
NOAT_GP39-1_20080822.JPG	1777 m	8/22/08	67.84	-159.52	N
NOAT_GP39-2_20080822.JPG	1776 m	8/22/08	67.84	-159.52	N
NOAT_GP40-1_20080822.JPG	1827 m	8/22/08	68.01	-159.56	N
NOAT_GP40-2_20080822.JPG	1827 m	8/22/08	68.02	-159.56	N
NOAT_GP41-1_20080822.JPG	1810 m	8/22/08	68.19	-159.60	N
NOAT_GP41-2_20080822.JPG	1811 m	8/22/08	68.20	-159.60	N
NOAT_GP42-1_20080822.JPG	1764 m	8/22/08	68.38	-159.64	N
NOAT_GP42-2_20080822.JPG	1765 m	8/22/08	68.38	-159.64	N
NOAT_GP43-1_20080822.JPG	1969 m	8/22/08	68.56	-159.69	N
NOAT_GP43-2_20080822.JPG	1971 m	8/22/08	68.56	-159.68	N
NOAT_GP44-1_20080822.JPG	1975 m	8/22/08	67.67	-159.02	N
NOAT_GP44-2_20080822.JPG	1975 m	8/22/08	67.67	-159.02	N
NOAT_GP45-1_20080822.JPG	1923 m	8/22/08	67.85	-159.05	N
NOAT_GP45-2_20080822.JPG	1925 m	8/22/08	67.85	-159.05	N
NOAT_GP46-1_20080822.JPG	1783 m	8/22/08	68.03	-159.09	N
NOAT_GP46-2_20080822.JPG	1782 m	8/22/08	68.03	-159.09	N
NOAT_GP47-1_20080822.JPG	1835 m	8/22/08	68.21	-159.12	N
NOAT_GP47-2_20080822.JPG	1833 m	8/22/08	68.21	-159.12	N
NOAT_GP48-1_20080822.JPG	1865 m	8/22/08	68.39	-159.16	N
NOAT_GP48-2_20080822.JPG	1859 m	8/22/08	68.39	-159.16	N
NOAT_GP49-1_20080822.JPG	2224 m	8/22/08	68.57	-159.20	N
NOAT_GP49-2_20080822.JPG	2222 m	8/22/08	68.57	-159.20	N
NOAT_GP50-1_20080822.JPG	1962 m	8/22/08	67.68	-158.55	N
NOAT_GP50-2_20080822.JPG	1964 m	8/22/08	67.68	-158.55	N
NOAT_GP51-1_20080822.JPG	1718 m	8/22/08	67.86	-158.58	N
NOAT_GP51-2_20080822.JPG	1716 m	8/22/08	67.86	-158.58	N
NOAT_GP52-1_20080822.JPG	1695 m	8/22/08	68.04	-158.61	N
NOAT_GP52-2_20080822.JPG	1695 m	8/22/08	68.04	-158.61	N
NOAT_GP53-1_20080822.JPG	2105 m	8/22/08	68.22	-158.65	N
NOAT_GP53-2_20080822.JPG	2103 m	8/22/08	68.22	-158.65	N

Table A-36: Balser and George image metadata part 21

Image name	Altitude	Year	Center latitude	Center longitude	Processed?
NOAT_GP54-2_20080822.JPG	1835 m	8/22/08	68.40	-158.68	N
NOAT_GP55-1_20080822.JPG	1653 m	8/22/08	67.69	-158.08	N
NOAT_GP55-2_20080822.JPG	1654 m	8/22/08	67.69	-158.08	N
NOAT_GP56-1_20080822.JPG	1679 m	8/22/08	67.88	-158.11	N
NOAT_GP56-2_20080822.JPG	1678 m	8/22/08	67.87	-158.11	N
NOAT_GP57-1_20080822.JPG	1707 m	8/22/08	68.05	-158.14	N
NOAT_GP57-2_20080822.JPG	1706 m	8/22/08	68.05	-158.14	N
NOAT_GP58-1_20080822.JPG	1953 m	8/22/08	68.24	-158.17	N
NOAT_GP58-2_20080822.JPG	1953 m	8/22/08	68.24	-158.17	N
NOAT_GP59-1_20080822.JPG	1729 m	8/22/08	67.52	-157.59	N
NOAT_GP59-2_20080822.JPG	1728 m	8/22/08	67.52	-157.59	N
NOAT_GP60-1_20080822.JPG	1639 m	8/22/08	67.70	-157.61	N
NOAT_GP60-2_20080822.JPG	1637 m	8/22/08	67.70	-157.61	N
NOAT_GP61-1_20080822.JPG	1681 m	8/23/08	67.88	-157.64	N
NOAT_GP61-2_20080822.JPG	1677 m	8/23/08	67.89	-157.64	N
NOAT_GP62-1_20080822.JPG	1724 m	8/23/08	68.07	-157.67	N
NOAT_GP62-2_20080822.JPG	1716 m	8/23/08	68.07	-157.66	N
NOAT_GP63-1_20080822.JPG	2003 m	8/22/08	68.25	-157.69	N
NOAT_GP63-2_20080822.JPG	2002 m	8/22/08	68.25	-157.69	N
NOAT_GP64-1_20080822.JPG	2150 m	8/23/08	67.71	-157.14	N
NOAT_GP64-2_20080822.JPG	2146 m	8/23/08	67.71	-157.14	N
NOAT_GP65-1_20080822.JPG	1623 m	8/23/08	67.89	-157.17	N
NOAT_GP65-2_20080822.JPG	1622 m	8/23/08	67.89	-157.17	N
NOAT_GP66-1_20080822.JPG	1767 m	8/23/08	68.08	-157.19	N
NOAT_GP66-2_20080822.JPG	1765 m	8/23/08	68.08	-157.19	N
NOAT_GP67-1_20080822.JPG	1958 m	8/23/08	68.25	-157.21	N
NOAT_GP67-2_20080822.JPG	1954 m	8/23/08	68.26	-157.21	N
NOAT_GP68-1_20080822.JPG	2397 m	8/23/08	67.72	-156.66	N
NOAT_GP68-2_20080822.JPG	2397 m	8/23/08	67.72	-156.65	N
NOAT_GP69-1_20080822.JPG	1863 m	8/23/08	67.90	-156.70	N
NOAT_GP69-2_20080822.JPG	1861 m	8/23/08	67.90	-156.70	N
NOAT_GP70-1_20080822.JPG	1837 m	8/23/08	68.08	-156.71	N
NOAT_GP70-2_20080822.JPG	1839 m	8/23/08	68.08	-156.71	N
NOAT_GP71-1_20080822.JPG	1959 m	8/23/08	68.09	-156.23	N
NOAT_GP71-2_20080822.JPG	1956 m	8/23/08	68.09	-156.23	N
TT0_0621.JPG	3597 m	9/1/06	68.05	-159.30	N
TT0_0622.JPG	3595 m	9/1/06	68.04	-159.28	N
TT0_0623.JPG	3595 m	9/1/06	68.03	-159.27	N

Table A-37: Balser and George image metadata part 22

Image name	Altitude	Year	Center latitude	Center longitude	Processed?
TT0_0625.JPG	3596 m	9/1/06	68.00	-159.23	N
TT0_0626.JPG	3599 m	9/1/06	67.99	-159.22	N
TT0_0627.JPG	3605 m	9/1/06	68.15	-158.58	N
TT0_0628.JPG	3599 m	9/1/06	68.17	-158.57	N
TT0_0629.JPG	3592 m	9/1/06	68.18	-158.56	N
TT0_0630.JPG	3598 m	9/1/06	68.19	-158.55	N
TT0_0631.JPG	3594 m	9/1/06	68.20	-158.54	N
TT0_0632.JPG	3589 m	9/1/06	68.21	-158.53	N
TT0_0633.JPG	3578 m	9/1/06	68.22	-158.52	N
TT0_0634.JPG	3576 m	9/1/06	68.24	-158.51	N
TT0_0635.JPG	3583 m	9/1/06	68.28	-158.23	N
TT0_0636.JPG	3577 m	9/1/06	68.28	-158.20	N
TT0_0637.JPG	3573 m	9/1/06	68.28	-158.17	Y
TT0_0638.JPG	3576 m	9/1/06	68.27	-158.15	N
TT0_0639.JPG	3584 m	9/1/06	68.27	-158.12	N
TT0_0640.JPG	3584 m	9/1/06	68.27	-158.09	Y
TT0_0641.JPG	3579 m	9/1/06	68.26	-158.06	Y
TT0_0642.JPG	3583 m	9/1/06	68.26	-158.03	N
TT0_0643.JPG	3582 m	9/1/06	68.26	-158.00	Y
TT0_0644.JPG	3595 m	9/1/06	68.26	-157.98	N
TT0_0645.JPG	3598 m	9/1/06	68.25	-157.95	N
TT0_0646.JPG	3590 m	9/1/06	68.25	-157.92	N
TT0_0647.JPG	3589 m	9/1/06	68.25	-157.89	N
TT0_0648.JPG	3601 m	9/1/06	68.24	-157.86	N
TT0_0649.JPG	3597 m	9/1/06	68.24	-157.83	N
TT0_0650.JPG	3594 m	9/1/06	68.24	-157.81	N
TT0_0651.JPG	3592 m	9/1/06	68.23	-157.78	N
TT0_0652.JPG	3588 m	9/1/06	68.23	-157.75	N
TT0_0653.JPG	3710 m	9/1/06	68.25	-157.77	N
TT0_0654.JPG	3708 m	9/1/06	68.26	-157.74	N
TT0_0655.JPG	3709 m	9/1/06	68.26	-157.71	N
TT0_0656.JPG	3720 m	9/1/06	68.27	-157.69	N
TT0_0657.JPG	3722 m	9/1/06	68.27	-157.66	N
TT0_0658.JPG	3730 m	9/1/06	68.27	-157.63	N
TT0_0659.JPG	3738 m	9/1/06	68.28	-157.61	N
TT0_0660.JPG	3745 m	9/1/06	68.28	-157.58	N
TT0_0661.JPG	3739 m	9/1/06	68.29	-157.55	N
TT0_0662.JPG	3735 m	9/1/06	68.29	-157.53	N

Table A-38: Balser and George image metadata part 23

Image name	Altitude	Year	Center latitude	Center longitude	Processed?
TT0_0664.JPG	3743 m	9/1/06	68.30	-157.47	N
TT0_0665.JPG	3563 m	9/1/06	68.09	-157.46	N
TT0_0666.JPG	3552 m	9/1/06	68.09	-157.49	N
TT0_0667.JPG	3567 m	9/1/06	68.09	-157.52	N
TT0_0668.JPG	3573 m	9/1/06	68.09	-157.54	N
TT0_0669.JPG	3585 m	9/1/06	68.08	-157.57	N
TT0_0670.JPG	3587 m	9/1/06	68.08	-157.60	N
TT0_0671.JPG	3599 m	9/1/06	68.08	-157.63	N
TT0_0672.JPG	3593 m	9/1/06	68.08	-157.65	N
TT0_0673.JPG	3599 m	9/1/06	68.07	-157.68	N
TT0_0674.JPG	3597 m	9/1/06	68.07	-157.71	N
TT0_0687.JPG	2077 m	9/1/06	67.87	-156.79	N
TT0_0688.JPG	2075 m	9/1/06	67.87	-156.77	N
TT0_0689.JPG	2084 m	9/1/06	67.87	-156.76	N
TT0_0690.JPG	2081 m	9/1/06	67.87	-156.74	N
TT0_0691.JPG	2086 m	9/1/06	67.86	-156.73	N
TT0_0692.JPG	2102 m	9/1/06	67.70	-156.02	N
TT0_0693.JPG	2099 m	9/1/06	67.70	-156.01	N
TT0_0694.JPG	2095 m	9/1/06	67.70	-155.99	N
TT0_0695.JPG	2093 m	9/1/06	67.70	-155.98	N
TT0_0696.JPG	2094 m	9/1/06	67.70	-155.96	N
TT0_0697.JPG	2084 m	9/1/06	67.66	-155.68	N
TT0_0698.JPG	2084 m	9/1/06	67.66	-155.67	N
TT0_0699.JPG	2086 m	9/1/06	67.66	-155.65	N
TT0_0700.JPG	2082 m	9/1/06	67.65	-155.64	N
TT0_0701.JPG	2088 m	9/1/06	67.65	-155.62	N
TT0_0702.JPG	2084 m	9/1/06	67.65	-155.61	N
TT0_0703.JPG	2081 m	9/1/06	67.65	-155.60	N
TT0_0704.JPG	2096 m	9/1/06	67.66	-155.44	N
TT0_0705.JPG	2088 m	9/1/06	67.66	-155.42	N
TT0_0706.JPG	2084 m	9/1/06	67.65	-155.41	N
TT0_0707.JPG	2086 m	9/1/06	67.65	-155.39	N
TT0_0708.JPG	2085 m	9/1/06	67.65	-155.38	N
TT0_0709.JPG	2089 m	9/1/06	67.65	-155.36	N
TT0_0710.JPG	2084 m	9/1/06	67.62	-155.24	N
TT0_0711.JPG	2082 m	9/1/06	67.61	-155.23	N
TT0_0712.JPG	2076 m	9/1/06	67.61	-155.22	N
TT0_0713.JPG	2069 m	9/1/06	67.60	-155.21	N

Table A-39: Balser and George image metadata part 24

Image name	Altitude	Year	Center latitude	Center longitude	Processed?
TT0_0715.JPG	2066 m	9/1/06	67.59	-155.20	N
TT0_0716.JPG	2066 m	9/1/06	67.59	-155.19	N
GAAR_GP05-1_20090821.JPG	1585 m	8/22/09	66.65	-155.67	N
GAAR_GP05-2_20090821.JPG	1585 m	8/22/09	66.65	-155.67	N
GAAR_GP05-3_20090821.JPG	1583 m	8/22/09	66.65	-155.67	N
GAAR_GP06-1_20090821.JPG	1423 m	8/21/09	66.83	-155.67	N
GAAR_GP06-2_20090821.JPG	1423 m	8/21/09	66.83	-155.68	N
GAAR_GP06-3_20090821.JPG	1423 m	8/21/09	66.83	-155.68	N
GAAR_GP11-1_20090821.JPG	1789 m	8/22/09	66.66	-155.22	N
GAAR_GP11-2_20090821.JPG	1789 m	8/22/09	66.66	-155.22	N
GAAR_GP11-3_20090821.JPG	1790 m	8/22/09	66.66	-155.21	N
GAAR_GP12-1_20090821.JPG	1401 m	8/21/09	66.84	-155.22	N
GAAR_GP12-2_20090821.JPG	1402 m	8/21/09	66.84	-155.22	N
GAAR_GP12-3_20090821.JPG	1402 m	8/21/09	66.84	-155.23	N
GAAR_GP19-1_20090821.JPG	1521 m	8/22/09	66.66	-154.77	N
GAAR_GP19-2_20090821.JPG	1521 m	8/22/09	66.66	-154.77	N
GAAR_GP19-3_20090821.JPG	1522 m	8/22/09	66.66	-154.77	N
GAAR_GP20-1_20090821.JPG	1452 m	8/21/09	66.84	-154.77	N
GAAR_GP20-2_20090821.JPG	1452 m	8/21/09	66.84	-154.77	N
GAAR_GP20-3_20090821.JPG	1452 m	8/21/09	66.84	-154.77	N
GAAR_GP21-1_20090821.JPG	1376 m	8/21/09	67.02	-154.77	N
GAAR_GP21-2_20090821.JPG	1376 m	8/21/09	67.02	-154.78	N
GAAR_GP21-3_20090821.JPG	1377 m	8/21/09	67.02	-154.78	N
GAAR_GP28-1_20090821.JPG	1425 m	8/21/09	67.02	-154.31	N
GAAR_GP28-2_20090821.JPG	1422 m	8/21/09	67.02	-154.32	N
GAAR_GP28-3_20090821.JPG	1420 m	8/21/09	67.02	-154.32	N
GAAR_GP36-1_20090821.JPG	2025 m	8/21/09	67.20	-153.86	N
GAAR_GP36-2_20090821.JPG	2024 m	8/21/09	67.20	-153.86	N
GAAR_GP36-3_20090821.JPG	2023 m	8/21/09	67.20	-153.86	N
GAAR_GP37-1_20090821.JPG	2011 m	8/21/09	67.38	-153.85	N
GAAR_GP37-2_20090821.JPG	2012 m	8/21/09	67.38	-153.86	N
GAAR_GP37-3_20090821.JPG	2012 m	8/21/09	67.38	-153.86	N
GAAR_GP43-1_20090821.JPG	1968 m	8/21/09	67.38	-153.39	N
GAAR_GP43-2_20090821.JPG	1968 m	8/21/09	67.38	-153.40	N
GAAR_GP43-3_20090821.JPG	1968 m	8/21/09	67.38	-153.40	N
GAAR_GP50-1_20090821.JPG	1981 m	8/21/09	67.38	-152.93	N
GAAR_GP50-2_20090821.JPG	1979 m	8/21/09	67.38	-152.93	N
GAAR_GP50-3_20090821.JPG	1977 m	8/21/09	67.38	-152.94	N

Table A-40: Balser and George image metadata part 25

Image name	Altitude	Year	Center latitude	Center longitude	Processed?
GAAR_GP57-2_20090821.JPG	2102 m	8/21/09	67.56	-152.46	N
GAAR_GP57-3_20090821.JPG	2101 m	8/21/09	67.55	-152.46	N
GAAR_GP58-1_20090821.JPG	1961 m	8/21/09	67.74	-152.45	N
GAAR_GP58-2_20090821.JPG	1961 m	8/21/09	67.74	-152.45	N
GAAR_GP58-3_20090821.JPG	1961 m	8/21/09	67.73	-152.45	N
GAAR_GP59-1_20090821.JPG	1987 m	8/21/09	67.92	-152.44	N
GAAR_GP59-2_20090821.JPG	1986 m	8/21/09	67.92	-152.44	N
GAAR_GP59-3_20090821.JPG	1983 m	8/21/09	67.92	-152.44	N
GAAR_GP60-1_20090821.JPG	2192 m	8/21/09	68.10	-152.43	N
GAAR_GP60-2_20090821.JPG	2192 m	8/21/09	68.10	-152.43	N
GAAR_GP60-3_20090821.JPG	2194 m	8/21/09	68.10	-152.43	N
GAAR_GP61-1_20090821.JPG	2303 m	8/21/09	68.28	-152.42	N
GAAR_GP61-2_20090821.JPG	2303 m	8/21/09	68.28	-152.42	N
GAAR_GP61-3_20090821.JPG	2303 m	8/21/09	68.28	-152.42	N
GAAR_GP62-1_20090821.JPG	2246 m	8/21/09	67.55	-151.99	N
GAAR_GP62-2_20090821.JPG	2246 m	8/21/09	67.55	-152.00	N
GAAR_GP62-3_20090821.JPG	2245 m	8/21/09	67.55	-152.00	N
GAAR_GP63-1_20090821.JPG	2134 m	8/21/09	67.73	-151.98	N
GAAR_GP63-2_20090821.JPG	2135 m	8/21/09	67.73	-151.98	N
GAAR_GP63-3_20090821.JPG	2135 m	8/21/09	67.73	-151.98	N
GAAR_GP64-1_20090821.JPG	2314 m	8/21/09	67.91	-151.97	N
GAAR_GP64-2_20090821.JPG	2314 m	8/21/09	67.91	-151.97	N
GAAR_GP64-3_20090821.JPG	2313 m	8/21/09	67.91	-151.97	N
GAAR_GP65-1_20090821.JPG	2072 m	8/21/09	68.09	-151.96	N
GAAR_GP65-2_20090821.JPG	2072 m	8/21/09	68.09	-151.95	N
GAAR_GP65-3_20090821.JPG	2071 m	8/21/09	68.09	-151.95	N
GAAR_GP66-1_20090821.JPG	2277 m	8/21/09	68.27	-151.94	N
GAAR_GP66-2_20090821.JPG	2277 m	8/21/09	68.27	-151.94	N
GAAR_GP66-3_20090821.JPG	2277 m	8/21/09	68.27	-151.94	N
GAAR_GP67-1_20090821.JPG	2275 m	8/21/09	67.73	-151.51	N
GAAR_GP67-2_20090821.JPG	2279 m	8/21/09	67.72	-151.51	N
GAAR_GP67-3_20090821.JPG	2280 m	8/21/09	67.72	-151.51	N
GAAR_GP68-1_20090821.JPG	2380 m	8/21/09	67.91	-151.49	N
GAAR_GP68-2_20090821.JPG	2380 m	8/21/09	67.91	-151.49	N
GAAR_GP68-3_20090821.JPG	2377 m	8/21/09	67.90	-151.49	N
GAAR_GP69-1_20090821.JPG	2261 m	8/21/09	68.09	-151.48	N
GAAR_GP69-2_20090821.JPG	2258 m	8/21/09	68.09	-151.48	N
GAAR_GP69-3_20090821.JPG	2257 m	8/21/09	68.08	-151.48	N

Table A-41: Balser and George image metadata part 26

Image name	Altitude	Year	Center latitude	Center longitude	Processed?
GAAR_GP70-2_20090821.JPG	1818 m	8/21/09	67.18	-151.10	N
GAAR_GP70-3_20090821.JPG	1820 m	8/21/09	67.18	-151.10	N
GAAR_GP71-1_20090821.JPG	1802 m	8/21/09	67.54	-151.06	N
GAAR_GP71-2_20090821.JPG	1802 m	8/21/09	67.54	-151.06	N
GAAR_GP71-3_20090821.JPG	1802 m	8/21/09	67.54	-151.06	N
GAAR_GP72-1_20090821.JPG	2021 m	8/21/09	67.72	-151.04	N
GAAR_GP72-2_20090821.JPG	2021 m	8/21/09	67.72	-151.04	N
GAAR_GP72-3_20090821.JPG	2020 m	8/21/09	67.72	-151.04	N
GAAR_GP73-1_20090821.JPG	2409 m	8/21/09	67.90	-151.02	N
GAAR_GP73-2_20090821.JPG	2407 m	8/21/09	67.90	-151.02	N
GAAR_GP73-3_20090821.JPG	2404 m	8/21/09	67.90	-151.02	N
GAAR_GP74-1_20090821.JPG	2504 m	8/21/09	68.08	-151.00	N
GAAR_GP74-2_20090821.JPG	2504 m	8/21/09	68.08	-151.00	N
GAAR_GP74-3_20090821.JPG	2503 m	8/21/09	68.08	-151.00	N
GAAR_GP75-1_20090821.JPG	2586 m	8/21/09	68.26	-150.98	N
GAAR_GP75-2_20090821.JPG	2588 m	8/21/09	68.26	-150.98	N
GAAR_GP75-3_20090821.JPG	2589 m	8/21/09	68.26	-150.98	N
GAAR_GP76-1_20090829.JPG	1764 m	8/29/09	67.17	-150.65	N
GAAR_GP76-2_20090829.JPG	1761 m	8/29/09	67.17	-150.65	N
GAAR_GP76-3_20090829.JPG	1759 m	8/29/09	67.17	-150.64	N
GAAR_GP77-1_20090829.JPG	2298 m	8/29/09	67.35	-150.62	N
GAAR_GP77-2_20090829.JPG	2299 m	8/29/09	67.35	-150.62	N
GAAR_GP77-3_20090829.JPG	2300 m	8/29/09	67.35	-150.62	N
GAAR_GP78-1_20090829.JPG	2250 m	8/29/09	67.53	-150.60	N
GAAR_GP78-2_20090829.JPG	2249 m	8/29/09	67.53	-150.60	N
GAAR_GP78-3_20090829.JPG	2248 m	8/29/09	67.53	-150.60	N
GAAR_GP79-1_20090829.JPG	2241 m	8/29/09	67.71	-150.57	N
GAAR_GP79-2_20090829.JPG	2242 m	8/29/09	67.71	-150.57	N
GAAR_GP79-3_20090829.JPG	2243 m	8/29/09	67.71	-150.57	N
GAAR_GP80-1_20090829.JPG	2374 m	8/29/09	67.89	-150.55	N
GAAR_GP80-2_20090829.JPG	2374 m	8/29/09	67.89	-150.55	N
GAAR_GP80-3_20090829.JPG	2374 m	8/29/09	67.89	-150.55	N
GAAR_GP81-1_20090829.JPG	2259 m	8/29/09	68.07	-150.53	N
GAAR_GP81-2_20090829.JPG	2258 m	8/29/09	68.07	-150.53	N
GAAR_GP81-3_20090829.JPG	2258 m	8/29/09	68.07	-150.52	N
GAAR_GP83-1_20090829.JPG	2228 m	8/29/09	67.70	-150.11	N
GAAR_GP83-2_20090829.JPG	2227 m	8/29/09	67.70	-150.11	N
GAAR_GP83-3_20090829.JPG	2225 m	8/29/09	67.70	-150.11	N

Table A-42: Balser and George image metadata part 27

Image name	Altitude	Year	Center latitude	Center longitude	Processed?
GAAR_GP84-2_20090829.JPG	2662 m	8/29/09	67.88	-150.08	N
GAAR_GP84-3_20090829.JPG	2658 m	8/29/09	67.88	-150.08	N
GAAR_GP85-1_20090829.JPG	2636 m	8/29/09	68.06	-150.05	N
GAAR_GP85-2_20090829.JPG	2634 m	8/29/09	68.06	-150.05	N
GAAR_GP85-3_20090829.JPG	2631 m	8/29/09	68.06	-150.05	N
TT0_2372.JPG	2552 m	8/19/08	67.96	-161.70	N
TT0_2373.JPG	2548 m	8/19/08	67.95	-161.68	N
TT0_2374.JPG	2537 m	8/19/08	67.95	-161.66	N
TT0_2375.JPG	2536 m	8/19/08	67.95	-161.64	N
TT0_2376.JPG	2534 m	8/19/08	67.95	-161.62	N
TT0_2377.JPG	2534 m	8/19/08	67.95	-161.60	N
TT0_2378.JPG	2542 m	8/19/08	67.94	-161.58	N
TT0_2379.JPG	2547 m	8/19/08	67.94	-161.56	N
TT0_2380.JPG	2545 m	8/19/08	67.94	-161.54	N
TT0_2381.JPG	2547 m	8/19/08	67.94	-161.52	N
TT0_2382.JPG	2552 m	8/19/08	67.94	-161.50	N
TT0_2383.JPG	2542 m	8/19/08	67.93	-161.48	N
TT0_2384.JPG	2545 m	8/19/08	67.93	-161.46	N
TT0_2385.JPG	2539 m	8/19/08	67.93	-161.44	N
TT0_2386.JPG	2535 m	8/19/08	67.93	-161.42	N
TT0_2387.JPG	2540 m	8/19/08	67.92	-161.40	N
TT0_2388.JPG	2554 m	8/19/08	67.92	-161.38	N
TT0_2389.JPG	2555 m	8/19/08	67.92	-161.36	N
TT0_2390.JPG	2546 m	8/19/08	67.92	-161.34	N
TT0_2391.JPG	2546 m	8/19/08	67.92	-161.32	N
TT0_2392.JPG	2531 m	8/19/08	67.91	-161.30	N
TT0_2393.JPG	2509 m	8/19/08	67.91	-161.28	N
TT0_2394.JPG	2502 m	8/19/08	67.91	-161.26	N
TT0_2395.JPG	2517 m	8/19/08	67.91	-161.25	N
TT0_2396.JPG	2660 m	8/19/08	67.88	-161.13	N
TT0_2397.JPG	2650 m	8/19/08	67.87	-161.15	N
TT0_2398.JPG	2649 m	8/19/08	67.87	-161.17	N
TT0_2399.JPG	2651 m	8/19/08	67.87	-161.20	N
TT0_2400.JPG	2646 m	8/19/08	67.87	-161.22	N
TT0_2401.JPG	2645 m	8/19/08	67.86	-161.24	N
TT0_2402.JPG	2644 m	8/19/08	67.86	-161.27	N
TT0_2403.JPG	2647 m	8/19/08	67.86	-161.29	N
TT0_2404.JPG	2639 m	8/19/08	67.86	-161.31	N

Table A-43: Balser and George image metadata part 28

Image name	Altitude	Year	Center latitude	Center longitude	Processed?
TT0_2406.JPG	2655 m	8/19/08	67.85	-161.36	N
TT0_2407.JPG	2649 m	8/19/08	67.85	-161.38	N
TT0_2408.JPG	2651 m	8/19/08	67.85	-161.40	N
TT0_2409.JPG	2651 m	8/19/08	67.84	-161.42	N
TT0_2410.JPG	2640 m	8/19/08	67.84	-161.45	N
TT0_2411.JPG	2643 m	8/19/08	67.84	-161.47	N
TT0_2412.JPG	2648 m	8/19/08	67.84	-161.49	N
TT0_2413.JPG	2644 m	8/19/08	67.83	-161.51	N
TT0_2414.JPG	2638 m	8/19/08	67.83	-161.53	N
TT0_2415.JPG	2633 m	8/19/08	67.83	-161.56	N
TT0_2416.JPG	2636 m	8/19/08	67.83	-161.58	N
TT0_2417.JPG	2631 m	8/19/08	67.82	-161.60	N
TT0_2418.JPG	2628 m	8/19/08	67.82	-161.63	N
TT0_2419.JPG	2627 m	8/19/08	67.82	-161.65	N
TT0_2420.JPG	2627 m	8/19/08	67.82	-161.67	N
TT0_2421.JPG	2626 m	8/19/08	67.81	-161.69	N
TT0_2422.JPG	2624 m	8/19/08	67.81	-161.70	N
TT0_2423.JPG	2613 m	8/20/08	67.81	-161.45	N
TT0_2424.JPG	2606 m	8/20/08	67.80	-161.44	N
TT0_2425.JPG	2601 m	8/20/08	67.80	-161.44	N
TT0_2426.JPG	2598 m	8/20/08	67.79	-161.43	N
TT0_2427.JPG	2604 m	8/20/08	67.78	-161.43	N
TT0_2428.JPG	2604 m	8/20/08	67.77	-161.43	N
TT0_2429.JPG	2605 m	8/20/08	67.76	-161.42	N
TT0_2430.JPG	2602 m	8/20/08	67.75	-161.42	N
TT0_2431.JPG	2606 m	8/20/08	67.75	-161.41	N
TT0_2432.JPG	2611 m	8/20/08	67.74	-161.41	N
TT0_2433.JPG	2616 m	8/20/08	67.73	-161.41	N
TT0_2434.JPG	2609 m	8/20/08	67.72	-161.40	N
TT0_2435.JPG	2606 m	8/20/08	67.71	-161.40	N
TT0_2436.JPG	2617 m	8/20/08	67.70	-161.39	N
TT0_2437.JPG	2632 m	8/20/08	67.69	-161.39	N
TT0_2438.JPG	2619 m	8/20/08	67.69	-161.39	N
TT0_2439.JPG	2611 m	8/20/08	67.68	-161.38	N
TT0_2440.JPG	2607 m	8/20/08	67.67	-161.38	N
TT0_2441.JPG	2599 m	8/20/08	67.66	-161.37	N
TT0_2442.JPG	2596 m	8/20/08	67.73	-161.25	N
TT0_2443.JPG	2592 m	8/20/08	67.72	-161.27	N

Table A-44: Balser and George image metadata part 29

Image name	Altitude	Year	Center latitude	Center longitude	Processed?
TT0_2445.JPG	2604 m	8/20/08	67.72	-161.31	N
TT0_2446.JPG	2602 m	8/20/08	67.71	-161.33	N
TT0_2447.JPG	2591 m	8/20/08	67.71	-161.35	N
TT0_2448.JPG	2606 m	8/20/08	67.71	-161.37	N
TT0_2449.JPG	2608 m	8/20/08	67.70	-161.39	N
TT0_2450.JPG	2603 m	8/20/08	67.70	-161.41	N
TT0_2451.JPG	2604 m	8/20/08	67.70	-161.43	N
TT0_2452.JPG	2600 m	8/20/08	67.69	-161.45	N
TT0_2453.JPG	2601 m	8/20/08	67.69	-161.47	N
TT0_2454.JPG	2606 m	8/20/08	67.68	-161.49	N
TT0_2455.JPG	2607 m	8/20/08	67.68	-161.51	N
TT0_2456.JPG	2609 m	8/20/08	67.68	-161.53	N
TT0_2457.JPG	2608 m	8/20/08	67.67	-161.55	N
TT0_2458.JPG	2607 m	8/20/08	67.67	-161.57	N
TT0_2459.JPG	2615 m	8/20/08	67.67	-161.59	N
TT0_2460.JPG	2610 m	8/20/08	67.66	-161.61	N
TT0_2461.JPG	2611 m	8/20/08	67.66	-161.63	N
TT0_2478.JPG	2581 m	8/20/08	67.65	-161.69	N
TT0_2479.JPG	2582 m	8/20/08	67.64	-161.67	N
TT0_2480.JPG	2573 m	8/20/08	67.64	-161.65	N
TT0_2481.JPG	2570 m	8/20/08	67.64	-161.63	N
TT0_2482.JPG	2577 m	8/20/08	67.64	-161.61	N
TT0_2483.JPG	2571 m	8/20/08	67.64	-161.59	N
TT0_2484.JPG	2570 m	8/20/08	67.63	-161.57	N
TT0_2485.JPG	2578 m	8/20/08	67.63	-161.55	N
TT0_2486.JPG	2576 m	8/20/08	67.63	-161.53	N
TT0_2487.JPG	2575 m	8/20/08	67.63	-161.52	N
TT0_2488.JPG	2570 m	8/20/08	67.62	-161.50	N
TT0_2489.JPG	2565 m	8/20/08	67.62	-161.48	N
TT0_2490.JPG	2570 m	8/20/08	67.62	-161.46	N
TT0_2491.JPG	2573 m	8/20/08	67.62	-161.44	N
TT0_2492.JPG	2579 m	8/20/08	67.62	-161.42	N
TT0_2493.JPG	2578 m	8/20/08	67.61	-161.40	N
TT0_2494.JPG	2584 m	8/20/08	67.61	-161.38	N
TT0_2495.JPG	2582 m	8/20/08	67.61	-161.36	N
TT0_2462.JPG	2629 m	8/20/08	67.72	-161.73	N
TT0_2463.JPG	2626 m	8/20/08	67.71	-161.73	N
TT0_2464.JPG	2621 m	8/20/08	67.70	-161.74	N

Table A-45: Balser and George image metadata part 30

Image name	Altitude	Year	Center latitude	Center longitude	Processed?
TT0_2466.JPG	2630 m	8/20/08	67.69	-161.76	N
TT0_2467.JPG	2627 m	8/20/08	67.68	-161.76	N
TT0_2468.JPG	2623 m	8/20/08	67.68	-161.77	N
TT0_2469.JPG	2626 m	8/20/08	67.67	-161.78	N
TT0_2470.JPG	2621 m	8/20/08	67.66	-161.78	N
TT0_2471.JPG	2612 m	8/20/08	67.66	-161.79	N
TT0_2472.JPG	2610 m	8/20/08	67.65	-161.80	N
TT0_2473.JPG	2605 m	8/20/08	67.64	-161.81	N
TT0_2474.JPG	2600 m	8/20/08	67.63	-161.81	N
TT0_2475.JPG	2605 m	8/20/08	67.63	-161.82	N
TT0_2476.JPG	2603 m	8/20/08	67.62	-161.83	N
TT0_2477.JPG	2610 m	8/20/08	67.62	-161.83	N
TT0_2496.JPG	2582 m	8/20/08	67.60	-161.47	N
TT0_2497.JPG	2587 m	8/20/08	67.60	-161.48	N
TT0_2498.JPG	2585 m	8/20/08	67.60	-161.51	N
TT0_2499.JPG	2584 m	8/20/08	67.60	-161.52	N
TT0_2500.JPG	2588 m	8/20/08	67.61	-161.54	N
TT0_2501.JPG	2587 m	8/20/08	67.61	-161.56	N
TT0_2502.JPG	2583 m	8/20/08	67.61	-161.58	N
TT0_2503.JPG	2584 m	8/20/08	67.61	-161.60	N
TT0_2504.JPG	2576 m	8/20/08	67.61	-161.62	N
TT0_2505.JPG	2652 m	8/20/08	67.66	-161.80	N
TT0_2506.JPG	2660 m	8/20/08	67.67	-161.80	N
TT0_2507.JPG	2659 m	8/20/08	67.68	-161.81	N
TT0_2508.JPG	2661 m	8/20/08	67.68	-161.81	N
TT0_2509.JPG	2667 m	8/20/08	67.69	-161.81	N
TT0_2510.JPG	2666 m	8/20/08	67.70	-161.82	N
TT0_2511.JPG	2667 m	8/20/08	67.70	-161.82	N
TT0_2512.JPG	2667 m	8/20/08	67.71	-161.82	N
TT0_2513.JPG	2669 m	8/20/08	67.72	-161.82	N
TT0_2514.JPG	2671 m	8/20/08	67.72	-161.82	N
TT0_2515.JPG	2673 m	8/20/08	67.73	-161.82	N
TT0_2516.JPG	2675 m	8/20/08	67.74	-161.81	N
TT0_2517.JPG	2682 m	8/20/08	67.74	-161.80	N
TT0_2518.JPG	2683 m	8/20/08	67.75	-161.80	N
TT0_2519.JPG	2656 m	8/20/08	67.75	-161.79	N
TT0_2520.JPG	2663 m	8/20/08	67.76	-161.78	N
TT0_2521.JPG	2657 m	8/20/08	67.77	-161.78	N

Table A-46: Balser and George image metadata part 31

Image name	Altitude	Year	Center latitude	Center longitude	Processed?
TT0_2523.JPG	2651 m	8/20/08	67.78	-161.76	N
TT0_2524.JPG	2652 m	8/20/08	67.79	-161.75	N
TT0_2525.JPG	2643 m	8/20/08	67.79	-161.74	N
TT0_2526.JPG	2636 m	8/20/08	67.80	-161.73	N
TT0_2527.JPG	2619 m	8/20/08	67.80	-161.72	N
TT0_2528.JPG	2574 m	8/20/08	67.81	-161.71	N
TT0_2529.JPG	2572 m	8/20/08	67.81	-161.69	N
TT0_2530.JPG	2589 m	8/20/08	67.82	-161.68	N
TT0_2531.JPG	2564 m	8/20/08	67.82	-161.66	N
TT0_2532.JPG	2551 m	8/20/08	67.83	-161.65	N
TT0_2533.JPG	2515 m	8/20/08	67.83	-161.63	N
TT0_2534.JPG	2487 m	8/20/08	67.83	-161.61	N
TT0_2535.JPG	2448 m	8/20/08	67.84	-161.59	N
TT0_2536.JPG	2428 m	8/20/08	67.84	-161.58	N
TT0_2537.JPG	2391 m	8/20/08	67.85	-161.52	N
TT0_2538.JPG	2357 m	8/20/08	67.85	-161.51	N
TT0_2539.JPG	2315 m	8/20/08	67.86	-161.49	N
TT0_2540.JPG	2278 m	8/20/08	67.86	-161.47	N
TT0_2541.JPG	2225 m	8/20/08	67.86	-161.45	N
TT0_2542.JPG	2193 m	8/20/08	67.86	-161.43	N
TT0_2543.JPG	2176 m	8/20/08	67.87	-161.41	N
TT0_2544.JPG	2158 m	8/20/08	67.87	-161.39	N
TT0_2545.JPG	2143 m	8/20/08	67.87	-161.37	N
TT0_2546.JPG	2101 m	8/20/08	67.87	-161.35	N
TT0_2547.JPG	2053 m	8/20/08	67.88	-161.33	N
TT0_2548.JPG	2018 m	8/20/08	67.88	-161.31	N
TT0_2549.JPG	2003 m	8/20/08	67.89	-161.29	N
TT0_2550.JPG	1990 m	8/20/08	67.89	-161.28	N
TT0_2551.JPG	1984 m	8/20/08	67.89	-161.26	N
TT0_2552.JPG	1974 m	8/20/08	67.90	-161.25	N
TT0_2553.JPG	1964 m	8/20/08	67.91	-161.23	N
TT0_2554.JPG	1950 m	8/20/08	67.91	-161.22	N
TT0_2555.JPG	1941 m	8/20/08	67.92	-161.20	N
TT0_2556.JPG	1947 m	8/20/08	67.92	-161.19	N
TT0_2557.JPG	1944 m	8/20/08	67.92	-161.17	N
TT0_2558.JPG	1942 m	8/20/08	67.93	-161.15	N
TT0_2559.JPG	1952 m	8/20/08	67.93	-161.14	N
TT0_2560.JPG	1946 m	8/20/08	67.93	-161.12	N

Table A-47: Balser and George image metadata part 32

Image name	Altitude	Year	Center latitude	Center longitude	Processed?
TT0_2562.JPG	1960 m	8/20/08	67.94	-161.10	N
TT0_2563.JPG	1974 m	8/20/08	67.95	-161.09	N
TT0_2564.JPG	1983 m	8/20/08	67.95	-161.08	N
TT0_2565.JPG	1990 m	8/20/08	67.95	-161.07	N
TT0_2566.JPG	1931 m	8/20/08	67.93	-161.23	N
TT0_2567.JPG	1943 m	8/20/08	67.93	-161.25	N
TT0_2568.JPG	1942 m	8/20/08	67.93	-161.27	N
TT0_2569.JPG	1953 m	8/20/08	67.93	-161.29	N
TT0_2570.JPG	1957 m	8/20/08	67.93	-161.30	N
TT0_2571.JPG	1971 m	8/20/08	67.92	-161.32	N
TT0_2572.JPG	1998 m	8/20/08	67.92	-161.34	N
TT0_2573.JPG	2004 m	8/20/08	67.92	-161.36	N
TT0_2574.JPG	2002 m	8/20/08	67.92	-161.38	Y
TT0_2575.JPG	2002 m	8/20/08	67.92	-161.40	N
TT0_2576.JPG	2003 m	8/20/08	67.92	-161.42	N
TT0_2577.JPG	2000 m	8/20/08	67.92	-161.44	N
TT0_2578.JPG	2004 m	8/20/08	67.92	-161.45	N
TT0_2579.JPG	1996 m	8/20/08	67.91	-161.48	N
TT0_2580.JPG	1990 m	8/20/08	67.91	-161.49	N
TT0_2581.JPG	2001 m	8/20/08	67.91	-161.52	N
TT0_2582.JPG	2002 m	8/20/08	67.91	-161.53	N
TT0_2583.JPG	1989 m	8/20/08	67.91	-161.55	N
TT0_2584.JPG	1979 m	8/20/08	67.91	-161.57	N
TT0_2585.JPG	1977 m	8/20/08	67.91	-161.60	N
TT0_2586.JPG	1979 m	8/20/08	67.91	-161.61	N
TT0_2587.JPG	1975 m	8/20/08	67.91	-161.64	N
TT0_2588.JPG	1962 m	8/20/08	67.91	-161.65	N
TT0_2589.JPG	1966 m	8/20/08	67.91	-161.68	N
TT0_2590.JPG	1973 m	8/20/08	67.91	-161.69	N
TT0_2591.JPG	1980 m	8/20/08	67.91	-161.72	N
TT0_2592.JPG	1984 m	8/20/08	67.92	-161.73	N
TT0_2593.JPG	1990 m	8/20/08	67.92	-161.90	N
TT0_2594.JPG	1984 m	8/20/08	67.92	-161.92	N
TT0_2595.JPG	1976 m	8/20/08	67.93	-161.94	N
TT0_2596.JPG	1967 m	8/20/08	67.93	-161.96	N
TT0_2597.JPG	1964 m	8/20/08	67.93	-161.97	N
TT0_2598.JPG	1962 m	8/20/08	67.93	-161.98	N
TT0_2599.JPG	1964 m	8/20/08	67.93	-162.00	N

Table A-48: Balser and George image metadata part 33

Image name	Altitude	Year	Center latitude	Center longitude	Processed?
TT0_2601.JPG	1961 m	8/20/08	67.93	-162.23	N
TT0_2602.JPG	1960 m	8/20/08	67.93	-162.25	N
TT0_2603.JPG	1957 m	8/20/08	67.93	-162.26	N
TT0_2604.JPG	1952 m	8/20/08	67.93	-162.28	N
TT0_2605.JPG	1952 m	8/20/08	67.94	-162.29	N
TT0_2606.JPG	1949 m	8/20/08	67.94	-162.30	N
TT0_2607.JPG	1949 m	8/20/08	67.94	-162.32	N
TT0_2608.JPG	1956 m	8/20/08	67.94	-162.33	N
TT0_2609.JPG	1955 m	8/20/08	67.94	-162.35	N
TT0_2610.JPG	1954 m	8/20/08	67.94	-162.36	N
TT0_2611.JPG	1958 m	8/20/08	67.94	-162.37	N
TT0_2612.JPG	1962 m	8/20/08	67.94	-162.39	N
TT0_2613.JPG	1962 m	8/20/08	67.94	-162.40	N
TT0_2614.JPG	1960 m	8/20/08	67.94	-162.42	N

A.5: 1984 and 1985 flightlines over the coastal plain of ANWR

An extension of this work involves characterizing shrub expansion on the coastal plain of the Arctic National Wildlife Refuge (ANWR), which is managed by the U.S. Fish and Wildlife Service (FWS). In the mid-1980s, FWS arranged to have vertical aerial photographs acquired of the coastal plain of ANWR. Some of these were used to assess tectonic faults, but they have since been used to assess coastal erosion and vegetation change at regular grid intervals. These images are particularly useful for these kinds of studies because they are color-infrared and are at a scale of 1:6000 or 1:18,000. Shrub development can be facilitated by the development of patterned ground, a periglacial landscape feature. Patterned ground is clearly visible in these images.

I acquired a series of images from the FWS because of the high level of detail that these images afford (vs. the AHAP images), and because I am interested in gaining a better understanding of the extent of shrub expansion across northern Alaska. Future work will focus on deriving vegetation change data from these images.

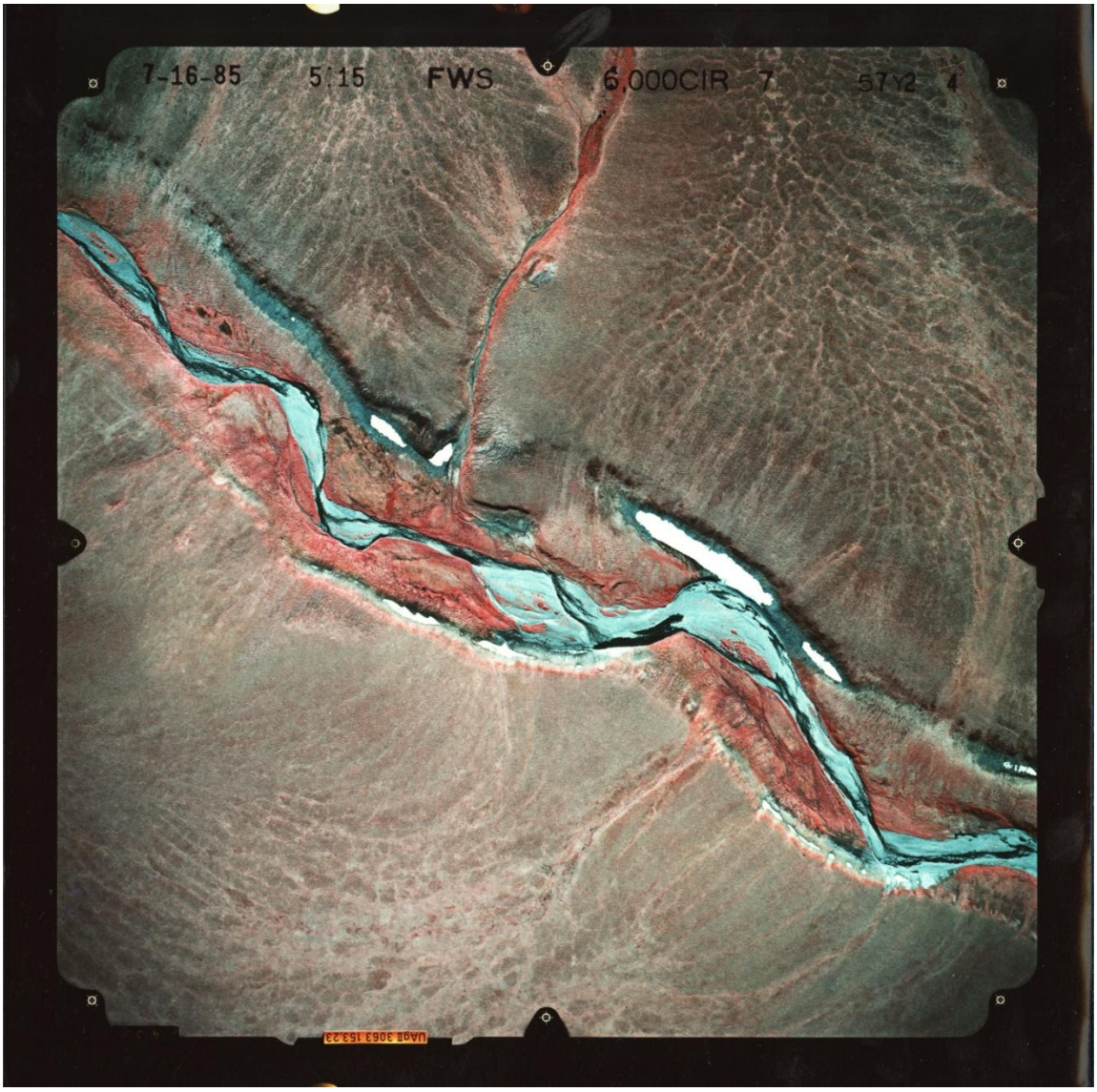

Figure A-28: An example of one of the 1:6000, 1985 color infrared vertical aerial photographs from the coastal plain of ANWR.

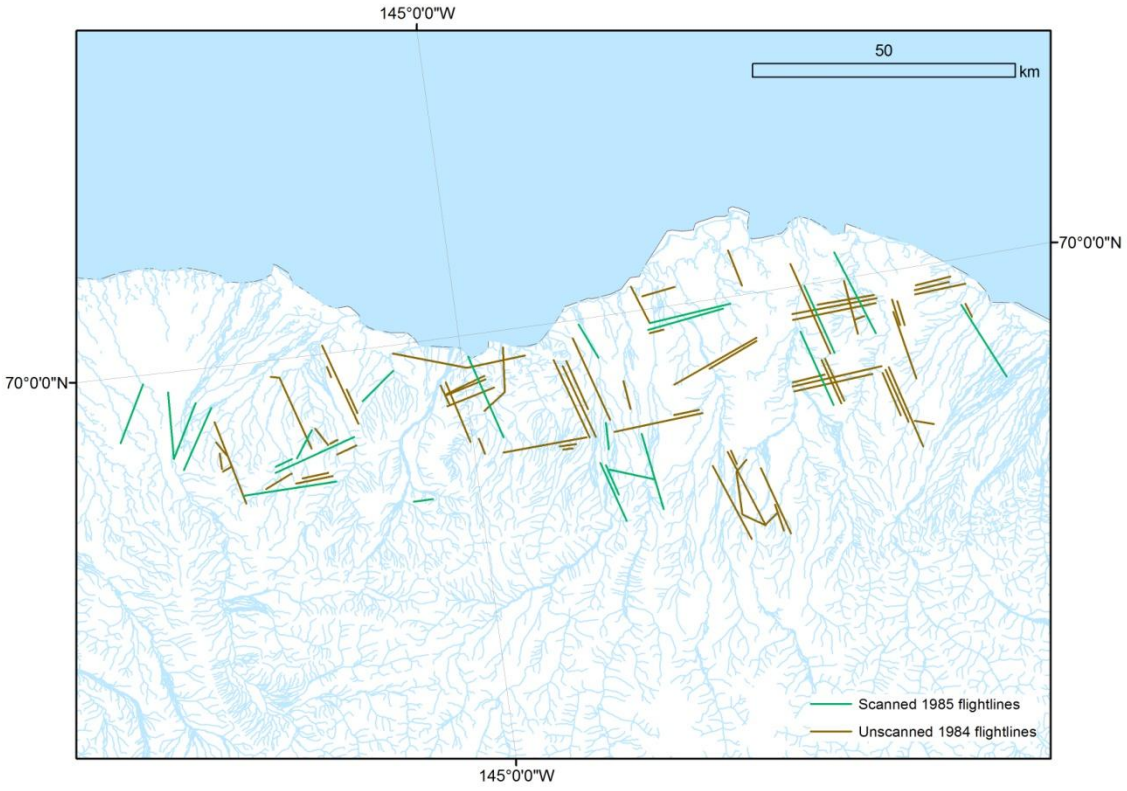

Figure A-29: Location of the flightlines for the 1984/1985 ANWR images.

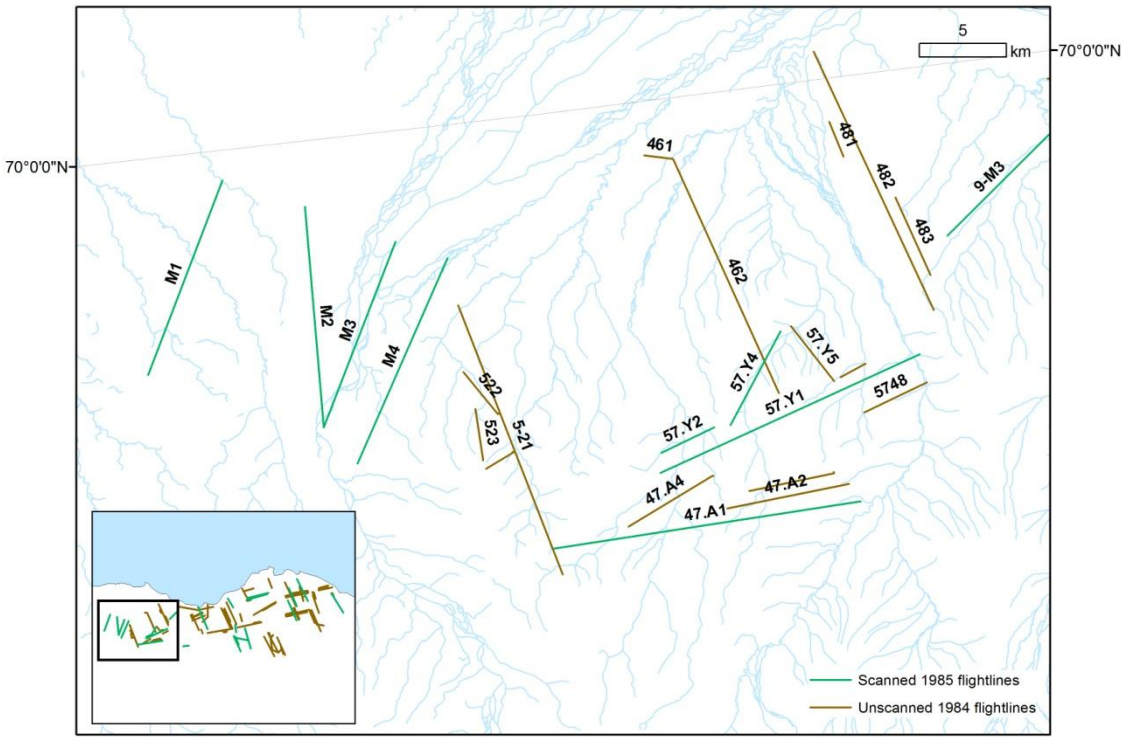

Figure A-30: Location of the flightlines for the 1984/1985 ANWR images, subsection 1.

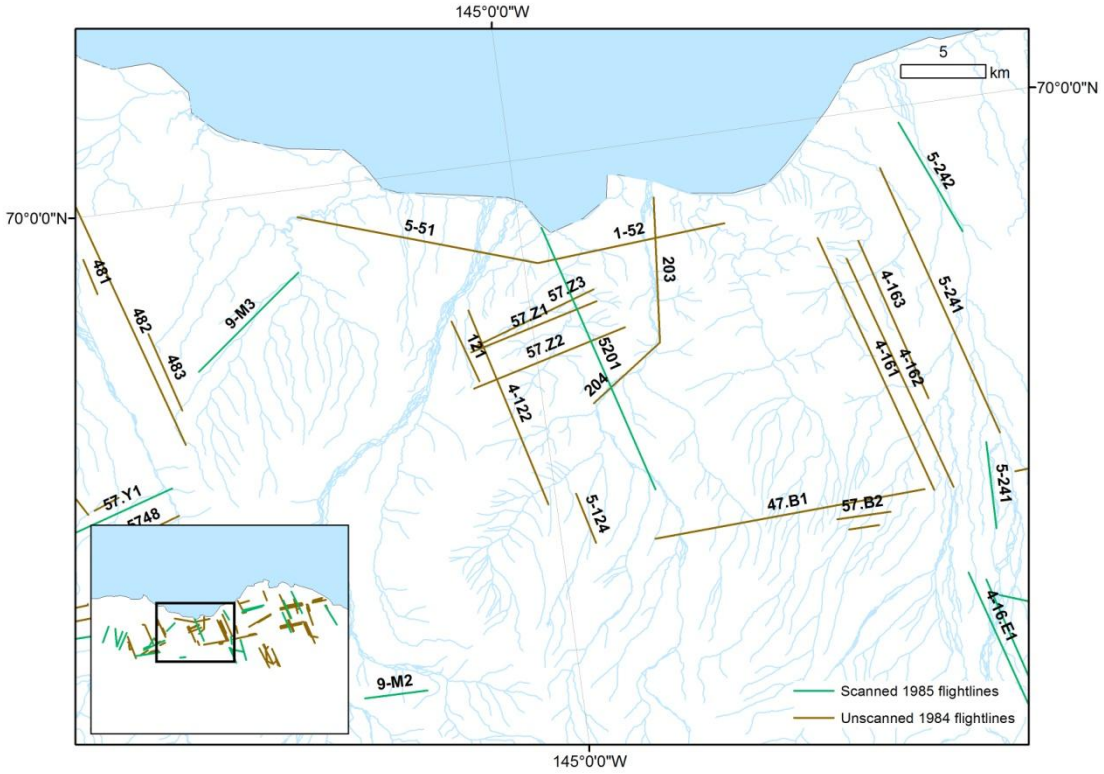

Figure A-31: Location of the flightlines for the 1984/1985 ANWR images, subsection 2.

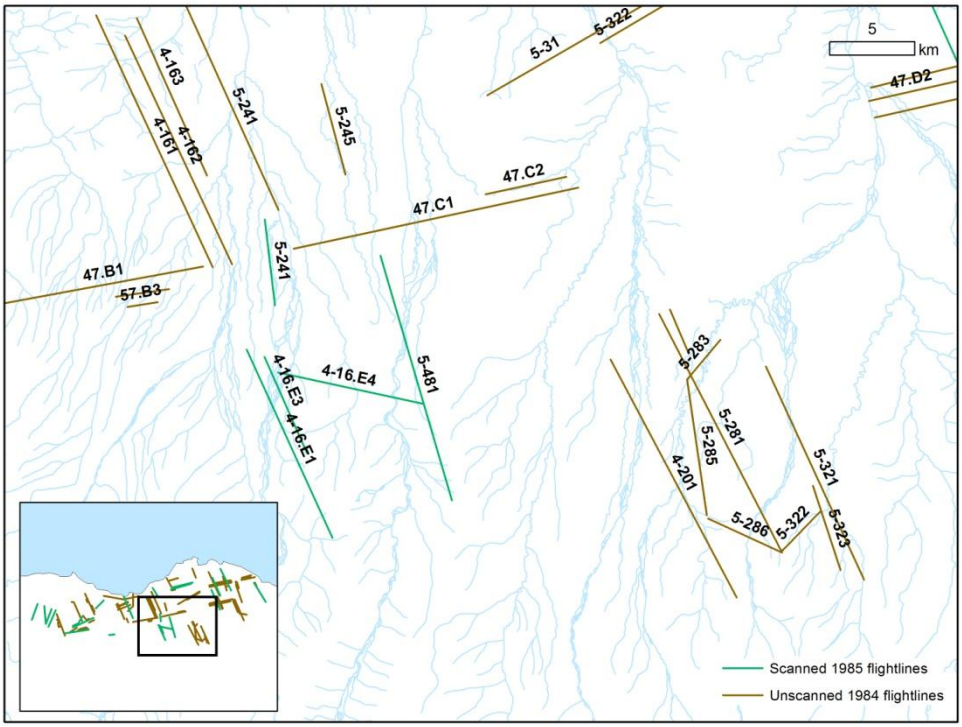

Figure A-32: Location of the flightlines for the 1984/1985 ANWR images, subsection 3.

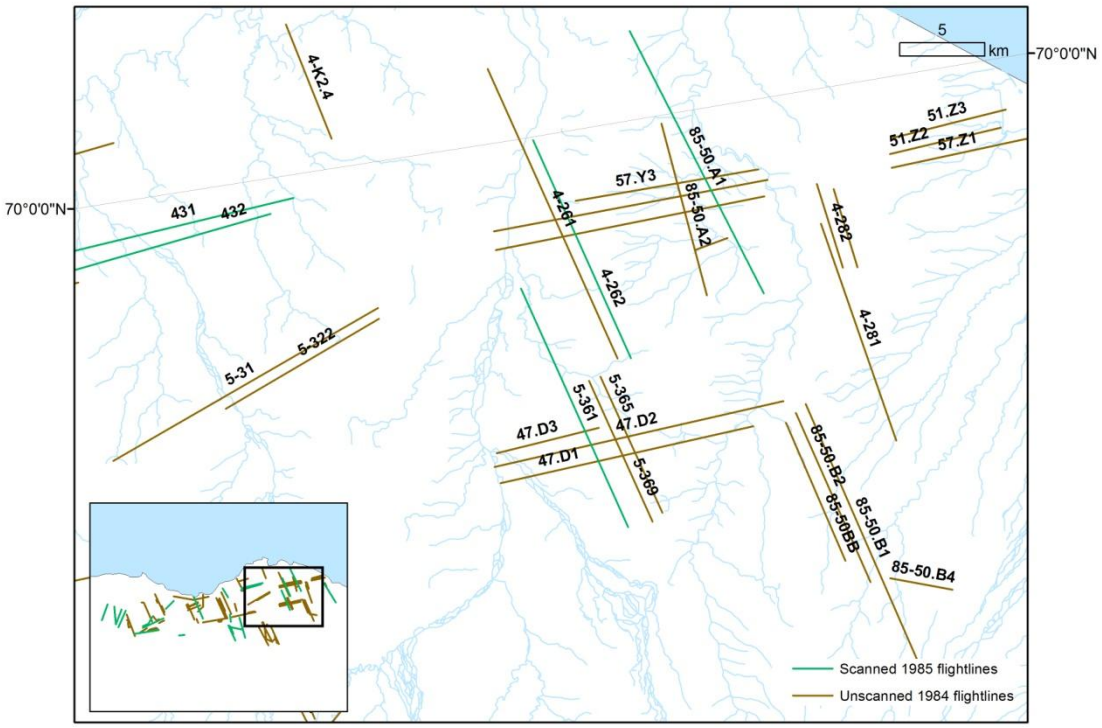

Figure A-33: Location of the flightlines for the 1984/1985 ANWR images, subsection 4.

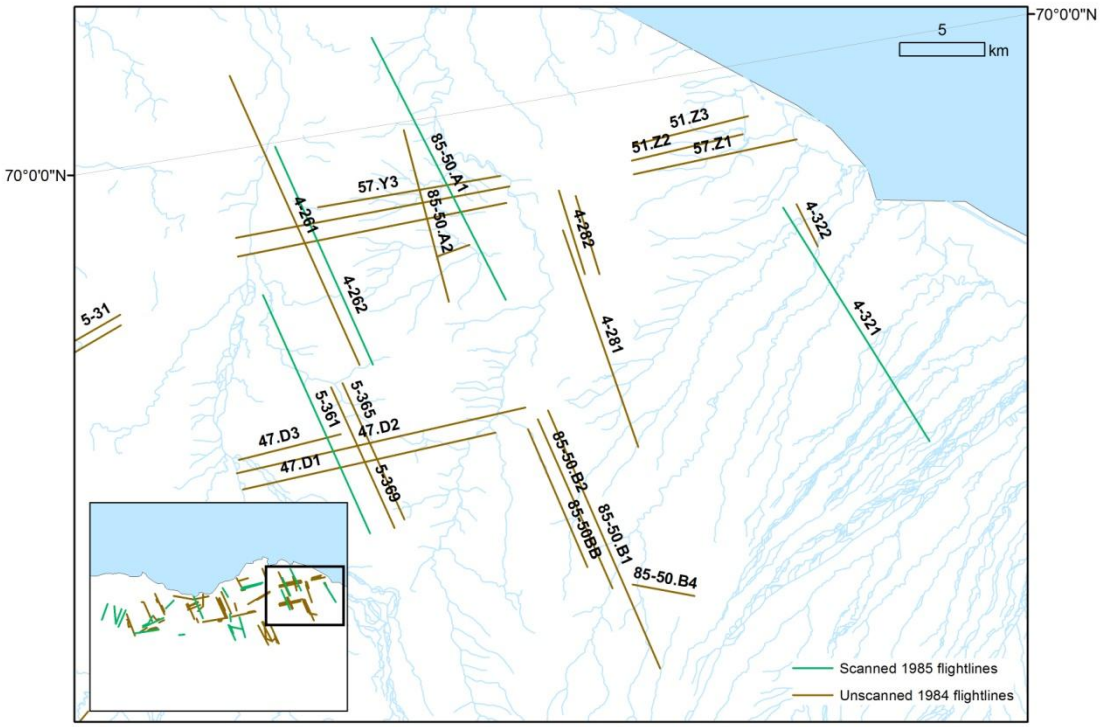

Figure A-34: Location of the flightlines for the 1984/1985 ANWR images, subsection 5.

Table A-49: ANWR 1984/1985 images part 1

Flightline	Image name	Scale	Source
1-85361	00001	6000	FWS
1-85362	00002	6000	FWS
1-85363	00003	6000	FWS
1-85364	00004	6000	FWS
1-85365	00005	6000	FWS
1-85366	00006	6000	FWS
1-85367	00007	6000	FWS
1-85368	00008	6000	FWS
1-85369	00009	6000	FWS
1-85370	00010	6000	FWS
1-85371	00012	6000	FWS
1-85372	00014	6000	FWS
416.E1	00001	6000	FWS
416.E1	00002	6000	FWS
416.E1	00003	6000	FWS
416.E1	00004	6000	FWS
416.E1	00005	6000	FWS
416.E1	00006	6000	FWS
416.E1	00007	6000	FWS
416.E1	00008	6000	FWS
416.E1	00009	6000	FWS
416.E1	00010	6000	FWS
416.E1	00011	6000	FWS
416.E1	00012	6000	FWS
416.E1	00013	6000	FWS
416.E1	00014	6000	FWS
416.E1	00015	6000	FWS
416.E1	00016	6000	FWS
416.E1	00017	6000	FWS
416.E1	00018	6000	FWS
416.E1	00019	6000	FWS
416.E1	00020	6000	FWS
416.E1	00021	6000	FWS
416.E1	00022	6000	FWS
416.E1	00023	6000	FWS
416.E1	00024	6000	FWS
416.E3	00001	6000	FWS
416.E3	00002	6000	FWS
416.E3	00003	6000	FWS

Table A-50: ANWR 1984/1985 images part 2

Flightline	Image name	Scale	Source
416.E3	00005	6000	FWS
416.E3	00006	6000	FWS
416.E3	00007	6000	FWS
416.E3	00008	6000	FWS
416.E3	00009	6000	FWS
416.E3	00010	6000	FWS
416.E3	00011	6000	FWS
416.E3	00012	6000	FWS
416.E4	00001	6000	FWS
416.E4	00002	6000	FWS
416.E4	00003	6000	FWS
416.E4	00004	6000	FWS
416.E4	00005	6000	FWS
416.E4	00006	6000	FWS
416.E4	00007	6000	FWS
416.E4	00008	6000	FWS
416.E4	00009	6000	FWS
416.E4	00010A	6000	FWS
416.E4	00011A	6000	FWS
416.E4	00012A	6000	FWS
416.E4	00013A	6000	FWS
416.E4	00014A	6000	FWS
416.E4	00015	6000	FWS
416.E4	00016	6000	FWS
416.E4	00017	6000	FWS
4262	00001	6000	FWS
4262	00002	6000	FWS
4262	00003	6000	FWS
4262	00004	6000	FWS
4262	00005	6000	FWS
4262	00006	6000	FWS
4262	00007	6000	FWS
4262	00008	6000	FWS
4262	00009	6000	FWS
4262	00010	6000	FWS
4262	00011	6000	FWS
4262	00012	6000	FWS
4262	00013	6000	FWS
4262	00014	6000	FWS

Table A-51: ANWR 1984/1985 images part 3

Flightline	Image name	Scale	Source
4262	00016	6000	FWS
4262	00017	6000	FWS
4262	00018	6000	FWS
4262	00019	6000	FWS
4262	00020	6000	FWS
4262	00021	6000	FWS
4262	00022	6000	FWS
4262	00023	6000	FWS
4262	00027	6000	FWS
4262	00029	6000	FWS
4262	00030	6000	FWS
4262	00031	6000	FWS
4262	00032	6000	FWS
431	0003	6000	FWS
431	0004	6000	FWS
431	0005	6000	FWS
431	00006	6000	FWS
431	00007	6000	FWS
431	00008	6000	FWS
431	00009	6000	FWS
431	00010	6000	FWS
431	00011	6000	FWS
431	00015	6000	FWS
431	00016	6000	FWS
431	00017	6000	FWS
431	00018	6000	FWS
431	00019	6000	FWS
431	0020	6000	FWS
431	00021	6000	FWS
431	00022	6000	FWS
431	00023	6000	FWS
431	00024	6000	FWS
431	00025	6000	FWS
431	00025-20120518093025	6000	FWS
431	0026	6000	FWS
431	00027	6000	FWS
431	00028	6000	FWS
431	00029	6000	FWS
431	00029-20120518093025	6000	FWS

Table A-52: ANWR 1984/1985 images part 4

Flightline	Image name	Scale	Source
432	00001	6000	FWS
432	00003	6000	FWS
432	00005	6000	FWS
432	00008	6000	FWS
432	00010	6000	FWS
432	00012	6000	FWS
432	00013	6000	FWS
433	00014	6000	FWS
434	00015	6000	FWS
435	00016	6000	FWS
436	00017	6000	FWS
437	00018	6000	FWS
438	00019	6000	FWS
439	00028	6000	FWS
47.A1	00004	6000	FWS
47.A1	00005	6000	FWS
47.A1	00007	6000	FWS
47.A1	00024	6000	FWS
47.A1	00025	6000	FWS
47.A1	00002	6000	FWS
47.A1	00005	6000	FWS
47.A1	00006	6000	FWS
47.A1	00007	6000	FWS
47.A1	00008	6000	FWS
47.A1	00009	6000	FWS
47.A1	00010	6000	FWS
47.A1	51.Z1.01	6000	FWS
5201	00001	6000	FWS
5201	00002	6000	FWS
5201	00003	6000	FWS
5201	00004	6000	FWS
5201	00005	6000	FWS
5201	00006	6000	FWS
5201	00007	6000	FWS
5201	00008	6000	FWS
5201	00009	6000	FWS
5201	00010	6000	FWS
5201	00011	6000	FWS
5201	00012	6000	FWS

Table A-53: ANWR 1984/1985 images part 5

Flightline	Image name	Scale	Source
5201	00014	6000	FWS
5201	00015	6000	FWS
5201	00016	6000	FWS
5201	00017	6000	FWS
5201	00018	6000	FWS
5201	00019	6000	FWS
5201	00020	6000	FWS
5201	00021	6000	FWS
5201	00022	6000	FWS
5201	00023	6000	FWS
5201	00024	6000	FWS
5201	00025	6000	FWS
5201	00026	6000	FWS
5201	00027	6000	FWS
5201	00028	6000	FWS
321	00001	6000	FWS
321	00003	6000	FWS
321	00005	6000	FWS
321	00014	6000	FWS
321	00015	6000	FWS
321	00016	6000	FWS
321	00017	6000	FWS
321	00018	6000	FWS
321	00019	6000	FWS
321	00020	6000	FWS
321	00021	6000	FWS
321	00022	6000	FWS
321	00023	6000	FWS
321	00024	6000	FWS
321	00025	6000	FWS
321	00026	6000	FWS
321	00027	6000	FWS
321	00028	6000	FWS
321	00029	6000	FWS
321	00030	6000	FWS
5361	00001	6000	FWS
5361	00002	6000	FWS
5361	00003	6000	FWS
5361	00004	6000	FWS

Table A-54: ANWR 1984/1985 images part 6

Flightline	Image name	Scale	Source
5361	00006	6000	FWS
5361	00007	6000	FWS
5361	00008	6000	FWS
5361	00009	6000	FWS
5361	00010	6000	FWS
5361	00011	6000	FWS
5361	00014	6000	FWS
5361	00016	6000	FWS
5361	00031	6000	FWS
5361	00032	6000	FWS
57.Y1	00001	6000	FWS
57.Y1	00002	6000	FWS
57.Y1	00003	6000	FWS
57.Y1	00004	6000	FWS
57.Y1	00005	6000	FWS
57.Y1	00006	6000	FWS
57.Y1	00007	6000	FWS
57.Y1	00008	6000	FWS
57.Y1	00009	6000	FWS
57.Y1	00010	6000	FWS
57.Y1	00011	6000	FWS
57.Y1	00012	6000	FWS
57.Y1	00013	6000	FWS
57.Y1	00014	6000	FWS
57.Y1	00015	6000	FWS
57.Y1	00016	6000	FWS
57.Y1	00017	6000	FWS
57.Y1	00018	6000	FWS
57.Y1	00019	6000	FWS
57.Y1	00020	6000	FWS
57.Y1	00021	6000	FWS
57.Y2	00001	6000	FWS
57.Y2	00002	6000	FWS
57.Y2	00003	6000	FWS
57.Y2	00004	6000	FWS
57.Y2	00005	6000	FWS
57.Y2	00006	6000	FWS
57.Y2	00007	6000	FWS
57.Y2	00008	6000	FWS

Table A-55: ANWR 1984/1985 images part 7

Flightline	Image name	Scale	Source
57.Y3	00002	6000	FWS
57.Y3	00003	6000	FWS
57.Y3	00004	6000	FWS
57.Y4	00001	6000	FWS
57.Y4	00002	6000	FWS
57.Y4	00003	6000	FWS
57.Y4	00004	6000	FWS
57.Y4	00005	6000	FWS
57.Y4	00006	6000	FWS
57.Y4	00007	6000	FWS
57.Z1	00001	6000	FWS
57.Z1	00002	6000	FWS
57.Z1	00003	6000	FWS
57.Z1	00004	6000	FWS
57.Z1	00005	6000	FWS
57.Z1	00006	6000	FWS
57.Z1	00007	6000	FWS
57.Z1	00008	6000	FWS
57.Z1	00009	6000	FWS
57.Z1	00013	6000	FWS
8431(84)	00001	6000	FWS
8431(84)	00002	6000	FWS
8431(84)	00003	6000	FWS
8431(84)	00004	6000	FWS
8431(84)	00005	6000	FWS
8431(84)	00006	6000	FWS
8431(84)	00007	6000	FWS
8431(84)	00008	6000	FWS
8431(84)	00009	6000	FWS
8431(84)	00010	6000	FWS
8431(84)	00011	6000	FWS
8431(84)	00012	6000	FWS
8431(84)	00013	6000	FWS
8431(84)	00014	6000	FWS
8431(84)	00015	6000	FWS
8431(84)	00016	6000	FWS
8431(84)	00017	6000	FWS
8431(84)	00018	6000	FWS
8431(84)	00019	6000	FWS

Table A-56: ANWR 1984/1985 images part 8

Flightline	Image name	Scale	Source
8431(84)	00021	6000	FWS
8431(84)	00022	6000	FWS
8431(84)	00023	6000	FWS
8431(84)	00024	6000	FWS
8431(84)	00026	6000	FWS
8431(84)	00027	6000	FWS
8431(84)	00028	6000	FWS
8431(84)	00030	6000	FWS
8431(84)	00032	6000	FWS
8431(84)	00033	6000	FWS
8431(84)	00034	6000	FWS
8431(84)	00035	6000	FWS
85-50.A1	00001	6000	FWS
85-50.A1	00002	6000	FWS
85-50.A1	00003	6000	FWS
85-50.A1	00004	6000	FWS
85-50.A1	00005	6000	FWS
85-50.A1	00006	6000	FWS
85-50.A1	00007	6000	FWS
85-50.A1	00008	6000	FWS
85-50.A1	00009	6000	FWS
85-50.A1	00010	6000	FWS
85-50.A1	00011	6000	FWS
85-50.A1	00012	6000	FWS
85-50.A1	00013	6000	FWS
85-50.A1	00014	6000	FWS
85-50.A1	00015	6000	FWS
85-50.A1	00016	6000	FWS
85-50.A1	00017	6000	FWS
85-50.A1	00019	6000	FWS
85-50.A1	00020	6000	FWS
85-50.A1	00021	6000	FWS
85-50.A1	00022	6000	FWS
85-50.A1	00023	6000	FWS
85-50.A1	00024	6000	FWS
85-50.A1	00025	6000	FWS
85-50.A1	00026	6000	FWS
85-50.A1	00027	6000	FWS
85-50.A1	00028	6000	FWS

Table A-57: ANWR 1984/1985 images part 9

Flightline	Image name	Scale	Source
9M-3	00019	6000	FWS
9M-3	00020	6000	FWS
9M-3	00021	6000	FWS
9M-3	00022	6000	FWS
9M-4	00001	6000	FWS
9M-4	00002	6000	FWS
9M-4	00003	6000	FWS
9M-4	00004	6000	FWS
9M-4	00005	6000	FWS
9M-4	00006	6000	FWS
9M-4	00007	6000	FWS
9M-4	00008	6000	FWS
9M-4	00019	6000	FWS
9M-4	00020	6000	FWS
9M-4	00021	6000	FWS
9M-4	00022	6000	FWS
9M-4	00023	6000	FWS
9M-4	00024	6000	FWS
M-1	00001	6000	FWS
M-1	00002	6000	FWS
M-1	00003	6000	FWS
M-1	00004	6000	FWS
M-1	00005	6000	FWS
M-1	00006	6000	FWS
M-1	00007	6000	FWS
M-1	00008	6000	FWS
M-1	00009	6000	FWS
M-1	00010	6000	FWS
M-1	00011	6000	FWS
M-1	00013	6000	FWS
M-1	00014	6000	FWS
M-1	00015	6000	FWS
M-1	00016	6000	FWS
M-1	00019	6000	FWS
M-1	00021	6000	FWS
M-1	00022	6000	FWS
M-1	00023	6000	FWS
M-2	00001	6000	FWS
M-2	00002	6000	FWS

Table A-58: ANWR 1984/1985 images part 10

Flightline	Image name	Scale	Source
M-2	00004	6000	FWS
M-2	00005	6000	FWS
M-2	00006	6000	FWS
M-2	00007	6000	FWS
M-2	00008	6000	FWS
M-2	00009	6000	FWS
M-2	00010	6000	FWS
M-2	00011	6000	FWS
M-2	00012	6000	FWS
M-2	00013	6000	FWS
M-2	00014	6000	FWS
M-2	00015	6000	FWS
M-2	00016	6000	FWS
M-2	00017	6000	FWS
M-2	00018	6000	FWS
M-2	00019	6000	FWS
M-2	00020	6000	FWS
M-2	00021	6000	FWS
M-2	00022	6000	FWS
M-2	00023	6000	FWS
M-2	00024	6000	FWS
M-2	00040	6000	FWS
M-2	00041	6000	FWS

Table A-59: Shrub cover maps generated for project.

Area	Year available	Area	Year available
Atigun	1972	Killik	1977
	2010		1982
Ayiyak	1979		2004
	1985	Kurupa	1977
	2010		1985
Canning	1955		2007
	1978	Nanushuk I	1955
	2009		1978
Chandler	1978		2004
	1985	Nanushuk II	1955
	2010		1978
Colville	1974		2004
	1980	Nigu	1977
	2004		1985
Colville II	1955		2008
	1980	Nimiuktuk I	1977
	2004		2009
Colville III	1980		
	2004		

Table A-60: Availability of geomorphologic, hydrologic, and elevation data for the project.

Area	Geomorphic Unit Boundaries	Elevation (30 m DEM)	River/lake polygons	Digitized River Centerlines
Atigun	✓	✓		
Ayiyak	✓	✓	✓	✓
Canning	✓	✓	✓	✓
Chandler	✓	✓	✓	✓
Colville 1	✓	✓	✓	✓
Colville 2,3,4	✓	✓		
Killik	✓	✓	✓	✓
Kurupa	✓	✓	✓	✓
Nanushuk 1,2	✓	✓	✓	✓
Nigu	✓	✓	✓	✓
Nimiuktuk 1	✓	✓		
Nimiuktuk 2	✓	✓		
Nimiuktuk 3	✓	✓		
Oolamnagavik	✓	✓		